Scaffold surface modifications and culture conditions as key parameters to develop cartilage and bone tissue engineering implants

Joaquín Ródenas Rochina

Valencia, 09/12/2014

UNIVERSITAT POLITÈCNICA DE VALÈNCIA

Thesis supervisors:
Jose Luis Gomez Ribelles
Myriam Lebourg

UNIVERSITAT POLITÈCNICA DE VALÈNCIA

Scaffold surface modifications and culture conditions as key parameters to develop cartilage and bone tissue engineering implants

Thesis submitted by:

Joaquín Ródenas Rochina

To obtain the degree of Doctor at the

Universitat Politècnica de València

Thesis supervisors:

Jose Luis Gomez Ribelles

Myriam Lebourg

Valencia, 09/12/2014

The question is not how far. The question is,
do you possess the constitution, the depth of faith,
to go as far is as needed?
-Noah MacManus-

Acknowledgement.

I would like to say thank you first to Generalitat Valenciana for the VALi+d grant I receive, which helped me in a big way to complete this work, and allowed me to enjoy a time in Dublin´s Trinity College with the BEFPI grant.

At the same time, I am enormously grateful to the Industry and Commerce ministery for funding the Cenit intelimplant project though their Ingenio 2010 initiative

I am specially indebted to my thesis directors, Jose Luis Gomez Ribelles and Myriam Lebourg, who gave me the chance to complete my thesis in the Center for Biomaterials and Tissue Engineering under their supervision. Their help and support have been essential for me in every moment.

Thanks, too, to Julio Jose Suay for allowing me to contribute in project Cenit.

Thank you, also, to all my lab partners, Carmen, Maria, Manu, Alex, Irene and everybody else, for the help they gave me although this years. Specially, I want to thank Keila for helping me with histology protocols.

It's worth to mention here Laura, our lab´s technician, who always had an answer for everything.

I must thank the Intituto Principe Felipe and its confocal microscopy service, most than anybody else, their technician Eva. In the same way, I give my thanks to the UPV's microscopy service for all the support they gave me, especially Alicia, Jose Luis and Merche.

Even from the distance, my deepest thank you to Dr. Daniel Kelly and Dr. Yurong Liu, who let me work part of my thesis at Trinity Center for Bioengineering, and to my lab partners there, Henrique, Tariq, Lu and Tomas.

Finally, thanks to my family. For everything

.

Index

Abstract

This thesis is focused on the development and evaluation of different hybrid scaffolds for the treatment of injuries in cartilage or bone. These hybrid materials were three-dimensional polycaprolactone macroporous scaffolds obtained through freeze extraction and particle leaching combined method and modified with hyaluronic acid or mineral particles. In order to facilitate the description of the obtained results, the thesis is divided in two sections dedicated to bone and cartilage tissue engineering respectively.

In the case of bone tissue engineering we addressed the treatment of disorders associated with the spine that require spinal immobilization. This Thesis proposes the development of a synthetic macroporous support for intervertebral fusion as an alternative to commercial bone substitutes. Macroporous scaffolds were developed with bare polycaprolactone or its blends with polylactic acid in order to increase its mechanical properties and degradation rate. Furthermore, the scaffolds obtained were reinforced with hydroxyapatite or Bioglass®45S5 to improve their mechanical properties and turn them in bioactive scaffolds. The supports were characterized physicochemically and biologically to determine if they met the requirements of the project. Finally, materials were tested *in vivo* in a bone critical size defect preformed in a rabbit model against a commercial support.

Cartilage engineering has been extensively studied in the last years due to the inherent limited self repair ability of this tissue. The second part of the thesis was focused in developing a construct composed by *in vitro* differentiated chondrocyte like cells in a hybrid scaffold for cartilage tissue engineering. Polycaprolactone hybrid substrates coated with hyaluronic acid scaffold were developed obtaining a substrate with positive influence over the development of chondrocyte phenotype in

culture and able to protect the cells from excessive mechanical loading in the joint. Cell-scaffolds constructs were obtained combining hybrid scaffolds with mesenchymal stem cells and differentiating them to chondrocytes using chondrogenic culture medium combined with hypoxia, mechanical stimulus or co-culture. Finally the cellularized scaffolds were mechanically, biochemically and histologically characterized to determine the production of extracellular matrix and expression of chondrogenic markers.

Resumen

La presente tesis se centró en el desarrollo y evaluación de diversos soportes tridimensionales híbridos para el tratamiento de las lesiones de cartílago o hueso. Dichos materiales híbridos eran soportes tridimensionales macroporosos de prolicaprolactona obtenidos por el método combinado de *freeze extraction* y *particle leeaching* posteriormente modificados con ácido hialurónico o partículas minerales. Para facilitar la compresión de los resultados obtenidos la tesis se estructura en dos secciones dedicadas a ingeniería tisular de hueso y de cartílago respectivamente.

La ingeniería tisular ósea abarca distintas patologías, tales como determinados desordenes asociados con la columna vertebral que requieren de la inmovilización de esta mediante la fusión de vertebras. En esta tesis proponemos el desarrollo de un soporte macroporoso sintético para fusión intervertebral como alternativa a los sustitutos óseos comerciales. Se diseñaron soportes macroporosos de policaprolactona pura o mezclada con ácido poliláctico para incrementar las propiedades mecánicas del constructo y su velocidad de degradación. Por otro lado los andamios obtenidos fueron reforzados adicionalmente con hydroxyapatita o Bioglass®45S5 a fin de mejorar sus propiedades mecánicas y dotarlos de bioactividad. Los soportes fueron caracterizados fisicoquímicamente y biológicamente para determinar si cumplían los requisitos del proyecto. Finalmente los materiales fueron testados *in vivo* en un modelo de defecto óseo de tamaño crítico realizado en conejo frente a un soporte comercial.

El cartílago ha sido ampliamente estudiado debido a la escasa capacidad del cartílago para autorrepararse. El segundo bloque de la tesis se centró en el desarrollo de un constructo formado por células diferenciadas *in vitro* a condrocito en un soporte híbrido para ingeniería tisular. Se desarrollaron soportes híbridos de policaprolactona recubiertos con ácido hialurónico obteniendo así un andamio

celular con una influencia positiva sobre el fenotipo celular y capaz de proteger las células de cargas mecánicas excesivas de la articulación. Se prepararon constructos de células mesenquimales en *scaffolds* y diferenciaron a condrocitos mediante el uso de medio de cultivo condrogénico combinado con el uso de hipoxia, estímulo mecánico o cocultivo. Finalmente los constructos fueron caracterizados mecánicamente, bioquímicamente e histológicamente a fin de estudiar la producción de matriz extracelular y la expresión de marcadores fenotípicos correctos.

Resum

La present tesi es centrà en el desenvolupament i avaluació de diversos suports tridimensionals híbrids per al tractament de les lesions de cartílag i ós. Aquestos materials híbrids són suports tridimensionals macroporosos de prolicaprolactona obtinguts pel mètode combinat de *freeze extraction* i *particle leeaching* posteriorment modificats amb àcid hialurònic o partícules minerals. Per facilitar la comprensió dels resultats obtinguts la tesi s'estructura en dues seccions dedicades a l'enginyeria tissular d'ós i cartílag respectivament.

L'enginyeria tissular òssia abasta diferents patologies tal com determinats desordres associats amb la columna vertebral que requereixen de la immobilització d'aquesta mitjançant la fusió de vertebres. En aquesta tesi proposem el desenvolupament d'un suport macroporós sintètic per fusió intervertebral en lloc dels substituts ossis comercials. Amb aquesta finalitat es van dissenyar suports macroporosos de policaprolactona pura o barrejada amb àcid polilàctic per incrementar les propietats mecàniques del constructe i la seva velocitat de degradació. D'altra banda suports macroporosos obtinguts addicionalment es varen reforçar amb hydroxyapatita o Bioglass® per tal de millorar les seves propietats mecàniques i dotar-los de bioactivitat. Els suports van ser caracteritzats fisicoquímicament i biològicament per determinar si acomplien amb els requisits del projecte. Finalment els materials van ser testats *in vivo* en un model de defecte ossi de mida crítica en conill comparant-lo amb un suport comercial.

El cartílag a sigut àmpliament estudiat a causa de l'escassa capacitat del cartílag per regenerar-se. El segon bloc de la tesi es va centrar en el desenvolupament d'un constructe format per cèl·lules diferenciades *in vitro* a condròcit en un suport híbrid per enginyeria tissular. Es van desenvolupar suports híbrids de policaprolactona recoberts amb àcid hialurònic obtenint així un *scaffold* amb una influència positiva

sobre el fenotip cel·lular i que protegeix les cèl·lules de les càrregues mecàniques excessives de l'articulació. Es varen preparar constructes de cèl·lules mesenquimals en *scaffolds* i es van diferenciar a condròcits mitjançant l'ús de medi de cultiu condrogènic combinat amb l'ús d'hipòxia, estímul mecànic i cocultiu. Finalment els constructes formats per un *scaffold* amb cèl·lules van ser caracteritzats mecànicament, bioquímicament e histològicament a fi d'estudiar la producció de matriu extracel·lular y la expressió dels marcadors fenotípics correctes.

.

General objective and specific purposes

General objective

The aim of this thesis is the development of three-dimensional scaffolding systems for bone and cartilage regeneration. Bone regeneration supports were developed having in mind their application as bioactive spinal fusion strips (although they can find application in other bone diseases) while cell/scaffold constructs were developed for articular cartilage tissue engineering.

Specific purposes

- To produce polycaprolactone and polycaprolactone/polylactic acid blend macroporous scaffolds by freeze extraction and particle leaching in order to obtain a bimodal porosity composed by interconnected macropores whose pore walls are in turn microporous.
- For the synthetic spinal fusion strips these scaffolds were combined with mineral coating or containing particles to favour bone anchorage. Morphologic and physical properties will be characterized while biological response will be assessed by *in vitro* culture. Samples of optimized composition were produced for an *in vivo* study performed at the Instituto of Biomecánica de Valencia
- Supports for cartilage engineering will be based on PCL scaffolds whose pore walls were coated with hyaluronic acid. Different approaches to produce this coating will be tested. Cell-scaffold constructs will be produced by seeding the scaffolds with mature chondrocytes or mesenchymal stem cells and culturing them in chondrogenic conditions. The effect of hypoxia, mechanical stimulation and co-culture of chondrocytes and MSCs will be assessed.

1. INTRODUCTION

1. Introduction

1.1. Connective tissue: Bone and cartilage

Connective tissue is derived from embryonic mesoderm and is commonly formed by few cells immersed in a huge amount of extracellular matrix (ECM), composed principally by fibrillar proteins and the ground substance (adhesion proteins, proteoglycans and interstitial fluid). Connective tissues are widely distributed along the body and consist of a huge variety of specialized structures and cell types that provide binding, support, protection and insulation to other tissues.[1] Connective tissue types are embryonic connective tissue, adult connective tissue and special connective tissue. Embryonic connective tissue is developed during early embryonic stages and found mainly in the umbilical cord. Adult connective tissue is comprised of both loose and dense connective tissue; which are differentiated on the cell/ECM ratio.[2] Loose connective tissue shows a high cell/collagen ratio and provides support and insulation while dense connective tissue shows a low cell/collagen ratio and provides flexible and strong connections between tissues.[2,3] On the other hand, the so-called special connective tissues are tissues with a unique extracellular matrix structure, cell type and functions which are not found in the other connective tissues.[2,3] Special connective tissues includes four types, which are hematopoietic tissue, adipose tissue, bone and cartilage.[2] The present thesis is focused on bone and cartilage connective tissues.

1.1.1. Bone

Bone is a highly vascularized and mineralized tissue with a dual structure: cortical and cancellous bone. Bone is a natural composite consisting of mineral crystals

(70% of dry weight) and an organic phase (30% of dry weight)[4]. The combination of mineral crystals and collagen results in a tissue with outstanding mechanical properties.[5] The mechanical properties of the composite are adapted to their load-bearing function much better than the separated components since collagen provides toughness that compensates hydroxyapatite brittle fracture while mineral phase provides the hardness and the rigidity which bare collagen is lacking.

Cortical bone shows the highest mechanical properties and is a dense and slightly porous tissue composed by osteons that are concentric extracellular matrix lamellae surrounding the Haversian canal which is, itself, crossed by a blood vessel[4,6,7] as shown in **figure 1-1**. On the other hand cancellous bone is a highly porous structure (75-95%) localized between the diaphysis and the bone end in long bones as shown in **figure 1-2** and filling short and flat bones.[4,6-8] Cancellous bone is organized in trabeculae or spicules showing lower mechanical properties than cortical bone.[4,6,8,9]

Figure 1-1. Cortical bone osteon structure diagram [6]. [Ross MH and Pawlina W: Histology: A Text and Atlas 6th edition. Lippincott WIlliams & Wilkins, 2011]

Figure 1-2. Long bone structural organization.[6] [Ross MH and Pawlina W: Histology: A Text and Atlas 6th edition. Lippincott WIlliams & Wilkins, 2011]

Bone cells are called osteoblasts (osteocytes) and osteoclasts, they regulate bone homeostasis, which is a highly dynamic process of tissue remodelling. [10] Osteoblasts are non-migratory cells derived from mesenchymal stem cells (MSC), which show different behaviours and characteristics along their maturation steps. Active osteoblast is a mononucleated cell found in the osteoid (non-mineralized extracellular matrix region) that shows a high alkaline phosphatase expression. Osteoblast secretes collagen type I and non-collagenous proteins to form the extracellular matrix, cytokines and growth factors which regulate the osteoid and mineralization as final step. Once osteoid is mineralized and the osteoblast is surrounded with mineralized extracellular matrix, it is called osteocyte and remains quiescent, although still playing a role in the regulation of bone homeostasis.[10] On the other hand osteoclast is a cell type derived from hematopoietic stem cells that

regulates bone resorption through the acidification of mineralized extracellular matrix and the enzymatic degradation of ECM proteins. Osteoclast attaches to the mineralized matrix and acidify the zone using a carbonic anhydrase that dissolves the bone mineral.[10]

As shown in **figure 1-1**, cells are distributed among the extracellular matrix, a complex macromolecular network composed of highly mineralized collagen fibres which allows cell anchorage and structural support.

Protean extracellular matrix is composed by collagen type I and non-collagenous proteins. Collagen type I is formed by three polypeptide, composed by glycine, proline and hydroxyproline, associated in helix conformation. Collagen is assembled staggered in parallel with the unit ends separated by gaps of 40nm with an overlap of 27nm constituting a 67nm zone called "hole zone". Hydroxyapatite crystals nucleate in this space, but its growth is limited due to the gap size.[4] On the other hand non collagenous proteins are a diverse pool of proteins, like bone sialoprotein, osteopontin, osteonectin and osteocalcin, which represent just a 10% of bone ECM proteins. Non-collagenous protein functions are not entirely understood, but it is known that they affect hydroxyapatite crystal nucleation and growth, cell signalization and ion homeostasis.[4]

Mineral phase is composed by hydroxyapatite crystals that nucleate and grow inside the hole zone, a gap between collagen fibres. Hydroxyapatite formation is regulated by proteins that generate a dynamic equilibrium between the bone remodelling and the mineral needs of the organism.[4] Hydroxyapatite found in bones is similar to geological hydroxyapatite ($Ca_5(PO_4)_3(OH)$) but with a lower Ca/P molar ratio than 1.67 for stoichiometric hydroxyapatite. Comparing with geological apatite crystal, biological apatite is smaller and show differences in chemical composition such as

several ionic substitutions (presence of carbonate, magnesium, etc) associated with calcium or hydroxyl deficiencies that disrupt the crystalline network.[4,11]

1.1.2. Cartilage

Cartilage is an avascular and aneural connective tissue composed by chondrocytes dispersed in an extracellular matrix composed by proteoglycans and collagen.[12] Three types of cartilage tissues can be distinguished: fibrocartilage, elastic and hyaline cartilage that are classified by its appearance, mechanical properties and extracellular matrix characteristics.[6] Fibrocartilage is present on intervertebral discs and insertion points of bone with ligament or tendons. This cartilage is structured in chondrocytes surrounded by a small amount of cartilaginous matrix composed by collagen type I parallel fibre groups with lack amorphous matrix rich in chondroitin sulphate and dermatan sulphate surrounding the chondrocytes. Elastic cartilage is present on ear canal, epiglottis and larynx and compared to hyaline cartilage shows less extracellular matrix. The ground substance is composed mainly by elastic fibres highly ramified.[12]

On the other hand hyaline cartilage is a tissue with a highly complex and specialized structure, localized mainly on bone surface joints. It is a tissue with a low cellularity (3-5% of wet weight) with a highly hydrated extracellular matrix composed by collagen (mainly collagen type II) and proteoglycans.[6] As shown in **figure 1-3**, four different zones compose hyaline cartilage structure with differences in the distribution and composition of their extracellular matrix. From cartilage surface to bone they are: Superficial, intermediate, deep zone and calcified zone. Superficial zone is the thinnest zone of hyaline cartilage, it is composed by two layers rich in collagen, fibronectin and water. This structure adds resistance to shear stress at the

articular joint but it is important as well sustaining compressive strength. The upper layer of this zone is a collagen acellular sheet that covers the joint while the bottom one is composed by flattened chondrocytes immersed in a collagen matrix with fibres oriented parallel to the articular joint surface. The intermediate zone is composed by spherical chondrocytes that show synthetic organelles surrounded by an ECM with fibrils obliquely or randomly oriented with respect to superficial zone. Extracellular matrix shows a higher content of proteoglycans but lesser collagen and water content. The deep zone is the thickest part of the cartilage, and it is composed by highly biosynthetic round chondrocytes aligned in columns. Finally the calcified zone is the closest zone to subchondral bone and is composed by small round chondrocytes with low metabolic activity and surrounded by calcified extracellular matrix. [6,13]

Figure 1-3. Hyaline cartilage structure diagram (a) and histology (b)[6] [Ross MH and Pawlina W: Histology: A Text and Atlas 6th edition. Lippincott WIlliams & Wilkins, 2011]

Cartilage cellular population is composed exclusively by chondrocytes that derive from mesenchymal stem cells and are isolated in ECM structures called lacunae. These structures vary in shape and orientation along with cartilage deepness, but cells adapt to the lacunae shape independently of this.[12,13] Furthermore, cellular membrane presents cilia that penetrate the extracellular matrix in some chondrocytes and are suspected to act as mechanical signal sensors.[13] Finally chondrocytes shows two different subpopulations inside the hyaline cartilage tissue: mature chondrocytes and hypertrophic chondrocytes.[13] Mature chondrocytes are not able to proliferate and occupy the main part of the tissue, where they secrete collagen and other macromolecules to maintain hyaline cartilage homeostasis. On the other hand hypertrophic chondrocytes are the final chondrocyte development stage and occupy the calcified zone near to bone. [12,13]

Cartilage ECM is composed by collagen and glycosaminoglycans distributed so as to resist mechanical loading. Collagen fibril network provides tensile and shear strength while glycosaminoglycans fill the interstices, as a water-retaining gel, absorbing shock compression forces and providing the joint with non adherent surface.[12,13] Collagen is the most abundant protein in hyaline cartilage ECM and collagen type II is the most representative collagenous protein (80% of total collagen).[6] Cartilage type II forms fibres of 15 to 45 nm of diameter that, in association with other collagen types, form a mesh that entraps other molecules.[12,13] The remaining amount of collagen is composed by collagen types VI, IX, X and XI. Collagen type IX and XI are associated to collagen type II and stabilize it. Collagen type IX participates in the interaction between proteoglycans and collagen type II mesh. Collagen type XI regulates collagen type II fibril size.[6,12,13] Collagen type X is present only in calcified zones and organizes collagen fibrils in hexagonal lattices that contribute to bone mineralization.[6] The other principal component of hyaline cartilage extracellular matrix are the

proteoglycans. Proteoglycans composition is a 5% of protein and a 95% of unbranched polysaccharides.[13] Proteoglycans are one of largest molecules produced by cells with molecular weights that can reach 3.5 x 10^6 Dalton; they are composed by a core protein of 200 to 300 nm length with glycosaminoglycans attached to it.[12] Glycosaminoglycans attached to core protein are linear polysaccharides composed by disaccharide monomers (an amino sugar and another monosaccharide) with a carboxylate or sulfate groups. The main glycosaminoglycans present in hyaline cartilage are hyaluronic acid, chondroitin sulfate, dermatan sulfate, keratan sulfate and heparan sulfate.[13] Proteoglycans *in vivo* are commonly bound to a hyaluronic acid molecule constituting a huge molecule that is trapped by the collagen fibre network filling the intrafibrillary space and retaining water as a hydrogel.[12]

1.2. Regenerative capacity of bone and cartilage.

1.2.1. Bone healing

Bone shows a high regeneration capacity that generally grants a complete bone fracture healing without external intervention. Fracture healing is a complex process regulated by cells and the huge amount of biological molecules that they secrete.[14] Fracture healing is divided in two types: direct and indirect fracture healing. Direct fracture healing requires that bone ends do not show any gap and a stable fixation. This process is characterized by presenting only intramembranous bone healing. On the other hand, the most typical process is indirect fracture healing that show intramembranous and endochondral bone healing.[15] Indirect fracture healing start after trauma when bone fracture is covered with a hematoma produced by blood flowing from bone marrow and peripheral blood vessels. Cells start secreting tumor necrosis factor-α and diverse interleukins which regulate the inflammatory response

by recruiting inflammatory cells and promoting angiogenesis.[15] After hematoma formation the callus formation between the fracture ends helps to stabilize the structure.[14,15] Mesenchymal stem cells recruitment is fundamental in this step.[15] Mesenchymal stem cells are a population of stromal cells with low presence in bone marrow (less than 0.01%) that show a high self-renewal capacity and are able to differentiate into different cell types, including osteocyte and chondrocyte lineage.[16,17] MSCs are recruited from bone marrow, surrounding soft tissues and peripheral blood and attracted to the hematoma due to chemotactic signals like cell-derived factor-1 and bone morphogenetic proteins such as BMP-7.[15] Once MSCs migrate towards the hematoma they start secreting signalling molecules and an extracellular matrix containing collagen type I and II, that start forming the callus tissue.[15] Blood supply is essential for bone regeneration,[14,15] thus angiogenesis promotion during endochondral fracture healing is combined with chondrocyte apoptosis and matrix degradation to allow enough space to the growth of new blood vessels. Callus tissue becomes mineralized and cartilage callus tissue is substituted by bone tissue[15] while mesenchymal stem cells differentiate to osteoblasts. Cell differentiation is regulated by biologic signals like bone morphogenetic proteins[14,18,19] and physical signals such as mechanical stimulus[20]. Finally bone remodelling starts as a lamellar bone deposition and mineralized callus resorption to rebuild the functional bone structure.[15] On the other hand in some clinical cases like those which imply bone filling, pathological bone loss, fracture nonunion or in spinal fusion need be improved[21,22] and bone grafting is a well-recognised strategy[21]. Bone autograft have a important role in orthopaedic surgery because is biocompatible, osteogenic, osteoinductive and osteoconductive.[21] Nevertheless, autologous tissue availability is limited and bone graft surgery shows postoperative pain and morbidity.[21] Allogenic bone graft is an alternative when extensive grafting is required.[21] Bone allografts are used frozen or freeze-dried but rarely fresh due to the risk of disease transmission and host

rejection.[21] On the other hand tissue preparation and sterilization minimize the immune response and disease risk transmission but also affect the graft properties.[21]

1.2.2. Cartilage healing

Cartilage shows very little self-repair ability.[13] Cartilage injuries are catalogued in three types: matrix disruption, partial thickness defect and full thickness defect. [13] Matrix disruption occurs when extracellular matrix damage is not excessive. Traumatized tissue is restored through the surrounding chondrocytes which increase their biosynthetic activity to repair the matrix.[13] Partial thickness defects are fissures or some other kind of visible tissue disruption that do not reach the subchondral bone. Cells adjacent to the injury start proliferating and increasing the ECM production, but for unknown reasons this process usually stops before the injure is repaired.[13,23] In full thickness defect the injury reaches the subchondral bone and induces bleeding, thereby filling the injury with a fibrin clot. Due to this characteristic, full-thickness defect is able to recruit mesenchymal stem cells in contrast to previous cartilage injury types and fill the defect with a tissue intermediate between hyaline cartilage and fibrocartilage.[13,23,24] The lack of self repair ability compared to bone tissue can be explained by three features: 1) chondrocytes do not proliferate and have a low metabolic activity; 2) Cartilage extracellular matrix may impede chondrocyte migration and cell adhesion; 3)mesenchymal stem cells are only recruited when subchondral bone is damaged.[13] Classical therapeutic solutions for repairing damaged cartilage are two: tissue transplantation and induction of spontaneous regeneration.[13,23,25] The tissue transplantation intends to fill the cartilage defect with a tissue graft that can be osteochondral plugs, periosteal and perichondrial grafts.[13,24,25] Osteochondral

plugs transplantation (autologous or allogenic) allows filling the cartilage defect to substitute damaged cartilage but does not induce tissue regeneration.[13,24,25] Autologous grafts are extracted from non-load bearing cartilage areas and are used to fill small cartilage defects. On the other hand allogenic grafts are used in large defects[24] but this procedure showed the typical drawbacks associated to allografts, such as host reject immunoreaction and disease risk transmission. [13,25] Immunogenic response can be reduced by freezing the graft, thereby increasing the graft shelf-life and allowing a disease screening prior to implantation, but at the same time, it comes with a reduction of tissue viability.[13] The other tissue grafts options are periosteal and perichondrial grafts, that have been used in humans to repair cartilage defects. This technique solves the problem of donor morbidity site of autologous osteochondral plugs but 70% of perichondrial grafts fails after five years due to graft ossification.[13] On the other hand, induction of spontaneous regeneration consists in stimulating the regeneration, giving access to bone marrow MSCs to invade the defect and regenerate it like in natural full-thickness defect healing.[13,25] Subchondral bone penetration is performed by abrasion, drilling or microfracture that induces fibrin clot formation thus serving as scaffold for mesenchymal stem cell migration and differentiation.[13,25] Microfracture is many times the preferred option since it can be performed arthroscopically and only generates a minimal iatrogenic tissue damage.[25] On the other hand regenerated tissue varies from fibrocartilage to hyaline cartilage, but even regenerated hyaline cartilage formed by this technique shows worse mechanical properties and durability compared to healthy tissue.[13]

1.3. Cell free and cell based approaches in cartilage and bone tissue engineering

Tissue engineering is a promising alternative based on the use of engineering and biological sciences to understand the relationship between structure and function of mammalian tissues to design substitutes that restore and support the tissue functions.[26] Tissue engineering tries to mimic the tissues using scaffolds as extracellular matrix, expanded cells obtained from a donor and adding growth factors.[26, 27] Main tissue engineering approaches are two: (1) using acellular scaffolds that should be invaded by surrounding host tissue or (2) implanting cell-scaffold constructs. One of the key factors in both approaches is the scaffold that is a three-dimensional porous structure fabricated with synthetic or natural based biomaterials. It plays the role of a synthetic extracellular matrix allowing cell colonization, migration, proliferation and differentiation.[26] Cell free scaffold implantation has the objective to induce cell invasion by providing migration paths, but also to guide the organization of new-formed extracellular matrix. On the other hand cell-scaffold construct are based on cell seeded scaffolds that have been cultured *in vitro* to induce cell proliferation (even cell differentiation) and ECM deposition prior to implantation.

Both approaches have also been proposed in bone tissue engineering [28].Viability of transplanted cells in bone defects depends of local blood supply, as 150-200µm is the maximum distance from blood vessel where optimally effective nutrient diffusion takes places;[29] cell death is observed when cells are too far away from blood supply. This points to that seeded scaffold implantation as not the best choice if the construct is not pre-vascularized *in vitro* through co-culture with endothelial cells[30]. Acellular osteoconductive scaffold implantation may induce mesenchymal stem cell migration from bone marrow and posterior differentiation working as a guide to bone fracture healing process.[31,32] Thereby the scaffold properties such

as biocompatibility, biodegradation rate, pore size, pore interconnectivity, volume porosity, mechanical behaviour and surface topography and chemistry are essential to achieve a successful tissue regeneration.[33] Among other factors, those properties determine not only MSCs adhesion and osteoblastic differentiation inside the scaffold, but also angiogenesis inducing the growth of a network of blood vessels inside the pore structure simultaneously to the formation of new bone tissue. Scaffold must have a pore size between to 200-400 μm, enough to leave space to osteon formation (223μm of size in humans)[28] that defines the Haversian canal (50-70μm of diameter) that contains the capillary.[34] On the other hand angiogenesis promotion can be improved using scaffolds that release angiogenic factors such as vascular endothelial growth factor or grafting the scaffold surface with proangiogenic peptide like Ser-Val-Val-Tyr-Gly-Leu-Arg derived from osteopontin or promote selectively human endothelial cell adhesion with Arg-Glu-Asp-Val sequence from fibronectin.[30] Other important feature in bone tissue engineering is bioactivity, the ability of the material to bond to bone tissue[35] that can be predicted *in vitro* through the formation of an apatite layer over the scaffold when it is immersed in simulated body fluid.[36,37] Bioactivity can be improved with the addition of bioactive particles in the scaffold materials or by surface modifications[36,38].

In cartilage tissue engineering, cell-free scaffold implantation[39-44] and cell-scaffold construct[45-49] approaches have been proposed. Acellular scaffold implantation serves as an improvement of cartilage regeneration induction therapies based on subchondral bleeding[50]. The scaffold fills the defect overcoming the critical-size limit for spontaneous healing because the pores are filled with blood and bone marrow derivates that form a fibrin clot and allow the MSC attachment[50] guiding spontaneous cartilage healing; the scaffold also provides a mechanical support to the regenerating tissue. On the other hand, scaffolds can be seeded with

chondrogenic cells and cultured *in vitro* to induce cell proliferation, ECM deposition and differentiation prior to the implantation. Present option allows the graft manipulation at three levels: scaffolds, cells and construct assembly procedure.[51] To develop a cell/scaffold construct, the first step is the cell population isolation and *in vitro* expansion to reach the required cell numbers to seed the scaffold.[51] In cartilage tissue engineering research adult autologous chondrocytes or mesenchymal stem cells are currently used[52] previously expanded *ex vivo* in monolayer. Mature chondrocytes isolated from hyaline cartilage have been considered a logical option.[53] However, chondrocytes expanded in monolayer cultures dedifferentiate[13,53-56] losing the typical chondrocyte phenotype.[13,52] The huge number of cells required for this approach is limited because an extensive number of passages induces cell dedifferentiation[55,57] and chondrocyte isolation is limited by tissue rareness and donor zone morbidity[52,53,58]. On the other hand MSCs are considered an interesting option due to the availability, high expansion capacity *in vitro* and their ability to differentiate to chondrocytes.[53] These characteristics allow two different tissue engineering approaches based on mesenchymal stem cells: to differentiate them to chondrocytes *in vitro* inside the scaffold and implant the construct when cells show the correct phenotype markers or seeding the scaffold with MSCs and implant it in the host body to allow the neighbour tissues inducing cell differentiation *in vivo*.[59] Drawbacks of MSCs imply phenotypic instability[60,61] and it has been pointed that *in vivo* environment is not enough to drive a correct chondrogenic differentiation of implanted uncommitted MSC[62].

Scaffolds are fabricated with biomaterials, which are materials able to interact with the biologic systems and replace the tissue.[63] Biomaterials commonly used in bone and cartilage tissue engineering are biodegradable polymers that can be synthetic or of natural origin.[9,35] Natural polymers are proteins or polysaccharides that present adhesion motives and are biocompatible. Natural-based polymers

present problems of purification, they can transmit diseases [63] and their processing to produce scaffolds with predesigned pore architectures is quite limited. On the other hand, synthetic polymers resolve most of natural polymer drawbacks but do not present biological cues as natural origin polymers[35,64]. Synthetic polymers are produced from simple monomers with known structure, with a high impurities control showing reproducible and predictable properties[9,22,35] and are compatible with a variety of processing technologies that have been developed to produce sponges with a variety of pore architectures.[35,65]

1.3.1. Bone tissue engineering cell-free approach: Biomaterials and mineral composite scaffolds.

Biodegradable synthetic polymers are a huge group of biomaterials with different properties. This work is focused on saturated aliphatic polyesters. Polyesters are polymers widely used in tissue engineering research and approved by the Food and Drug Administration of United States for many medical applications.[9] The most important polyesters are polylactic acid, polyglycolic acid and polycaprolactone.[9,22] Aliphatic polyesters have a common basic chemical structure that show a similar degradation mechanism, the hydrolysis of ester bonds and weight loss through oligomers diffusion. Finally the short chains are degraded to monomeric subunits that are metabolized or excreted.[9,22]

Polycaprolactone (PCL) is a semicrystalline polyester with a low melting point (58ºC)[9,22] synthesized by the ε-caprolactone monomer ring aperture and polymerization[22] (Chemical structure showed on **figure 1-4**). Polycaprolactone is a non-toxic polymer approved for medical applications by the Food and Drugs

Administration [35] and a widely used polymer in bone[66-71] and cartilage[39,48] tissue engineering.

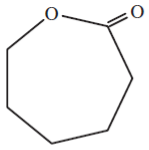

Caprolactone

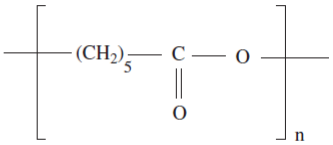

Poly(caprolactone)

Figure 1-4. Chemical structure of cyclic caprolactone and polycaprolactone[63] [Reprinted from Progress in Polymer Science, 32, Nair LS, Laurencin CT. Biodegradable polymers as biomaterials, 762-798, ©2007, with permission from Elsevier]

Polycaprolactone is a flexible polymer as its glass transition point is at -60ºC[63] thus at body temperature the amorphous phase is in rubbery state. Young modulus (0.4 GPa) are in range with the modulus for cancellous bone.[22] On the other hand the ester bonds make it degradable in presence of water by hydrolysis but its degradation speed is lower than polylactic acid.[9,22] Finally polycaprolactone is a polymer soluble in a huge variety of organic solvents[22]. All these characteristics allow producing polycaprolactone scaffolds with a wide range of fabrication protocols.[22]

Polylactic acid is a polymer widely used in tissue engineering composed by a monomeric unit that is a chiral compound that shows two optical isomers D and L-lactic.[22,63] The polymer synthesis happens through ring opening polymerization of cyclic lactic acid dimer[22], chemical structure of Polylactic acid is shown in **figure 1-5**.

Figure 1-5. Chemical structure of cyclic lactide and polylactide[63] [Reprinted from Progress in Polymer Science, 32, Nair LS, Laurencin CT. Biodegradable polymers as biomaterials, 762-798, ©2007, with permission from Elsevier]

The poly-L-lactic acid (PLLA) is a semicrystalline polymer with high mechanical properties (young modulus of 2.7 GPa) quite similar to cortical bone.[22] The mechanical properties of polylactic acid are higher than those of polycaprolactone due to the higher glass transition temperature of the amorphous phase, 60-65ºC, that makes it to be in the glassy state at body temperature.[9] The degradation is consequence of ester bond hydrolysis and its degradation is faster than that of polycaprolactone due to a higher density of ester groups in the main polymer chain. It is worth noting that hydrolysis of polylactic acid release lactic acid that is a cell metabolizable non toxic chemical[9,22]. On the other hand, lactic acid reduces the pH acting as a catalyser of the degradation reaction.[9,22] Finally polylactic acid like polycaprolactone is soluble in various organic solvents[22] and compatible with diverse scaffold fabrication protocols.

Synthetic polymer scaffolds for bone tissue engineering have downsides. Saturated aliphatic polyesters are hydrophobic thus impairing cell invasion[35], they show a lack of bioactivity that inhibits bone tissue integration due to a deficient surface mineralization[9] and they do not show biological cues[35].To solve these limitations hybrid or composite scaffolds are developed to try to mimic the bone tissue composite nature that is composed by collagen type I mineralized with nanometric hydroxyapatite crystals. Composite material is a mixture of two (or more) different materials that show the better properties of both components.[9]

Polymer/ceramic composites showed improvement of mechanical properties[72-74], protein adsorption [75,76] and subsequently the cell adhesion on polymer scaffolds with respect to any of its components. Polymer phase provides the formability while the ceramic provides the composite with higher mechanical properties, as well as bioactivity[9] and hydrophilicity[77]. Finally composites show particular surface properties compared to naked polymer scaffold that can affect cell behaviour. Since polymeric scaffolds do not show biological motives, cell-material interaction is mediated by proteins adsorbed from serum or biologic fluid (blood, synovial fluid, etc). The amount and conformation of adsorbed proteins is determined in large extent by surface chemistry or surface energy.[78] In this way changes on substrate stiffness, or chemistry can affect the fate of mesenchymal stem cells cultured on it.[79,80] The two main strategies to develop a polymeric composite scaffold are the biomineralization to coat the pore walls with a mineral layer and mixing the polymer with mineral particles before the sample fabrication[9,81].

Biomineralization is a surface modification to coat the implant with a hydroxyapatite layer.[81] Diverse methods are used to mineralize polymer scaffolds but the easiest and most common is the immersion in simulated body fluid to precipitate calcium phosphate over the polymeric scaffold (natural or synthetic) in aqueous solution.[81] This technique has two important advantages over the other techniques. Simulated body fluid allows a complete and uniform surface coating with a mineral layer almost identical in composition and structure to the mineral bone phase.[81] On the other hand coating conditions are not toxic and do not need to expose the scaffold to high temperature or pressure.[81] The technique consists in the immersion of the sample in simulated body fluid that is an aqueous solution with ions concentration similar to that of human plasma.[81] Anionic chemical groups like carboxyl or hydroxyl present on sample surface attract and lead to the adsorption of calcium ions at the surface when it is immersed in simulated body

fluid.[81,82] Later calcium cations abundance leads in turn to attraction and adsorption of phosphate anions and the cycle repeats itself leading to the growth of a phosphate calcium coating. On the other hand the success of this method depends of surface scaffold properties that could not promote enough hydroxyapatite deposition.[81] To resolve this drawback, scaffold surfaces are modified to improve hydroxyapatite deposition.[81] An easy option is to increase the number of anionic functional groups such as carboxyl or hydroxyl moieties on the scaffold surface; this can be easily done by plasma treatment or chemical degradation. [38,81,82] Plasma treatment is based on plasma reaction with polymer surface.[83] Plasma contains ions, electrons and free radicals which react with polymer,[82] affecting only the surface (10nm or less) without modifying the bulk properties.[82,83] Oxygen and air plasma increase the presence of oxygen containing chemical groups.[82,83] Hydrophilicity and mineral layer deposition have been increased after polymer substrate exposure to plasma.[36,38,82] On the other hand, in the case of polyesters, a chemical degradation can increase the presence of carboxyl groups that are related with apatite nucleation initiation.[81,82] Hydrolysis is usually performed with sodium hydroxide that cleaves the ester bonds thereby eroding the polymer, which increases the roughness and the presence of carboxyl group that has been related to an increased mineralization.[81,82]

Composite scaffold fabrication by mineral particle addition is achieved by fabricating scaffolds with a mixture of mineral particles with polymer solution[9] or polymer melt[84]. The addition of particles to the polymer matrix can reinforce mechanically the scaffold and improve scaffold hydrophilicity.[9,77] The degradation kinetics of the polymer phase is altered too, due to the changes in equilibrium water content and water transport properties in the composites; besides, mineral phase may buffer the polymer acidic degradation residues thus limiting autocatalysis.[9] Finally the presence of bioactive particles improves the

biomineralization (described above)[38] and the obtained hydroxyapatite layer is chemically and structurally equivalent to bone mineral phase and works as a bonding interface with tissues.[9,81] Not only the presence of particles is important, the different bioactive particles have different properties and can affect the composite final properties. Among all the possible reinforcements, (hydroxyapatites, bioactive glasses, tricalcium phosphate, bicalcium phosphate, calcium sulphate, calcium silicide, etc.) in this work hydroxyapatite and Bioglass®45S5 particles, widely described in the literature [66-68,70,85-88], have been studied.

Hydroxyapatite (HAp) is widely used in bone tissue engineering as it promotes a faster bone regeneration and bonding to the neighbouring tissue without intermediary tissue[89]. Polycaprolactone composites reinforced with hydroxyapatite [67,68] for bone tissue engineering have been described in literature. Biological response of these composites was improved, compared to naked polymer scaffold [68].

Bioglass® 45S5 (BG) (45% SiO_2, 24.54% Na_2O, 24.4% CaO y 6% P_2O_5) is a bioactive glass that shows good biocompatibility and osseous integration[9] and do not show cytotoxicity[90]. Bone bonding is achieved through the development of a calcium deficient carbonate phosphate layer over the surface in presence of biological fluid that allows the chemical bonding to the bone.[9] Another important feature of bioactive glasses is the release of soluble ionics compounds that alter the osteoblast gene expression profile of genes related with bone homeostasis and cell metabolism (extracellular matrix remodelling, cell-cell adhesion and cell-matrix adhesion).[91] Composite scaffolds that use bioactive glasses like Bioglass®45S5 as ceramic reinforcement showed an increase in mechanical properties [88].

1.3.2. Cartilage tissue engineering cell-scaffold construct approach: Polymer/hydrogel scaffolds and cells.

Scaffolds for cell-scaffold construct must define the space for the engineered tissue to guide the restructuring and allow oxygen and nutrients diffusion.[51] On the other hand, scaffolds should show structural integrity and transmit the mechanical forces[51]to create the adequate biomechanical environment for the cells lodged in the pores. Scaffolds and hydrogels are used for cell transplantation in cartilage tissue engineering.[46-49] Hydrogel research for cartilage tissue engineering has increased in the last years[92] due to hydrogels seem the most logical option in order to mimic the natural environment of hyaline cartilage matrix[92,93] to allow the chondrogenic differentiation. Hydrogels are three-dimensional networks of crosslinked hydrophilic polymers (natural or synthetic) able to retain huge amount of water.[53,92-94] Many hydrogels present adequate biocompatibility, biodegradability and proper nutrients and waste residues diffusion due to the pores and the water retained.[92-94] Hydrogels based on natural polymers are the most suitable option since they offer biological cues for adherent cells[82,92] and mimic clue aspects of extracellular matrix and can direct cell migration, proliferation and cell organization.[93] Natural hydrogels are natural highly hydrophilic polymers (proteins or polysaccharides) like collagen, chondroitin sulphate, alginate or agarose that can be crosslinked through physical, ionic or covalent bonding[92,93].

Hyaluronic acid (also called hyaluronan) is an interesting natural hydrogel for cartilage tissue engineering. It is a non-sulphated glycosaminoglycan component of hyaline cartilage. Hyaluronic acid is a linear polysaccharide composed by N-acetyl-D-glucosamine and glucuronic acid disaccharide units, [22] as shown in **figure 1-6**.

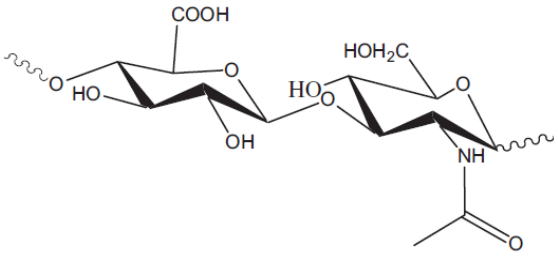

Figure 1-6. Chemical structure of hyaluronic acid[63] [Reprinted from Progress in Polymer Science, 32, Nair LS, Laurencin CT. Biodegradable polymers as biomaterials, 762-798, ©2007, with permission from Elsevier]

Hyaluronan promotes mesenchymal stem cell migration, differentiation and collagen deposition.[22] This polymer show a hydrophilic surface that impedes non-specific protein adsorption obstructing cell attachment[95], avoiding cell spreading; instead it provides a specific cue that promotes adhesion specifically through the CD44 receptor[96], furthermore hyaluronic acid may increase proliferation and chondrogenesis.[97-101]

Nevertheless, due to their low rigidity, hydrogels could not be the best support for chondrocytes from the point of view of stress transmission and generation of the right biomechanical environment, since they are too compliant. When cartilage cells are exposed to compressive loading, they change their secretion profile[102,191] and when the loading is excessive, the extracellular matrix loses proteoglycans[103,191] leading to a degeneration of the extracellular matrix. On the other hand, increasing hydrogel modulus to match cartilage modulus is not the best option as it implies a crosslink degree increase that can compromise cell viability[104,191]. Hydrogels like agarose and alginate, which show better mechanical properties than other hydrogels, are not tough enough to resist wear and tear due to joint friction in large animal model.[105] On the other hand, scaffolds made with synthetic polymers like polyesters showed better mechanical properties than polymers of natural origin and are more resistant to joint friction[105] and can

be fabricated as foams, woven and non-woven fibre meshes[105] with a defined size and adjusted to fit in the injured tissue. Finally saturated aliphatic polyesters do not offer biological signals (like biological adhesion sites) that may enhance chondrocyte phenotype and ECM secretion[64]. Cell material interaction is mediated by the interaction of membrane integrins with the proteins adsorbed over the material surface[95] such as fibronectin, laminin or vitronectin. Polyesters are adhesive substrates that induce cell spreading, which is related to a decrease in chondrogenic marker expression; furthermore cell-matrix interactions mediated by integrin have been shown to inhibit MSC chondrogenesis[106,107]. On the other hand, hydrophilicity promotes cell rounding and expression of chondrocyte-like phenotype[108]due to the lower protein absorption over the hydrogel[95] that reduces cell adhesion and spreading; it is for this reason that synthetic polymer drawbacks may be resolved modifying the surface, increasing the hydrophilicity or adding biological macromolecules.[95]

Scaffold embedding approach is an interesting option to develop hybrid polymer/hydrogel for cartilage tissue engineering since composite scaffold combines the load bearing capacity of polymeric macroporous scaffold with the biologic properties of a natural hydrogel as a cell carrier to increase the cell seeding[109]. This approach is not a cell-free approach as cells must be placed inside the hydrogel phase before the hydrogel infiltration, which must be crosslinkable *in situ* by photo-crosslinking, chemical crosslinking, enzymatic crosslinking or temperature and pH inducible gelation.[93] Natural biopolymers present these properties or can be modified to acquire them. The chemical crosslink is the crosslink (reversible or not) between polymer chains by adding a crosslinker, a molecule with at least two reactive groups able to bond two polymer chains or two points of same molecule[93,110]. On the other hand gelling time depends of concentrations of polymer and crosslinker.[93] Photo-crosslink is based on grafting polimerizable

vinyl groups graft on hydrogel chain and crosslinking by polymerization in presence of ultraviolet light;[93] concentrations and exposure time must be controlled to avoid cell damages or death.[93] It may not be the best option for our purpose to produce hybrids since scaffolds may absorb ultraviolet light. Enzymatic crosslink can be performed by the reaction between phenol derivatives groups present on polymer chains catalyzed by peroxidases.[93] This approach is applicable to polymers without phenol groups such as hyaluronic acid provided that they are modified substituting the carboxyl group of glucuronic acid with tyramine.[111] Enzymatic crosslink procedure shows a good biocompatibility and provide a good control over the reaction, but the presence of reactive oxygen species can have cytotoxic effects.[93] Finally certain polymers are able to gel through physical crosslink in response to temperature or pH variations.[93] In thermosensitive hydrogels changes in temperature can affect the molecular interaction with water and at a certain critical temperature, their polymer have more affinity to polymer chains that to water, inducing a phase separation between water and polymer phase.[93] On the other hand it has been reported that chitosan in water solution can jellify when the pH of the solution increases[93].

1.3.2.1 Cells and cell culture protocols for cartilage tissue engineering. Cell-scaffold construct.

Cell-scaffold construct to repair damaged cartilage tissue requires *in vitro* culture of cells seeded in a scaffold to induce cell proliferation, extracellular matrix deposition and differentiation prior to implantation. Apart from scaffold type, important factors which influence the quality of the engineered tissue are the type of cells selected and the chondrogenic culture conditions used.

As we said above, both mature chondrocytes and MSCs are used in cartilage tissue engineering.[52] Chondrocytes from hyaline cartilage are the current gold standard[53]. Chondrocyte harvesting is limited by tissue availability[52,53], and chondrocytes start dedifferentiating when expanded in monolayer[13,53] losing the spherical shape, showing a fibroblastic shape, a reduced expression of collagen type II and a higher expression of collagen type I.[13,52] On the other hand, culture in three-dimensional substrate allow cell redifferentiation,[52,54] via the use of external stimulus such as growth factors, mechanical stimulus or oxygen level tension that can induce cell redifferentiation[52] and raise the number of passages up to which cells can be efficiently redifferentiated.[54]. Mesenchymal stem cells are an alternative to mature chondrocytes as they are able to differentiate towards chondrocytes.[53] Mesenchymal cells can be isolated easily from diverse tissues from which the most common are bone marrow and adipose tissue[53,112]. Mesenchymal stem cells *in vitro* can be differentiated to chondrocyte in presence of growth factors, hypoxia or mechanical stimulus.[52] Nevertheless, a current drawback to this technology is that mesenchymal stem cells usually fail to develop good quality, long lasting mature hyaline cartilage[113] because they show a transient chondrocyte phenotype showing hypertrophy markers[60,61]; moreover, there is still no consensus about the optimal combination of culture conditions that may lead to a stable phenotype.[54]

Chondrocytes and mesenchymal stem cells require of extrinsic factors to obtain a functional phenotype[52,53] through regulation of cell differentiation pathways (**figure 1-7**). Chondrogenesis is a complex process regulated by key transcription factors[114], the first stage of which is the pre-cartilage condensation that is the chondroprogenitor mesenchymal cell aggregation.[115] This stage is regulated through Sox9, which is member of the Sox proteins family, a group of transcription factors.[114,116] Sox9 probably regulates the expression of membrane proteins that

are necessary for mesenchymal condensation.[114] Next step is the chondrocyte differentiation, which is regulated by Sox5, Sox6 and Sox9[114,115] when cells start to secrete of collagen type II, IX, XI and aggrecan, components of cartilage extracellular matrix.[115] Sox5 and Sox6 are co-expressed with Sox9 in this step (but not at mesenchymal condensation)[115]but unlike Sox9 they do not show transcriptional activation domain[114]. On the other hand, Sox9 establishes a complex with Sox5 and Sox6 to work cooperatively, where they (Sox5 and Sox6) act as architectural proteins that organize the DNA to facilitate the access of other transcription factors (as Sox9) to chondrocyte target genes enhancing the expression.[114,116] Finally chondrocytes can differentiate to hypertrophic chondrocyte, characterized by the expression of collagen type X and alkaline phosphatase[115] and extracellular matrix mineralization. Chondrocyte hypertrophy is regulated through Runx2 (a transcription factor of the runt family) expressed in prehypertrophic chondrocytes due to in deficient Runx2 mice hypertrophy is blocked.[115,117] On the other hand Sox9 negatively regulates this stage because it suppresses the earlier chondrocyte conversion to hypertrophic chondrocyte. [117,118]

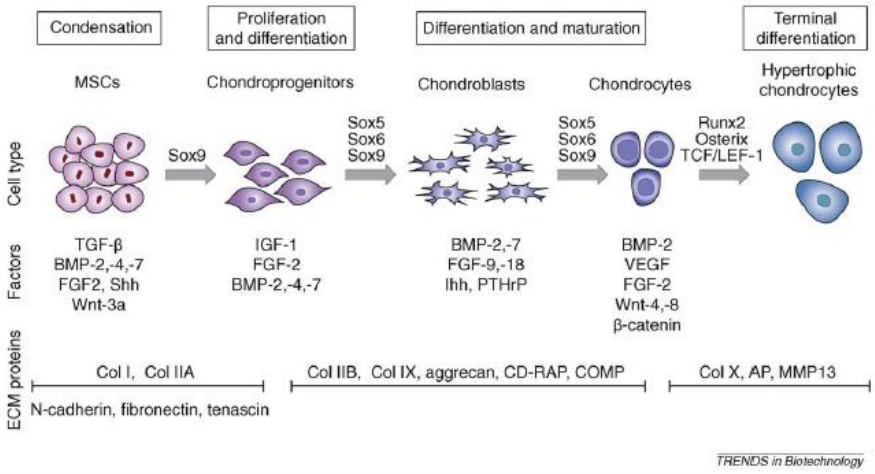

Figure 1-7. Sequence of mesenchymal stem cell chondrogenesis stages.[53] [Reprinted from Trends in biotechnology, 27, Vinatier C, Mrugala D, Jorgensen C, Guicheux J, Noël D. Cartilage engineering: a crucial combination of cells, biomaterials and biofactors, 307-314, ©2009, with permission from Elsevier]

Current cell culture protocols prescribe the use of growth factors such as transforming growth factor-β or fibroblast growth factor which are necessary to induce and maintain the correct chondrocyte phenotype[53]. Transforming growth factor-β family are the most commonly used factors in cartilage tissue engineering, as they are able to improve biochemical and mechanical properties of tissue construct through their effect as stimulator of extracellular matrix production in chondrocytes and inductor of MSC differentiation.[52,53] Fibroblast growth factor-2 is usually used during cell expansion due to its mitogenic effect over adult chondrocytes while in mesenchymal stem cells it induces proliferation and increases chondrogenic differentiation potential.[53] Chondrocytes expanded in presence of fibroblast growth factor-2 and transforming growth factor-β1 and subsequently redifferentiated with transforming growth factor-β1 and dexamethasone under serum-free conditions were reported to show an increment of chondrogenic markers.[52,119] In addition to growth factors, biophysical stimulus such as hypoxia, mechanical stimulus and recently coculture conditions can act as extrinsic

chondrogenic factors and are increasingly studied as factors to drive chondrogenic differentiation or redifferentiation. [52,53]

1.3.2.1.1. Oxygen level tension

Low oxygen tension is a key factor in the proliferation and differentiation of chondrocytes and mesenchymal stem cells.[53] Hyaline cartilage is an avascular tissue where the oxygen and nutrient supply occurs via diffusion from the synovial fluid.[53] This hypoxic environment varies from 7% of oxygen to 1% depending on tissue depth.[53,120] Cell survival to hypoxia is given by the hypoxia inducible factor activity. The hypoxia inducible factor is an heterodimeric transcription factor that binds to hypoxic inducible genes initiating the transcription.[121] This transcription factor is composed by hypoxia inducible factor-1α (HIF-1α), 2α or 3α that heterodimerize with the aryl hydrogen receptor nuclear translocator (also called hypoxia inducible factor-1β [53,121] under hypoxic conditions and bind to hypoxia responsive element initiating the transcription (**figure 1-8**).[53,121] On the other hand hypoxia inducible factor-1α under normoxia conditions have residues that show a oxygen-dependent hydroxylation through the prolyl-4 hydroxylase that allows recognition by the E3 ubiquitin ligase Von Hippel-Lindau that mark HIF-1α for proteasomal degradation.[122]

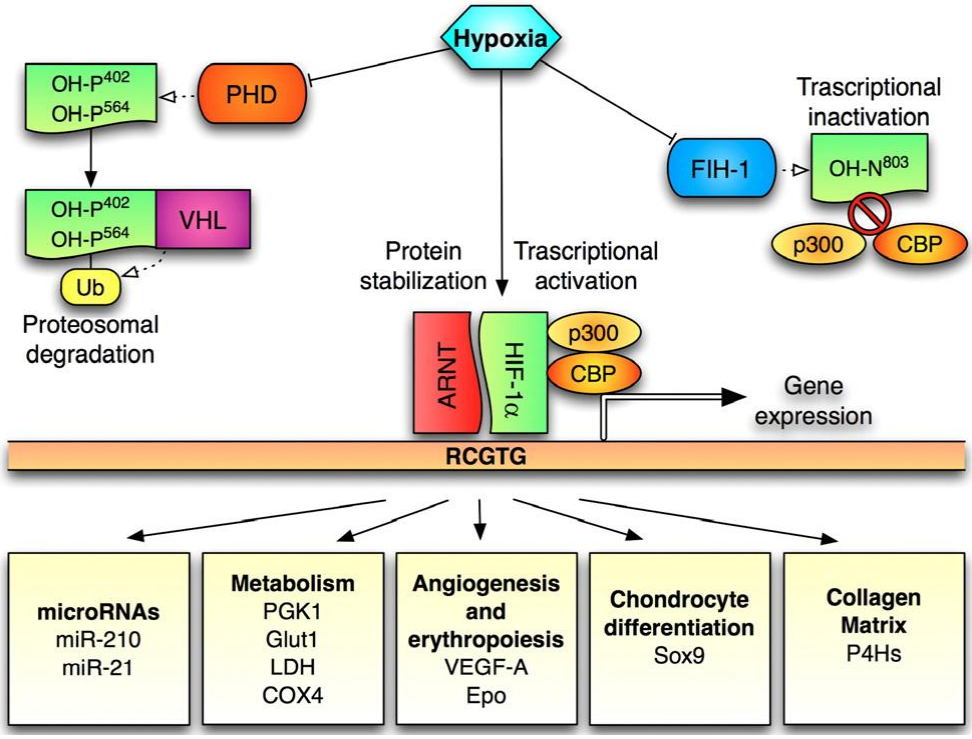

Figure 1-8. Sketch of hypoxia inducible factor pathways. Prolyl-4 hydroxylase (PHD), E3 ubiquitin ligase Von Hippel-Lindau(VHL), hypoxia inducible factor-1α (HIF-1α) and aryl hydrogen receptor nuclear translocator (ARNT) [122] [Reprinted from Bone, 47, Araldi E, Schipani E, Hypoxia, HIFs and bone development., biomaterials and biofactors, 190-196, ©2010, with permission from Elsevier]

Hypoxia (oxygen levels of 1.5-5%) application on *in vitro* cultured three-dimensional substrates showed an increment of cell redifferentiation and phenotype stability in chondrocytes that showed an induction of Sox9 and biosynthetic activity. [52] Literature suggests that HIF-1α is responsible of chondrocyte survival while hypoxia inducible factor-2α is essential for the induction of chondrocyte phenotype maybe through Sox9 induction. [52,53] On the other hand hypoxia has been shown to induce mesenchymal stem chondrogenesis and inhibits hypertrophy and apoptosis. [52,53] HIF-1α is considered responsible of promoting chondrogenesis in monolayer culture[52] and inhibiting hypertrophy through the downregulation of

Cbfa/Runx2 promoter expression and affinity for DNA.[123] On the other hand hypoxic conditions have been shown to enhance the quality of *in vitro* engineered tissue through secreted enzymes that stabilize the extracellular matrix.[124]

1.3.2.1.2. Mechanical loading stimulation

Hyaline cartilage *in vivo* supports mechanical forces like shear strain, compression or hydrostatic pressure that are key factors in chondrogenesis.[20,53] Mesenchymal stem cell differentiation and chondrocyte redifferentiation can be induced *in vitro* by mimicking these mechanical stimuli through different kinds of bioreactors that reproduce shear strain, uniaxial compression or hydrostatic pressure.[20,52,125,126] On the other hand cell-scaffold constructs show differences in secretion and organization of extracellular matrix depending on the mechanical stimulus type, duration and magnitude applied[52,53] but the response to the culture conditions has also been shown to depend on the substrate used.[107] Transmission of mechanical signals through surface cell receptors interaction with the substrate has been proposed as one possible way for cells to sense mechanical cues[127]. Cells show differences in integrin expression and cell differentiation in response to substrate stiffness,[79] chemistry[80] or presence of biologic adhesion motives[128] that can explain the substrate-dependent response.

The current strategies to apply mechanical stimulus *in vitro* are the use of bioreactors to generate fluid flow, compression or hydrostatic pressure. Fluid flow is based on continuous or discontinuous shear stress application on culture medium. Fluid flow induces MSC proliferation and upregulates both Sox9 and Runx2 expression, suggesting that expression of transcription factors implied in different differentiation fate can be affected by fluid flow.[20] Compression stimulus aims to

mimic the compressive load that happens in articular joint. Dynamic compression stimulus induce chondrogenesis of mesenchymal stem cells showing an induction of Sox9 and transforming growth factor β1[20] but this effect seems dependant on the time of application showing a detrimental effect on cells at earlier time points when the pericellular matrix is not yet developed.[20,129] Finally, hydrostatic compression is the application of physiological levels of cyclic hydrostatic pressure that mimics the "strain-free" stress experienced by cells in the nearly incompressible fluid inside the cartilage matrix during joint loading.[130] Cyclic hydrostatic pressure loading applied at physiological levels (1-10MPa)[130-132] induces the expression of chondrogenic markers such as sulphated glycosaminoglycan or collagen type II in mesenchymal stem cells and chondrocytes[132-134] and reduces the expression of hypertrophic markers such as collagen type I, MMP-13 and calcification of engineered grafts[107,135,136].

1.3.2.1.3. Co-culture

Cells in tissues *in vivo* communicate with each other through membrane proteins or soluble signals. Mature hyaline chondrocytes *in vivo* are isolated from other cells by an ECM that prevents cell-to-cell contact allowing only paracrine signalling. On the other hand, surface chondrocytes of articular cartilage and mesenchymal stem cells during the cartilage development show cell-to-cell contacts. [137] Co-culture intends to restore direct or indirect interaction between two cell populations in the same culture in order to mimic their natural, physiological interplay. In cartilage tissue engineering, this interaction appears usually between a cell type that induces the chondrogenesis and a second type that presumably will repair the objective lesion.[137] Chondrocyte coculture with mesenchymal stem cells showed increase chondrocyte proliferation, increased extracellular matrix synthesis and construct

functional properties.[137] The mechanisms by which cells interact with each other is not clear but literature reports point towards a combination of cell-to-cell and soluble mediators signalization. Cell-to-cell contact formation mechanisms remain unknown but different membrane proteins such as gap junction proteins connexins can affect chondrocyte differentiation.[137] On the other hand, another co-culture signal way are the soluble paracrine mediators, given that chondrocyte culture medium supernatant can induce chondrocyte redifferentiation and promote mesenchymal stem cell chondrogenesis and hypertrophy prevention.[52,137,138] Parathyroid hormone related peptide secreted by chondrocytes in co-culture[138] has been reported to inhibit hypertrophic markers expression[125,138], probably through Runx2 blocking and Sox9 phosphorylation[139]. Parathyroid hormone related peptide in combination with other soluble paracrine molecules may hold the key for efficient mesenchymal stem cell differentiation and phenotype stabilization in co-culture.[138]

Co-culture experimental designs have two main variables: cell types used and co-culture design. Cell type selection is really important. Most common choices are chondrocyte-chondrocyte and chondrocyte-mesenchymal stem cell, but other cell types such as dermal fibroblast, osteoblast or synovial fibroblast have been studied.[137] Chondrocyte-chondrocyte co-culture showed that a small number of primary chondrocytes are able to rescue phenotype of dedifferentiated chondrocytes even if one cell type in co-culture is from a xenogenic source.[52] The importance of chondrocyte-chondrocyte strategy is its capacity to upregulate gene expression of aggrecan, collagen type II and SOX9 while downregulating collagen type I.[52] On the other hand chondrocyte-mesenchymal stem cells show a more interesting interaction. Mesenchymal stem cells in pellet co-culture with chondrocytes can promote chondrocyte redifferentiation. While this does not happen when MSC are substituted with other cells, such as dermal fibroblasts, this reduces the need of high

numbers of chondrocytes substituting part of them by MSC.[140] On the other hand, co-culture with chondrocytes induces MSC chondrogenesis and inhibits hypertrophy in direct and indirect coculture.[138,140,141]

Cell co-culture strategies can be divided as direct and indirect co-culture as shown on **figure 1-9**. Direct co-culture experiments uses two cell types seeded together, allowing to establish both cell-to-cell contacts and paracrine signal communication.[137] Many direct co-culture designs have been proposed, but the most common involved a mixed monolayer cell culture, pellet or mixed seeding on scaffold or hydrogel[137,138,140,142-146]. Direct co-culture has been proposed as a preferential method for mesenchymal stem cell chondrogenesis and hypertrophy inhibition.[140] On the other hand indirect co-culture is based on the physical separation of both cell types using monocultures (in monolayer or three-dimensional) separated by a porous membrane that impedes cell migration, using chondrocyte conditioned culture medium or retaining cells separated in two gels or scaffolds.[137,138,140-142,146,147] In indirect co-culture, only the effect of paracrine signalling is thus relevant, as direct cell-to-cell contact between different cell types is not allowed. Indirect co-culture has showed contradictory findings[137]; while some works point towards a positive effect of indirect co-culture[138,141,147] other works suggest that only direct co-culture have a chondrogenic effect[140,145]. Described differences between works probably are due to differences in cell types selected and co-culture systems used.[137]

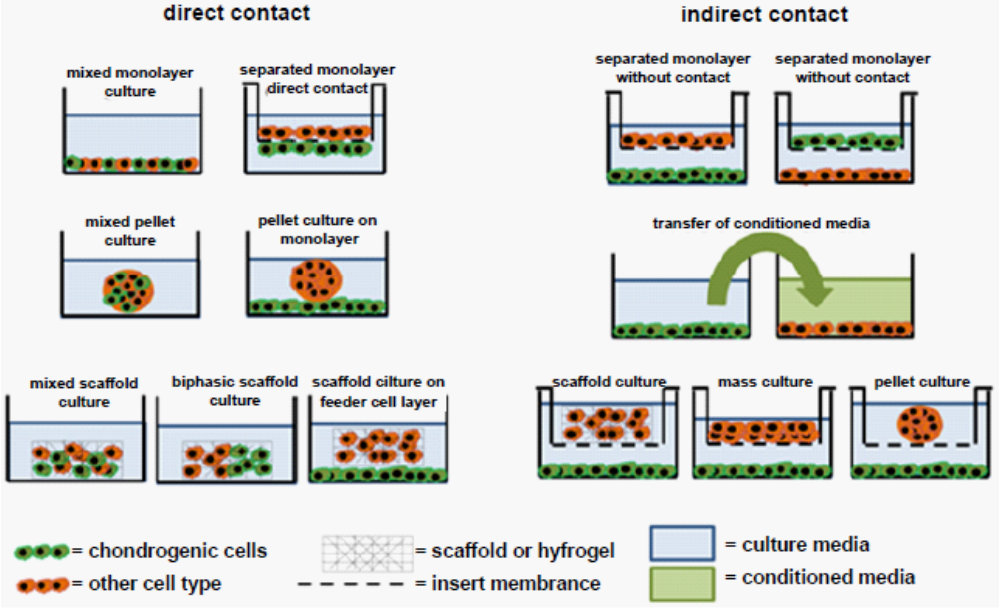

Figure 1-9. Overview of different direct and indritect co-culture systems in two and three dimensional cultures[137]

2. MATERIALS AND METHODS

2. Materials and methods

2.1. Materials:

2.1.1. Polymers and chemicals

2.1.1.1. Polycaprolactone

Polycaprolactone, is a semicrystalline aliphatic polyester obtained through ring opening polymerization of ε-caprolactone and has been approved by the Food and Drugs Administration.[22,35,63] The polymer is formed by ester bonds which degrade by hydrolysis with a small degradation rate.[22,35,63] The PCL used in these experiments was supplied by Polyscience. (MW 43,000–50,000 Da, Polysciences)

2.1.1.2. Polylactic acid

Poly(L-lactic acid) is also a Food and Drugs Administration approved polyester which degradation kinetic is higher than PCL and its degradation end product is lactic acid, a normal by-product of cell metabolism.[9,22,63] The polylactic acid was supplied by Cargill Dow.

2.1.1.3. Elvacite 2043

Elvacite 2043 is an acrylic resin soluble in ethanol and with a low molecular weight composed by polyethylmethacrylate (PEMA). Elvacite 2043 beads with a mean diameter of 200μm were supplied by Lucite International.

2.1.1.4. Hydroxyapatite

Hydroxyapatite is a biocompatible crystalline ceramic that shows osteoinductive properties.[89] The synthetic hydroxyapatite $[Ca_5 (OH)(PO_4)_3]_X$ used in this work is similar but more crystalline than the hydroxyapatite from biologic source. Hydroxyapatite with a 200nm particle size was supplied by Sigma-Aldrich(Hydroxyapatite, 677418).

2.1.1.5. Bioglass®45S5

Bioactive glasses are biocompatible and bioactive materials which in dissolution release ions able to modify the gene expression[9]. The chosen bioactive glass is Bioglass® 45S5 (45% SiO_2, 24.5% Na_2O, 24.5% CaO y 6% P_2O_5). The Bioglass® with a 20µm particle size was supplied by MO-Sci Corporation(GL-0160).

2.1.1.6. Hyaluronic acid

Hyaluronic acid (HA) is a linear and non-sulphated glycosaminoglycan, component of hyaline cartilage.[22,63] Furthermore hyaluronic acid promotes mesenchymal stem cell migration and differentiation.[22]The bacterial obtained HA, from Streptococcus Equi, was supplied by Sigma-Aldrich (Hyaluronic acid sodium salt from *Streptococcus equi*, 53747).

2.1.1.7. Divinyl sulfone

Divinyl sulfone (DVS) is a non colored chemical able to react and crosslink with HA hydroxyl groups establishing ether bonds under alkaline pH[148] without affecting the biologically active groups[149]. The divinyl sulfone was supplied by Sigma-Aldrich (Divinyl sulfone, V3700).

2.1.1.8. Tyramine

Tyramine is a chemical compound derived from the amino acid tyrosine. Tyramine is able to react and substitute the carboxyl group of glucuronic sub-unit and form a biodegradable chain crosslink when exposed to active oxygen radicals; this allows for *in situ* crosslinking using peroxidase and peroxide in presence of cells.[111] Tyramine was supplied by Sigma-Aldrich(Tyramine hydrochloride, T2879).

2.1.1.9. Alginate

Alginic acid (also called alginate), is a linear polysaccharide obtained from brown algae able to gel in presence of calcium.[35,63] Alginate sodium salt was supplied by Sigma-Aldrich (Alginic acid sodium salt from brown algae, 71238).

2.1.1.10. Fibronectin

Fibronectin (FN) is an extracellular matrix glycoprotein that allows integrin-mediated cell adhesion.[6] Interaction of cells with fibronectin influences a wide range of biological aspects such as cell adhesion and differentiation.[95] The fibronectin was supplied by Sigma-Aldrich (Fibronectin from human plasma, F2006)

2.1.2. Cells and culture medium

2.1.2.1. Cells:

2.1.2.1.1. Cell lines:

2.1.2.1.1.1. MC3T3-E1

MC3T3-E1 cell line was used for the biological characterization of composite scaffolds for bone tissue engineering. This cell line is derived from mouse calvaria and is often used in bone tissue engineering and the study of osteoblastic differentiation, as it shows robust proliferation and a physiologically relevant coupling between proliferation and differentiation[150]. Cells were purchased from the Riken Cell Bank (Japan).

2.1.2.1.2. Primary cell culture

2.1.2.1.2.1. Human chondrocytes

Human chondrocytes were harvested from knees of patients undergoing arthroplasty after their informed consent following the guidelines of the ethical committees of Universitat Politècnica and Clínica de la Salud of Valencia. The cartilage was dissected from subchondral bone, finely diced and then washed with supplemented 100 U penicillin, 100 µg streptomycin Dulbecco's modified Eagle's medium (DMEM) (Gibco). For chondrocyte isolation, finely diced cartilage was incubated for 30 min with 0.5 mg/ml hyaluronidase (Sigma– Aldrich) while shaking at 37C, and then with 1 mg/ml pronase (Merck, VWR International SL) during 60 min in the same conditions. Subsequently the cartilage pieces were washed with supplemented Culture medium and digested with 0.5 mg/ml of collagenase-I (Sigma–Aldrich) in a shaking water bath at 37ºC overnight. The resulting cell suspension was filtered through a 70 µm pore nylon filter (BD Biosciences) to remove tissue debris. Cells were centrifuged and washed with culture medium supplemented with 10% foetal bovine serum(FBS) (Invitrogen SA).

2.1.2.1.2.2. Bovine chondrocytes

Bovine chondrocytes were harvested from the metacarpophalangeal joints of an animal obtained from a local slaughterhouse. The cartilage was dissected from subchondral bone following the same protocol than for human chondrocytes.

2.1.2.1.2.3. Mesenchymal stem cells

Porcine mesenchymal stem cells were harvested from the femoral bone marrow. The femur bone was cut in the upper part in aseptic conditions and the gelatinous bone marrow was removed. Bone marrow was grinded and centrifuged to remove the non-desired hematopoietic cells. The cells were seeded at $4x10^5$ cells/cm in a $T75cm^2$ culture flask and non adherent cells were removed when the medium was changed. Cells were harvested and isolated at the Trinity Centre of Bioengineering (TCBE) of Trinity College Dublin (Ireland).

2.1.2.2. Cell culture medium

Cell culture mediums are classified in the present thesis as expansion cell culture medium and cell culture medium of cells seeded in scaffolds. Expansion medium is used to expand cells in monolayer in order to obtain the cell number necessary to seed the scaffolds. On the other hand culture medium contains different supplements in order to induce cell differentiation or maintain the correct phenotype. The different culture mediums used on present work for each cell type are listed in **table 2-1**.

	MC3T3-E1		Human chondrocyte		Porcine mesenchymal stem cell			Bovine chondrocyte	
	Expansion culture medium	Osteoblast differentiation culture medium	Expansion culture medium	Culture medium	Expansion culture medium	Chemically defined chondrogenic media		Expansion culture medium	Chemically defined chondrogenic media
						Hypoxya/ bioreactor experiment	Coculture experiment		
Glucosa (g/l)	1	1	4.5	4.5	4.5	4.5	4.5	4.5	4.5
Glutamine (µg/ml)	584	584	292	292					
GlutamaX (µg/ml)					862	862	431	431	431
Penicilin/streptomicin (U/ml / µg/ml)	100/100	100/100	100/100	100/100	100/100	100/100	100/100	100/100	100/100
Foetal bovine serum (%)	10	10	10	10	10			10	
β-glycerophosphate sodium (mM)		2.1							
ascorbic acid (µg/ml)		50	50	50		50	50		50
Sodium Pyruvate (µg/ml)				110		110	110		110
Bovine serum albumin (mg/ml)						1.5	1.5		1.5
L-Proline (µg/ml)						40	40		40
Linoleic Acid (µg/ml)						5.37	4.7		4.7
ITS (%)						1			
ITS + PREMIX (%)							1		1
Dexamethasone (nM)						100	100		100
TGF-β3 (ng/ml)						10	10		10
FGF-2 (ng/ml)					5			5	

Table 2-1. Table with culture medium composition for cell expansion and culture in scaffolds of each cell type.

2.2. Methods

2.2.1. Scaffold manufacture

2.2.1.1. Polymeric scaffolds obtained through freeze-extraction and particle leaching combined technique.

The scaffolds fabrication protocol is a combination of two methods, one being freeze extraction (a modification of freeze drying proposed by Wang et al.[151]) and the other, the particle leaching method using polymer beads as porogen. This protocol generates both micropores -when the polymer solvent crystallizes as consequence of thermal induced phase separation between polymer and solvent on the other hand removing porogen leads to an interconnected macroporosity (**figure 2-1**).

To fabricate the different scaffolds of polycaprolactone and polycaprolactone/polylactic acid blend at (80/20) or (20/80) the polymer (or combination of both) is dissolved at 20% (polycaprolactone) or 15% (polymer blend) calculated in weight/volume in dioxane. As porogen Elvacite 2043 beads with a mean diameter of 200 μm were used. The polymer solution was mixed with PEMA beads at a weight ratio 1:1 and immediately frozen in liquid nitrogen. Solvent extraction was performed in cold ethanol at -20ºC in a freezer; ethanol was changed three times. Subsequently particle leaching to extract the porogen was performed at 37ºC in ethanol that was changed over 14 times. When no more PEMA is detected in the extraction solvent the samples are removed, ethanol is evaporated and the samples packed. [158, 191]

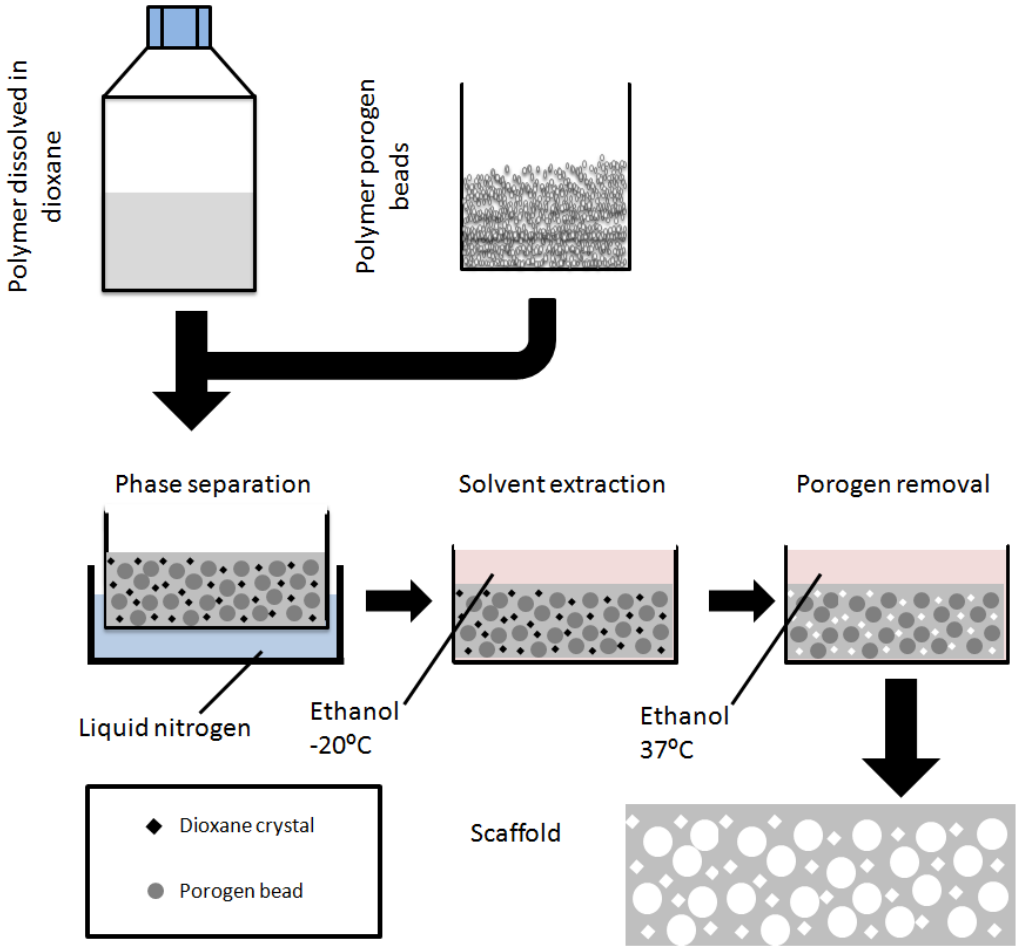

Figure 2-1. Mixed process of freeze extraction with particle leaching.

2.2.1.2. Polymer-ceramic composite scaffolds fabrication

With the aim of improving the mechanical properties and the osteoactivity of polycaprolactone scaffolds, polymer-ceramic composite scaffolds were prepared.

To do so, polymer solutions were mixed with different amounts of mineral particles (5, 10 or 20 % by weight with respect to polymer). The ceramic reinforcements used

were synthetic hydroxyapatite and Bioglass® 45S5. Particles were homogenezed by ultrasonic dispersion in dioxane (Ultrasonic homogenizer, Sonopuls HD 3200) and subsequently the polymer was dissolved by continuous stirring. The scaffold fabrication protocol used was the same as for non-reinforced scaffolds. [158]

2.2.1.3. Polycaprolactone scaffold composites obtained by biomimetic apatite coating

Seeking to increase the polycaprolactone scaffold bioactivity and to improve wettability they were coated with a calcium phosphate layer. The mineral coating protocol is divided in three steps (**figure 2-2**): to enhance the surface capacity to nucleate crystals, to nucleate calcium phosphate crystals over scaffold surfaces and to coat the scaffold surface with a biomimetic hydroxyapatite layer.

Surface modification to improve the presence of functional chemical groups to enhance crystal deposition was performed with two methods: Air plasma treatment and chemical degradation. Air plasma treatment attacks the polymer surface with ions, electrons, radicals and neutral molecules that react with polymer and increase the presence of oxygen containing chemical groups[82,83]. Samples were placed in plasma chamber (Plasma Electronic GmbH) at 40% of potency and at 20% of gas flow. Chemical degradation was performed with sodium hydroxide to degrade polymer ester bonds to increase the number of carboxyl groups present on the scaffold surface. Samples were immersed in ethanol to fill the pores and the solvent was substituted with ethanol/water 50/50 and finally substituted with water using a vacuum pump to ensure the filling of the sample. Then samples were filled with sodium hydroxide solution using a vacuum pump and incubated at 37ºC. Finally samples were washed with water.

Nucleation treatment consists in nucleating phosphate calcium crystals over scaffold surface. Samples were filled with ethanol/water 50/50 using a vacuum pump and drying the water excess. The procedure was the following: sample immersion in calcium chloride, blot over tissue paper and washing in ethanol/water 50/50. The second step consisted in drying the water excess and immersing in phosphate potassium. Finally samples were washed in water.

Biomimetic hydroxyapatite coating was performed immersing the samples in simulated body fluid allowing crystal growth. Samples were infiltrated with water and immersed in simulated body fluid and incubated at 37ºC. Finally samples were washed with water and dried.

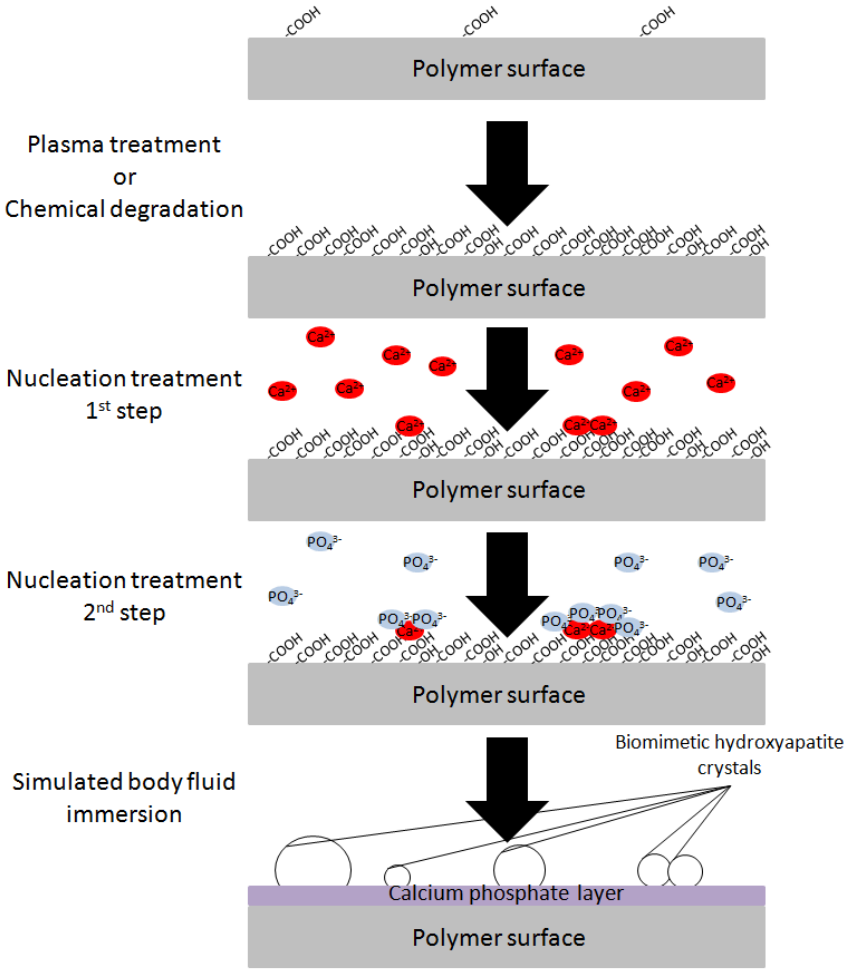

Figure 2-2. Polymer surface biomineralization process.

2.2.1.4. Polycaprolactone scaffold coating with hyaluronic acid

With the aim to increase the wettability and biological response of naked scaffolds the PCL scaffolds were coated with HA. To do so, a hyaluronic acid solution was infiltrated and crosslinked under alkaline conditions to allow the reaction between DVS, and hyaluronic acid hydroxyl groups. This obtained hydrogel is crosslinked

through ether bonds[148] yielding a stable link between the hyaluronic acid chains without affecting the biologically active groups.[149]

The effect of hyaluronic acid coating conformation was studied for three coating methods(**figure 2-3**): 1step, 1 step modified and 2 step crosslinking.

The 1 step crosslinking's purpose was to fill the scaffold's pores with swollen hyaluronic acid hydrogel. In the first step, a 2% hyaluronic acid solution in 0.2M sodium hydroxide (Scharlau) aqueous solution was mixed with a 2:1 molar ratio of DVS. The scaffolds were placed in the solution and then connected to a vacuum pump for 2 min to infiltrate de hyaluronic acid and fill the pores. Excess hyaluronic acid was removed and the samples were incubated for 2 hours at room temperature (RT) to carry out the crosslink reaction. Subsequently samples were washed with acetone/water mixture 50/50 and dried.[191]

In the 1 step crosslinking modified protocol, the purpose was to leave a thin and low swelling hyaluronic acid coating on the scaffold pore walls. To obtain the thin coating, after infiltration with the HA mixed with DVS as in the precedent paragraph, samples were left for 1 hour at room temperature to allow the crosslink reaction and dried at 37ºC for 48 hours. Then scaffolds were washed repeatedly with water to wash out unreacted DVS.

The 2 step crosslinking also aims to coat the scaffold pore walls with a thin hyaluronic acid layer. In the first step a 1% hyaluronic acid (w/v) is dissolved in distilled water. The scaffolds were placed in the hyaluronic acid solution and connected to a vacuum pump for two minutes. After eliminating excess hyaluronic acid the samples were placed in an oven at 37ºC for one day and finally dried with vacuum. HA coating step was repeated three times. Subsequently the samples were immersed in acetone/water mix (80/20) at pH 12 with a 2:1 molar ratio of DVS with

respect to HA reactive moieties calculated from hyaluronic acid coating dry weight. The acetone/water solution avoids hyaluronic acid dissolution but permits HA swelling and the de-protonation of hydroxyl groups of hyaluronic acid[148] necessary for the crosslink reaction to take place. The samples were incubated for 24 hours and after incubation the samples were washed with 80/20 (v/v) acetone/water mixture and dried. [191]

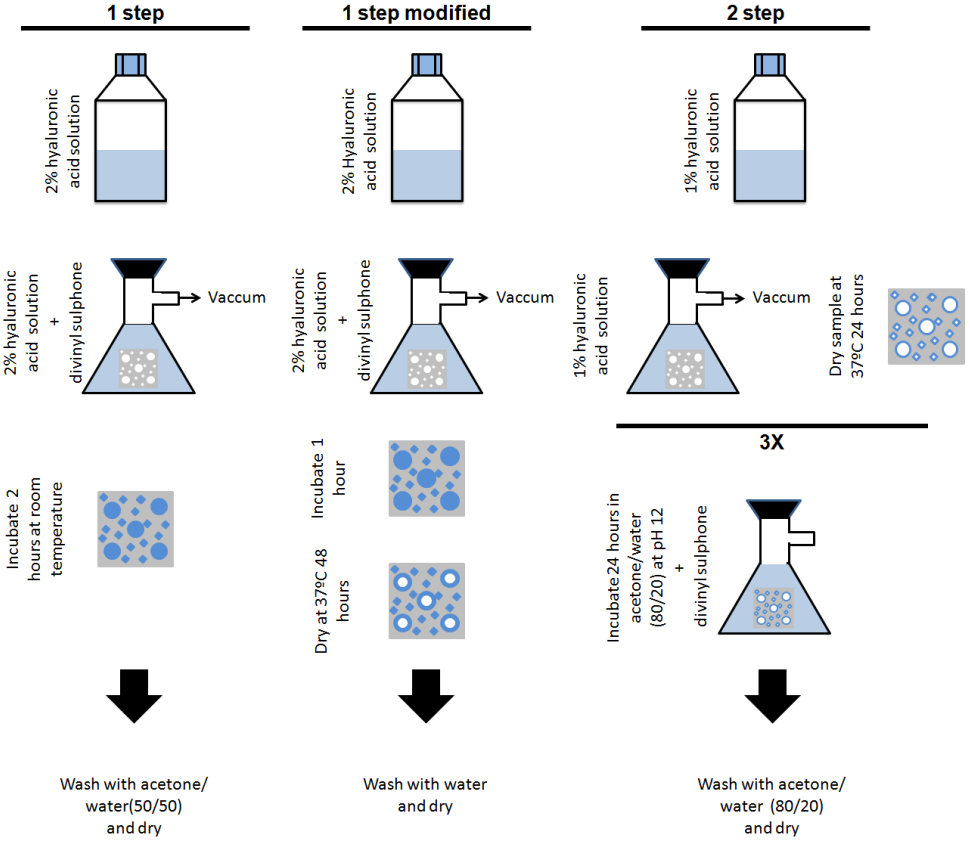

Figure 2-3. Scaffold coating with hyaluronic acid.

2.2.1.5. Tyramine substituted hyaluronic acid tyramine substituted hyaluronic acid

To obtain a hyaluronic acid crosslinkable *in situ* the carboxyl acid group of glucuronic acid was substituted with tyramine. The protocol for peroxidase crosslink of hyaluronic acid was inspired by Dr Calabro[111].

To substitute the hyaluronic acid, 500 mg of hyaluronic acid were dissolved slowly in a reaction buffer (4-Morpholineethanesulfonic acid at 5.4%w/w in 100 ml of NaCl 150mM equilibrated at pH 5.75 using 1.5 ml of NaOH 5M diluted). Once the hyaluronic acid was homogenously dissolved, 434 mg of tyramine HCl (molar 2:1 to hyaluronic acid) were added and after its complete dissolution, 480 mg of N-(3-Dimethylaminopropyl)-Nomethylcarbodiimide (molar 1:1 to tyramine HCl) and 57.6 mg N-Hydroxysuccinimide (molar 1:10 to N-(3-Dimethylaminopropyl)-N′-ethylcarbodiimide) were added, too. The reaction was carried out at 37ºC with agitation for 24 hours. When the reaction was stopped the tyramine substituted hyaluronic acid was dialyzed against 150 mM NaCl solution for 48 hours changing the buffer each 8 hours, and subsequently against miliQ water. Finally the tyramine substituted hyaluronic acid was lyophilized for 24 hours at-80ºC and 0.001mbar in a Telstar Lyoquest lyophilizer.

2.2.1.5.1. Tyramine substituted hyaluronic acid crosslink

Tyramine substituted hyaluronic acid allows *in situ* crosslinking which permits to encapsulate the cells inside the scaffold. The crosslink is catalyzed by horseradish peroxidase that generates two free radicals between tyramine hydroxyl groups.

The tyramine substituted hyaluronic acid was dissolved at 20mg/ml in Dulbecco's phosphate buffered saline (DPBS) with 2g/l glucose (DPBSG), and mixed with 2

U/ml horseradish peroxidase (HRP) (final concentration: 1U/ml). Then, if it was to be used for cell seeding, the solution was mixed with cell suspension (1:1) and injected in the scaffold at 10 µl/sample and incubated with 30µl H_2O_2 at 0.01% for 30 min. Finally, the sample was washed with culture medium supplemented with FBS; the medium was further changed after 1, 2 and 4 hours to remove any free radicals or peroxide residues.

2.2.2. Physico-chemical characterization

2.2.2.1. Scanning electron microscopy and cryo scanning electron microscopy

Observation of the scaffold morphology was carried out using scanning electron microscopy (SEM) in secondary mode. To do so, samples were cryofractured (to preserve the microstructure of the scaffolds), mounted on copper stubs with a graphite conductive tape and gold sputtered. For CryoSEM, wet samples were carefully wiped with filter paper, mounted in a clamp, ultrafrozen, and then cryofractured. Samples were sublimated at -50ºC and gold sputtered inside the microscopy vacuum chamber. The microscope used was JEOL JSM6300 scanning electron microscope at an acceleration voltage of 15 kV. [158, 191]

2.2.2.2. Energy dispersion X-ray analysis

The scaffold's surface composition was analysed using energy dispersive X-ray (EDX) analysis to confirm the presence of ceramic particles.

Samples were cryofractured, mounted on copper stubs with a graphite conductive tape and carbon sputtered. The microscope used was JEOL JSM6300 scanning electron microscope at an acceleration voltage of 15 kV. [158]

2.2.2.3. Differential scanning calorimetry

Differential scanning calorimetry (DSC) measurements were carried out in a Mettler Toledo 823e DSC on samples with a weight between 5-10mg. A first heating scan at 10ºC/min from 0ºC to 220ºC enabled to characterize the structure of the sample after degradation. After annealing at 220ºC for three minutes, and cooling down at 10ºC/min to 0ºC, a second heating scan at 10ºC/min was recorded to analyze the behaviour after having erased thermal history.

The degree of crystallinity and melting enthalpy of the scaffolds, was determined using the DSC software, and crystallinity was calculated for each phase of the blend assuming that melting heat for pure crystals of polylactic acid and polycaprolactone are ΔH^{o}_{PLLA}=90.95 J/g [152] and ΔH^{o}_{PCL}=136.1 J/g[153]respectively.

2.2.2.4. Ceramic content in composite samples

Ceramic content in composite scaffolds was assessed using a calcination technique; the samples were submitted to a temperature scan up to 800ºC so that the polymer was thermally degraded, and mineral residue was measured. [158]

The thermogravimetric analysis (TGA) was performed using a SDT Q600 analyser from TA Instruments or a tubular oven to determine the residue produced by the

calcination of the sample as an indicator of the actual amount of reinforcement present in the scaffolds.

When using the SDT Q600, the sample was placed in a platinum pan and subjected to a heating scan from 50 to 800ºC at 20ºC/min under nitrogen atmosphere. The mass was monitored as a function of the temperature and results were analysed using software TA Analyzer from the device.

When the thermo gravimetric analyser was not available, samples were tested in a tubular oven (Gallur; HC300 CONATEC, version 10-1-2000) .Samples were weighed before and after calcination of the polymer at 600ºC to calculate the percentage of mineral phase. [158]

2.2.2.5. Polymer content in blend and hybrid samples

Thermogravimetric analysis was performed in a SDT Q6000 from TA Instruments to determine the amount of polymer (polylactic acid, polycaprolactone or crosslinked hyaluronic acid) present in hyaluronic acid coated scaffolds or blend scaffolds. Weight loss of each polymer component was determined applying a linear relationship between the scaffold and the pure polymer weight loss between the temperatures in the range of the weight derivate peak of pure polymers. The samples were placed in the platinum pan and the temperature was raised from 50 to 1000ºC at a heating rate of 10ºC/min (for blend scaffolds) or 20ºC/min (HA coated scaffolds) under nitrogen atmosphere. The mass was monitored as a function of the temperature; results were analyzed using the software TA Analyzer from the instrument.[191]

2.2.2.6. Porosity measurement by gravimetry

The porosity of the scaffolds was determined by gravimetry: samples were weighted dry and wet to determine the weight increase and relate it to the pore volume.

The porous samples were cut in pieces with a defined size, weighed dry and filled with ethanol (introduced under vacuum). Porosity was calculated as the quotient of the volume of pores to the total volume of the sample according to the following equation

$$p = \frac{V_{pores}}{V_{polymer+}V_{pores}}$$

where the volume of pores (V_{pores}) was deduced from the quotient of the mass difference between dry (m_{dry}) and wet (m_{wet}) scaffold and the ethanol density ($d_{ethanol}$). For this experiment we assumed that the amount of ethanol absorbed by the polymer phase is negligible.

$$V_{pores} = \frac{m_{wet}\text{-}m_{dry}}{d_{ethanol}}$$

Volume of polycaprolactone ($V_{polymer}$) was calculated from the quotient of dry weight (m_{dry}) of the scaffold and the density of the polymer ($d_{polymer}$).

$$V_{polymer} = \frac{m_{dry}}{d_{polymer}}$$

[158, 191]

2.2.2.7. Water absorption behaviour

For water absorption analysis five samples were immersed in distilled water and allowed to take up water until equilibrium was reached (48 h). Samples were weighed dry (Wd) and wet (Ws) and a ratio describing water uptake was calculated according to equation.

$$\text{Swelling ratio} = \frac{W_s}{W_d}$$

[191]

2.2.2.8. Mechanical analysis: Compression assays

Scaffold's mechanical properties were determined following the American Society for Testing and Mmaterials D1621-04a *''Compressive properties of rigid cellular plastics''* guidelines.

Uniaxial compression tests were performed using a Microtest Universal Testing Machine with a 15 N load cell. The sample was compressed at room temperature using a crosshead speed of 1mm/min. The load ramp up to -15 N was performed and a stress–strain curve was traced. The standard stress-strain curve obtained in the compression assay in porous scaffolds can be divided in 4 sections (**figure 2-4**). The first section is the adaptation zone (a). This zone represents the approximation of load cell to the sample. Linear elasticity zone (b) represents the non plastic deformation of trabeculae where the stress shows a linear dependence of the strain. The plateau zone (c) is the sample plastic deformation as a consequence of trabeculae buckling. When the stress overpasses the yield strength, the trabeculae buckle and the pores collapse, showing the plateau zone due to the sample strain increase at nearly no stress. When the trabeculae are collapsed the densification zone

starts (d). Elastic modulus was determined as the slope of initial segment of the curve, Yield strength was determined as the stress at the inflexion point between elastic zone and plateau zone and densification modulus was determined as the tangent of the maximum modulus reached during densification zone. [158, 191]

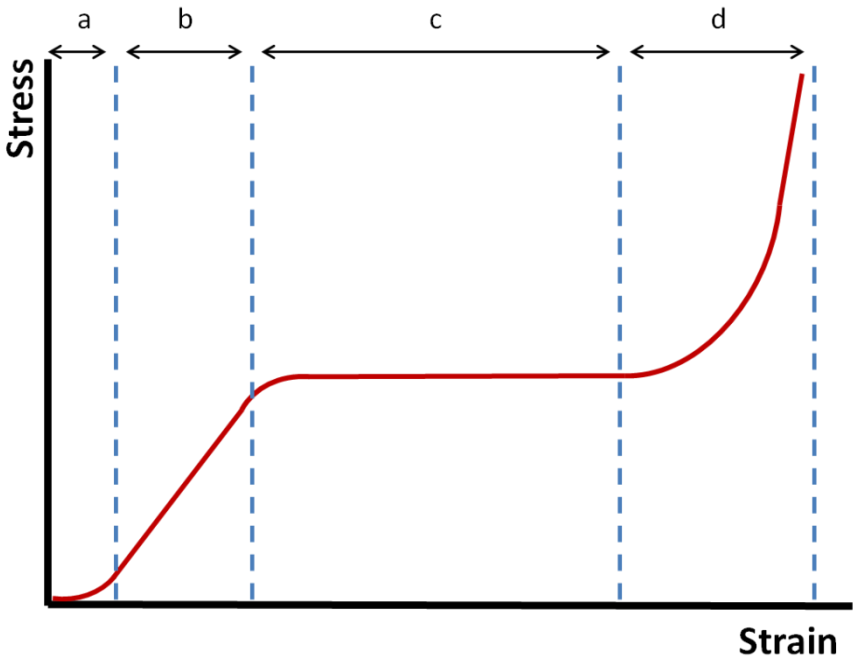

Figure 2-4. Scaffold's stress-strain curve for compression assay divided in 4 sections. Adaptation (a), linear elasticity zone (b), plateau zone (c) and densification zone (d).

2.2.2.9. Dynamic mechanical analysis: Equilibrium and dynamic modulus

Void scaffolds were incubated in sterile culture medium (supplemented with acid ascorbic, bovine serum albumin, dexamethasone and sodium azide) at 37ºC during up to 35 days to determine the mechanical contribution of hydrolytic degradation in the construct properties. This effect was assessed through the measurement of

equilibrium and dynamic modulus using a thermal mechanical analyser, and the determination of elastic modulus using the Microtest Universal testing machine at different time points.

Samples were removed at 1, 17 and 35 days, washed with Dulbecco's phosphate buffered saline and placed in DPBS at 4ºC until analysis was performed. The samples were compressed at room temperature in immersion on DPBS. Stress relaxation test was performed using a thermal mechanical analyser. Compressive equilibrium modulus was determined from the equilibrium values reached by the samples after applying 10% strain and holding it for 30 min. Dynamic modulus was determined overlaying a cyclic strain of 1% of amplitude at 0.1 Hz to the 10% equilibrium strain for 10 cycles.[134]

2.2.2.10. Stability in physiological medium

In the case of composite samples, the dissolution of the mineral phase can affect the pH of the culture medium and thus cell fate. Thus, evolution of the pH of phosphate buffer in contact with the composite samples was studied for up to 48 h. (phosphate buffer was chosen over more physiological carbonate buffer due to the high instability of carbonate buffer pH in normal atmosphere).

For each material, three samples were cut and incubated with 1 ml phosphate buffer 1 M at 37 ºC after vacuum infiltration. pH was measured at 0, 0.5, 1, 3, 8 and 24hours. [158]

2.2.2.11. Degradation study

Degradation study was performed to determine the effect of hydrolytic degradation in different polycaprolcatone/polylactic acid blends. Assay was performed with a low saline buffer to avoid salt precipitates that can interfere with the weight measures.

Samples were incubated with phosphate buffer (NaH2PO4 3,12g/l, Na2HPO4 28.66g/l and 0.02% NaN3 pH=7.4) in a ratio of 0.5% sample weight in buffer volume, samples were incubated at 37ºC for 78 weeks and medium was changed every two weeks. Samples were removed and stored at 0, 30, 44, 60 and 78 weeks.

2.2.3. Cell Culture

2.2.3.1. Disinfection protocol, sample preconditioning and cell seeding protocol

Scaffold seeding protocols were adapted to each type of scaffold developed. Polymeric scaffolds are hydrophobic and do not show biologic adhesion motives, and for this reason they were preconditioned. First step of sample preconditioning was the sample disinfection. Absolute ethanol was infiltrated inside the samples and incubated and after one hour was changed with sterile ethanol 70% at 4ºC during 72 hours. The preconditioning step consists in washing the samples with DPBS three times to remove ethanol and incubating the samples overnight at 37ºC in culture medium supplemented with FBS, and penicillin/streptomycin. This protocol allows filling the scaffold with culture medium and coating the surface with adhesive proteins. MC3T3-E1 were seeded on polycaprolactone and composite scaffolds by depositing a small drop of concentrated cell solution on the scaffold surface. Samples were incubated for 30 minutes at 37ºC and then cell culture medium was

added. On the other hand, human chondrocytes were injected in PCL and hyaluronic acid coated samples using a Hamilton syringe (**figure 2-5**). [158, 191]

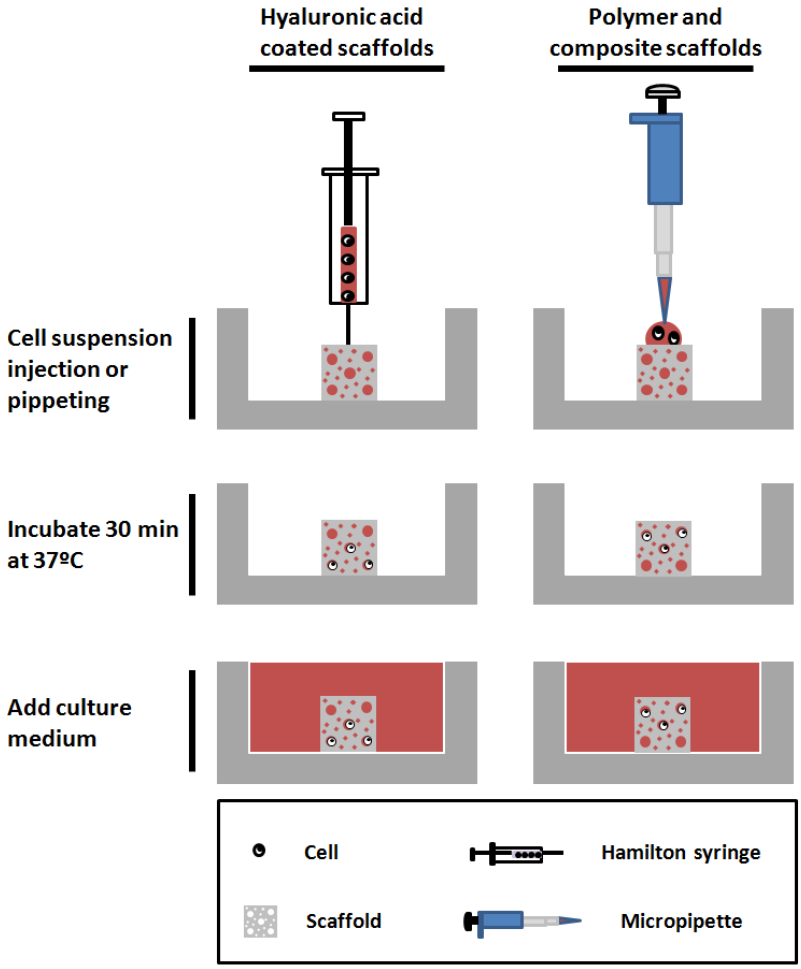

Figure 2-5. Chondrocyte and MC3T3-E1 seeding in polymeric scaffolds.

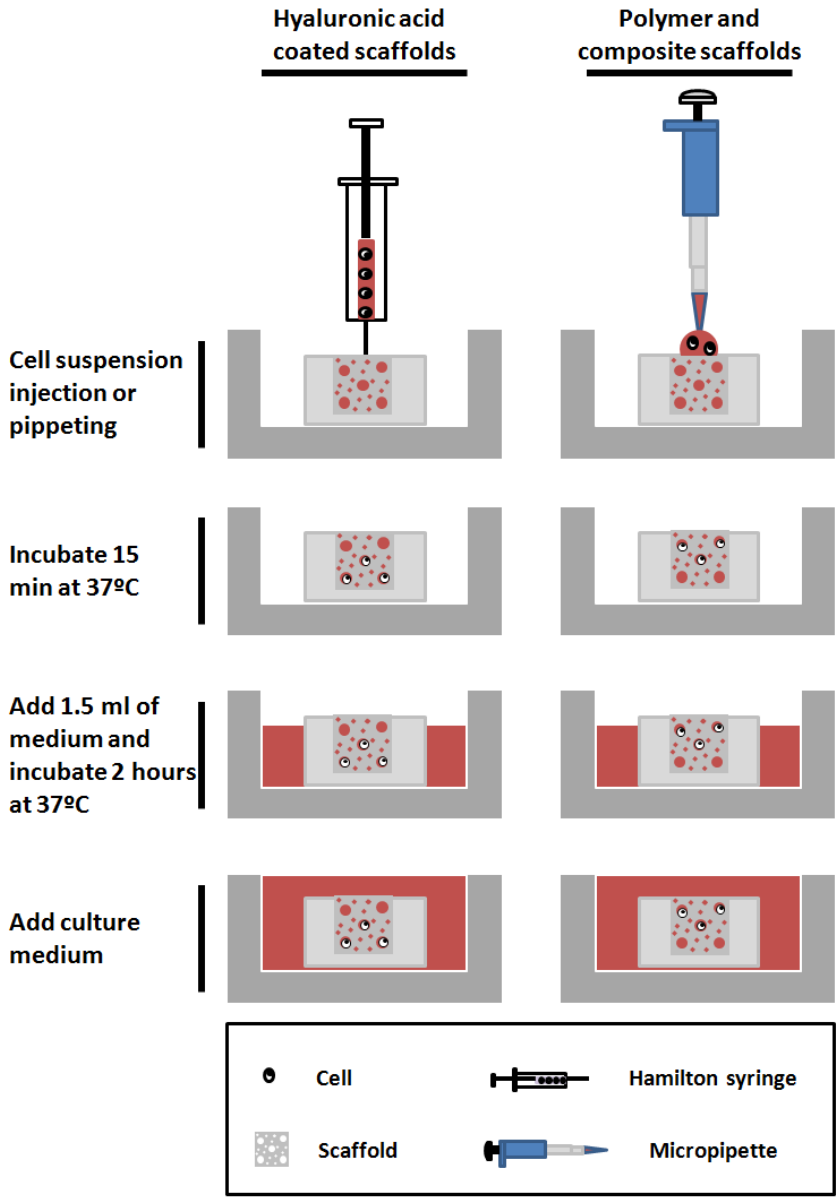

Figure 2-6. Mesenchymal stem cells seeding in polymeric scaffolds using agarose molds.

Finally polycaprolactone, Bioglass composite and hyaluronic acid seeded with MSCs were previously deposited on agarose moulds that surrounded all the samples sides except for the top side to improve the cell seeding. Mesenchymal stem cells were concentrated and injected (hyaluronic acid samples) or deposited in a drop on the scaffold top and incubated at 37ºC. Fifteen minutes after 1 ml of culture medium was added and they were incubated for 2 hours prior to cover the sample with cell culture (**figure 2-6**). MC3T3-E1 were seeded at $2.5X10^5$ cells/scaffold ($12.5X10^6$ cells/ml), chondrocytes at $4X10^5$ cells/scaffold ($10X10^6$ cells/ml) and mesenchymal stem cells at $5X10^5$ cells/scaffold ($10X10^6$ cells/ml).

On the other hand polycaprolcatone scaffolds used in co-culture experiments were sterilized with gamma ray radiation (25kGy performed by Aragogamma) and preconditioned with phosphate saline buffer. PCL scaffolds were coated with 20µg/ml of fibronectin for 1 hour. Fibronectin coated scaffolds were washed with phosphate saline buffer and seeded with the same protocol than mesenchymal stem cells. On the other hand tyramine substituted hyaluronic acid was sterilised by filtration and cells-hyaluronic acid mixture was injected on PCL scaffolds (**figure 2-7**) and crosslinked *in situ* as is described on **section 2.2.1.5.1**. Mesenchymal stem cells were seeded at $3X10^5$ cells/scaffold ($10X10^6$ cells/ml).

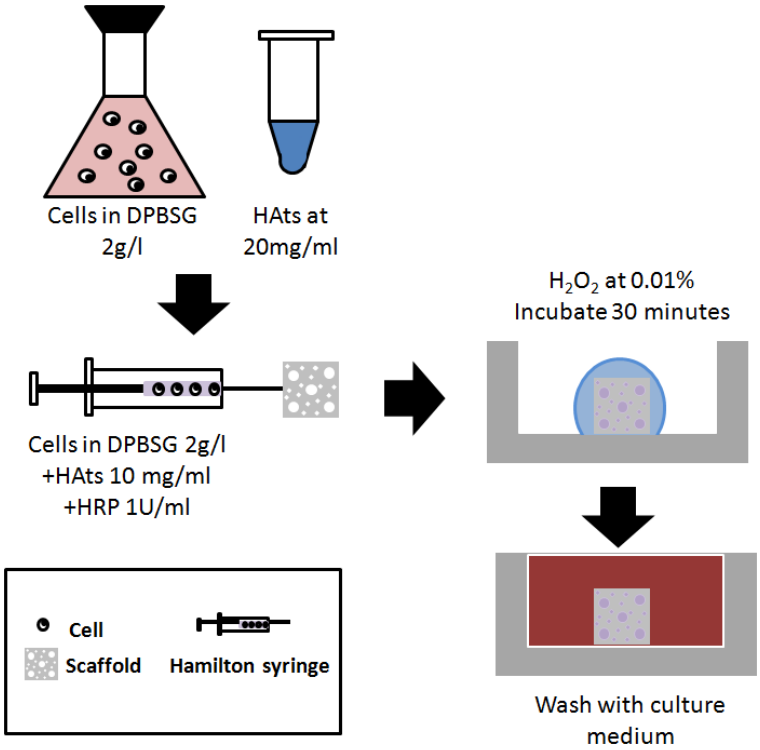

Figure 2-7. Cell seeding with tyramine substituted hyaluronic acid crosslinkable *in situ*.

2.2.3.2. Normoxia and hypoxia

Cell cultures were performed at 37ºC in normoxia conditions with a 20% of oxygen and 5% of carbon dioxide. On the other hand for cell culture in hypoxic conditions an incubator connected to a nitrogen flow was used to reduce the oxygen concentration to 5% and 5% of carbon dioxide.

2.2.3.3. Hydrostatic pressure

Cell culture stimulated with hydrostatic pressure was performed using a custom made bioreactor developed in the Trinity College Dublin. The bioreactor (sketch showed on picture 2-8) is a metallic cylinder filled with water in which the samples are immersed. The pressure cylinder is then sealed and connected to a compression machine that compresses water generating an intermittent hydrostatic pressure increment inside the vessel.

Figure 2-8. Sketch of the bioreactor system used to stimulate samples with hydrostatic pressure. (1-Water deposit valve, 2-Main system valve, 3-Pressure cylinder in-valve, 4-Pressure cylinder out-valve) To open the pressure cylinder to put or remove sealed plastic bags with samples valve 3 is closed and 4 open to remove cylinder cap. To fill the bioreactor valves 1, 2, 3 and 4 are opened. When the bioreactor is working only valves 2 and 3 are opened to transmit the hydrostatic pressure generated by fatigue testing machine through pneumatic piston.

To stimulate cells with hydrostatic pressure samples of each material, at day 14 they were divided in two groups and sealed inside sterile plastic bags with 2.5 ml/sample of chondrogenic culture medium during the loading period (3 weeks). The hydrostatic pressure group samples were placed inside the bioreactor and the free swelling control samples were placed into an open water bath, both inside a 37ºC incubator. The hydrostatic pressure loading protocol consisted in a dynamic pressure (max pressure 10MPa) at a frequency of 1 Hz for a period of 2hours/day five times each week.[134]

2.2.3.4. Co-culture

A co-culture study was designed to develop an indirect coculture system between chondrocytes and mesenchymal stem cells (**figure 2-8**). Chondrocytes were mixed with alginate to obtain $7X10^6$ cells/ml dissolved in 0.5% solution of alginate. Cell-alginate suspension was placed in negative teflon-agarose mould composed by a teflon part at the bottom part and an agarose mould over teflon. The bottom part was a rectangular teflon piece with vertical cylindrical inserts 3 mm in diameter and 3 mm height. Top part was a 3% agarose with 0.1M of calcium piece with 4mm height and holes of 8mm of diameter where the cell suspension is deposited that matched with the teflon inserts. The agarose mould part is made pouring molten agarose in a sterile plastic plate and putting a negative teflon mould to generate the holes. Chondrocytes-alginate construct is a cylinder of 8 mm in diameter and 4 mm height with a hole in the middle of 3 mm in diameter and 3 mm height (**figure 2-9**).

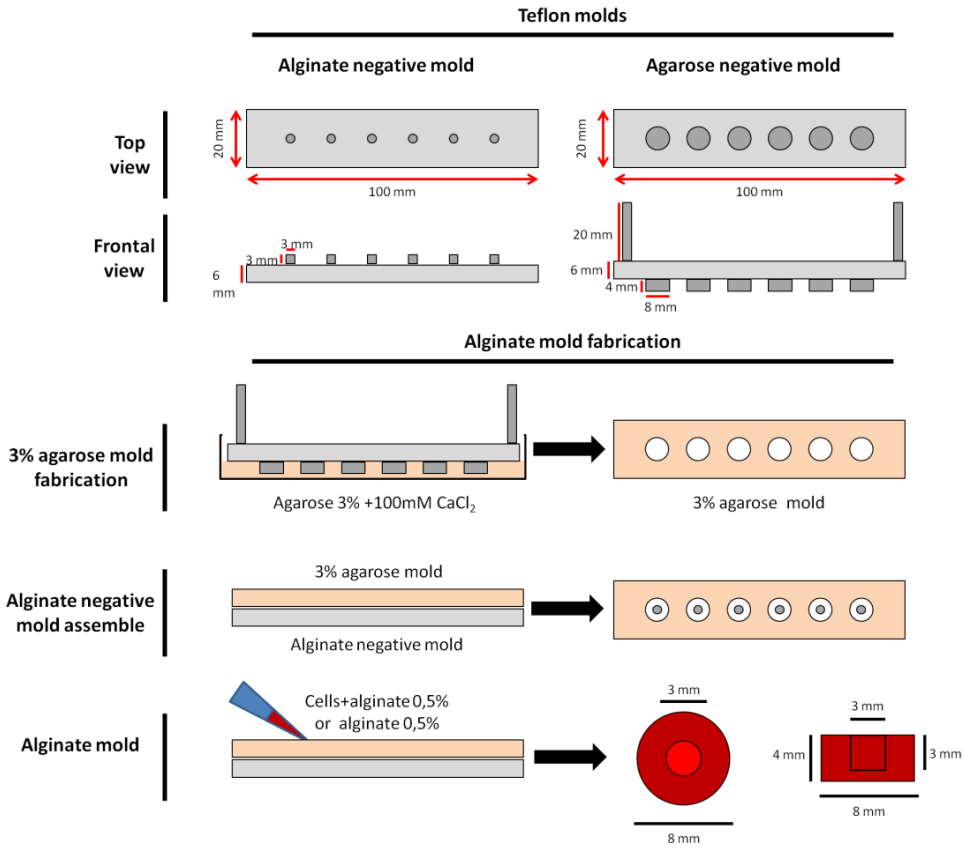

Figure 2-9. Alginate mold fabrication protocol.

Scaffolds seeded with mesenchymal stem cells were inserted in that hole. As a result the two types of cell were expected to grow separately and only can interact through soluble signals. Porcine mesenchymal stem cells were seeded at $3X10^5$ cells/scaffold and chondrocytes at $1.2X10^6$ cells/alginate gel and cultured with chondrogenic media under normoxia conditions for 35 days.

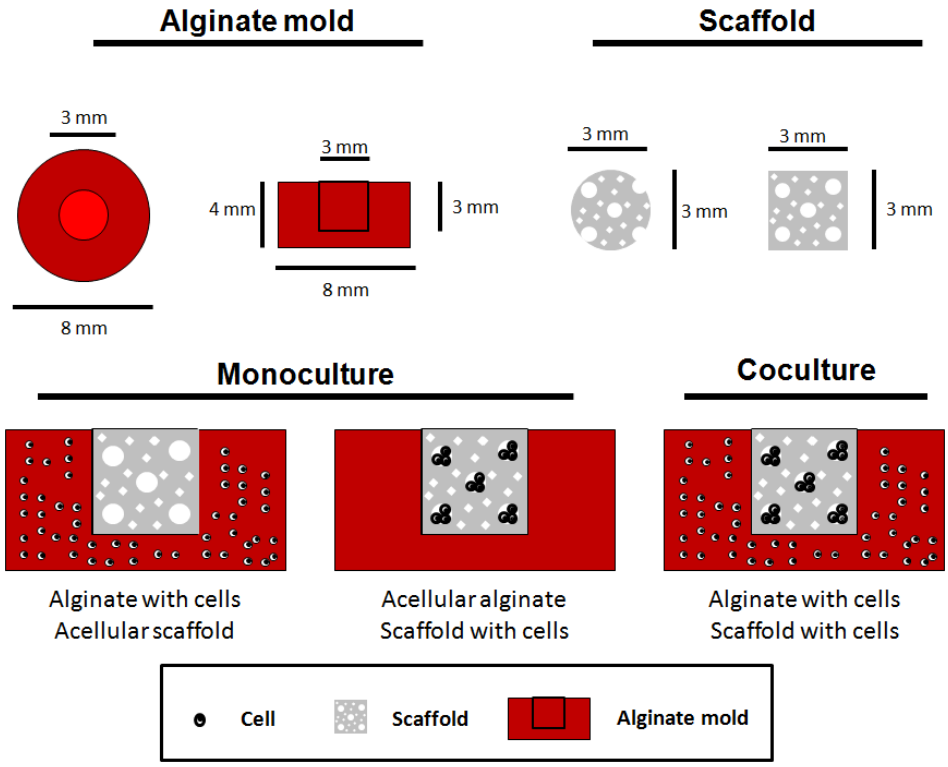

Figure 2-10. Co-culture sketch. Monocultures are defined as only one material with cells the alginate mold or scaffold and co-culture defined as scaffold and alginate mold seeded with cells.

2.2.4. Biological characterization

2.2.4.1. Cytotoxicity determined by MTS

Cytotoxicity was evaluated using a contact-free assay. Basal DMEM without phenol red with 1 % P/S was incubated with 5 % w/v of the samples to be tested and with latex (positive cytotoxic control) during 48 h at 37ºC. MC3T3-E1 cells were seeded in a P24 multiwell plate in standard growth medium without phenol red. At 24 hours, when reaching subconfluence, the medium was replaced with the medium

incubated with the materials (n = 3). The culture medium was removed after 24 h and medium with MTS reagent (dilution 1:5) was added. Cultures were incubated for 3 h in the incubator at 37º C protected from light and absorbance at 490 nm was read in a Perkin-Elmer VICTOR microplate reader. Metabolic activity was determined using a standard curve provided in the kit. [158]

2.2.4.2. Sample enzymatic digestion for biochemical assays

Biochemical analyses were performed on digested samples. Enzymatical digestion allows to solubilize the biomolecules to test and protect them from endogenous enzymes released from lysed cells. Samples were washed with DPBS and stored at -80ºC in a microtube until the analyses were performed. After thawing, cells were digested adding papain (Sigma-Aldrich) or proteinase K (Roche) and finally the sample was analysed or stored at -80º.

Papain digestion was performed incubating the samples during 18 h at 60°C adding 3.875 U/ml of enzyme in Activated Papain Enzyme Digestion Solution (100mM Sodium Phosphate Buffer, 5mM Na2EDTA, 10mM L-cysteine, pH 6.5). On the other hand proteinase K digestion was done at 60ºC during 16 hours followed by enzyme inactivation at 90ºC for 10 min with 50 µg/ml of enzyme dissolved in DPBS at pH 8.1. Samples were assayed immediately or stored at -80ºC. [158, 191]

2.2.4.3. DNA content

Total DNA content present in the samples was measured using P7589 Quant-iT PicoGreen dsDNA assay kit (Invitrogen) or DNA Quantitation Kit, Fluorescence Assay. Quantitation of DNA using PicoGreen reagent (invitrogen) and bisBenzimide H 33258 dye (Hoechst 33258) (Sigma) was performed following the manufacturer's instructions. Previous to the DNA quantification assay the samples were tested to determine the optimal dilution.

Samples and standards were put in a black P96 multiwell plate in triplicate and added 200 µl of working solution and then incubated 5 min at room temperature protected from light. The fluorescence for PicoGreen was read at 520 nm using a multiwell plate reader (VICTOR3 from Perkin-Elmer) and for Hoechst at 460 nm in a microplate reader (SynergyTM HT from BioTek). The DNA content was determined using the DNA standard calibration curve and the cell seeding efficiency as the sample's total DNA divided by the amount of DNA present in a cell and then divided by the theoretical number of seeded cells. [158,191]

2.2.4.4. Sulfated glycosaminoglycans content

The total glycosaminoglycans (GAGs) content present in the samples was measured using Blyscan assay kit (Biocolor), a modified version of 1,9-dimethylmethylene blue assay following the manufacturer's instructions. Previous to the glycosaminoglycans quantification assay the samples were tested to determine the optimal dilution.

Samples and standards were spun and the optimal volume of supernatant was diluted with papain buffer extract up to a total of 200ul and mixed with 1 ml of Blyscan in a

centrifuge microtube. Samples were incubated for 30min in an orbital shaker and then were centrifuged at 15000g for 10 min and supernatant was discarded. The resulting precipitate was dissolved in 1 ml dissociation reagent and placed at 200µl/well in P96 multiwell plate and absorbance was read at 656nm in a microplate reader (SynergyTM HT from BioTek or VICTOR3 from Perkin-Elmer). Quantities of sulphated glycosaminoglycan were determined from a calibration curve performed using chondroitin sulphate standard provided in the kit.[191]

2.2.4.5. Hydroxyproline content

Collagen content present in the samples was measured determining the hydroxyproline content using the protocol described by Kafienah.[154] Previous to the hydroxyproline quantification assay the samples were tested to determine the optimal dilution.

Samples were spun and the optimal volume of supernatant was mixed with papain buffer extract up to a total sample volume of 200µl, then 200µl of 38% HCl was added and incubated 18h at 110ºC. Samples were dried by evaporation at 45ºC and then samples dissolved in 200 µl of MiliQ water. Finally, 60 µl/well were put in P96 multiwell plate and was mixed Chloramine T reagent to allow for hydroxyproline oxidation. Finally 4-(Dimethylamino)benzaldehyde reagent was added. The amount of hydroxyproline was measured by reading the absorbance at 570nm in a microplate reader (SynergyTM HT from BioTek or VICTOR3 from Perkin-Elmer). Quantities of hydroxyproline were determined from a calibration curve realized using hydroxyproline standard and the amount of collagen was calculated using a value of hydroxyproline-to-collagen ratio of 1:7.69.[155]

2.2.4.6. Collagen type II and X ELISA

Collagen type II and X presence in the sample was measured through a colorimetric immunoassay. The Enzyme-linked immunosorbent assay for collagen type II (Collagen type II ELISA, mdbioproducts) was performed using a heterogeneous sandwich ELISA and collagen type X (Porcine collagen type 10 (CoL-10) Elisa kit, BlueGene) was quantified with a competitive enzyme immunoassay technique. The assays were performed following the kit's user manual

Samples were washed with DPBS and stored at -80ºC. Samples were homogenized in 200 µl of cold NaCl 0.9% solution. Samples were sonicated 5 min and centrifuged at 1500 g for 15 min. Then 100 µl of supernatant was stored at -80ºC for Collagen type X assay. Remaining sample with construct debris was mixed with 450 µl of pepsin at 1.1 mg/ml (pepsin from porcine gastric mucosa, Sigma) in 62.5mM of acetic acid (pH=3.00) and incubated for 72 h at 4ºC with gentle mixing. After the incubation period 50 ul of TBS 10X (1M Trizma® base, 2M NaCl, 50mM $CaCl_2$ in water) were added and samples adjusted to pH 8.00. Then 50 ul of elastase (Elastase from porcine pancreas; Sigma) were added and incubated for 24 h at 4ºC with gentle mixing. Samples were removed and centrifuged at 10000 rpm for 5 minutes. The supernatant was collected and stored at -80ºC.

Collagen type II ELISA was performed following the kit's user manual. Samples and standards were pipetted at 100 µl on coated multiwell plate and incubated for 2 hours. Microplate was washed 6 times with 200 µl of wash buffer. 100 µl of conjugated antibody were added and incubated for 2 hours. After washing the plate, 100 µl of streptavidin-HRP were added and incubated for 30 min. Wells were washed and 100 µl of substrate were added and incubated for 20 minutes. Finally the reaction was stopped with 100 µl of stop solution. The absorbance was read at 450 nm with the Perkin-Elmer VICTOR3 multiplate reader.

Collagen type X ELISA protocol. Samples and standards were pipetted at 100 µl and 50 ul of conjugate on coated multiwell. The multiwell plate was incubated for 1 hour at 37ºC. Samples were washed 5 times with 400 µl of wash buffer. Then 50 µl of substrate A and substrate B were incubated for 15 minutes at 37ºC and stopped with 50 µl of stop solution. The absorbance was read at 450 nm with the Perkin-Elmer VICTOR3 multiplate reader.

2.2.4.7. Alkaline phosphatase analysis

The alkaline phosphatase (ALP) presence in the sample was measured both in released form from the culture medium as well as in intracellular form by measuring the activity of lysed cells extract.

Activity of alkaline phosphatase as the conversion of P-nitrophenyl phosphate to p-nitrophenol was measured as the result number of product millimol obtained by the activity of a cellular extract. Samples were washed with DPBS and then fragmented using a scalpel and dispersed in lysis buffer (0.2 % Triton X-100, 10 mM Tris–HCl pH 7.2) on ice for 7 min, and further sonicated for 2 min. The samples were centrifuged at 13000 rpm at 4ºC for 7 min to precipitate cellular and scaffold debris. Supernatant was mixed (1:1) with p-nitrophenylphosphate (p-nitrophenyl phosphate, Sigma) at 1 mg/ml and incubated for 2 h at 37ºC. Reaction then was stopped adding 1 M NaOH. Finally aliquots of 100 µl were put in a P96 in duplicate and were read at 405 nm with the Perkin-Elmer VICTOR3 multiplate reader. The p-nitrophenyl phosphate conversion was determined using a nitrophenol standard curve. [158]

The amount of ALP released to the media was determined measuring the substrate conversion using SensoLyte® pNPP Alkaline Phosphatase Assay kit *Colorimetric*

(AnaSpec) following the manufacturer's instructions. Samples were collected from the culture media 2 days after the media change. The samples were centrifuged at 1500 rpm for one minute to precipitate cellular and scaffold debris. Supernatant was placed at 50µl/well in triplicate in P96 well plate, and then 50 µl of colorimetric alkaline phosphatase substrate was added and incubated for 40 min at room temperature protected from light. The absorbance was read at 405 nm with the Perkin-Elmer VICTOR3 multiplate reader. Sample's ALP content was determined using the enzyme standard calibration curve.

2.2.4.8. Scanning electron microscopy and CryoSEM

The cell distribution and morphology was analyzed using scanning electron microscopy. Samples were fixed with 2.5% glutaraldehyde 1 hour at 4ºC. The samples were washed and stored in DPBS at 4ºC. The samples were dehydrated through a series of increasing percentages of alcohol and finally dried at air. Samples were mounted on copper stubs with a graphite conductive tape and gold sputtered. The microscope used for both methodologies was a JEOL JSM6300 scanning electron microscope at an acceleration voltage of 15 kV. [158, 191]

2.2.4.9. Sample inclusion

Samples were fixed, included in a inclusion media and cut to obtain the tissue sections used to staining protocols. Samples for microscopy were washed in DPBS and fixed with 10% neutral buffered formalin (1 hour at 4ºC) for optimum cutting temperature compound embedding and 4% paraformaldehyde (16 hour at 4ºC) for

polyester wax embedding. Samples were washed twice with DPBS to remove the fixing agent and stored in DPBS 4ºC.

Optimum cutting temperature compound (Tissue Tek) embedded samples were incubated in 30 % of sucrose solution overnight. Samples were wiped in order to remove excess solution, included in a mould with optimum cutting temperature compound and frozen rapidly at -80ºC. The embedded scaffolds were cut longitudinally using the cryotome Microm HM 500 at -30 ºC in 200 µm thick sections. Sections were washed gently with DPBS two times to eliminate optimum cutting temperature compound. On the other hand polyester wax (Electron Microscopy Sciences) embedded samples were first dehydrated through a series of increasing percentage alcohol substituting the water with ethanol, after this was immersed in absolute ethanol/ polyester wax 50:50 overnight and finally included in a mould with polyester wax and cured 48 hours at room temperature. The embedded scaffolds were cut longitudinally using the microtome Leica RM2025 in 10 µm thick sections. [158, 191]

2.2.4.10. Immunostaining

Presence of cell proteins used as differentiation markers was determined through immunostaining, performed as immunofluorescence or immunohistochemistry.

Immunofluorescence samples were washed to remove the mounting media and permeabilized to allow the antibody diffusion. Samples were incubated in presence DPBS with bovine serum albumin (BSA) at 1% to avoid the antibodies non specific binding points. The primary antibody diluted to the optimum concentration in DPBS with BSA at 1% was incubated with the sample and washed with DPBS/TWEEN

0.5% to remove non specific bindings. The antibodies chosen were divided in osteogenic markers, chondrogenic markers and adhesion proteins. Osteogenic markers selected were osteocalcin (Abcam) and Runx2 (Abcam). Positive chondrogenic markers used were collagen type II (Chemicon International), aggrecan (Invitrogen) and CD-44(Abcam) while collagen type I (Chemicon International) was used as negative marker. Adhesion protein markers were integrin α5 (Santa Cruz Biotechnology), α_V (Millipore), β_1 (Millipore) and CD-44 (Invitrogen). To reveal staining the samples were incubated in presence of immunofluorescence conjugated antibody Alexa 488 (Invitrogen) or Alexa 647 (Invitrogen) and FICT conjugated phalloidin (Invitrogen) diluted both in DPBS with BSA at 1%. Finally samples were mounted with Fluorsave Vectashield mounting medium with DAPI (Atom). Pictures were taken using an immunofluorescence or a confocal microscope.

Immunohistochemical staining of collagen type I (Abcam) and Collagen type II (Chemicon International)was carried out following a modified Dako kit staining protocol (EnVision®+dual Link System-HRP, DakoCytomation), adding an antigen retrieval step after endogenous peroxidase activity inactivation. After endogenous peroxidase inactivation, samples were incubated with pepsin (5mg/ml in 5mM HCl) 45 minutes at 37ºC. The samples were blocked with DPBS with BSA at 1% and incubated in presence of primary antibody. After antibody incubation the samples were washed and incubated in presence of HRP-labelled polymer. Finally the sample was revealed adding the substrate-chromogen, dehydrated and mounted with Entellan mounting media (Electron Microscopy Sciences). Pictures were taken using a stereoscopic microscope (Leica MZ APO).

2.2.4.11. Histochemistry

Presence and distribution of cells and ECM components was determined through different histochemistry staining.

Histological staining for mineralization of fresh tissue samples was the Von Kossa staining. Samples were cut at 1 mm thick with a scalpel, washed with distilled water and incubated in 5 % AgNO3 (Sigma) for 20 min under ultraviolet light. Samples were washed with distilled water and revealed incubating in 2% Na2S2O3 (Sigma) for 2 min. Then samples were washed in distilled water and counterstained with neutral red solution (Fluka) for 2 min. Finally the samples were dehydrated through washes in solutions of increasing grade ethanol and after air drying for later viewing using a stereoscopic microscope (Leica MZ APO).[158]

Collagen, glycosaminoglycans and calcium staining was performed on polyester wax tissue sections. Samples were deparaffined with ethanol 100% and rehydrated with deionised water. Samples were stained for GAGs with 1% Alcian Blue for 30 min, washed with water and counterstaining for nuclei with 0.1% nuclear fast red for 5 minutes. Collagen staining was performed with 0.1% Picro-Sirius for 30 min, washed with acetic acid 0.5% and water. Cells were counterstained with Harris hematoxylin 5 min. ECM calcium deposits were detected with alizarin red. Samples were immersed tin 2% alizarin red solution for 2 minutes to remove the dye excess. Finally the samples were washed with water, dehydrated and mounted with Entellan mounting media (Electron Microscopy Sciences) for later viewing using a stereoscopic microscope (Leica MZ APO).

2.2.4.12. Dynamic mechanical analysis of cell-scaffolds constructs

To determine the effect of ECM grown inside the pores over the mechanical properties, the equilibrium and dynamic modulus were determined using a Zwick Z005 (Roell) with 5N load cell for samples of 5 mm diameter and a thermal mechanical analyser for samples with a diameter of 3mm. Elastic modulus was determined using the Microtest Universal testing machine at different time points.

Eventually the elastic modulus was determined using the Microtest Universal Testing Machine with a 15 N load cell. In order to preserve the samples for future biochemical assays a non-destructive test was performed. Five cycles of compression were applied until 15% of deformation was reached. First curve was discarded to study the elastic modulus after the plastic deformation that would be present in a physiological load. Elastic modulus was determined as the slope of initial segment of the second cycle curve. On the other hand analysis for equilibrium and dynamic modulus was performed as is described on **section 2.2.2.9.**

2.3. Statistical analysis

Samples homogeneity was analyzed doing a Levene's test to choose the correct statistical analysis. If Levene's test was positive a Student t-test or one factor ANOVA was chosen; but if it was negative a non-parametric test was used; differences were considered significant for $p<0.05$. In all figures, error bars represent standard deviation.

RESULTS AND DISCUSSION.

3. MACROPOROUS PCL COMPOSITE SCAFFOLDS FOR BONE TISSUE ENGINEERING: RESULTS AND DISCUSSION

3. Macroporous PCL composite scaffolds for bone tissue engineering: Results and discussion.

3.1. Abstract

The present chapter contains the results obtained in the development of a polymer-ceramic composite scaffold for bone tissue engineering as part of a project focused in obtaining a prototype for spinal fusion applications. Spinal diseases usually require intervertebral joint immobilization that can be performed with pedicle screw devices or bone graft implantation, but for long term stability, bone formation between vertebrae is required.[17,156] For spinal fusion, the preferred type of graft is the bone autograft but it is limited by availability and donor site morbidity.[17,156] This is why other graft types as allografts and synthetic materials are proposed, in spite of the known drawbacks associated to allogeneic transplants or synthetic biopolymers. [156] The objective of this study was to develop and characterize a composite scaffold from the beginning up to *in vivo* evaluation for its application as spinal fusion strip prototype. Composite scaffolds are a great approach for designing bone substitutes because they combine the advantages of two biomaterials classes[9], bioactive inorganic materials and polymers. Composite scaffolds used in this work were based on synthetic biodegradable polymers such as PCL or PLLA[63] scaffold. For this work hydroxyapatite nanoparticles or 45S5 Bioglass® microparticles were selected as bioactive inorganic material for reinforcement as they are similar in composition to bone mineral phase (HAp)[89] and promote cell differentiation (BG)[157].

Spinal fusion strip prototype development was divided in four steps. (I) Characterization and validation of ceramic-polymer composite scaffolds. (II) Development of several composite scaffolds series with different compositions. (III) PCL/PLLA composite scaffolds degradation study and (IV) *in vitro* selection and *in*

vivo evaluation. Physical properties were measured (mechanical behaviour, morphology, composition, stability in physiological medium) and biological response was characterized using osteoblast-like cells and animal model. The *in vivo* study was beyond the scope of the present thesis although it was part of the global project. The results obtained in the experiments performed at Inasmet Tecnalia (*in vitro* evaluation) and at Instituto de Biomecanica de Valencia (*in vivo* evaluation) are presented for the sake of global comprehension of the general design process.

3.2. Characterization and validation of ceramic-polymer composite scaffolds.

The objective was developing PCL composite scaffolds containing ceramic reinforcement to test the viability of the fabrication process and characterizing them as candidates for a spinal fusion strip. Composite scaffolds were prepared using PCL solutions with different amounts of mineral particles (5, 10 and 20 % by weight with respect to PCL). Morphological, mechanical and other physical properties were measured as a function of scaffold composition and biological characterization was performed using MC3T3-E1 cell line under normoxia conditions. Cells were seeded at 250000 cells/scaffold with culture medium for osteoblast differentiation and cultured for 28 days. This work has been published in the Journal of Materials Science: Materials in Medicine entitled "Comparative study of PCL-HAp and PCL-BG composite scaffolds for bone tissue engineering."[158].

Samples	Polymer composition	Ceramic reinforcement
PCL	Polycaprolactone	-
PCL-5BG	Polycaprolactone	5% Bioglass
PCL-10BG	Polycaprolactone	10% Bioglass
PCL-20BG	Polycaprolactone	20% Bioglass
PCL-5HAp	Polycaprolactone	5%HAp
PCL-10HAp	Polycaprolactone	10%HAp
PCL-20HAp	Polycaprolactone	20%HAp

Table 3-1. Table with tested samples composition.

The influence of mineral reinforcement over the scaffold features was performed with mechanical tests in compression, TGA analysis and EDX analysis.

The influence of different composite scaffolds over MC3T3-E1 differentiation was assessed using biochemical quantitative analysis of DNA and ALP as well using immunofluorescent staining of Runx2 and osteocalcin.

"Present section was removed due to copyright statements. Section content is available in Ródenas-Rochina J, Ribelles JL, Lebourg M. Comparative study of PCL-HAp and PCL-bioglass composite scaffolds for bone tissue engineering. Journal of Materials Science: Materials in Medicine 2013; 24:1293-308"

3.3. Development and evaluation of polymer based composite scaffolds: Development of composite scaffolds series and characterization.

This subchapter was developed as part of Cenit Intelimplant project coordinated by Tequir I+D+i and funded by Spanish Ministry of Industry, Tourism and Commerce through INGENIO 2010 program. The objective was developing a spinal fusion strip prototype and proceeding to its *in vivo* evaluation. The objective of this section was the development of particular materials in the line of those described in the preceding section but addressed to the intended application in the framework of Cenit Intelimplant project.

In this project, scaffolds as described in the former section were used with different surface modifications. Here, a different polymer (polymer 2) was added to the formulation still looking for a less compliant matrix and higher degradation rate. Polymer 1used in this work is a quite compliant material even if the objective is the development of a vertebral fusion strip that must sustain low loading after implantation during bone invasion. Moreover, degradation of polymer 1 is very slow and may not be adapted to the rate of bone remodelling, which is relatively fast. Composite scaffolds were prepared using polymer 1 and polymer blends solutions with mineral particles. Samples were cut to 2 different sizes. Samples for mechanical test were 4x4x7 mm^3 and samples for remaining physico-chemical tests were 4x4x4 mm^3. Finally sample's surface was modified with plasma treatment, nucleation or hydroxyapatite coating.

The effect of polymer blends and mineral reinforcement was determined using SEM, compression mechanical test and DSC analysis.

Samples compositions were omitted due to a confidentiality agreement between the center and the company owner of the results.

3.3.1. Morphology and microstructure

Figure 3-1 shows the developed samples. All samples showed the same interconnected porous structure with a high porosity with a bimodal pore structure divided in macropores and micropores. Macropores were obtained after porogen removal along the particle leaching and micropores as consequence of dioxane crystallisation along the phase separation induced by the freeze extraction as described in the previous section. Mineral particles addition did not show any important effect over the scaffold architecture or pore structure but surface roughness was increased. On the other hand EDX spectroscopy analysis, was performed to confirm if mineral particles are present on the pore wall surface. The EDX spectrum (**figure 3-2**) of both mineral particles composite samples surface showed the peaks corresponding with the expected respective mineral particles formula. Composition 13 and composition 17 showed calcium and phosphate peaks that corresponds to expected spectrum for mineral particles 1 introduced. On the other hand composition 9 showed specific element peaks that matched with mineral particles 2 composition.

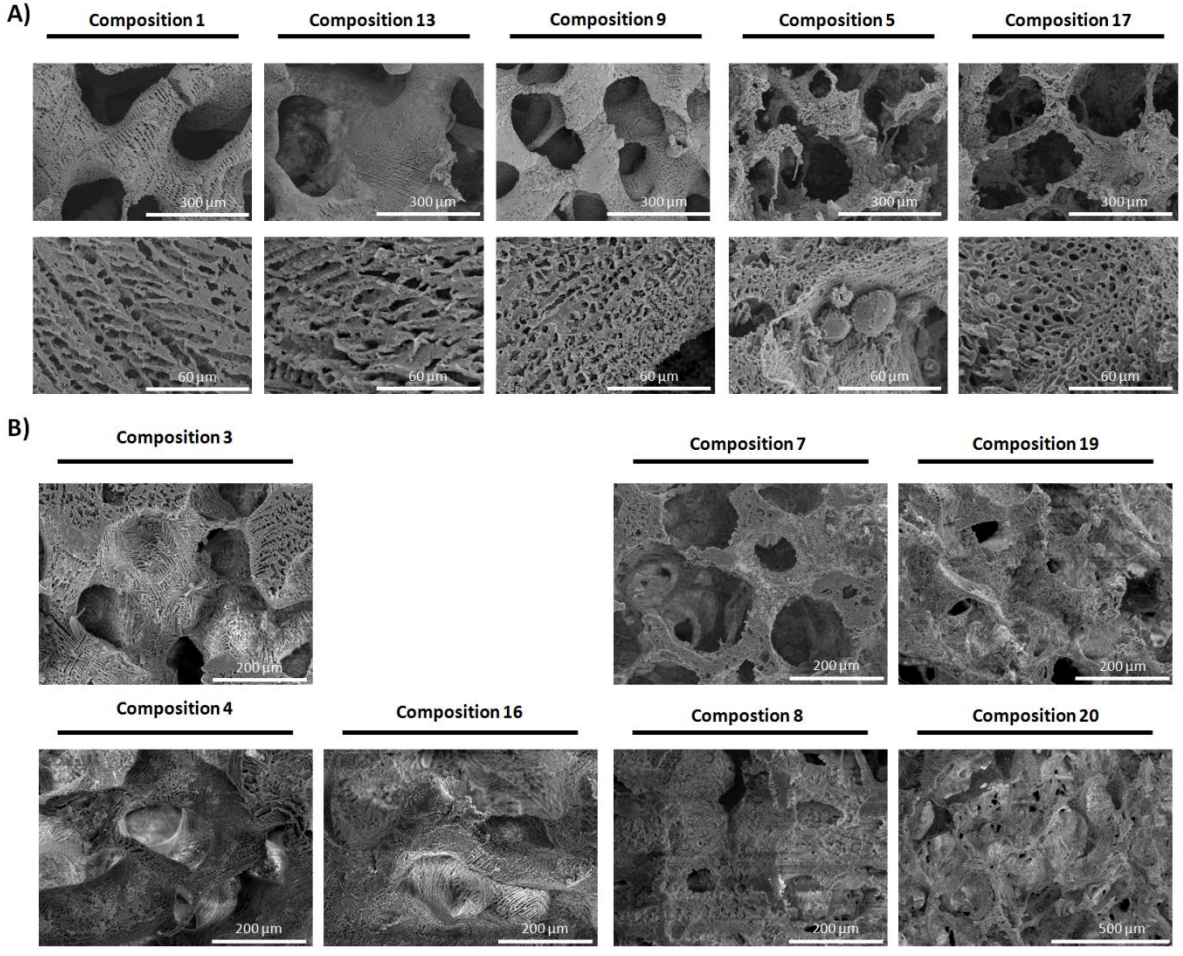

Figure 3-1. Micrographs of developed scaffolds (A). Micrographs of developed scaffolds (B). (magnification/scale bar = X100/500 µm; X200/300 µm and X1000/60 µm).

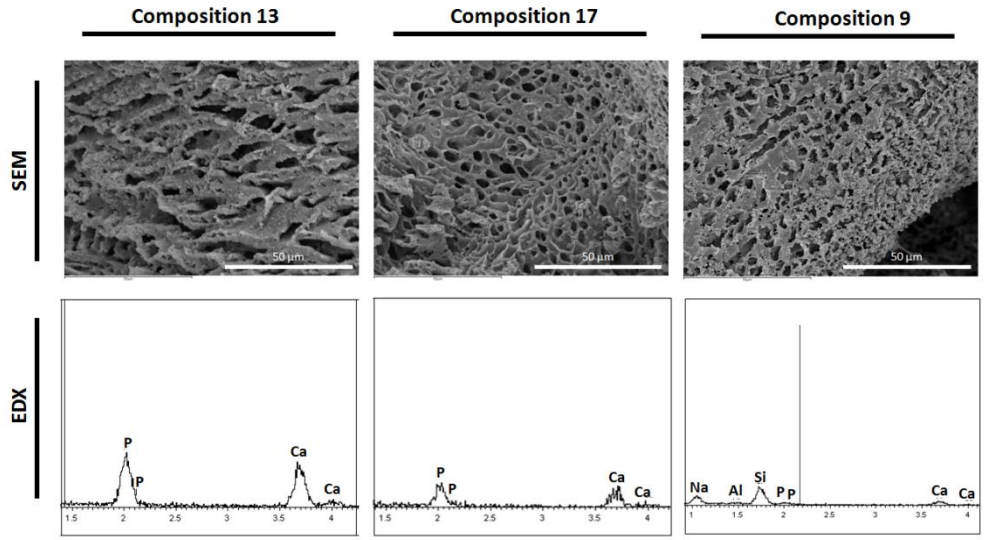

Figure 3-2. Micrographs and energy-dispersive X-ray spectroscopy spectra of scaffolds. (magnification/scale bar = X1000/50µm).

Nucleation and coating treatment were performed to increase scaffold bioactivity. Samples with nucleation and coating treatment at low magnifications did not show any differences over scaffold structure. On the other hand at high magnifications a mineral layer was observed coating part of the scaffold surface hiding the micropores. In order to determine if layer composition was calcium phosphate crystals, it was analyzed with EDX spectroscopy. EDX results show that surface treatments allow the growth of phosphate-calcium crystals. Plasma treatment combined with nucleation allows calcium phosphate crystal nucleation on the sample surface confirmed by the EDX spectroscopy spectrum that showed calcium and phosphate presence. On the other hand, samples that were subjected to the complete coating protocol (plasma, nucleation and coating) exhibited the presence of typical “cauliflower-like" structure of biomimetic hydroxyapatite.

Polymer blend scaffolds (composition 5 and composition 17 scaffolds) showed a particular microstructure characterized by dispersed spherical aggregates (**figure 3-1**) on the pore walls. Polymer blend seems not to compromise the correct scaffold structure where macropores are still well interconnected, although trabeculae are thinner and with a more irregular shape. On the other hand composition 5 and composition 17 showed a statistically significant porosity increment compared to composition 1 scaffold.

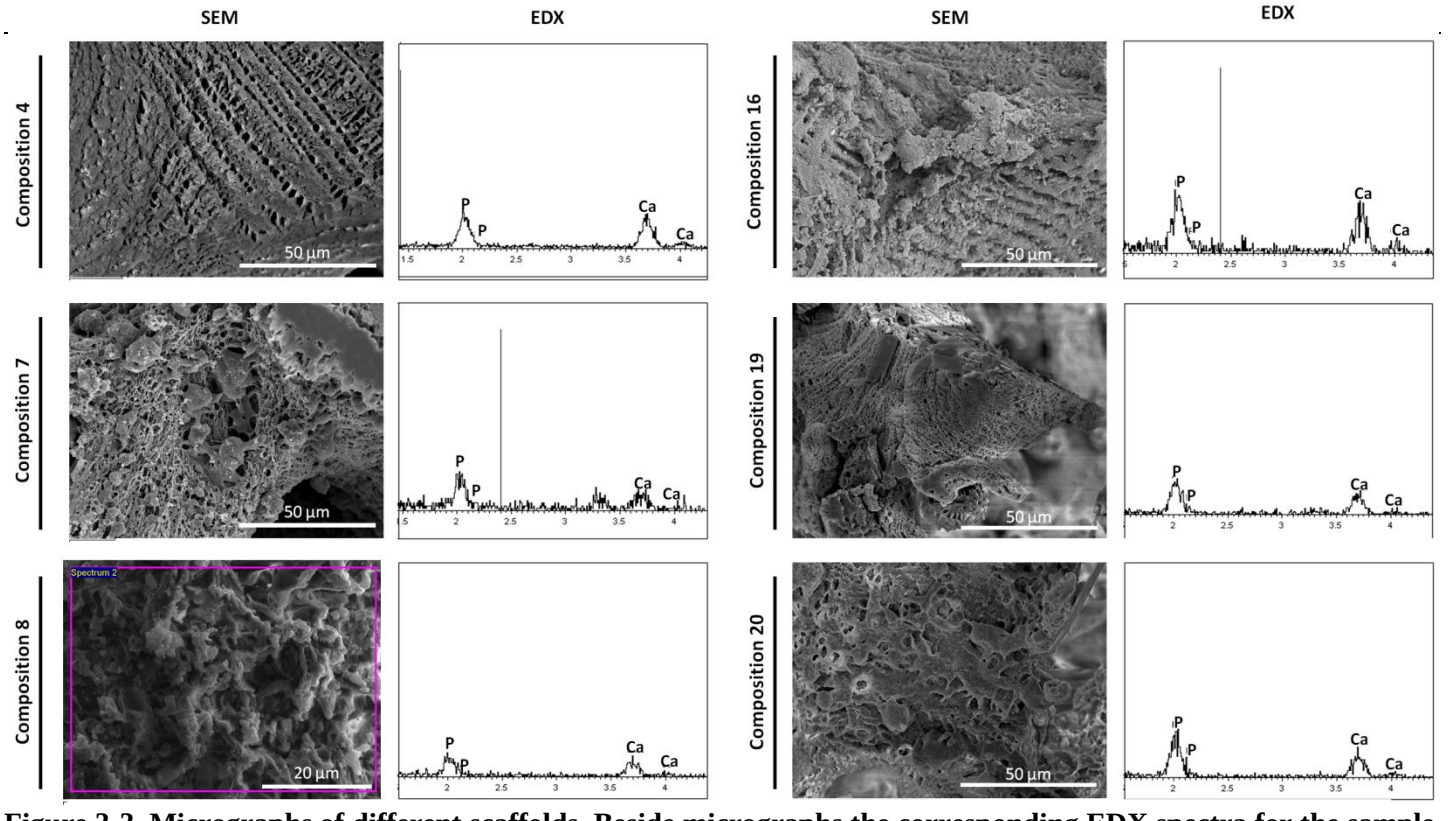

Figure 3-3. Micrographs of different scaffolds. Beside micrographs the corresponding EDX spectra for the sample surfaces are shown. (magnification/scale bar= X1000/50 µm).

3.3.2. Crystallinity and ceramic content.

Heating thermograms obtained with DSC are shown in **figure 3-4**. Thermograms showed that polymer blend samples have two melting points corresponding to polymer 1 and polymer 2. Melting temperature of polymer 1 phase is very close to that of pure homopolymer scaffold. Mineral particle inclusion produced a slight reduction of melting temperature. Crystallinity was calculated from the DSC heating thermograms (**table 3-2)**. For composition 1 scaffolds crystallinity changes from 67.9% for bare samples to 66.4% for composition 13. In composition 5 crystallinity of polymer 1 was a 10% lower compared to composition 1 scaffold. On the other hand introduction of mineral particles in the compostition 17 decreased more dramatically the crystallinity than in composition 13. In composition 17, polymer 1 crystallinity was reduced around a 8% compared to composition 5 wich polymer 2 phase crystallinity decreased around 17% whereas in composition 13 crystallinity only dropped about 2% with respect to composition 1.

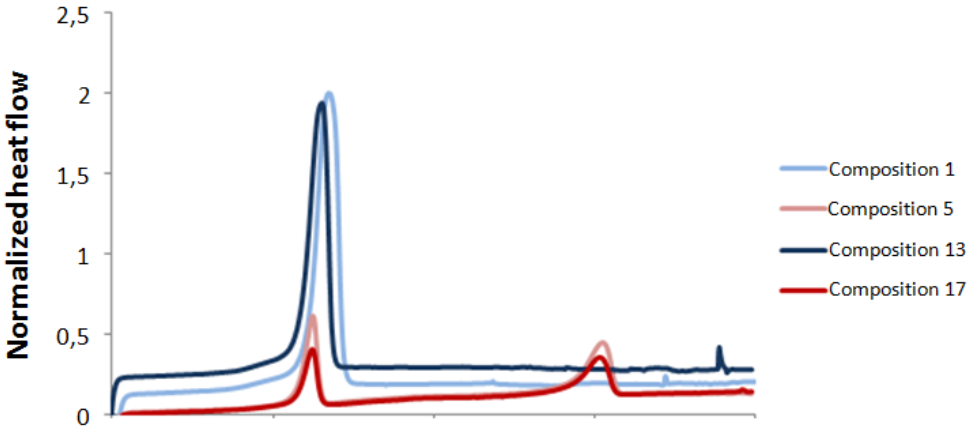

Figure 3-4. Differential scanning calorimetry graphs of developed scaffolds.

Percentage of ceramic phase shown in **table 3-2** was determined through the residue obtained after pyrolysis of composite samples. Tested samples showed a mineral content smaller than expected. Reinforcement content was around 6% lower than the theoretical one in mineral particles containing samples (composition 13 and composition 17) the difference was still higher in the case of composition 9 that had a 16% mineral content less than theoretical.

3.3.3. Mechanical properties

Table 3-4 presents the values of the mechanical properties (elastic modulus and yield strength) for the fabricated scaffolds. Introduction of mineral particles 1 reduced the elastic modulus whereas mineral particles 2 increased it, differences in both cases are small but statistically significant. Composition 5 showed higher mechanical properties with an elastic modulus 7 times higher than composition 1 samples. On the other hand, mineral particles 1 introduction in composition 17 scaffolds decreased dramatically the mechanical properties although the modulus of composition 17 is still higher than that of composition 1 and composition 13 scaffolds.

	Porosity (%)	Solid residue		Mechanical properties		Crystallinity	
		Mean (%)	Diff. (%)	Elastic modulus (MPa)	Yield strength (MPa)	Xpol1	Xpol2
Composition 1	87.7 ± 1.1			0.55 ± 0.12	0.06 ± 0.01	67.9	
Composition 13	87.8 ± 0.1	19 ± 0.2 **	-4.9	0.38 ± 0.07 *	0.05 ±0.01 *	66.4	
Composition 9	83.9 ± 1.5 *	16.7 ± 0.2	-16.7	0.8 ± 0.07 *	0.11 ± 0.01 *		
Composition 5	89.2 ± 0.4 *			3.94 ± 0.45 *	0.23 ± 0.07 *	60.2	26.5
Composition 17	90.5 ± 0.5 *	18.7 ± 0.4 **	-6.3	1.12 ± 0.28 *	0.07 ± 0.01	55.6	22.1

Table 3-2. Total porosity, solid residue analysis, crystallinity and mechanical analysis of the different scaffolds. The Diff. (%) means the difference in the amount of microparticles detected in the composites and the nominal value. Samples that show significant differences ($p<0.05$) with composition 1 sample are pointed with (*) and (**) for samples compared to composition 9.

3.3.4. Discussion

Polymer 1 is a semicrystalline polymer with a viscoelastic behaviour that is very interesting for different tissues, but quite compliant for bone substitutes even to sustain the low loading to which the vertebral fusion strip is subjected after implantation during bone invasion. In the previous section the particulate mineral filler plays the role of increasing the stiffness of polymer matrix, in addition to provide the scaffold with bioactive properties. To further increase stiffness of the polymeric component of the hybrid scaffold polymer blends of with other biodegradable polymers were used in present part of the work.

The pore architecture described above was considered adequate for invasion of bone tissue and vascularization. It was shown that the different modification of the material blending polymer 1 with polymer 2 or increasing the mineral content did not alter the general characteristics of the pore size and interconnectivity. As in the previous section, mineral particles 1 or mineral particles 2 reinforcement did not have any effect over scaffold structure but increased surface roughness as a consequence of mineral particle presence on the polymer surface. Polymer blending only showed a slight effect over scaffold structure and showed heterogeneous polymer structures on scaffold's pore walls compared to composition 1 scaffold. In our blends the polymer that was present in lower proportion was isolated in small spherical domains included in a continuous matrix of the other polymer. These structures were a consequence of phase separation between polymer 1 and polymer 2. Phase separation takes place when the solution in solvent is frozen as a first step of freeze extraction. At room temperature the solution of polymer 1 and polymer 2 in solvent is homogeneous but on cooling, not only solvent crystallizes, but also the two polymers crystallize or vitrify. In addition porosity in blends was statistically higher than composition 1 reference control. Porosity increment was related with

microporosity because the polymer concentration in the initial solution in blends was at 15% compared to 20% in other samples. Micropores are dependent of polymer/solvent proportion because freeze extraction technique generated the micropores when the solvent (solvent A in the present work) starts to crystallize after thermally induced phase separation between solvent and polymer. When the solvent proportion increased the number of micropores increased too increasing global porosity. The difference in the solution concentration was forced by the high viscosity of blend; moreover, homogeneous solutions of polymer 1 and polymer 2 in solvent could not be obtained at concentrations higher than 15%.

Ceramic content determined by the residues of pyrolysis was smaller than expected by the amount of mineral mixed in the initial solution, as happened in the previous section. Mineral loss can happen during freeze extraction if mineral particles get trapped inside the solvent phase; there may also be some release of poorly bound particles at the surface of the samples during the process of particle leaching. In composition 9 samples, the highest particle loss could be consequence of mineral particles dissolution in ethanol along particle leaching. On the other hand SEM showed that mineral particles were quite apparent on pore walls surfaces (**figure 3-2**) not only as deduced by the increase of roughness with respect with pure polymer scaffolds but its presence is also confirmed by EDX spectroscopy. Their presence on pore surfaces may not only allow to interact with the environment directly, but it may also increase protein adsorption[75] and mineral precipitation from body fluids[177]. On the other hand, the exhibition of mineral components on the pore walls was further improved using surface treatments. Synthetic polymer scaffolds have a low intrinsic bioactivity[9]. The first step of surface modification consisted in plasma treatment intending to increase the density of carboxyl groups on the polymer surface that can improve wettability and higher negative charge may favour both mineral deposition and cell adhesion.[82,83] The second step in order to

modify the surface of the implant was a nucleation treatment, in order to form crystallization nuclei on which calcium phosphate coating can later develop. The third and last step used for increasing bioactivity was a coating protocol using simulated body fluid. Coating follows previous treatments and consists in incubating the samples in simulated body fluid to allow the mineral deposition and hydroxyapatite crystal growth. As a result of this treatment, a layer of cauliflower shaped biomimetic hydroxyapatite is expected to be deposited, as described extensively in the literature[36,38]. This was observed in our work, where the coating formed over the scaffold surface as a result of the used protocol occluded part of micropores as shown in **figure 3-3** but did not cover the whole scaffold surface. Finally it seems that mineral particles affect the apatite coating on composition 13 samples. Composition 13 samples showed a higher number of cauliflower crystals than other tested scaffolds pointing that mineral particles introduction improves bioactivity in good agreement with other works[36,177].

As expected, mechanical properties were affected by particle inclusion and blending. Blend scaffolds showed the highest elastic modulus and yield strength of all tested scaffolds due the blend nature of polymer scaffold. On the other hand mineral particles introduction on composition 17 cause a downfall of mechanical properties. One possible explanation like in the previous section was the inhomogeneous dispersion of mineral particles that weakened the structure. Blend solution was a more viscous solution than non blend composition hampering particle dispersion in the solution and probably forms particle agglomerates that cause structure defects.

Finally polymer degradation is interesting in bone tissue engineering because bone has a fast regeneration rate compared with other tissues. Polymer 2 degradation is faster than polymer 1 and its presence in the polymer blend probably accelerates scaffold degradation. On other hand mineral particles could improve the degradation rate of developed scaffolds since degradation depends, among other factors, on the

polymer crystallinity and sample wettability.[9] The addition of mineral particles could improve degradation increasing sample hydrophilicity[9] and reducing polymer crystallinity. These properties configure a complex system that could be used to modulate the degradation properties of our developed samples.

3.3.5. Conclusion

Composite and bare polymer blend scaffolds were obtained with a porosity and morphology suitable for bone tissue engineering. Composite scaffolds showed similar features than composites obtained in the first section of this chapter. Polymer phase separation did not seem to compromise the correct scaffold structure, only a higher porosity was observed in blend samples due the lower proportion of polymer/solvent used. On the other hand mechanical properties were highly improved in polymer blend scaffold.

3.4. Development and evaluation of polymer based composite scaffolds: PCL/PLLA composite scaffolds degradation study.

Polycaprolactone is a semicrystalline polymer too compliant for bone substitutes. To resolve these drawbacks in the current thesis we add poly(lactic acid) in the form of polymer blend and use a mineral filler to increase the stiffness of PCL. In the present section we analyze the degradation rate of PCL/PLLA blends. Degradation is an important aspect of scaffold design: the material should be resorbed by the organism at the same time that new formed tissue grow in order to guide tissue regeneration. PCL/PLLA blend materials probably will show different degradation rates due to the huge difference between both components. The presence of PLLA in the blend can accelerate the bioresorption of the scaffold because it degrades faster than PCL and lactic acid subproduct decrease pH in the surrounding of the polymer increasing the chain cleavage[22].

In a previous work of our group hydrolytic degradation behaviour of microporous PCL/PLLA membranes was studied by Gaona et al.[179] In that work it was observed that PLLA phase suffer a more prominent degradation than PCL phase. On the other hand PLLA/PCL blends showed an intermediate behaviour between pure polymers. Present work introduces the presence of macropores and mineral microparticles. These changes probably increase the hydrolysis of the blend membrane since it will improve sample hydrophilicity and facilitate water diffusion inside the sample.

This work has been recently submitted for publication entitled “Effects of hydroxyapatite filler on long-term hydrolytic degradation of PLLA/PCL porous scaffolds”[180].

Scaffolds were prepared using PCL/PLLA (20/80) and PCL/PLLA (80/20) solutions at 15% in dioxane with (or not) 20% of HAp. Samples were cut to 6 mm diameter and 3.5 mm of height. Samples degradation was performed in phosphate-buffered solution (with sodium azide as biocide) at 37 ^{0}C in a water bath with orbital shaking, for up to 78 weeks.

Samples	Polymer composition	Mineral composites	
		Ceramic reinforcement	Surface modification
PCL/PLLA(20/80)	20%polycaprolactone / 80%poly-(L)-lactic acid	-	-
PCL/PLLA(80/20)	80%PCL / 20%poly-(L)-lactic acid	-	-
PCL/PLLA(20/80)-HAp	20%PCL / 80%poly-(L)-lactic acid	20%HAp	-
PCL/PLLA(80/20)-HAp	80%PCL / 20%poly-(L)-lactic acid	20%HAp	-

Table 3-3. Table with tested samples composition.

The influence of degradation performed in immersion in phosphate buffer at 78 weeks was evaluated by weight loss of each component using TGA analysis and morphologic and mechanical changes using SEM and mechanical test in compression.

3.4.1. Morphology and physico-chemical properties.

Figure 3-5 shows the double pore structure described along this chapter of developed PCL/PLLA blend scaffolds that showed a porosity around 90%. PCL and PLLA phase separation was also observed as shown by the inclusion of spherical domains of the minority phase inside the main phase. Phase separation features were more exacerbated for PCL rich blends, but inclusion of inorganic phase did not modify the morphology of the scaffolds as described previously. PCL/PLLA(20/80) based scaffolds showed thinner struts and more heterogeneity between the pores. Mineral nanoparticle content, crystallinity and mechanical properties were determined and are showed in **table 3-4**. Nanoparticle content was lower than expected with a 30% less in PCL/PLLA(20/80)-20HAp and 4% in PCL/PLLA(80/20)-20HAp. Crystallinity of PCL and PLLA phases was independent of blend composition. On bare blend scaffolds crystallinity of PCL phase was around 70% whereas PLLA phase it was around 40%. On the other hand, hydroxyapatite addition produces a crystallinity decrement in both polymer components. Crystallinity in PCL phase decreased around a 20% in both composite polymer blends and a 10% in PLLA phase. Composites showed decreasing mechanical modulus with hydroxyapatite addition or with the increase of PCL content. PCL/PLLA(20/80) showed the highest modulus followed by PCL/PLLA(20/80)-20HAp. PCL/PLLA(80/20) showed a modulus 2.6 times lower than PCL/PLLA(20/80). Finally PCL/PLLA(80/20)-20HAp showed the lowest modulus that was 30 times lower than non composite blend and 82 times lower than PCL/PLLA(20/80). On the other hand, the yield strength was not detectable on PCL/PLLA(80/20)-20HAp.

	Porosity (%)	Solid residue		Mechanical properties		Crystallinity		W_{PCL}/W_{PCL0}	W_{PLLA}/W_{PLLA0}
		Mean (%)	Diff. (%)	Elastic modulus (MPa)	Yield strength (MPa)	X_{CPCL}	X_{CPLLA}	Week 78 (%)	Week 78 (%)
PCL/PLLA (20/80)	89.6±0.4			1.64 ± 0.08	0.22 ± 0.08	65	36	80	31
PCL/PLLA (20/80)-20HAP	89.6±0.3	19.1±1.3	-4.33	1.37 ± 0.27	0.11 ± 0.07	48	19	87	31
PCL/PLLA (80/20)	85.4±0.3			0.61 ± 0.2 *	0.06 ± 0.01	70	38	72	43
PCL/PLLA (80/20)-20HAP	86.7±0.5	14.1±0.7 ***	-29.68	0.02 ± 0.01 **,***	- ± -	50	25	96	35

Table 3-4. Total porosity of composite scaffolds series, solid residue analysis of composite scaffolds series, mechanical analysis of scaffolds, crystallinity analysis of scaffolds series and relative weight loss at 78 weeks. The Diff. (%) means the difference in the amount of microparticles detected and the nominal value. Samples that show significant differences ($p<0.05$) with PCL/PLLA(20/80) sample are pointed with (*), (**) for PCL/PLLA(80/20) and (***) for samples compared to PCL/PLLA(20/80)-20HAP.

3.4.2. Morphology and microstructure evolution.

After 78-week degradation the overall gross morphology of the PCL/PLLA(80/20) scaffolds showed some visual differences compared to the day the experiment started and microstructure was generally preserved **(Figure 3-6)**. On the other hand, PLLA rich blends showed some loss of integrity, with a progressive structure collapse and broken struts, likely due to the fragile nature of PLLA (Tg above ambient temperature). In PCL rich blends, the size of polylactic acid inclusions decreased with time.

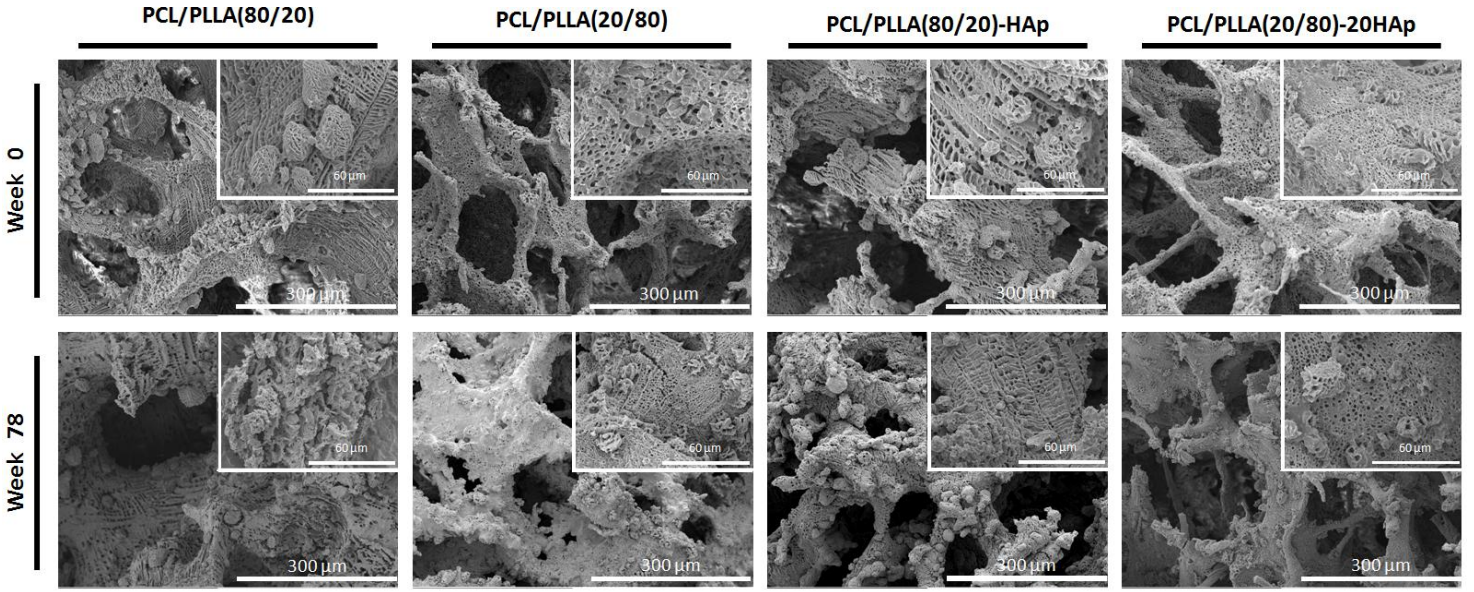

Figure 3-5. Microstructure of polyester scaffolds at week 0 and 78. Detail views of blend scaffolds in the upper right corner of each micrograph. (magnification/scale bar = 200X/300 µm and 1000X/60 µm).

3.4.3. Weight loss evolution

The structure changes as result of polymer chain degradation and structure erosion. Evolution of sample weight and sample composition with time is presented in **figure 3-7**. This kind of visualization allows simultaneous envisioning of the total weight loss and of the weight loss that can be attributed to each phase: PCL (Blue), PLLA (green) and inorganic content (red). Content of each polymer phase was determined from gravimetry measurements; PLLA degrades thermically around 320ºC while PCL degrades around 400ºC, and thus weight loss of each phase can be differentiated from each other by the temperature range where it occurs. During all the degradation period, PCL phase and PLLA phase were seen to be thermally degraded at easily distinguishable temperatures as seen in the defined and separated peaks seen in the derivate signal of the weight loss (although theses temperatures varied along the degradation time due to the changes in chain length). Weight loss of a particular phase was determined as the weight loss between the temperatures limited by the onset and offset of weight loss derivate peaks (see **figure 3-7**). Weight loss is most noticeable for PLLA rich blend sample, PCL/PLLA(20/80), and least noticeable for PCL rich composite sample, PCL/PLLA(80/20)-20HAp. In the case of the PCL rich blends (PCL/PLLA(80/20) and (PCL/PLLA(80/20)-20HAp), inclusion of HAp seems to limit the weight loss of the polymeric phase, while in the case of PLLA rich blends, (PCL/PLLA(20/80) and PCL/PLLA(20/80)-20HAp), HAp introduction leads to a retarded but increased loss of polymeric phase. In PCL rich blends, both phases lose weight in a similar proportion, whereas in PLLA rich blends, most of the weight loss can be ascribed to PLLA phase.

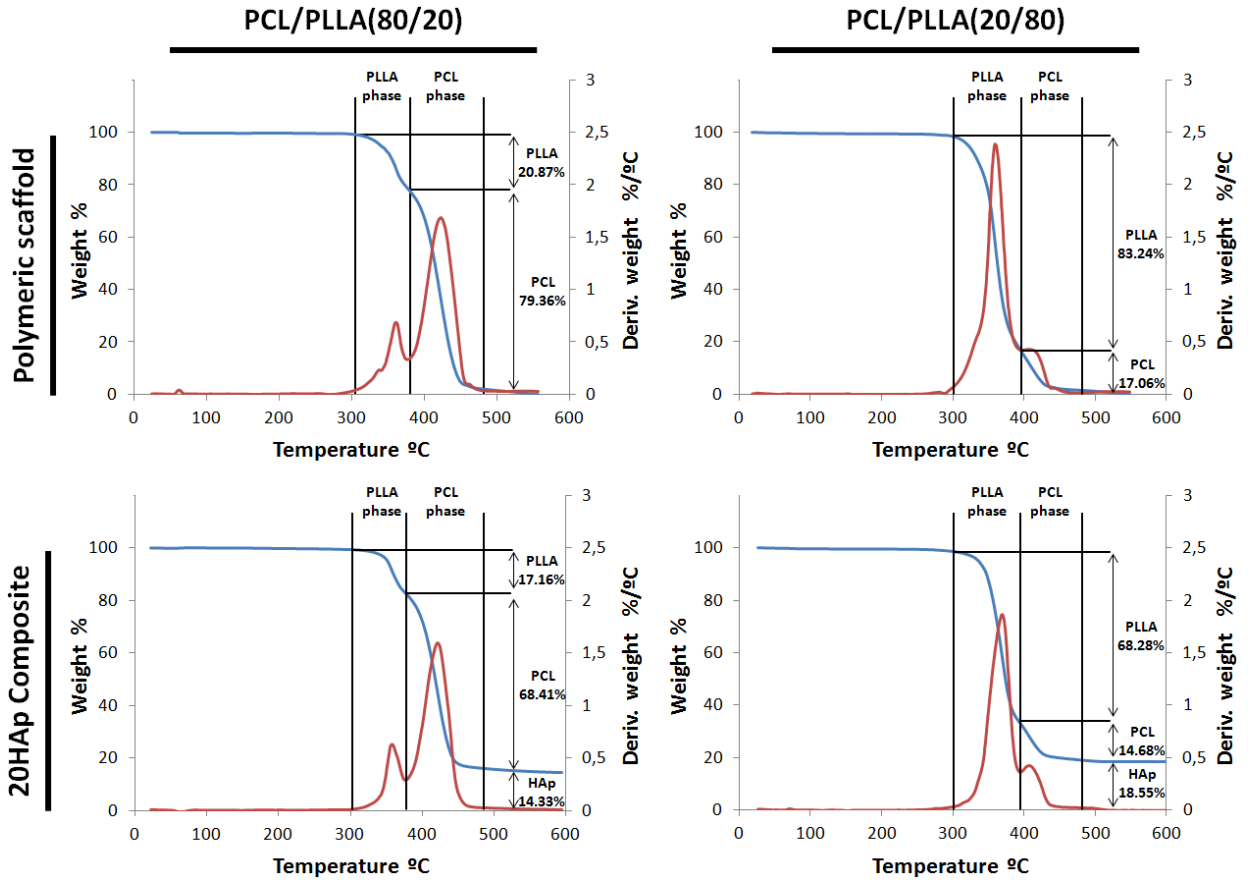

Figure 3-6. Representative TGA curve at day one for bare PCL/PLLA blends and composite. Weight loss of a particular phase was determined as the weight (blue curve) loss between the temperatures limited by the onset and offset of weight loss derivate peaks(red curve).

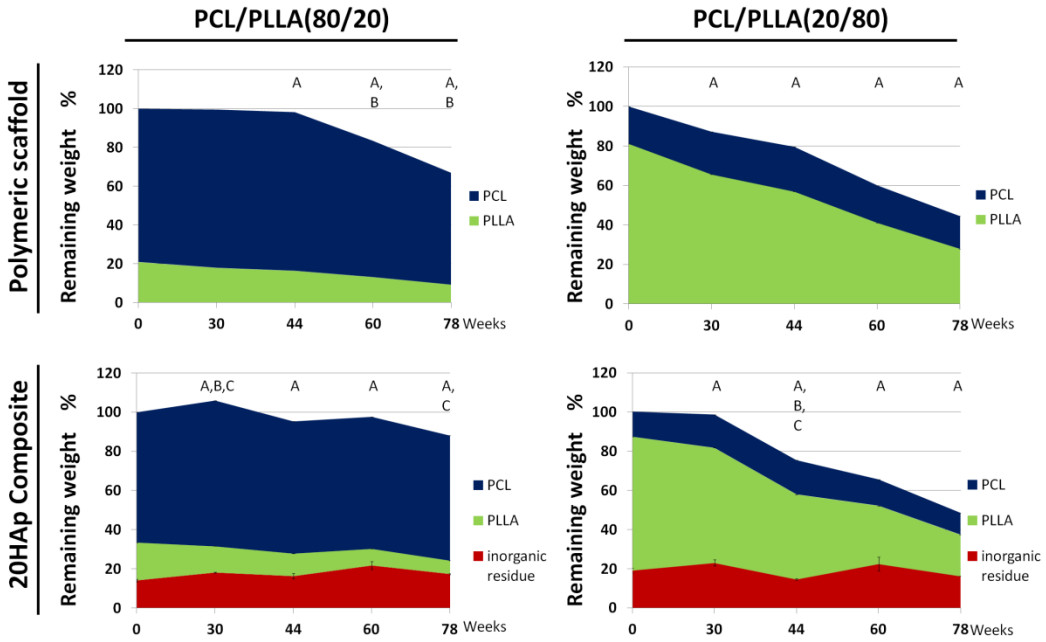

Figure 3-7. Evolution of sample weight and composition with time as determined by weighing and thermogravimetry. PCL (Blue), PLLA (green) and inorganic content (red). Error bars represent standard deviation. Significance ($p<0.05$) compared to same material phase at day 0 is signalled as: (A) PLLA, (B) PCL and (C) mineral particles.

3.4.4. Mechanical properties

Evolution of mechanical properties is shown in **figure 3-8**. Elastic modulus and yield strength of as-synthesized scaffolds were higher for PCL/PLLA(20/80) and PCL/PLLA(20/80)-20HAp than respective PCL/PLLA(80/20) blend, as can be seen in **figure 3-8 A** and **figure 3-8 B**. Inclusion of inorganic phase does not lead to a mechanical strengthening in the case of these materials: PCL/PLLA(80/20)-20HAp shows the lowest modulus and yield strength was undetectable for these samples. Nevertheless, after 30 weeks of degradation, PLLA rich scaffolds lost more than half of their strength and rigidity and there was no significant difference between PCL/PLLA(20/80) and PCL/PLLA(20/80)-20HAp on one side and PCL/PLLA(80/20) on the other side. On the contrary, densification modulus

increased with degradation time for PCL/PLLA(20/80) blends but in PCL/PLLA(80/20) did not show important differences with time.

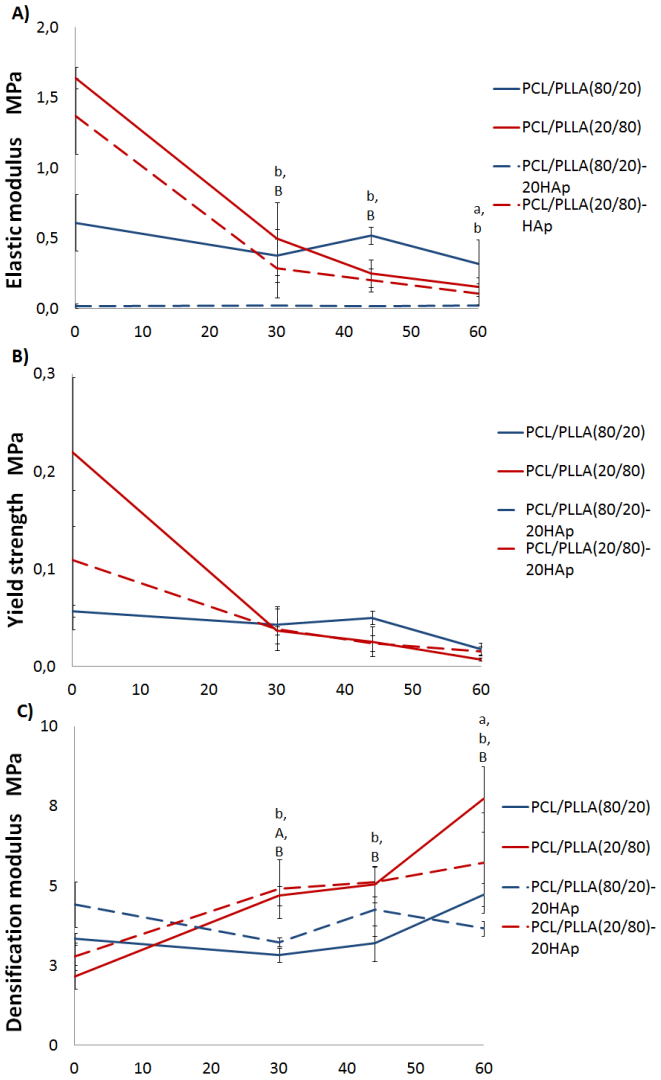

Figure 3-8. Mechanical compressive properties of the scaffolds. Evolution of the elastic modulus with time (A) evolution of the yield strength with time (B) and evolution of the densification modulus with time (C). Error bars represent standard deviation. Significance ($p<0.05$) compared to same scaffold at day 0 is signalled as: (a) PCL/PLLA(80/20), (b) PCL/PLLA(20/80), (A) PCL/PLLA(80/20)-20HAP and (B) PCL/PLLA(20/80)-20HAP.

3.4.5. Discussion

This work was focused on the study of degradation in PCL/PLLA blends eventually reinforced with HAp. We fabricated highly porous PCL/PLLA blend scaffolds reinforced with hydroxyapatite. Samples showed a phase separation between polycaprolactone and polylactic acid and an interconnected double pore structure as result of the fabrication process. Modulus of the scaffolds was in the same order of magnitude as samples developed in previous sections of this chapter but still they remain below the mechanical values of bone[22]; such supports should thus be used with external support for load bearing application. The ratio of PCL and PLLA content of the blend highly influenced the properties of the scaffold due to the large differences in mechanical and degradation properties of the two components. On the other hand hydroxyapatite addition have a negative effect over mechanical properties and crystallinity that decreased in presence of mineral reinforcement as already reported in previous sections.

Degradation of PCL/PLLA blends has been studied extensively and it has generally been shown that polylactic acid, was less degraded in polycaprolactone rich blends than in polylactic acid rich blends.[181] This is generally explained in terms of impaired water diffusion through the polycaprocatone matrix limiting the hydrolysis rate of polylactic acid inclusions. On present work weight loss associated to polylactic acid phase was higher in PCL/PLLA(20/80) blend than in PCL/PLLA(80/20) blend. On the other hand in the present work polycaprolactone phase weight loss cannot be explained by water diffusion as it was higher in PCL/PLLA(80/20) than in PCL/PLLA(20/80) in contradiction with the findings of Fukushima *et al.*[182] that found that PCL was degraded more rapidly in Poly(DL)lactic acid rich blends. On the other hand hydroxyapatite nanoparticles addition increased significantly the degradation of polymer phase in PCL/PLLA(20/80)-20HAp samples after an induction period of around 30 weeks.

Polylactic acid degradation increment as consequence of hydroxyapatite reinforcement is described in literature for in *in vitro* studies[183] and PLLA composites are reabsorbed *in vivo* faster than pure polylactic acid devices.[184] It is noteworthy that the main part of degraded polymer was the polylactic acid phase, but no differences were found in polylactic acid phase weight loss between reinforced samples and not. On the other hand, in polycaprolactone rich blends a reduction of polylactic acid phase weight was observed when hydroxyapatite was present. The present work showed that PCL, when reinforced with hydroxyapatite, was more resistant to hydrolysis, as shown by the reduced weight loss of these samples. The increase in degradation for polylactic acid samples could be explained with the lower crystallinity obtained in hydroxyapatite containing samples as degradation affects mainly the amorphous phase. Another explication is that hydroxyapatite increases sample hydrophilicity improving water diffusion through the sample, thus increasing polymer hydrolysis; nevertheless none of these explanations is able to explain polycaprolactone phase behaviour.

Weight loss of polymer samples was as consequence of polymer hydrolysis that caused sample erosion. After 78-week the polymer degradation affects substantially the scaffold structure. On PCL/PLLA(80/20) polymeric and composite scaffolds the most visible effect is the size reduction of PLLA spherical inclusions. On the other hand in PCL/PLLA(20/80) and PCL/PLLA(20/80)-20HAp the large weight lost affected substantially the scaffold structure. Scaffold was collapsed in polylactic acid rich blends due the weakening of the structure.

Finally scaffold's mechanical properties decreased with degradation time as expected. Although glassy PLLA is initially much more rigid than PCL (which is rubbery at ambient temperature), soon after 30 weeks there is no significant difference between the yield strength or elastic modulus of PLLA rich or PCL rich samples. Densification modulus of the PLLA based blends increased with

degradation time, whereas PCL based blends had relatively constant densification modulus.

3.4.6. Conclusion

The effect of hydroxyapatite filler on long-term (78 weeks) hydrolytic degradation of PCL/PLLA blend scaffolds was studied. Introduction of HAp shielded the PCL from degradation and decreasing the weight loss (more pronounced when PCL was the main phase). On the other hand, the presence of HAp had no significant effect on PLLA weight loss. Mechanical properties of the scaffolds decreased with degradation time as was expected. PCL/PLLA(20/80) was initially much more rigid than PCL/PLLA(80/20), but after 30 weeks hydrolysis there was no significant difference between the yield strength or elastic modulus of both bare blend polymer scaffolds.

3.5. Annex: *In vitro* and *in vivo* scaffold evaluation as potential spinal fusion strip.

This subchapter was developed as part of Cenit Intelimplant project coordinated by Tequir I+D+i and funded by Spanish Ministry of Industry, Tourism and Commerce through INGENIO 2010 program. The objective was developing a spinal fusion strip prototype and proceeding to its *in vivo* evaluation.

Samples compositions and results were omitted due to a confidentiality agreement between the center and the company owner of the results.

Previous to *in vivo* study an *in vitro* material selection was carried out by the group of Nerea Garagorri Ganchegui at Inasmet Tecnalia. The *in vitro* culture was performed with hFOB1.19 (human foetal osteoblast) cell line at 26 days. Experimental results will not be shown here. In summary it can be said that cell adhesion and cell viability were determined through WST-1 assay and osteogenic differentiation through ALP assay. WTS-1 assay is based on substrate transformation in a coloured product done by live cells and measured by absorbance. After the *in vitro* study were selected 3 biomaterials to perform the *in vivo* evaluation. *In vivo* evaluation to characterize the material properties to guide the bone regeneration was performed by Víctor Javier Primo Capella and Irene Lara Saez at the Instituto de Biomecanica de Valencia. Animal model selected was a critical resection in radius bone (25 mm) of New Zealand white rabbits and substitution with the selected material. Samples were implanted in five animals for each material and each time point and were sacrificed to evaluate the regenerated bone. *In vivo* study showed that developed biomaterials were able to regenerate the bone at same level than reference material. The Results were published in Revista de biomecánica, (56), 67-69 with the tittle of Biomateriales poliméricos flexibles para fusiones vertebrales.

3.5.1. Discussion

Final step of present work was select and validate the prototypes in a complex biological system. *In vitro* culture screening was performed by Inasmet-Tecnalia on all developed materials. *In vitro* tests allow reducing animal experiments and are a standardizable methodology to test cytotoxicity, cell proliferation and differentiation. Nevertheless, cell line, culture medium or physical factors can modify cell response *in vitro,* and *ex-vivo* experiments cannot reproduce tissue-material interaction.[185] For this reason animal models are necessary to test materials as a more accurately approximation to human. Rabbit as animal model for musculoskeletal studies is typically used (35% of studies are performed in rabbit) because has advantages over other models, such as a fast bone maturation (6 months), ease to house and handle.[185] On the other hand, bone histology, anatomy and bone remodelling is completely different to human, and for this reason it is commonly used as a previous stage to other animal models.[185] Implantation in rabbits performed in the Instituto de Biomecanica de Valencia had the objective of evaluate developed materials and compare them against commercial reference bone filler. Polymeric scaffolds did not show significant differences compared to reference material, with values near to healthy bone. Polymeric scaffolds developed on present work have advantages over bone substitutes actually available for human use as demineralised bone matrix, ceramics or collagen with calcium phosphate[186]. Advantages over cited substitutes are dismiss disease risk transmission of substitutes from animal or human source, are stiffer than collagen substitutes and are more manufacturable and flexible than ceramics.

3.6. Chapter discussion

The initial concept of bone substitute that we proposed evolved from PCL scaffolds with ceramic reinforcement until the final prototype. The initial hypothesis was tested and modified to obtain a prototype to test *in vivo*. In the first step of the research we tested different concentrations of Bioglass® and hydroxyapatite to obtain PCL composites. Samples obtained were homogeneous despite the variability of ceramic content. Particles addition improved surface roughness, sample hydrophilicity and mechanical properties that are important features in the development of a bone substitute. The mineral presence on the scaffold surface improves the adsorption of proteins and mineral precipitation[75,76,177] and makes more hydrophilic the material allowing cell invasion inside the scaffold[77]. Unexpectedly, mechanical improvement of composite scaffolds with high mineral reinforcement concentration was not found and samples with 20% of reinforcement showed modulus similar to naked PCL scaffold[158] remaining below the typical values measured for bone[22]. Experiments were performed with MC3T3-E1 and showed that 5% of mineral reinforcement improved cell adhesion but did not affect cell differentiation.[158] As consequence of this, materials formulation was reconsidered and were introduced new formulations. Effect of blending and hydroxyapatite reinforcement over degradation behaviour was tested on PCL/PLLA(20/80) and PCL/PLLA(80/20) blends (and composites) with an *in vitro* degradation study at 78 weeks. PCL/PLLA(20/80) samples degraded faster than PCL/PLLA(80/20) samples as expected. On the other hand hydroxyapatite reinforcement increased degradation only on PLLA phase but protected PCL phase. Finally biological analysis *in vitro* of all developed formulations and all surface treatments was performed. Materials that supported better cell proliferation and differentiation were selected for further research steps. Finally biomaterial 1, biomaterial 2 and biomaterial 3 were selected to be implanted in rabbits and showed

to be able to regenerate a critical bone lesion similarly than commercialized reference material. We can conclude as our developed materials are a promising candidate for spinal fusion applications.

4. MACROPOROUS PCL CONSTRUCTS FOR CARTILAGE TISSUE ENGINEERING: RESULTS AND DISCUSSION

4. Macroporous PCL constructs for cartilage tissue engineering: Results and discussion.

4.1. Abstract

This section presents the results obtained in the development of a hybrid scaffold as 3D support for articular cartilage regeneration. The objective of this study was to find a combination of a polymeric scaffold and cell seeding (bone marrow MSCs or mature chondrocytes) and culture protocol to develop an *in vitro* construct (scaffold and differentiated cells) to be implanted in a cartilage defect to induce new functional tissue formation. The supporting material will be based in a polycaprolactone, PCL, macroporous scaffold in which our research group have previous experience both *in vitro*[187-190] and in animal models[39,48]. PCL scaffold should provide the desired mechanical properties to the construct while its pore walls will be coated with hyaluronic acid that is meant to provide the surface to which cells adhere with the biological cues required for a correct cell differentiation and tissue integration.

In vitro construct development was divided in four steps: (I) The first step is the production of PCL+HA scaffolds series, their characterization and validation, then the study of culture conditions of mesenchymal stem cells inside the scaffold to enhance chondrogenic differentiation, including (II) the characterization of hypoxia as culture condition, (III) the characterization of mechanical stimulation to improve hypoxic effect and (IV) the characterization of co-culture of mesenchymal stem cells with mature chondrocytes. Physical properties of the cell-material construct after *in vitro* culture were measured (mechanical behaviour, morphology, composition).

4.2. Development of PCL+HA hybrid scaffolds: characterization and validation.

The main objective was to obtain PCL scaffolds with a double micro and macro porosity as described above and an homogeneous hyaluronic acid coating of the pore walls. Morphology, physical and mechanical properties of these supports were characterized and biological response of the *in vitro* construct (cells and scaffold) for cartilage reparation was evaluated.

PCL macroporous scaffolds were obtained by the combination of freeze extraction and porogen techniques as explained in materials and methods **section 2.2.1.1.** They are similar to those used in bone regeneration, with well connected macroporosity, macropores with spherical form and microporous pore walls.

Composite PCL+HA scaffolds were prepared by coating the pore walls with a solution of hyaluronic acid which was cross-linked with different protocols (in one or two steps). Biologic characterization was performed using mature human chondrocytes under normoxia conditions. This work has been published in the Journal of Biomedical Materials Research: Part A entitled "Different hyaluronic acid morphology modulates primary articular chondrocyte behaviour in hyaluronic acid-coated polycaprolactone scaffolds"[191].

The effect of hyaluronic acid coating over human chondrocytes was studied measuring the cell proliferation and ECM deposition using immunofluorescent staining of collagen and aggrecan as well as biochemical quantitative determination of DNA and GAGs.

Samples	Polymer composition	Hydrogel hybrid material	
		Hydrogel coating	Crosslink method
PCL	Polycaprolactone	-	-
PCL+HA1s	Polycaprolactone	Hyaluronic acid	One step with divinyl sulfone
PCL+HA2s	Polycaprolactone	Hyaluronic acid	Two steps with divinyl sulfone

Table 4-1. Table with tested samples composition.

4.2.1. Scaffold and coating structure.

As a result of the preparation process, scaffolds with high porosity (86.6% as determined by the weight increase when the pore structure is filled with ethanol[177]) and the desired double pore size distribution were obtained (**figure 4-1**). The coating techniques described on **section 2.2.1.4.** succeeded in producing two different coating morphology. Hybrid scaffolds produced by one step coating PCL+HA1s were prepared by filling the pore structure of PCL scaffold with a hyaluronic acid 2% solution in NaOH 0.2 M mixed with DVS (molar ratio of 2:1) to fill the macropores with hyaluronic acid hydrogel. One step filling and crosslinking of the scaffold pores produces a hyaluronic acid gel phase that fills the macropores. When the swollen hydrogel is frozen and water sublimated in the Cryo-SEM a micropore structure is shown by this gel which is quite similar to that of the pore walls of PCL scaffold. The arrows in **figure 4-1 B** indicate the hyaluronic acid structure filling one of the macropores. Coating in two steps consisted in infiltrating 1% hyaluronic acid solution and allowing it to dry. Dry coating was partially swollen in acetone/water (80/20) mixture at pH 12 and crosslinked with DVS to coat the scaffold surface with a hyaluronic acid film. In PCL+HA2s, hyaluronic acid only covers the pore walls, sometimes hiding the microporosity (white arrows in **figure 4-1 B**) while leaving the macropore space empty.

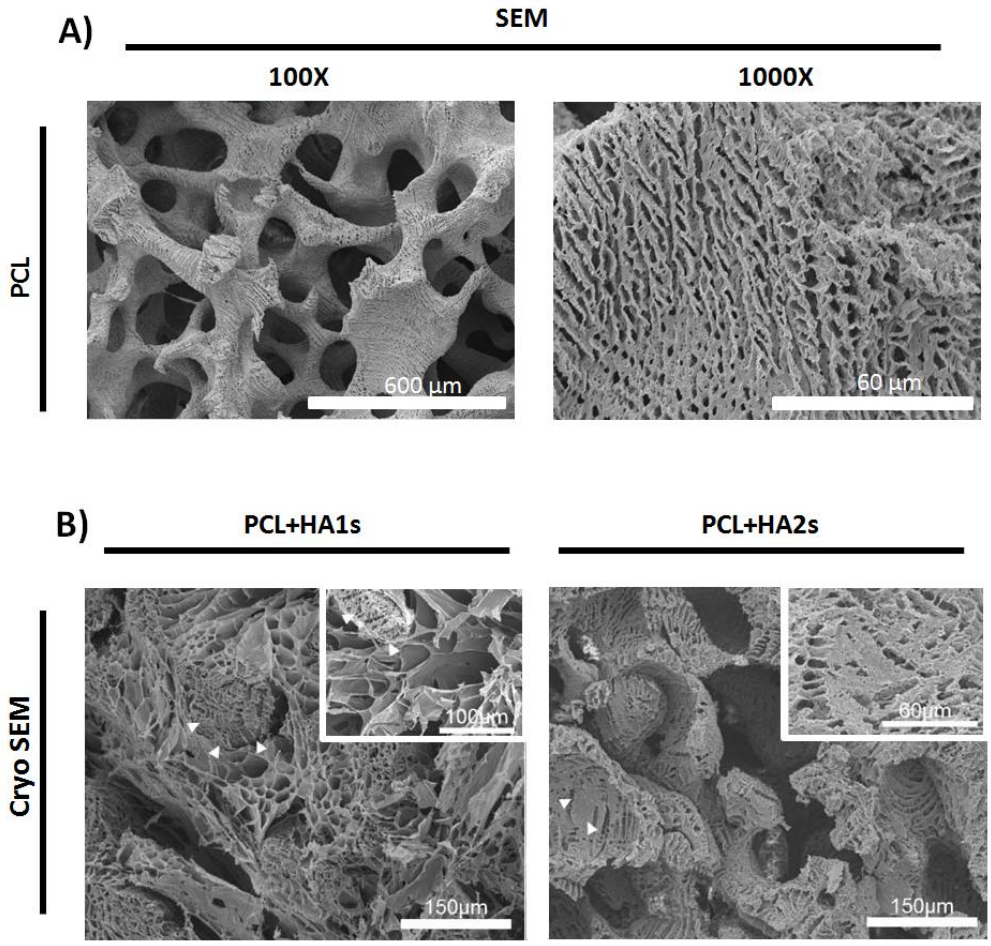

Figure 4-1. Scanning electron microscopy picture of PCL scaffold (A) and Cryo-scanning electron microscopy (swollen samples) micrographs of PCL+HA1s and PCL+HA2s (B). Detail views of hyaluronic acid coated scaffolds in the upper right corner of each micrograph.

HA content was determined performing a TGA. Analysis showed that PCL+HA1s contained 4.6±2.3% and PCL+HA2s 5.8±2.8% hyaluronic acid by weight. The amount of hyaluronan is not significantly different depending on the coating procedures, and there is some variability in both groups due to the preparation process. As can be seen in **table 4-2**, hyaluronic acid coating leads to an increased equilibrium water content, with a water uptake (measured on a dry basis) of nearly 3.5 (3.5 grams of absorbed water per gram of dry polymer) for both samples regardless of the coating type (3.57±0.36 for PCL+HA1s and 3.38±0.14 for PCL+HA2s, but the difference is not statistically significant).

4.2.2. Compression properties

As seen on **table 4-2**, compressive elastic modulus of the samples is not significantly influenced by the modification with hyaluronic acid, although PCL+HA1s have higher mean stiffness, probably due to the filling of the pores. The only significant difference appears between wet PCL+HA1s and wet PCL+HA2s. In general all wet samples have lower mean modulus.

			Elastic modulus (MPa)	
	Hyaluronic acid content (%)	Equilibrium water content	Dry	Swollen
PCL		1.45 ± 0.22	0.43 ± 0.02	0.34 ± 0.09
PCL+HA1s	4.6 ± 2.3	3.57 ± 0.36	0.56 ± 0.14	0.49 ± 0.1 *
PCL+HA2s	5.8 ± 2.8	3.38 ± 0.14	0.35 ± 0.12	0.29 ± 0.11 *

Table 4-2. Total porosity of hybrid scaffolds series, Hyaluronic acid content analysis of hybrid scaffolds series and mechanical analysis of scaffolds. Significance ($p<0.05$) between samples is signalled as (*).

4.2.3. Cell morphology and behaviour

Samples for cell culture were cut to 6 mm in diameter and 3 mm height. Human chondrocytes were seeded at 400000 cells/scaffold with standard culture media and cultured 21 days in normoxia.

As can be seen on **figure 4-2**, cell number is generally seen to increase with culture time; lower cell numbers are observed in PCL+HA hybrids at 7 and 14 days than in uncoated PCL scaffolds. In case of PCL+HA2s, some cells appear shrunk and may be suffering apoptosis (See **figure 4-2** at 7 days). The cells generally showed a fibroblastic shape with elongated cytoskeleton and filopodia, characteristic of dedifferentiated chondrocytes[192]. Only in a few occasions (see for example picture for PCL+HA1s at 14 days), rounded chondrocytes were found within the structure, mostly in PCL+HA1s and occasionally in PCL and PCL+HA2s samples.

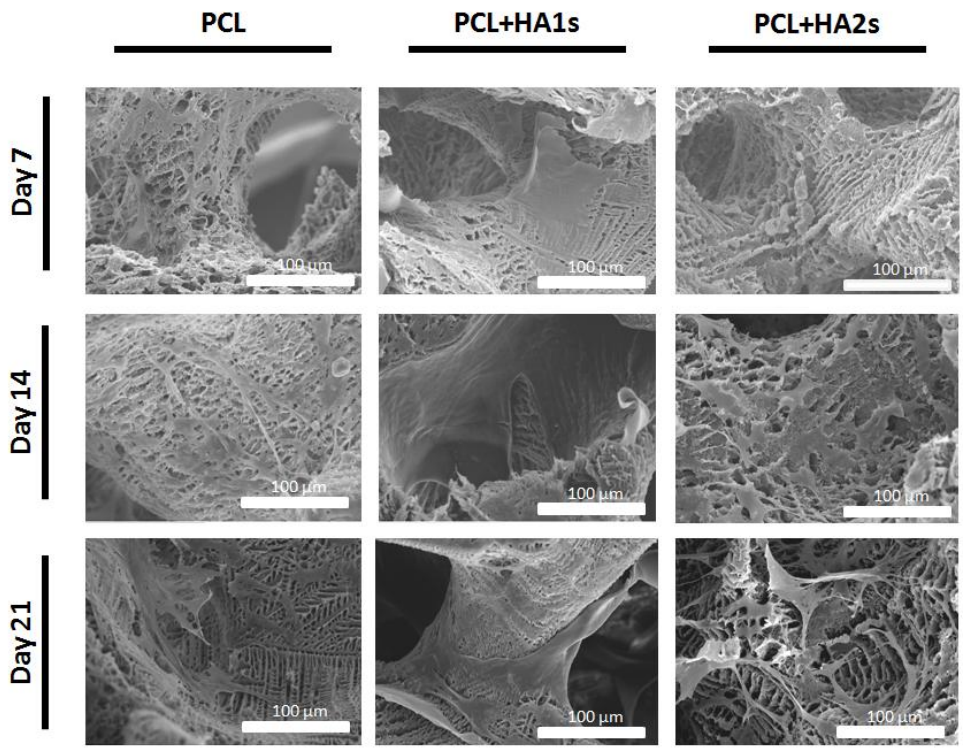

Figure 4-2. SEM images of PCL, PCL+HA1s and PCL+HA2s scaffolds seeded with human chondrocytes cells after 7, 14, and 21 days of culture. (magnification/scale bar = X1000/60µm).

In **figure 4-3** and **figure 4-4**, light microscopy pictures of the construct slices (100µm) have been combined with the immunofluorescent pictures from confocal laser scanning microscope to permit the simultaneous visualization of the cells and the construct structure. Scaffold material appears as black, pore space as gray; in PCL+HA1s samples, the hyaluronic acid phase appears as translucid fibres that cross the pore space. In **figure 4-3A** constructs are marked for collagen type I and II, in **figure 4-3B** for aggrecan and actin cytoskeleton and in **figure 4-4** for CD44. Cell distribution is different depending on the material type. Whereas in bare PCL cells are very homogenously distributed, in PCL+HA1s (and to a less extent in PCL+HA2s) cells tend to form aggregates. In general, in hyaluronic acid containing

samples, cells tend to grow in three dimensions, whereas in bare PCL scaffold, except in a few cases, cells are spread on the pore walls, and grow in volume only after locally reaching confluence. In PCL+HA1s, cell distribution varies from one sample region to another one, whereas in control samples and PCL+HA2s the behaviour is more homogenous.

The presence of collagen type I and II can be visualized in all samples. For instance, in bare PCL collagen type I and II are localized in the same parts of the construct and appear mostly intracellularly (**figure 4-3A**). In HA-coated samples there are domains with predominance of either one collagen type or the other, localized in different parts; in general, collagen type II is predominant in the areas of high cell density and cell aggregates, whereas collagen type I is predominant in the cells that are directly spread on the pore walls (**figure 4-3A**). The only exception to this behaviour is seen in PCL+HA2s at 21 days, where collagen type I and II appear in a homogenous manner within the pore space. Most collagen is intracellular, except for PCL+HA1s where some collagen deposition outside the cell is observed. Developed actin cytoskeleton is seen for an overwhelming majority of cells in PCL and PCL+HA2s construct; cells are generally spread on the pore surface or crossing the pore space; in contrast, in PCL+HA1s, nearby the spread cells on pore walls (likely where there was no or little HA), one can observe that in the cell clusters some cells lack the actin stress fibres network and their presence is only revealed by DAPI nucleus staining (see for example the two cells at the center of the picture at day 7).As can be seen in **figure 4-3B**, there is nearly no presence of aggrecan in the PCL construct. Aggrecan is most marked in PCL+HA1s samples, consistently with the data from quantitative GAGs analysis; in these samples, it appears mainly in the cell aggregates although not every cell cluster is marked for GAGs as can be seen for day 14 (right side of the picture). Here again, only in these samples aggrecan is found extracellularly, while in PCL+HA2s, it is mostly stained within the cell bodies

or close to the nucleus. In some cases, the repartition of the aggrecan as a sphere surrounding the cell is proper of a neoformed pericellular matrix (same cells as mentioned before, day 7). In the case of the clusters unfortunately the cell density leads to a very high signal intensity, making interpretation difficult. As can be seen on **figure 4-4**, staining for CD44 has very low intensity in PCL samples after 21 days, with many cells showing very little expression or no expression of CD44. On the other hand, there is staining for CD44 in PCL+HA1s and PCL+HA2s samples in most cells of the constructs. This shows a higher CD44 expression in cells that were cultured in the presence of hyaluronic acid.

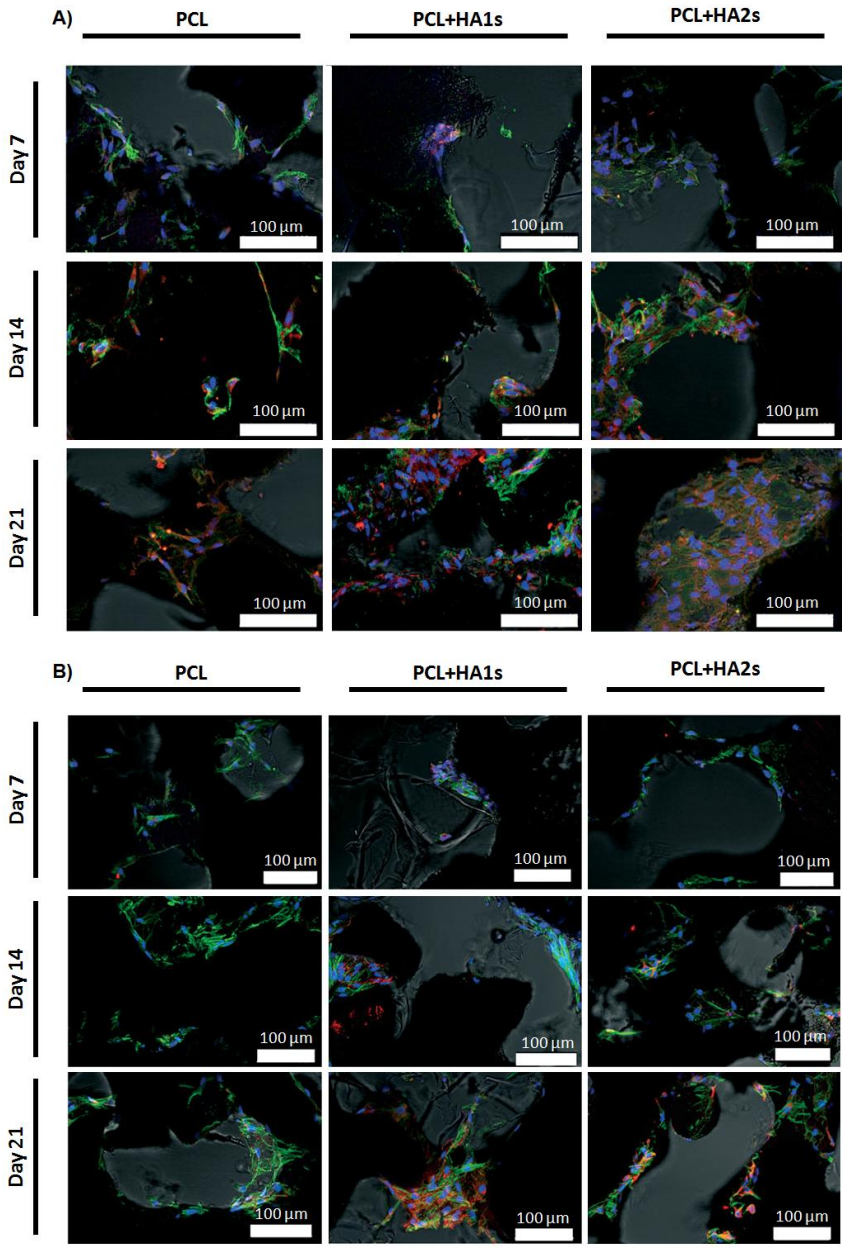

Figure 4-3. Composition of light microscopy and immunofluorescent staining for collagen type I (green) and II (red) and nuclei (blue) (A) and immunofluorescent staining for aggrecan (red) and actin (green) and nuclei (blue) (B) (magnification/scale bar= X40/100µm). The black areas of the pictures correspond to the scaffold.

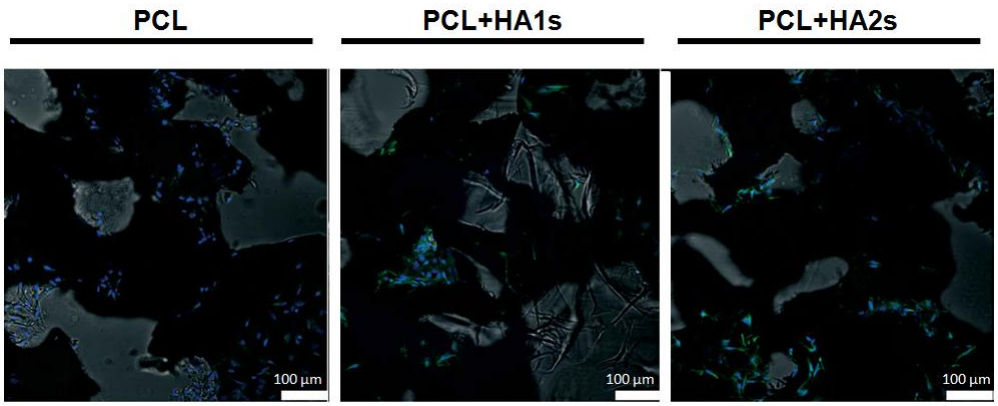

Figure 4-4. Composition of light microscopy and immunofluorescent staining for CD44 receptors (green) and nuclei (blue). The black areas of the pictures correspond to the scaffold. (magnification/scale bar= X40/100 µm).

4.2.4. Quantitative biochemical assays

Total DNA was always higher in bare PCL samples than in hyaluronic acid modified samples regardless of the modification type (**figure 4-5**). To simplify the presentation of results, significant differences are only pointed out between different materials at the same time or between day 21 and day 7. Cell seeding efficiency was determined comparing the theoretical number of seeded cells with the number of cells attached to the scaffold 3h after seeding. Cell number was calculated measuring total DNA and dividing the result by 11.2pg DNA/cell that is the theoretical DNA content by human chondrocyte[193]. Values obtained varied highly from one material to other, showing PCL+HA1s the worst value. In the case of PCL and PCL+HA1s, cell number grows with time, whereas in PCL+HA2s at 14 days there is a decrease in cell number and then cell number increases again at day 21 and becomes higher than in PCL+HA1s. All samples can be described as biocompatible and supporting cell adhesion and cell growth; no cytotoxicity due to DVS is observed. The proliferation ratio between day 21 and day 7 is the highest for

PCL+HA2s (2.4±0.5), followed by PCL+HA1s (1.9±1.7) (increase in cell number is not significant due to high dispersion); the minor ratio is observed for PCL (1.7±0.6).

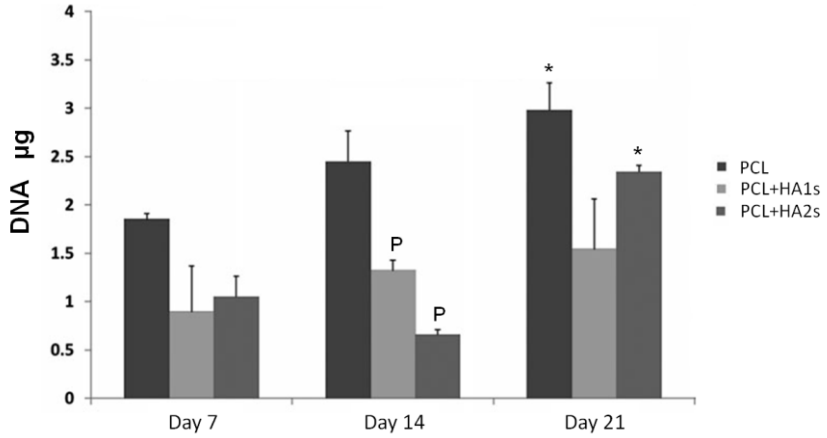

Figure 4-5. Total DNA of chondrocytes cell seeded in PCL, PCL+HA1s and PCL+HA2s. Results are averaged from n=3 experiments. Error bars represent standard deviation. Significance (p<0.05) compared to same group at day 7 is signalled as (*) and (P) for cultured samples compared to PCL samples at same time.

Sulfated glycosaminoglycan content in the constructs is presented in **figure 4-6**. To simplify the presentation of results, significant differences are only noticed between different materials at the same time or between day 21 and day 7. As can be seen, GAGs absolute content is higher in PCL control samples than in other samples, (statistically significant at day 14 with $p < 0.05$). Significant differences are found between day 21 and day 7 for both PCL and PCL+HA2s samples ($p < 0.05$). Based on the observation that GAGs content follows roughly the tendency of DNA content in the samples, it was decided to compare the ratio of GAGs to DNA as a qualification of the glycosaminoglycans production per cell. Results are shown in **figure 4-6**. As can be seen, at all times the glycosaminoglycan production per cell is

significantly higher ($p < 0.05$) in PCL+HA1s than in bare PCL; GAGs content normalized to cell number is not statistically different at day 21 when compared to day 7 in none of the samples, although an increasing trend is seen in PCL+HA1s and decreasing trend in other samples. PCL+HA2s shows a similar trend to PCL, with no significant difference unless at day 14 where the GAGs content is significantly lower than in PCL. At day 21 the most glycosaminoglycans per cell is found in PCL+HA 1step samples, with significant differences regarding PCL and PCL+HA2s ($p < 0.05$); this difference is not due to decreasing cell number in PCL+HA1s sample, as mean DNA content in PCL+HA1s samples increases with time as seen in **figure 4-5**.

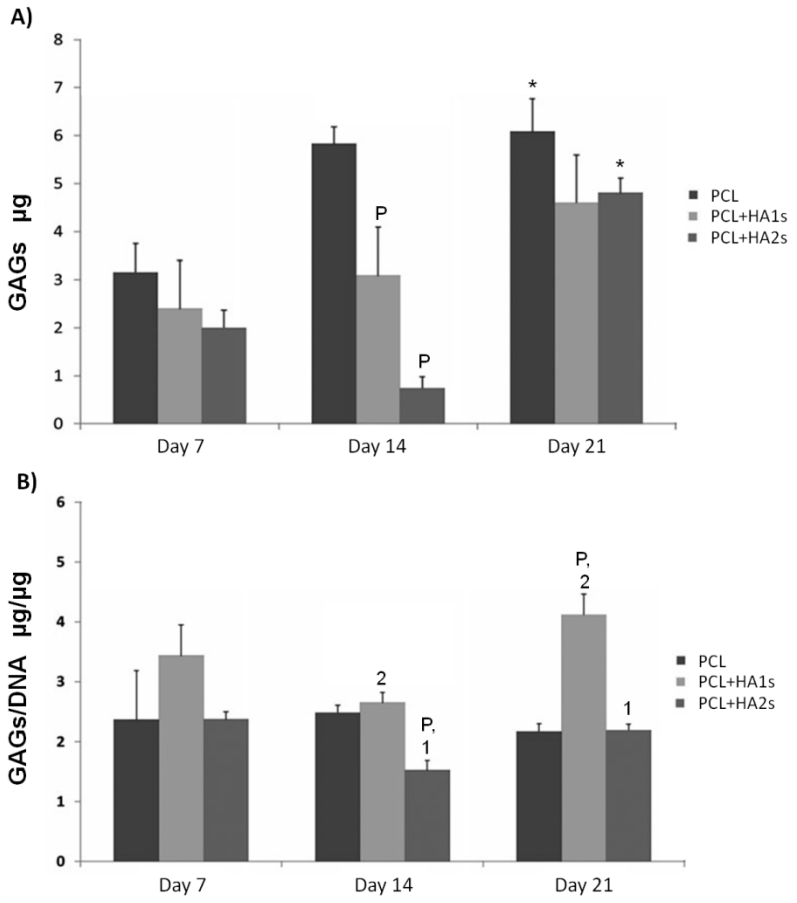

Figure 4-6. Total glycosaminoglycans (GAGs) (A) and glycosaminoglycans normalized to total DNA of chondrocytes at day 7, 14 and 21 in PCL, PCL+HA1s and PCL+HA2s. Results are averaged from n=3 experiments. Error bars represent standard deviation. Significance ($p<0.05$) compared to similar group is signalled as: (P) PCL, (1) PCL+HA1s and (2) PCL+HA2s samples for each group at the same time and compared to same sample group at day 7 is signalled is (*).

4.2.5. Discussion

In this section we tested the hypothesis that modifying PCL scaffolds with hyaluronan could improve cell redifferentiation and verify if this technique was effective to develop an *in vitro* construct for cartilage tissue engineering. The effect of hyaluronic acid on chondrocyte behaviour was tested in unfavorable conditions where dedifferentiation is likely to occur due to the use of FBS[188](which is employed to favour cell adhesion due to protein adsorption and to boost cell growth due to the presence of growth factors)[194] and to the low cell densities used due to the use of human primary cell line.

As described in the results section above, although both HA-modified samples contains similar amounts of HA, the incorporated hyaluronic acid shows a different microstructure depending on the methodology used, with homogenous crosslinking leading to a gel phase that fills the pores, whereas crosslinking of hyaluronic acid in two steps (PCL+HA2s) leads to a thin coating on the scaffolds' pore walls. Both samples are more hydrophilic than bare PCL sample due to the presence of hyaluronic acid. When the hydrophobic PCL scaffold was immersed in liquid water, the swelling ratio was only around 1.4 (**table 4-2**) as high hydrophobicity and surface tension impedes water penetration inside the scaffold, which can be a drawback when implanted *in vivo*. Hyaluronic acid coating improves wettability and allows water penetration inside the pore structure, regardless of the coating strategy used. Nevertheless, as seen by Cryo-scanning electron microscopy, microenvironment inside the hydrated scaffold is different, with presence of a gel phase in PCL+HA1s but a thin coating on the pore walls in PCL+HA2s. Lower swelling degree was observed in thin films made using the same two-step procedure (**table 4-2**) what explains that the hyaluronic acid coating in PCL+HA2s does not fill the pores when swollen.

Mechanical properties of the scaffolds tested were similar. There were initially some concerns about the effect of treatment because of the usage of sodium hydroxide (which can cause a cleavage of the ester bonds). As can be seen in **table 4-2**, there is no statistically significant difference in the moduli neither in dry nor in wet state; the effect of the treatment on PCL scaffolds mechanical properties is minimal and should not compromise the further use of the scaffold as a chondral implant. In the wet state, modulus decreases as described by other groups even when testing polycaprolactone based materials.[195, 196] Despite the high hydrophobicity, water diffusion inside the amorphous and crystalline part of PCL is very fast,[197] and may lower stiffness by decreasing interchain and intrachain interaction due to electrostatic interaction between water dipoles and carbonyl groups of PCL.

The elastic compressive moduli shown are in the range of moduli described for human articular cartilage by Athanasiou et al. [198] (0.5–1.82 MPa) although other groups have obtained higher values of 8–13.5 MPa[199] depending on the joint observed, when measuring with higher loading rate, described as ‘‘instantaneous modulus’’. In a previous work, our group implanted macroporous PCL scaffolds (with similar elastic modulus) in a rabbit knee model[48]; after 3 months, scaffolds seeded with allogenic chondrocytes were invaded by neoformed tissue; indentation measurements showed that the elastic modulus of the tissue–scaffold construct was the same than that of native cartilage controls (and significantly higher than pellet control). The values of the moduli measured here are similar those in that study and should grant adequate mechanical properties *in vivo* if the pore structure is successfully invaded by tissue. Higher initial modulus could be easily reached by varying the PCL content in the solution during the scaffold preparation (equilibrium modulus up to 4–5 MPa). Sample stiffness is an important factor in articular cartilage tissue engineering as articular cartilage is subjected to high dynamic compression loading *in vivo*. It has been shown that cartilage cells change their

secretion profile[102] when exposed to an excessive load: catabolic activity becomes faster than anabolic activity, which provokes a loss of proteoglycans,[103] matrix degradation and consequently a further decrease in mechanical properties. This usually leads to a repair tissue with inferior biochemical and biomechanical properties.[53] Matching rigidity of cartilage tissue using only a hydrogel is very difficult, and moreover the high chain density and network crosslinking necessary to obtain such rigidities using hydrogels has been shown to inhibit extracellular matrix production.[104] This type of structure (particularly PCL+HA1s) is thus interesting, as the polyester scaffolding guarantees adequate macroscopic mechanical behaviour, yielding a rigidity similar to cartilage while the microenvironment as sensed by the cells is a kind of diluted jelly, thus favouring cell migration, ECM production and diffusion.

Cells adhered to the material and proliferated in all three-dimensional supports. Seeding efficiency was lower in PCL+HA1s, what could be related to the presence of the gel phase inside the pores as seen in **figure 4-1**. This explains also the low densities found at day 7 in confocal microscopy; heterogeneous cell distribution may be due to limited diffusion throughout the gel. Hyaluronic acid may also be responsible for the reduced initial adhesion and seeding efficiency due to its hydrophilic character that does not permit non-specific adsorption of proteins.[64] As shown in the confocal microscopy images, the first and obvious differences in chondrocyte behaviour is the cell arrangement within the scaffold. Whereas in PCL scaffolds the cells tend to grow spread over the pore walls, in presence of hyaluronic acid cells are seen filling the pore space. Cell distribution in PCL–HA2s is quite uniform while in the case of PCL–HA1s it is less homogeneous appearing some cell clustering. It has been described in the literature that scaffolding materials, although presenting a 3D structure, do not necessarily encourage 3D growth *in vitro*, and that the behaviour of the cells seeded into macroporous scaffolds may be very similar to

that of 2D cultures if at the cell's scale, the pore wall appears as a flat surface.[200] This fact has motivated the use of a cell carrier together with the scaffolds,[201] or secondary gel phases inside the pores,[202] to get a three-dimensional tissue growth as occurs *in vivo* mainly due to the formation of a fibrin clot inside the implant. Here it appears that the modification of PCL with a hydrogel, in this case HA, can change this behaviour, although it is not clear why. Lower modulus of hyaluronic acid may allow for greater mobility of cells; it is known that in materials with rigidity gradients, cells tend to accumulate on the stiffer parts,[203] and that focal adhesions are strengthened by the increased rigidity.[204] As a matter of fact, formation of marked stress fibres in the actin cytoskeleton, which is associated with dedifferentiated phenotype,[188,192] is more prominent in PCL control than in other samples. This difference in growth mode may account for some of the effects observed in the immunofluorescent marking for collagen type I, II and aggrecan. Another clue feature may be the activation of intracellular pathways due to the binding of cells to hyaluronic acid through CD44; in fact CD44 expression at the end of culture time is higher in samples that contain HA, regardless of the structure of hyaluronic acid in the samples (**figure 4-4**). High levels of CD44 expression have been described as a clue for increased chondrogenic capacity in chondrocytes subpopulations and high expression of CD44 and integrin α3 was associated with more glycosaminoglycans production per cell and more mRNA of collagen type II.[205]

The formation of a pericellular matrix like surrounding the cells composed by aggrecan was observed occasionally in PCL+HA1s samples and may be triggered by the interaction of hyaluronic acid with CD44 and to the better retention of small proteoglycans due to constructive interaction with exogenous hyaluronic acid at specific binding sites.[206] Both in PCL+HA1s and PCL+HA2s, molecular weights between crosslinks are far higher than the number of hyaluronic acid saccharides

necessary for CD44 binding (observed already with hexasaccharides).[207] Nevertheless intracellular cascades that depend on CD44 may react in a different way upon binding; for instance clustering of CD44 with other membrane components may be hampered if CD 44 receptor is anchored to hyaluronic acid chain with very low mobility and high stiffness, as may be the case in PCL+HA2s. This may explain why scarce quantitative differences are observed between PCL+HA2s samples and PCL controls despite the qualitative differences observed by immunofluorescent staining. Another mechanism implied in the different response in PCL+HA1s and PCL+HA2s could be the influence of molecular crowding and of hyaluronic acid chain mobility on the ECM synthesis.[208] It is also likely that albeit due to restricted diffusion through the gel phase or due to an enhancement in the specific interaction between aggrecan and hyaluronic acid binding sites due to chain mobility glycosaminoglycans retention inside the construct is easier in PCL+HA1s. Higher normalized GAGs content could be due to better retention or to higher synthesis of GAGs; combination of quantitative analysis of gene expression and analysis of GAGs secreted in the medium will be necessary to clarify this point.

4.2.6 Conclusions

Primary articular chondrocytes were cultured in dedifferentiating conditions and the effect of two types of hyaluronic acid coating on cell proliferation, cell morphology, GAGs synthesis, ECM and cell markers was studied. Cells in PCL controls show signs of dedifferentiation such as reduced biosynthetic capacity, low staining for collagen type II and aggrecan and increased staining for collagen type I. In control samples the cells grow stuck on the pores walls, cells show a fibroblastic shape, and their behaviour can be assimilated to 2D behaviour. In samples modified with HA,

cell distribution is more heterogeneous and different cell sub-populations are found in the construct, with the formation of cell clusters that depending on localization or cell organization show either positive markers for collagen type I or collagen type II and aggrecan. In some zones the behaviour is similar to that observed in PCL control (cells spread on pore wall), while in other zones formation of cell clusters and three dimensional growth is observed; in these zones there is more presence of cartilage specific ECM like collagen type II and aggrecan. In both HA containing samples, markers for CD44 are detected on most cells whereas in pure PCL samples there is hardly any presence of CD44. ECM production per cell is higher in PCL-HA1s than in both PCL and PCL-HA2s samples.

All the mentioned results point towards a better phenotypic conservation in PCL-HA samples, with promising results when using PCL-HA1s. Enhanced hydrophilicity of the constructs and increased CD44 expression of chondrocytes in presence of HA shows that the strategy followed could be useful for cartilage tissue engineering in a cell-free approach if the increased hydrophilicity favours cell invasion and the presence of HA permits to home CD44 positive cells, which will be the subject of future works.

4.3. Characterization of hypoxia as culture condition to develop an *in vitro* construct.

Autologous cell implantation requires a huge number of cells, and bone marrow mesenchymal stem cells is generally considered as a suitable source.[53, 112] Nevertheless, as commented in the introduction, the technology for successful MSC-based cartilage tissue engineering is still lacking. The objective of this part of the work and the following sections was to test the influence of different culture conditions on chondrogenic differentiation of MSC cultured within the pores of our PCL+HA scaffolds. The results obtained in these scaffolds will be compared with those of pure PCL scaffolds and scaffolds made of a composite of PCL with 5% by weight of bioactive glass nanoparticles (PCL-5BG). This task was developed on Trinity Centre for Bioengineering (TCBE) under the supervision of Dr. Daniel J. Kelly and Dr. Yurong Liu. Present section is focused on the use of hypoxia during culture of mesenchymal stem cells in chondrogenic medium. The quality of the tissue produced by the cells *in vitro* was evaluated by testing its mechanical properties and measuring cell and extracellular matrix levels and distribution. Hyaluronic acid coating protocol selected was the one step but in order to improve cell seeding efficiency it was slightly modified, these samples will be called hereafter PCL+HA1s-m. The modified protocol sought to produce a thin layer of hyaluronic acid on the pore walls leaving more free space in the macropore during cell seeding than in PCL+HA1s samples. Protocol modification, described in the materials and methods section, was to dry the sample along the crosslink reaction to produce a hyaluronic acid coating with less swelling capacity when cell suspension is injected into the scaffold. On the other hand Bioglass® was introduced into PCL scaffolds to increase the scaffold hydrophilicity improving cell invasion and cell seeding efficiency. *In vitro* construct characterization was performed with porcine bone marrow mesenchymal stem cells under hypoxia conditions.

Samples	Polymer composition	Mineral composites	Hydrogel hybrid material	
		Ceramic reinforcement	Polysacharid coating	Crosslink method
PCL	Polycaprolactone	-	-	-
PCL+HA1s-m	Polycaprolactone	-	Hyaluronic acid	One step with divinyl sulfone
PCL-5BG	Polycaprolactone	5% Bioglass	-	-

Table 4-3. Table with tested samples.

Scaffolds of 5mm diameter and 3 mm height were seeded with porcine MSC at 500000 cells/scaffold and cultured with chondrogenic media under hypoxia conditions (5% CO2 - 5% O2) for 35 days. Control PCL, PCL+HA1s-m and PCL-5BG samples were cultured under normoxia conditions (5% CO2 - 20% O2) for 35 days.

Samples ID	Scaffold		Culture conditions	
	Scaffold	Scaffold ID	Culture condition	Culture condition ID
PCL NO	PCL	PCL	Normoxia	NO
HA NO	PCL+HA1s-m	HA	Normoxia	NO
BG NO	PCL-5BG	BG	Normoxia	NO
PCL HY	PCL	PCL	Hypoxya	HY
HA HY	PCL+HA1s-m	HA	Hypoxya	HY
BG HY	PCL-5BG	BG	Hypoxya	HY

Table 4-4. Table with cultured samples ID for present section, tested samples and scaffold culture conditions.

The influence of scaffold over cell response to hypoxia was performed evaluating the ECM using histological stain and immunostains to determine ECM distribution as well biochemical and mechanical evaluation of ECM.

4.3.1. Mechanical properties

Equilibrium elastic modulus (measured in a stress-strain compression ramp) and dynamic mechanical modulus (measured under dynamic compression loading) are depicted in **figure 4-7**. Contribution of the growing tissue over dynamic modulus increases with culture time in both conditions for all the materials. For PCL (NO and HY) and BG (NO and HY), increment was scarce in the first two weeks and increased between day 17 and day 35, while in HA (NO and HY) samples the increase was steady over the whole culture time. Oxygen tension in the culture did not have any significant effect over the mechanical properties in none of the samples. No significant trend was observed in the values of the equilibrium modulus, presented in **figure 4-7**.

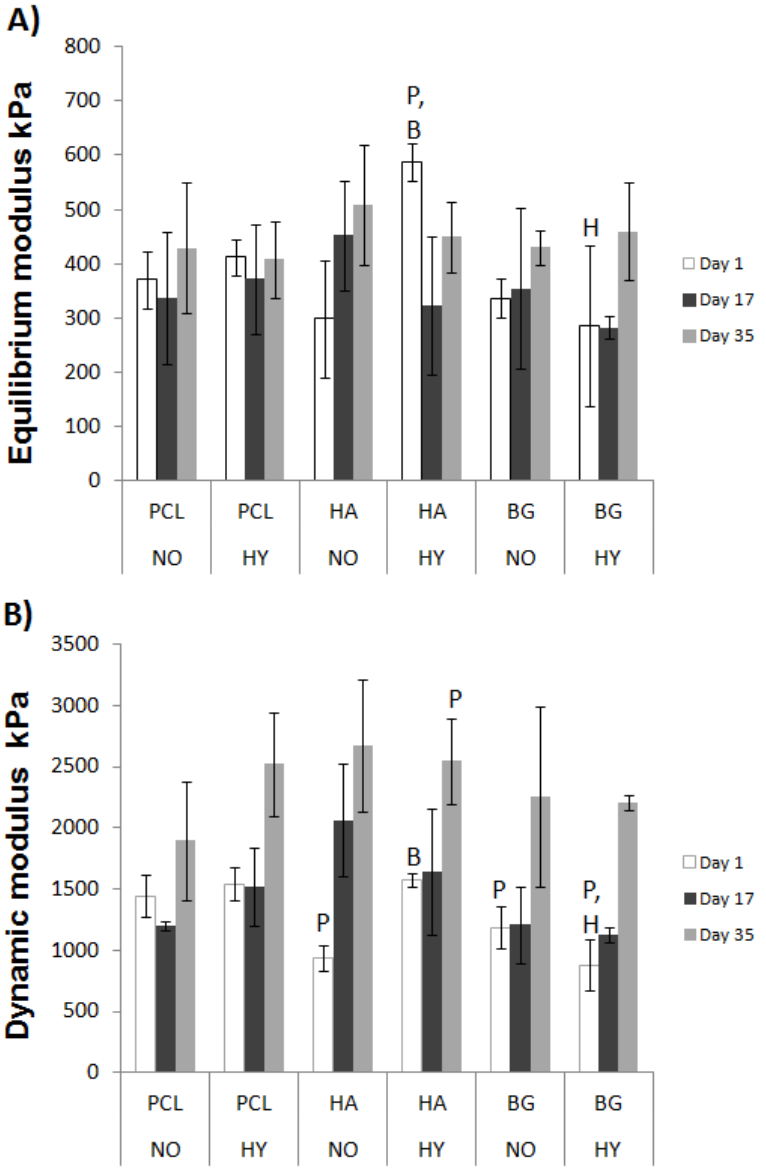

Figure 4-7: Mechanical results. Equilibrium modulus (A) and dynamic modulus (B) at day 1, 17 and 35 under normoxia (NO) and hypoxia (HY). Results are averaged from n=4 experiments. Error bars represent standard deviation. Significance ($p<0.05$) compared to similar group for normalized scaffolds is signalled as: (P) PCL, (B) BG and (H) HA samples for each group at the same time and culture condition.

4.3.2. Cell behaviour and differentiation

The evolution of DNA content in the constructs is shown in **figure 4-8**. Initial cell number at day 1 (a standard curve of mesenchymal stem cells numbers vs. DNA content was determined for this purpose) showed that seeding efficiency in BG (79.63 ± 12.26) and PCL (78.27% ± 8.02) scaffolds were similar, whereas seeding efficiency in HA (48.75% ± 11.71) constructs was lower. In all constructs cells proliferated up to day 17, showing that materials support mid-term survival of mesenchymal cells. Proliferation was slower in hypoxic conditions than in normoxic ones up to day 17, except for HA NO and HA HY samples, where proliferation was equal in both conditions. From day 17 to day 35, DNA content remained nearly constant for all samples in hypoxic conditions and for PCL NO. However, there was a strong decrease in DNA content in BG NO and HA NO samples during the same time.

MSC chondrogenic differentiation was studied by assessing the production of ECM components, such as glycosaminoglycans and collagen, by the cells. Glycosaminoglycans content normalized to total DNA is shown in **figure 4-9**. Glycosaminoglycans secretion increased with time for all samples. In normoxic conditions, glycosaminoglycans secretion was limited; hypoxia led to significant enhancement for most conditions (PCL HY at all times, HA HY at 35 days and BG HY at 17 days). Glycosaminoglycans secretion per cell was comparable for hypoxic cultures in all materials. In normoxic conditions, GAGs secretion remained low (increase seen in BG NO sample is mainly because the decrement in DNA levels at 35 days). Results for collagen secretion are shown in **figure 4-9**. collagen secretion per cell also increased over time, being superior at day 35 for all samples. At day 17, both HA (NO and HY) and BG (NO and HY) scaffolds showed inferior collagen secretion than PCL scaffolds both in normoxic and hypoxic conditions, whereas at day 35 only HA (NO and HY) showed inferior collagen level. Hypoxia did not show

a positive effect on collagen content per cell. The only two conditions where there was a significant difference was for PCL HY and BG HY at day 17, where normoxic samples showed increased collagen content with respect to the hypoxic ones.

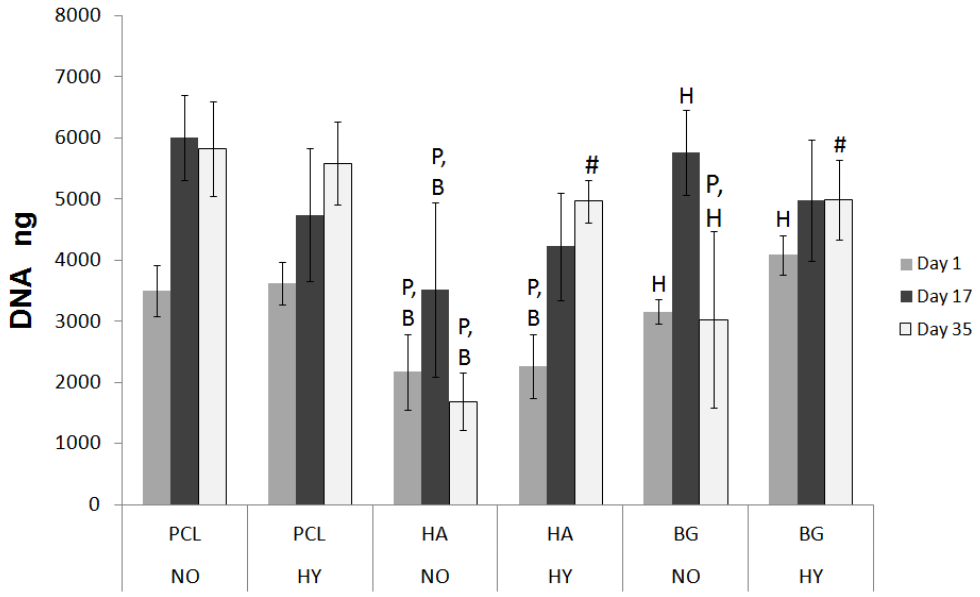

Figure 4-8. Total DNA of porcine mesenchymal stem cells after seeding at day 1, 17 and 35 in scaffolds under normoxia (NO) and hypoxia (HY). Results are averaged from n=4 experiments. Error bars represent standard deviation. Significance ($p<0.05$) compared to similar group for normalized scaffolds is signalled as: (P) PCL, (B) BG and (H) HA samples for each group at the same time and culture condition and (#) statically cultured sample from the same type at the same time.

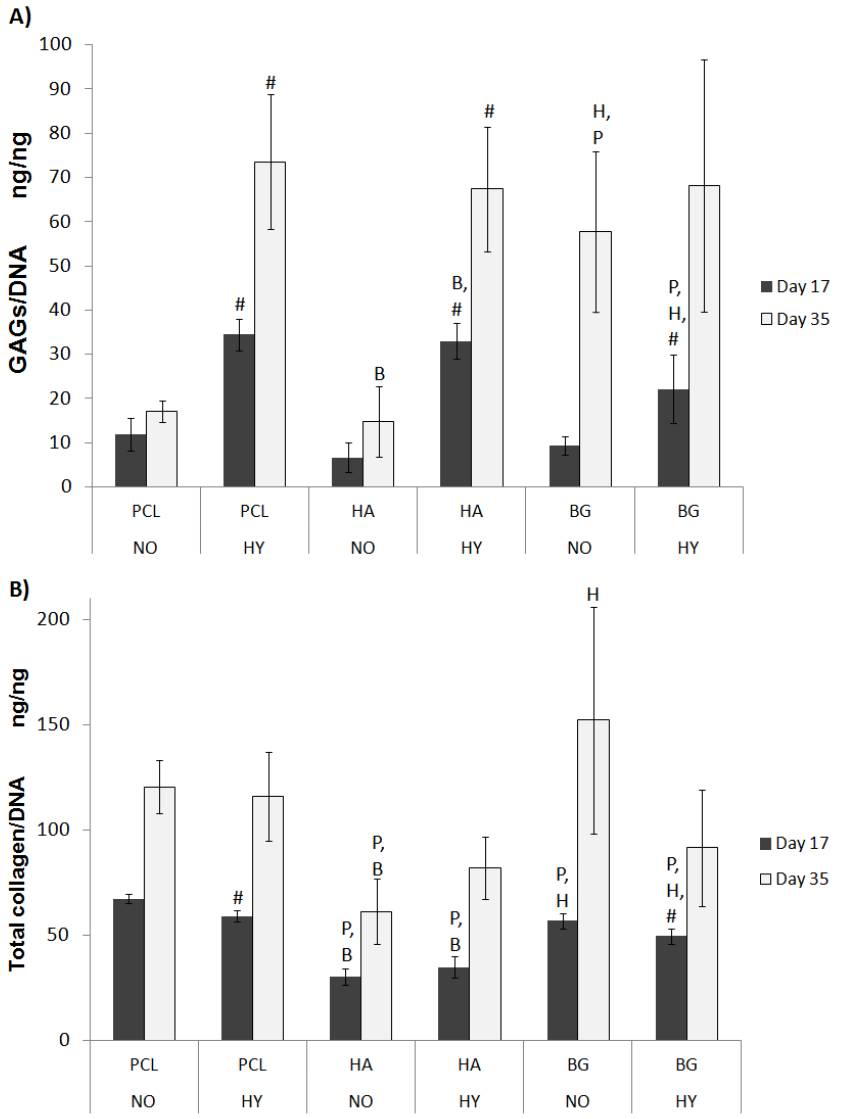

Figure 4-9. Glycosaminoglycans (GAGs) (A) and collagen (B) levels normalized to total DNA at day 17 and 35 under normoxia (NO) and hypoxia (HY). Results are averaged from n=4 experiments. Error bars represent standard deviation. Significance ($p<0.05$) compared to similar group for normalized scaffolds is signalled as: (P) PCL, (B) BG and (H) HA samples for each group at the same time and culture condition and (#) statically cultured sample from the same type at the same time.

A qualitative observation of extracellular matrix secretion at 35 days is provided in **figure 4-10**, **figure 4-11** and **figure 4-12**. Accumulation of glycosaminoglycans over culture time is shown in **figure 4-10**. In normoxic conditions, staining of mucopolysaccharides (shown in blue in **figure 4-10**) is limited, with a smooth blue staining filling the pores (PCL NO and BG NO) whereas in HA NO sample the secretion was limited to isolated cell clusters. In hypoxic conditions, in all materials there were significant amounts of matrix filling the scaffolds pores and in some zones of intense blue color, cells were embedded in lacunae within a glycosaminoglycans-rich matrix. Collagen deposition shown in red in **figure 4-11**; consistent with the findings of the biochemical analysis, collagen deposition is higher in PCL and BG samples, while in HA samples less intense stain is observed. Stained parts show either a rough and fibrous texture (such as in BG (NO and HY) samples or PCL NO sample) or a non textured pink background such as in PCL HY and HA HY samples.

Secretion of cartilage specific collagen was assessed using immunochemical stain against collagen type I (**figure 4-12**) and collagen type II (**figure 4-12**). In all samples both types of collagen are present; hypoxic culture mode leads to a reduction in collagen type I specific staining, whereas collagen type II staining was slightly more pronounced. In HA NO sample there was not much matrix stain either of collagen type I or collagen type II, but in HA HY sample there was a pronounced staining for collagen type II.

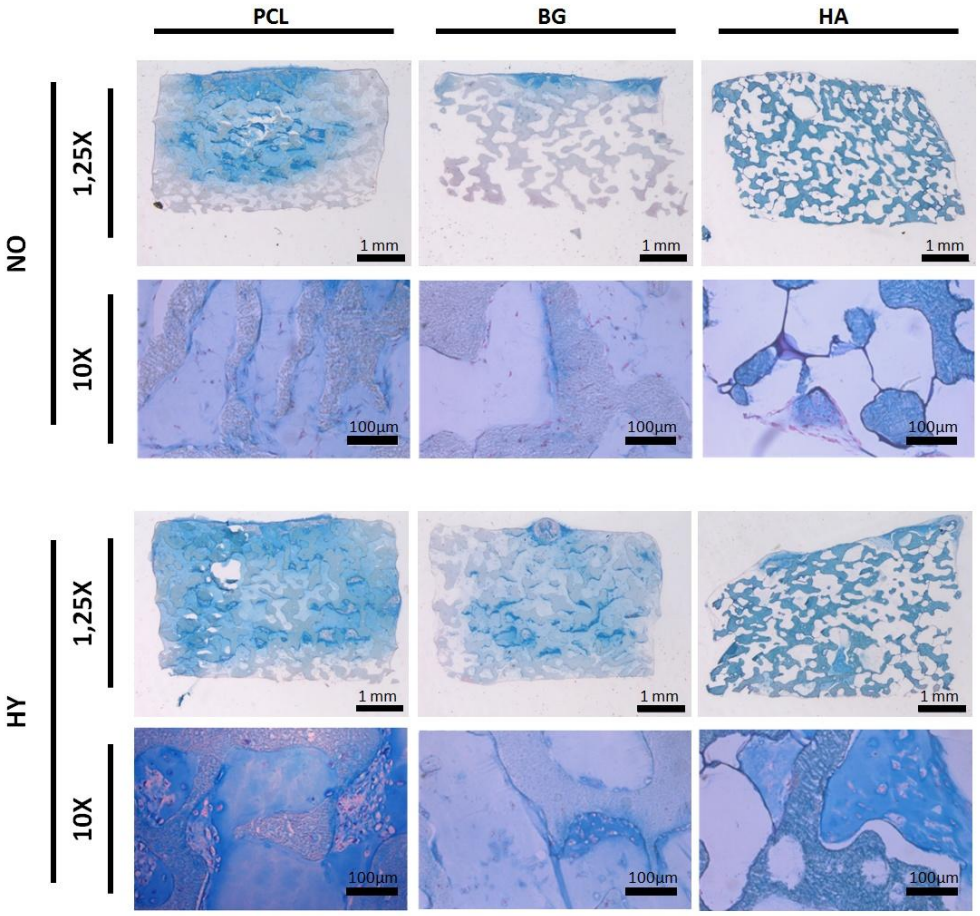

Figure 4-10. Alcian Blue staining for glycosaminoglycans at day 17 and 35 under normoxia (NO) and hypoxia (HY). Glycosaminoglycans appear in blue and cells in pink. (magnification/scale bar = X1.25/1mm and X10/100 µm).

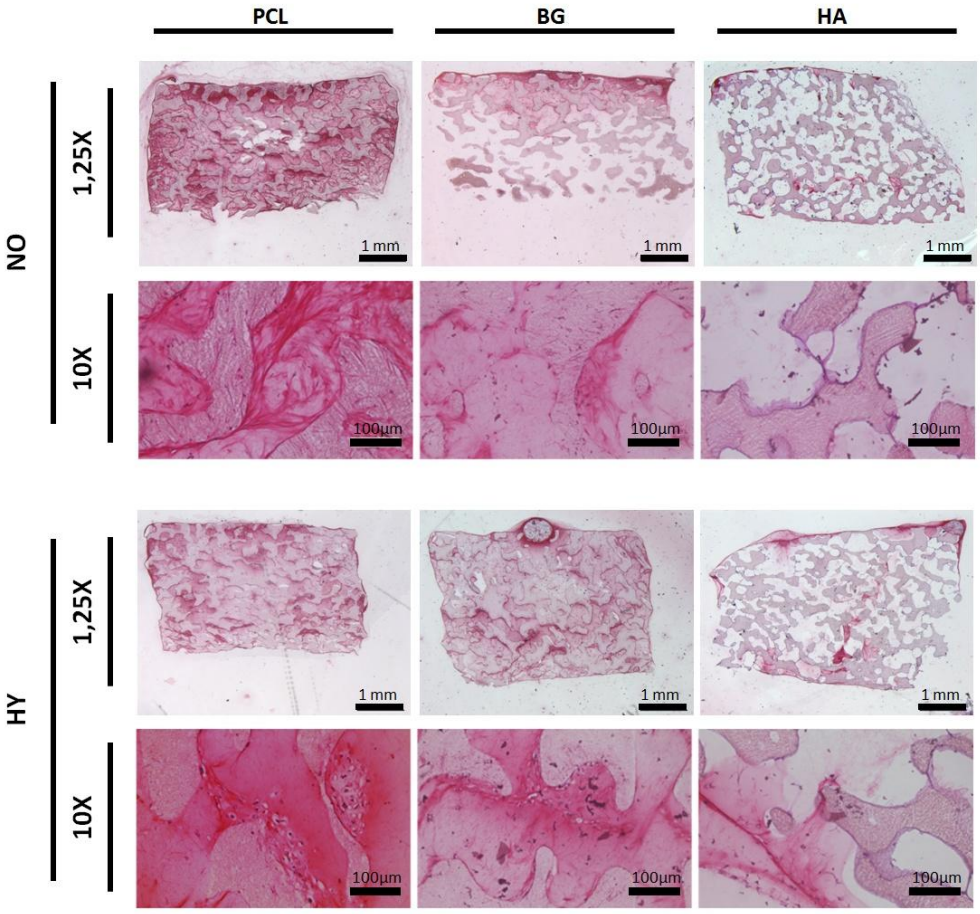

Figure 4-11. Picro-Sirius Red staining for collagen at day 17 and 35 under normoxia (NO) and hypoxia (HY). Collagen appears in red and cells in purple. (magnification/scale bar = X1.25/1mm and X10/100 µm).

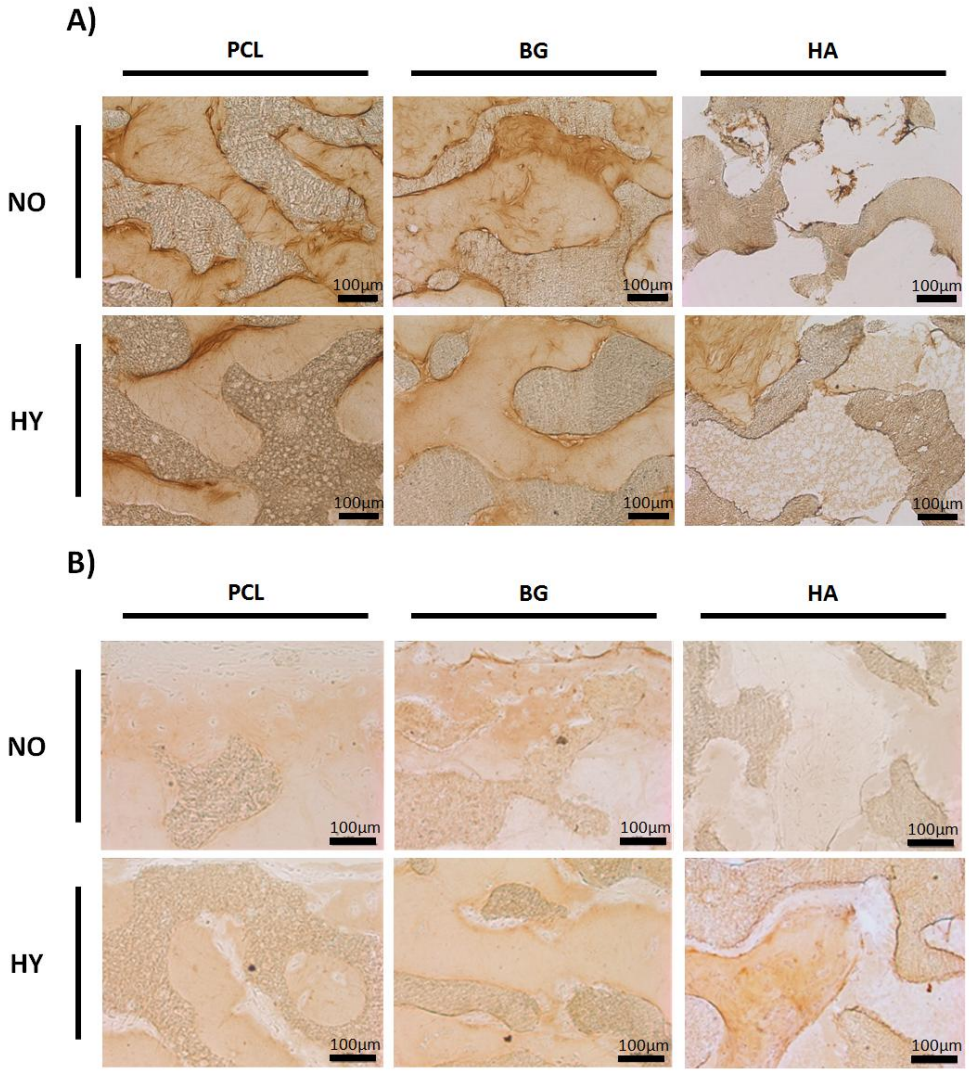

Figure 4-12: Microscopic views of anti- collagen type I (A) and anti-collagen type II (B) immunohistochemical staining of scaffolds cultured with mesenchymal stem cells at day 35 under normoxia (NO) and hypoxia (HY). Scaffold appears gray and collagen is brown. (magnification/Scale bar = X10/100µm).

4.3.3. Discussion

The hypothesis of this study was that hypoxia improves viability and chondrogenesis in *in vitro* culture in our scaffolds. Cartilage is constitutively hypoxic with oxygen levels between 1% to 7% depending on the depth inside the tissue[120]. Hypoxia has been seen to regulate chondrogenic induction of MSCs, partly through the activation of hypoxia inducible factors, mainly HIF-1α which accumulates inside the nucleus in hypoxic conditions and modulates DNA binding affinity of various gene promoters[209]. Not only SOX9 promoter's affinity for DNA is upregulated by HIF-1α, but also Cbfa/RUNX2 promoter affinity for DNA is downregulated in presence of HIF-1α, and the balance between SOX9 and RUNX2 has been shown to be critical in the switch between adult mature chondrocytes and hypertrophic chondrocytes[123]. Hypoxia may thus be an easy way to avoid terminal differentiation, as well as to improve the quality of the formed tissue; several enzymes implicated in matrix synthesis, including hydroxylases, are more stable in hypoxic conditions, contributing to enhance ECM quality[124,209].

In our work, agarose mould was used to improve cell seeding and in fact it was successful, obtaining a cell seeding efficiency higher than 50%. On the other hand. normoxic culture of chondroinduced MSCs during up to 35 days in synthetic scaffolds resulted in a decrease in DNA content in both HA NO and BG NO groups with respect to 17 days, whereas a slight decrease was seen in PCL NO group. Chondrogenic differentiation that follows into a terminal differentiation provokes apoptosis in MSCs[210], and hypoxia has been shown to inhibit apoptosis of chondrocytes and chondroinduced MSCs via both the HIF-1α and the PI3K/Akt pathway[211]. This could explain why hypoxia was necessary in order to maintain constant DNA content over a large culture period when cultivating MSCs along the chondrogenic pathway in our materials. Supplementing with TGFβ3, in our model, was not sufficient to maintain cell viability in high oxygen conditions over a large

period.

Hypoxia increased glycosaminoglycans/cell synthesis in PCL HY and HA HY materials, whereas no significant difference was seen in BG HY materials. Consistent with findings from the literature, total collagen content per cell in normoxic culture in PCL NO and BG HY was higher at 17 days than in their hypoxic counterparts, whereas in all other conditions no significant differences between normoxia and hypoxia were found.

Due to the lack of a general theoretical framework about the mechanisms of ECM deposition enhancement in hypoxic conditions and to the variety of the experimental setups (levels of oxygen employed:1, 2, 4, 5, 10%; timing of hypoxia; culture mode: scaffold, pellet/ aggregate, hydrogel; cell source: bone marrow, adult chondrocyte, synovium derived stem cells, infrapatellar fat stem cell) findings from literature often look contradictory and fuzzy. These findings can mean that the cells under hypoxia regulate the secretory profile from a non-specific one to a more hyaline cartilage profile. It has been reported that in hyaline cartilage the content of collagen is 15% and that of proteoglycans 9% percent of total cartilage wet weight[6] , thus the ratio collagen/proteoglycans is 1.67. In the present study we found that PCL NO and HA NO showed aberrant ratios of 6 while the ratio was 3 in BG NO. On the other hand in the same sample compositions (bare PCL, Bioglass® composite and PCL coated with hyaluronic acid) under hypoxia a ratio around 1.5 was determined. Our results suggest that ECM evaluation in base to increments or decrements of biochemical components levels is not enough. Collagen/proteoglycans ratio provides direct measurement about tissue quality. In our work hypoxia showed a powerful positive effect over cell differentiation more important than cell substrate. On the other hand Bioglass® composite showed a surprisingly positive effect over collagen/proteoglycans pointing that bioactive glasses can have a positive use on cartilage tissue engineering but need further studies to check if differentiation leads

to hypertrophic cartilage.

Increased GAGs synthesis as a result of hypoxic culture was observed in many[212,213] but not all published works [214,215] in literature. Increased collagen secretion by cells is not a common finding (in some cases even inferior values are found in hypoxic conditions[124]) although more specific staining for collagen type II and less staining for collagen type I is generally described [213**]**. In our work, both collagen type I and collagen type II were observed, although collagen type I deposition was limited and collagen type II increased under hypoxia; culture of the cells on a rigid substrate that appears as two-dimensional for cells due to the pore size may be related to the presence of collagen type I, which is very limited in hydrogel cultures [213]. One reason for this may be the regulation of cell fate through cell cytoskeleton and cytoskeletal tension. Whereas hydrogel culture promotes cell rounding and limits cytoskeletal pre-stress due to the presence of actin in a cortical form, adhesion to rigid materials and spreading is associated with developed actin fibres and cytoskeletal tension, which is known to favour the production of fibrous tissue[216]. This is concordant with the observation of marked fibrous texture observed in picrosirius stain in normoxic cultures. Interestingly, a great qualitative difference was observed under hypoxia, where a diffuse staining was observed whereas cells appeared more prone to cluster formation. Around these clusters that seem to mimic the condensation stage, glycosaminoglycans deposition was increased. Hyaline cartilage ECM is mainly formed of glycosaminoglycans, which provide compression resistance through osmotic retention of water in their negatively charged chains, and fibrillar collagen type II, which provides tensile resistance. Promotion of GAGs secretion through hypoxia promotes the balance between collagen and glycosaminoglycans content in the formed tissue, leading to a cartilage-like appearance of the formed tissue in all three materials. At the contrary, lack of glycosaminoglycans in the secreted ECM (which in our model is not

mimicked by the presence of an hydrogel phase, as when chondrocytes are cultured in alginate or agarose gels) leads to the formation of highly fibrous extracellular matrix that likely promotes excess cytoskeletal tension, which may lead to further phenotypic mismatch and production of collagen type I instead of collagen type II. Moreover, traditional models (hydrogel or pellet) enhance the retention of ECM[217]; in the case of pellet or aggregates, the dimension of the construct is determinant in restricting the diffusion of secreted macromolecules into the culture medium [218]. Despite of these pitfalls of our system with respect to *in vitro* culture (as they can be seen as positive for *in vivo* applications where the constraints are different), significant amounts of ECM were observed in all materials excepted HA NO. Hypoxia proved a more decisive influence than the material modification with respect to chondrogenesis, although hyaluronic acid modification in the present form did not show a positive response as expected. Modification with Bioglass® seemed to lead to some increase in glycosaminoglycans production and collagen type II staining in normoxic conditions, (although total collagen per cell was significantly lower than PCL control at 17 days in both hypoxic and normoxic conditions) but had no significant effect in hypoxic conditions. Release of phosphate ions may have contributed to cell apoptosis in these samples,[219] explaining the decrease in DNA content observed between day 17 and 35.

4.3.4. Conclusions

Our data suggests that in our scaffolds TGFβ3 induced chondrogenesis but let's to cell apoptosis in normoxic conditions as observed through the DNA values; thus, in our model, hypoxia conditions were necessary to maintain viability up to 35 days in culture. Additionally hypoxia regulated ECM synthesis. GAG/cell ratio was increased under hypoxic conditions in PCL and HA scaffolds. On the other hand the

collagen level was similar in normoxia and hypoxia conditions but staining for collagen type II was more prominent under hypoxia. Hypoxia induces a collagen/GAGs ratio closer to that of healthy cartilage the differences in this respect with normoxia culture conditions increases with culture time. An unexpected result was that BG reinforced scaffold showed the lower ratios in normoxia (2.7) compared to PCL and HA coated scaffold (6.4 and 5.7 respectively). Hypoxic conditions had more influence on biological response than substrate composition.

4.4. Characterization of mechanical stimulation to improve hypoxia effect.

The objective of this part of the work was to check if mechanical stimulation could improve the positive response obtained under hypoxic conditions. This task was developed in the Trinity Centre for Bioengineering (TCBE) and hydrostatic pressure was used as mechanical input to improve the previous results. The materials tested were PCL+HA1s-m, PCL-5BG and PCL. Samples were cultured in free swelling conditions up to 14 days before sealing the samples inside sterile plastic bags and starting to apply hydrostatic pressure during 3 weeks). Samples from the hydrostatic pressure group were placed inside the custom made bioreactor described in the materials and methods section while free swelling control samples were placed in an open water bath, both inside a 37ºC incubator. Porcine MSC were cultured with CDM+ media under hypoxia conditions (5% CO2 - 5% O2) for 35 days. This work has entitled "Compositional changes of synthetic biodegradable scaffolds modulate the influence of hydrostatic pressure on chondrogenesis of mesenchymal stem cells"[220] been recently submitted for publication.

		Mineral composites	Hydrogel hybrid material	
Samples	Polymer composition	Ceramic reinforcement	Polysacharid coating	Crosslink method
PCL	Polycaprolactone	-	-	-
PCL+HA1s-m	Polycaprolactone	-	Hyaluronic acid	One step with divinyl sulfone
PCL-5BG	Polycaprolactone	5% Bioglass	-	-

Table 4-5. Table with tested samples.

Scaffolds were seeded with porcine MSC at 500000 cells/scaffold and cultured with chondrogenic media under hypoxia conditions (5% CO2 - 5% O2) for 35 days sealed inside sterile plastic bags from day 14 to 35.

	Scaffold		Culture conditions	
Samples ID	Scaffold	Scaffold ID	Culture condition	Culture condition ID
PCL FS	PCL	PCL	Free swelling	FS
HA FS	PCL+HA1s-m	HA	Free swelling	FS
BG FS	PCL-5BG	BG	Free swelling	FS
PCL HP	PCL	PCL	Hydrostatic pressure	HP
HA HP	PCL+HA1s-m	HA	Hydrostatic pressure	HP
BG HP	PCL-5BG	BG	Hydrostatic pressure	HP

Table 4-6. Table with cultured samples ID for present section, tested samples and scaffold culture conditions.

The effect of substrate over MSC differentiation response to hydrostatic pressure was evaluated using a dynamic mechanical test to study the ECM contribution to construct mechanical properties as well biochemical and histological study was performed to evaluate the quality of obtained cell-scaffold construct.

4.4.1. Mechanical properties

Equilibrium and dynamic modulus shown in **figure 4-13** were normalized considering that scaffold and ingrowing tissue contribution to total modulus is additive, as in a parallel model (common strain, additive stress). The mechanical properties of polycaprolactone and polycaprolactone/hyaluronic acid scaffolds did not change significantly with time. In contrast, the equilibrium modulus of the PCL-5BG scaffolds increased with time in culture. The dynamic modulus of both hyaluronic acid and BG scaffolds significantly increased with time. The application of cyclic hydrostatic pressure did not significantly affect the equilibrium or the dynamic modulus of any of the three mesenchymal stem cells seeded scaffolds.

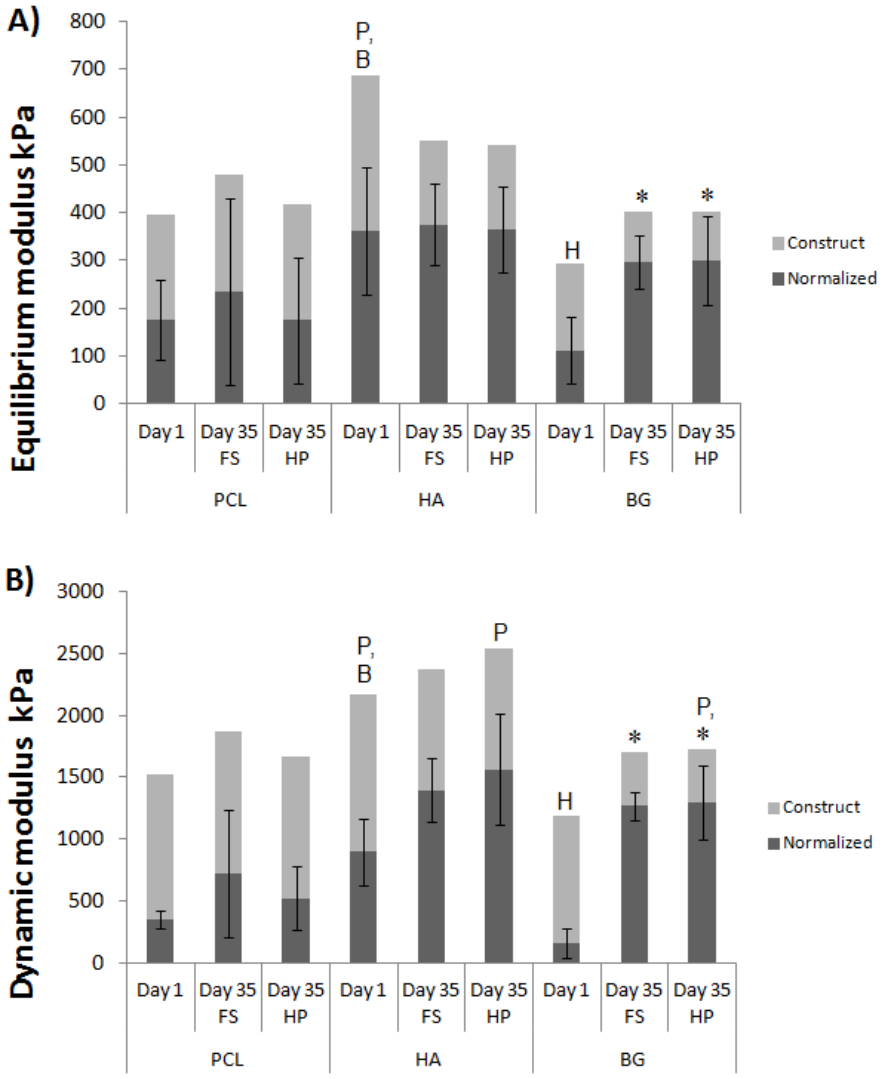

Figure 4-13: Mechanical results. Equilibrium modulus (A) and dynamic modulus (B) of whole construct (soft grey) and normalized (subtracting the value of the corresponding acellular scaffolds) (dark grey), at day 1 and at day 35 under free swelling (FS) and hydrostatic pressure (HP). Results are averaged from n=4 experiments. Significance ($p<0.05$) compared to similar group for normalized scaffolds is signalled as: (P) PCL, (B) BG and (H) HA samples for each group at the same time and culture condition; and (*) sample from the same type at day 1.

4.4.2. Cell behaviour and differentiation

The total DNA content of the scaffolds at day 1 was used as a measure of the cell seeding efficiency of the scaffolds (**figure 4-14**). Cell seeding efficiency was calculated as in the previous section; in HA scaffolds (27.5% ± 15.66) it was significantly lower compared with PCL (63.56% ± 11.21) and BG (88.08% ± 24.43) scaffolds which were not significantly different to each other. DNA content increased with time for all three scaffold types, demonstrating that they supported mesenchymal stem cells proliferation (ratios of proliferation between 1.5 and 4). Proliferation was highest in the HA scaffolds, its values at 35 days were similar to BG and PCL samples. Hydrostatic pressure did not significantly affect mesenchymal stem cells proliferation within the scaffolds.

On the other hand as seen from glycosaminoglycans and collagen levels normalized to total DNA at day 35 (**figure 4-15**), MSCs cultured inside PCL HP and BG HP scaffolds responded positively to the application of hydrostatic pressure, showing both significantly higher production of glycosaminoglycans and collagen than their respective free swelling control. In contrast, HA HP scaffolds loading had no significant effect on GAGs production, and moreover it had a significant and negative impact on normalized collagen levels. On the other hand collagen/GAG ratio results for all tested samples (in HP and FS conditions) was close to 1.67 the value reported for hyaline cartilage[6], but was more close in samples of HP group pointing that mechanical stimulation tends to approach slightly this ratio to *in vivo* data.

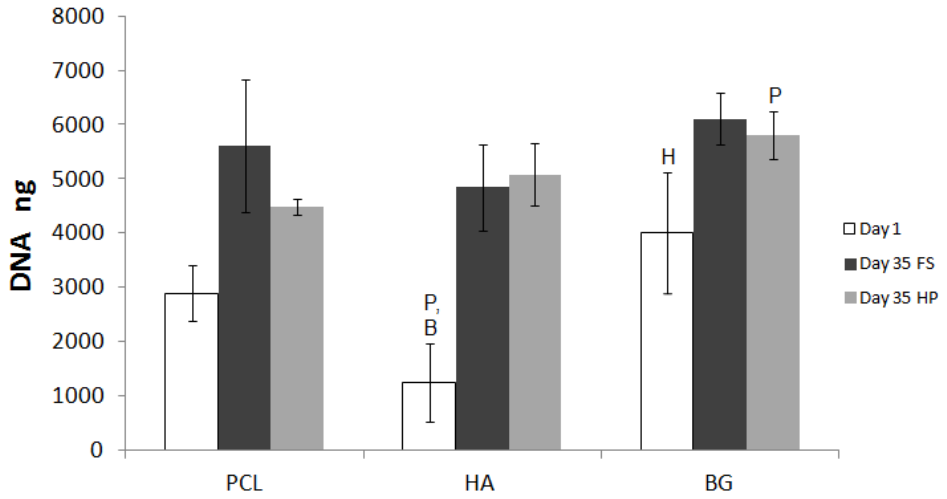

Figure 4-14. Total DNA of porcine mesenchymal stem cells after seeding at day 1 and 35 in scaffolds under free swelling (FS) and hydrostatic pressure (HP). Results are averaged from n=4 experiments. Significance ($p<0.05$) compared to similar group for normalized scaffolds is signalled as: (P) PCL, (B) BG and (H) HA samples for each group at the same time and culture condition.

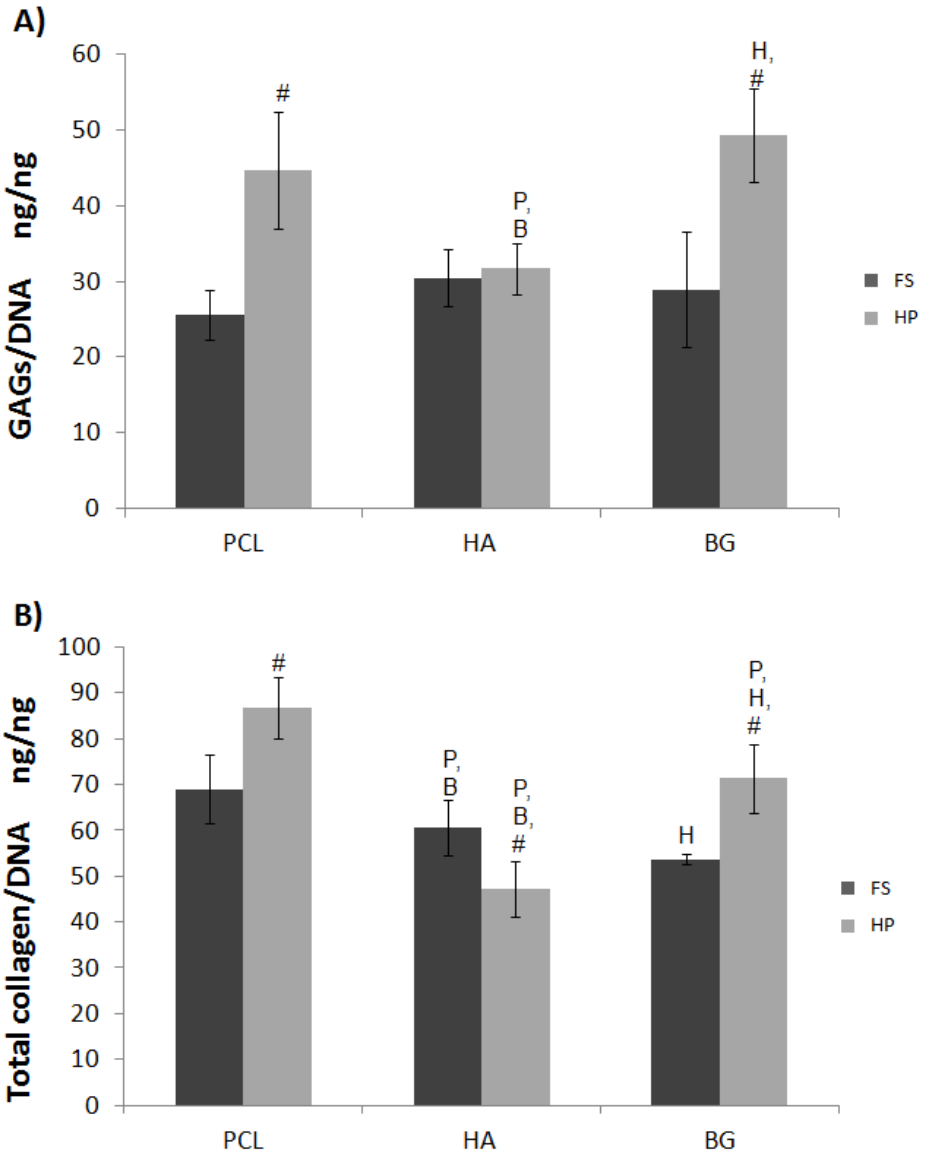

Figure 4-15. Glycosaminoglycans (GAGs) (A) and collagen (B) levels normalized to total DNA at day 35 under free swelling (FS) and hydrostatic pressure (HP) conditions in scaffolds. Results are averaged from n=4 experiments. Significance ($p<0.05$) compared to similar group is signalled as: (P) PCL, (B) BG and (H) HA samples for each group at the same time and culture condition and (#) statically cultured sample from the same type at the same time.

The Picro-Sirius Red and Alcian Blue staining, **figure 4-16**, show the distribution of the cells and secreted extracellular matrix in the different mesenchymal stem cells seeded scaffolds after 35 days in culture. In all the samples, the polymer matrix appears grey, whereas the pore space appears with the background color (if void) or coloured if it contains cells or extracellular matrix.

Collagen staining in all samples is more marked at the scaffold edge and around cell aggregates (**figure 4-16 A**). In free swelling conditions cells seem to aggregate into large clusters, mainly at or just under the surface of the scaffold. The pores of the PCL FS scaffolds appeared to be homogenously filled with a collagenous matrix. On the other hand in HA FS scaffolds, most of the collagen is deposited on the outside of the construct, whereas BG FS situation is intermediary, with most collagen on the surface but with some deposition within the bulk of the construct. Loading seems to improve the distribution of cells and the collagen repartition inside the samples. Mesenchymal stem cells cultured under hydrostatic pressure showed small cell aggregates distributed throughout the scaffold and similar collagen staining pattern filling the pores. Alcian blue staining (**figure 4-16 B**), which stains negatively charged proteoglycans and glycosaminoglycans, showed a different pattern. Generally staining for glycosaminoglycans was more prominent at the center of the samples whereas the edges were poorly stained. (In HA samples, scaffold colour changes from grey to blue-grey due to the staining of the pore walls by Alcian Blue; nevertheless, as hyaluronic acid is deposited as a very thin layer on the pore walls and inside the scaffold struts' microporosity, staining within the pores is not due to the presence of HA). Relatively homogenous Alcian blue staining was observed within HA scaffolds, whereas PCL and BG showed more localized staining.

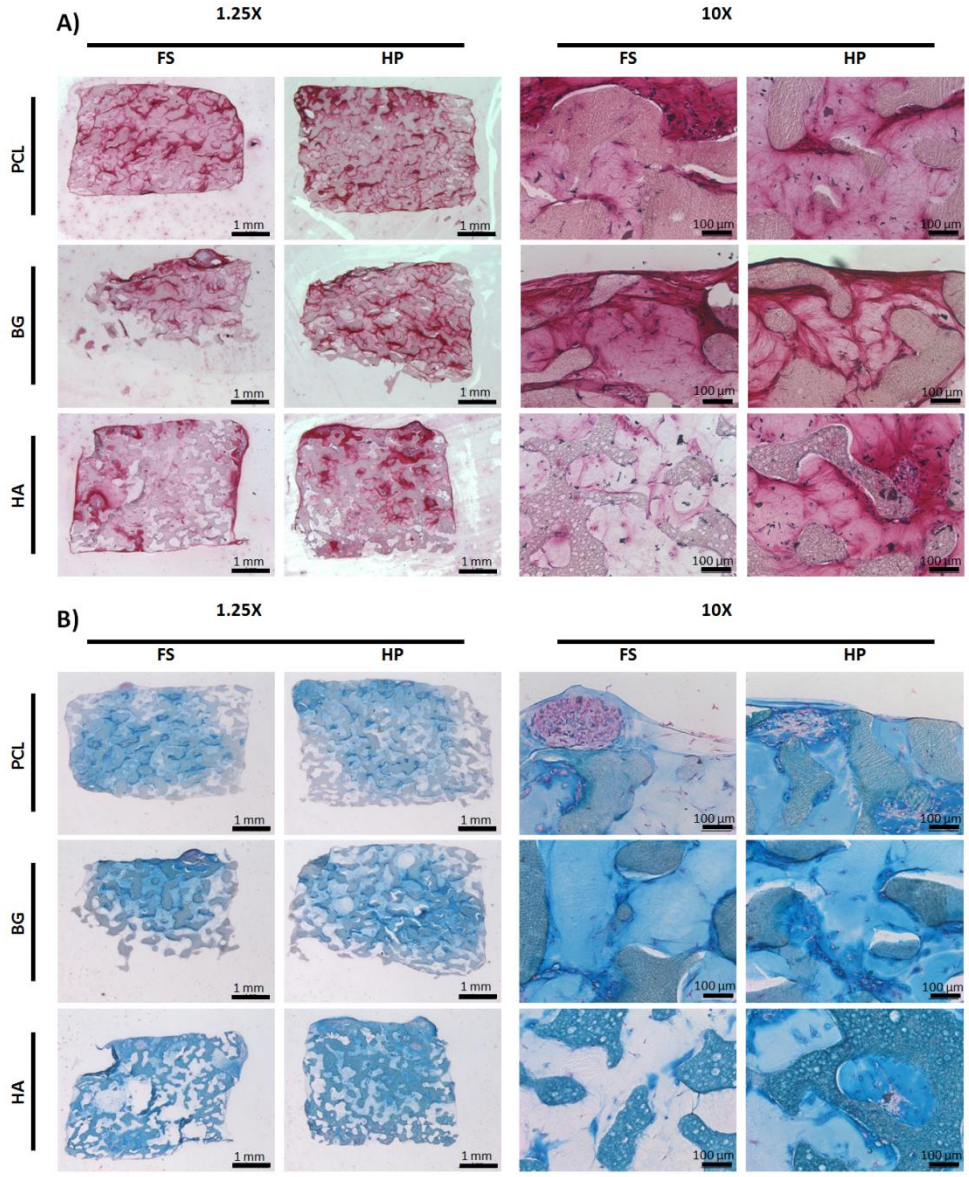

Figure 4-16: (A) Picro-Sirius Red staining for collagen and (B) Alcian Blue staining for glycosaminoglycans at day 35 under free swelling (FS) and hydrostatic pressure (HP). A: Collagen appears in red and cells in purple. B: glycosaminoglycans appear in blue and cells in pink. (magnification/scale bar = X1.25/1mm and X10/100 µm).

Modulation of cell differentiation through the interplay of scaffolding material and culture conditions was studied by examining collagen type I and II deposition using immunohistochemical staining. Immunochemical staining for collagen type I presented in **figure 4-17** follows the staining pattern for picro-sirius red. The macroscopic distribution was quite homogenous, only in HA samples some areas without extracellular matrix were observed, mainly in the bottom part of the scaffold. The common pattern of all samples for collagen type I was a darker staining at the scaffold's edge, either on top or bottom of the construct; moreover, there was heterogeneity at microscopic scale, with zones showing strong staining and zones with almost no stain inside the same pore. In the zones where staining was strong, a fibrillar collagen structure and organization of cells along the fibres were visible. Differences in the staining of collagen type I between adhesive materials (PCL FS and BG FS) and HA FS in free swelling conditions were observed. PCL FS and BG FS show a prominent collagen type I staining compared to HA FS samples that do not show the appearance of strong fibres as in the other samples. Loading conditions affect collagen type I staining profile, and this effect seems to be modulated by the material: whereas staining is more pronounced in free swelling condition for PCL HP and especially for BG HP in the three different zones observed, in the case of HA HP hydrostatic pressure did not show a dramatic effect on collagen type I deposition. The immunohistochemical staining for collagen type II, presented in **figure 4-18** follows the staining pattern for glycosaminoglycans. The macroscopic distribution was not homogenous, with greater type II collagen deposition observed in the center of the scaffolds and the upper surface as seen in the Alcian blue staining. Fibrillar appearance of collagen type II was much less marked than in the case of collagen type I for all samples. In some samples, the typical structure of chondrocytes in their lacunae can be observed, for example in PCL HP in or in HA FS samples. Here again, the effect of hydrostatic pressure was not observable.

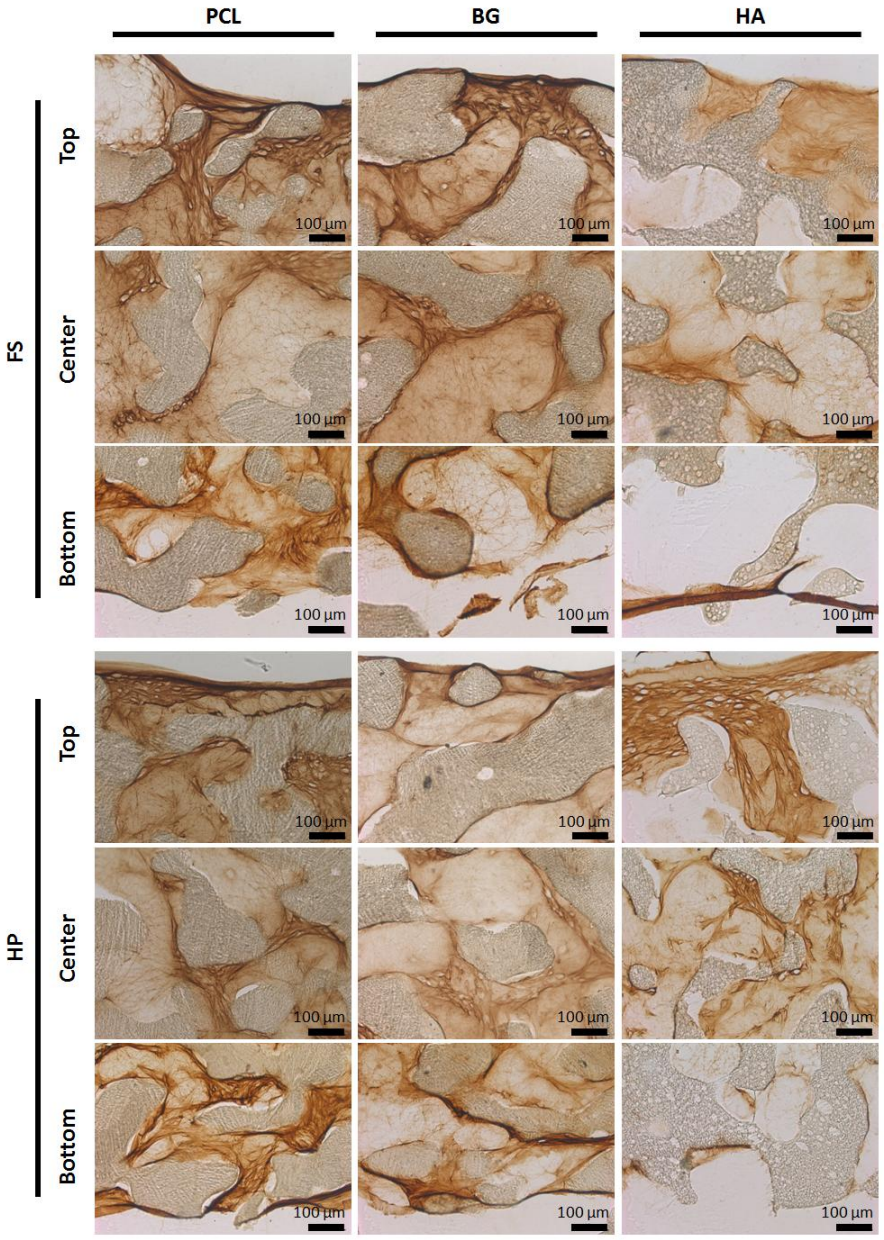

Figure 4-17: Microscopic views of anti- collagen type I immunohistochemical staining of scaffolds cultured with mesenchymal stem cells at day 35 under free swelling (FS) and hydrostatic pressure (HP). Scaffold appears gray and collagen is brown. (magnification/Scale bar = X10/100µm).

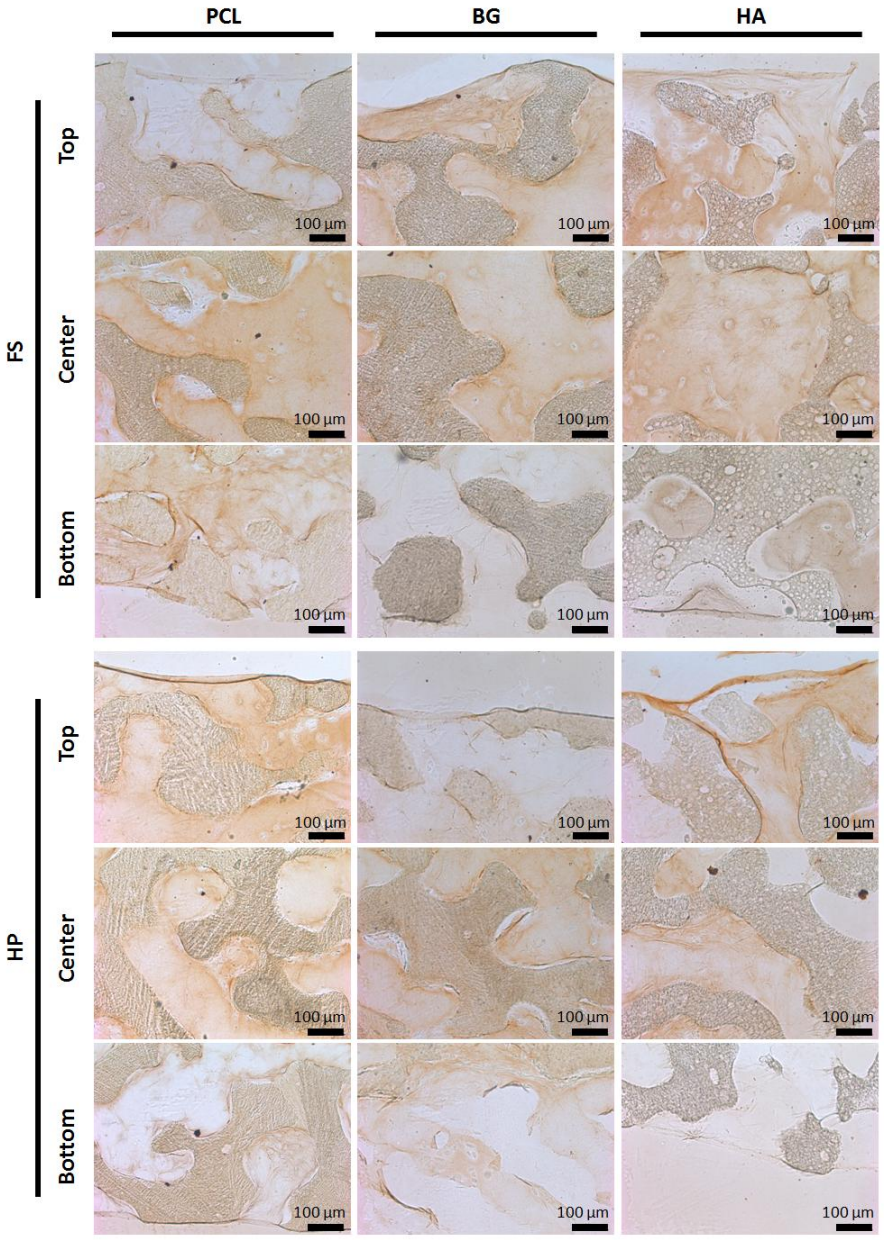

Figure 4-18: Microscopic views of anti- collagen type II immunohistochemical staining of scaffolds cultured with mesenchymal stem cells at day 35 under free swelling (FS) and hydrostatic pressure (HP. Scaffold appears gray and collagen is brown. (magnification/Scale bar = X10/100µm).

4.4.3. Discussion

Initial hypothesis was that hydrostatic pressure enhances the effect of hypoxia on chondrogenesis but this effect could be substrate dependent. In order to verify the hypothesis that simple material modifications may lead to a modulation of cell response to culture conditions, in the present work PCL scaffolds modified with hyaluronan or Bioglass® were used to study chondrogenic differentiation of MSCs under hydrostatic pressure, which is known to be a potent chondrogenic stimulus[107, 132].

Mechanical reinforcement of the scaffolds due to matrix deposition has been described in other works. The high rigidity of void scaffolds (in comparison with the formed tissue) may mask the effect of ECM deposition within the scaffolds, what may explain why no significant increases in the mechanical properties of the construct were observed with the application of hydrostatic pressure despite clear increases in extracellular matrix deposition. Mechanical properties should increase with time because the scaffold's pores are filled as a consequence of ECM deposition, increasing the resistance to fluid flow during mechanical tests due to the scaffold's permeability reduction. Normalized equilibrium and dynamic moduli were in the order of magnitude of the modulus observed in cartilage superficial region from porcine femoral condyle[221].

Scaffolds show a macroporous interconnected structure that allow for easy cell seeding and proliferation. The high hydrophobicity of PCL scaffold can represent a drawback to cell penetration and even distribution inside the scaffold; hyaluronic acid and Bioglass® were introduced inside the composites to lower the hydrophobicity. Bioglass® introduction increases the cell seeding efficiency compared with PCL or HA samples. Bioactive glass particles inclusion in polymer scaffolds has been reported to modify the surface hydrophilicity and protein

adsorption.[76,77] These characteristics of the modified scaffolds can explain the increased cell adhesion in BG samples. On the other hand, HA samples showed a significantly lower cell seeding efficiency compared to BG and PCL samples as already observed in previous section despite the use of an agarose mould. Lower cell seeding efficiency is thought to be due to the lower protein absorption over the hydrogel.[95] Nevertheless the cell proliferation inside HA samples was two -fold higher than the others groups. This may be due to an increased TGF production induced by CD44 interaction to hyaluronic acid or the modulation of pathways through the adhesion to hyaluronic acid.[98] Cell distribution was heterogeneous in all samples, but gained homogeneity when hydrostatic pressure was applied. As hydrostatic pressure has been previously shown to modulate cell migration[222] it is likely responsible for the more homogenous distribution of both cells and extracellular matrix. As a matter of fact, under hydrostatic pressure, small cell aggregates grew inside the ECM while under free swelling conditions cells grew in bigger aggregates. Moreover cell growth was affected by the substrate used; whereas PCL and BG induced cell attachment to the pores wall, growth of cell aggregates was observed inside the pores of PCL+HA1s-m samples.

These differences in cell distribution, growth and localization correlated with ECM histological staining. Hydrostatic pressure generally favoured a more marked extracellular matrix deposition and led to a more homogeneous staining, without the intense staining at the edges generally observed in the experiments performed in **section 3.2.** Hydrostatic pressure loading is known to increase the expression of proteoglycans and collagen:[133] in our study, cells' extracellular matrix synthesis was significantly affected by the mechanical stimulation, validating hydrostatic pressure as a promising culture stimulus to develop cell constructs *in vitro*. Enhanced deposition of matrix was seen in histological cuts stained with either Picro-Sirius Red or Alcian Blue. Sustained deposition of collagen was observed

possibly due to the hypoxic conditions,[223] as previous experiments with long cultures of mesenchymal stem cells in normoxic conditions in such scaffolds showed poor results (see **section 4.3.**). Collagen type II presented the same staining pattern as glycosaminoglycans and appeared generally where there was less collagen type I. Most of this collagen type II appeared in the center of the scaffolds whereas collagen type I deposition was generally favoured on the surface. This may be related with further central hypoxia that mediates expression of HIF-1α and increases lysylhydroxylation of collagen type II.[224]

On the other hand, most interestingly, the substrates modulated the cell response to hydrostatic pressure, whereas all substrates led to similar quantitative ECM synthesis levels under free swelling conditions; only the PCL HP and BG HP scaffolds showed a positive response to loading. In contrast hydrostatic pressure appeared to have little impact on ECM accumulation with HA HP scaffolds. This is likely related to the mechanism and strength of the cell adhesion to the different substrates. Whereas cells interact with BG and PCL scaffolds through adsorbed proteins and integrin signalling, in the case of HA samples protein adsorption is greatly reduced and interaction may occur through CD44 binding.[95,96] As observed in the results section, collagen type I deposition pattern was very different between adhesive (PCL and BG) and less adhesive (HA) samples. Strong fibres with intense stain, consistent with the application of significant cell contractility, were observed in PCL FS and BG FS samples, and lessened under hydrostatic pressure, whereas this was not observed to the same extent in hyaluronic acid samples. As force is applied by integrin binding, (in chondrocytes mechanical stress transmission and adhesion strength has been shown to be mainly due to β_1 integrin[225,226]), one could infer that hyaluronic acid limits integrin binding while PCL and BG promote it. Cell matrix interactions through integrin binding has been shown to inhibit MSCs chondrogenesis,[106, 107] and whereas agarose gels (that promote cell rounding)

were able to support chondrogenesis, fibrin gels (that induce cell spreading) showed less glycosaminoglycans expression.[107] On the other hand, in the same study, only fibrin gels showed a positive response to hydrostatic pressure whereas agarose samples did not; moreover mechanically induced enhancement of chondrogenesis in PEG hydrogels was shown to be integrin dependent[127]. Thus, different integrin implication in PCL and BG vs. HA scaffolds could explain why hydrostatic pressure showed a positive effect on ECM production in PCL HP and BH HP scaffolds but not in HA HP scaffolds, in which hydrostatic pressure had little or no effect. Immunofluorescence studies for different integrins was performed afterwards (results not shown), but at late times no significant differences were found in the studied cell surface receptors (α_v, α_5, β_1, CD44) most probably due to the abundance of ECM at this time and the predominance of cell-extracellular matrix interaction over cell-material interaction.

4.4.4.- Conclusions

Culture of MSCs on synthetic rigid scaffolds can lead to positive results when cultured using chondrogenic factors such as TGF-β3, hypoxia and intermittent hydrostatic pressure. Such scaffolds, once cultured, show modulus values in the range of normal cartilage tissue and should thus be biomechanically apt for implantation. Small composition changes in the scaffolding materials lead to different MSC response to intermittent hydrostatic pressure. As a result, a typical response (increase of ECM production; less prominent staining for collagen type I) is observed in bare PCL and Bioglass® containing scaffolds. Distribution and morphology of the deposited ECM was also greatly changed by HA coating. Such changes are thought to be related with differential expression and use of cell surface receptors and their associated pathways.

4.5. Characterization of coculture of MSCs and chondrocytes as culture condition to develop an *in vitro* construct.

Mesenchymal stem cell differentiation *in vitro* is a necessary step to develop effective cell-scaffold construct because the environment found in cartilage defect site could not be able to drive a correct *in vivo* differentiation.[62] MSC differentiation *in vitro* is performed using typical culture conditions such as growth factors supply, hypoxia and mechanical stimulation that were studied in previous sections. The use of such culture conditions showed to be able to induce MSC chondrogenesis but it has been pointed out that it does not prevent hypertrophy[52]. Co-culture is another approach used in order to obtain a satisfactory chondrogenesis and prevent hypertrophy. Co-culture is based on the premise that different cell types can generate a paracrine or cell-cell effect during *in vitro* culture that can direct cell fate to the desired phenotype.[52,137] The objective of this part of the thesis was to determine if indirect co-culture of mesenchymal stem cells with hyaline chondrocytes could improve chondrogenic differentiation of MSCs. Cell interaction was studied with a new indirect co-culture system that was developed trying to mimic the *in vivo* situation when a cell-scaffold construct is implanted in a cartilage defect and interact with the chondrocytes of host cartilage and also with subchondral bone cells only through secreted factors. With this system we wanted to study the influence of MSC and chondrocytes on each other, trying to determine on one hand if the presence of chondrocytes permits to stabilize the phenotype of differentiated MSCs and on the other hand if MSC signalling stimulates ECM production and chondrocytes redifferentiation.

To ensure the isolation of both cell types in our co-culture system they were seeded isolated in two different constructs. MSCs were cultured on two different substrates, one adhesive (fibronectin) and another non adhesive (hyaluronic acid). In previous parts of the thesis, hyaluronic acid coating was used but there were concerns about

the seeding efficiency and the effective interaction between cells and hydrogel. In the present work MSCs were dispersed in chemically modified hyaluronic acid solution before being injected into PCL scaffold, where the suspension was enzymatically crosslinked; in this way mesenchymal stem cells could be encapsulated in hyaluronic acid gel in order to limit interaction of MSCs with PCL scaffold, enhancing HA-cell interaction. Moreover, in previous sections PCL scaffolds were coated with FBS that is not defined protein solution but rather contains a wide range of adhesive proteins. In the present section the bare PCL control scaffolds were coated with fibronectin in order to obtain a homogenous cell attachment to the scaffold through integrin attachment to fibronectin adhesion domains. We expected that in these different and more controlled environments (HA vs. FN), MSC would express different adhesion protein patterns, which may modulate the way MSCs respond to co-culture stimulus; some findings in this line in the case of chondrocytes were reported in reference[128]. On the other hand chondrocytes were encapsulated in alginate gel that is a well known biomaterial in cartilage tissue engineering able to retain spherical morphology and chondrocyte phenotype while being inert and offering no specific biological cues to encapsulated chondrocytes.

Alginate mould fabrication process, sizes and scaffold assembling are described in **section 2.2.3.4.** Samples (**table 4-8**) were divided in three groups: Co-culture, MSC monoculture control and chondrocyte monoculture control. Samples mounting sketch is shown in **figure 2-9**. Co-culture was PCL+FN and PCL+HAts samples seeded with MSC cultured inserted in an alginate mould containing chondrocytes. MSC monoculture control was defined as PCL+FN and PCL+HAts seeded with MSC inserted in an acellular alginate mould without chondrocytes.

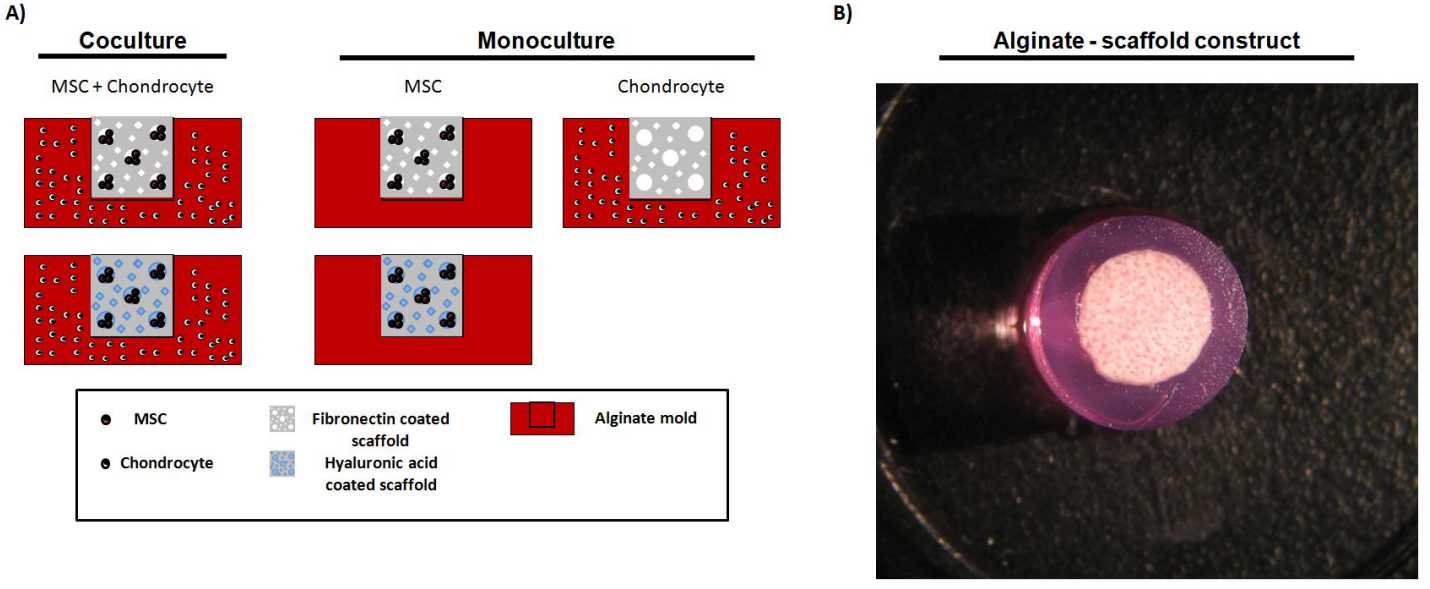

Figure 4-19. Coculture sketch (A) samples were divided in coculture constructs conformed by scaffolds seeded with MSC and an alginate mould seeded with chondrocytes. Control samples were monoculture of MSC without chondrocytes in alginate mould and chondrocyte monoculture seeded into the alginate mould with a scaffold without cells. Picture of assembled alginate-scaffold construct(B).

Samples	Polymer composition	Coating
PCL	Polycaprolactone	-
PCL+FN	Polycaprolactone	Fibronectin
PCL+HAts	Polycaprolactone	Tyramine substituted hyaluronic acid

Table 4-7. Table with tested samples.

Finally chondrocyte monoculture control was defined as an alginate mould seeded with chondrocytes (CHOmControl) with a PCL scaffold inserted. As a result the two types of cell were expected to grow separately and to interact only through soluble signals. Porcine MSCs were seeded in the scaffold and chondrocytes in alginate gel in a proportion of 1:4 and were cultured with chondrogenic media under normoxia conditions for 35 days. Samples were removed at day 1, 17 and 35 and prepared for mechanical, biochemical and histological analysis. Samples for mechanical and biochemical tests were removed from the culture plate, washed with DPBS and the scaffold was separated from the alginate mould. Alginate samples were stored at -80ºC while scaffolds were used to perform non-destructive mechanical assays, after which they were washed and stored at -80ºC until biochemical analysis was performed. On the other hand for histological analysis whole constructs (alginate + scaffold) were fixed and included in polyester wax.

	Cell coculture		Scaffold coculture		Alginate mould coculture
Samples	MSC	Chondrocyte	Scaffold	Sample ID	Sample ID
FNmo	Yes	No	PCL+FN	MSCmFN	-
HAmo	Yes	No	PCL+HAts	MSCmHA	-
FNco	Yes	Yes	PCL+FN	MSCcFN	CHOcFN
HAco	Yes	Yes	PCL+HAts	MSCcHA	CHOcHA
CHOmo	No	Yes	-	-	CHOmControl

Table 4-8. Table with cultured samples ID for present section, tested samples and scaffold coculture combination.

The influence of material on initial adhesion was performed using immunofluorescent staining of day 1 scaffolds for integrins β1, α_v, α_5, and surface receptor CD44.

The influence of MSC on chondrocyte ECM production was assessed using histological stains for collagen and glycosaminoglycans as well as biochemical quantitative analysis of collagen content and GAG content. Collagen type II was quantified by ELISA.

The influence of chondrocyte on MSC behaviour and phenotypic stability was studied both by assessing the content and quality of produced ECM (histological stain/ biochemical quantitative assay) as well as the expression of hypertrophic markers such as collagen type X by ELISA and ALP by enzymatic assay.

4.5.1. Characterization of materials.

PCL scaffolds showed the same structure (**figure 4-20**) and similar porosity and mechanical properties (**table 4-9**) as obtained in previous sections. Samples with hyaluronic acid were obtained by filling PCL scaffolds with an injectable *in situ* crosslinkable tyramine-substituted hyaluronic acid. In Cryo-scanning electron microscopy pictures (**figure 4-20**) swollen PCL+HAts samples' macropores were completely filled with a porous hydrogel. **Figure 4-21** shows Alcian blue staining picture corroborating that hyaluronic acid filled the whole scaffold. On the other hand Alcian blue staining showed a hole in the middle of the structure that probably was made by the needle insertion used to inject the hyaluronic acid. Scaffold porosity or mechanical properties (**table 4-6**) did not show significant differences compared to bare PCL scaffolds. On the other hand swollen PCL+HAts showed a decrement of elastic modulus in compression probably related with the hole made in the scaffold with the needle (showed on **figure 4-21** at HAts sample center), thus in further works another kind of mechanism would be needed in order to inject the viscous solution without damaging the scaffold.

		Elastic modulus (MPa)	
	Porosity (%)	Dry	Swollen
PCL	79,85 ± 1,89	0,90 ± 0,07	0,87 ± 0,2
PCL+Hats	78,71 ± 5,47	0,92 ± 0,23	0,63 ± 0,15

Table 4-9. Total porosity of and mechanical analysis of scaffolds.

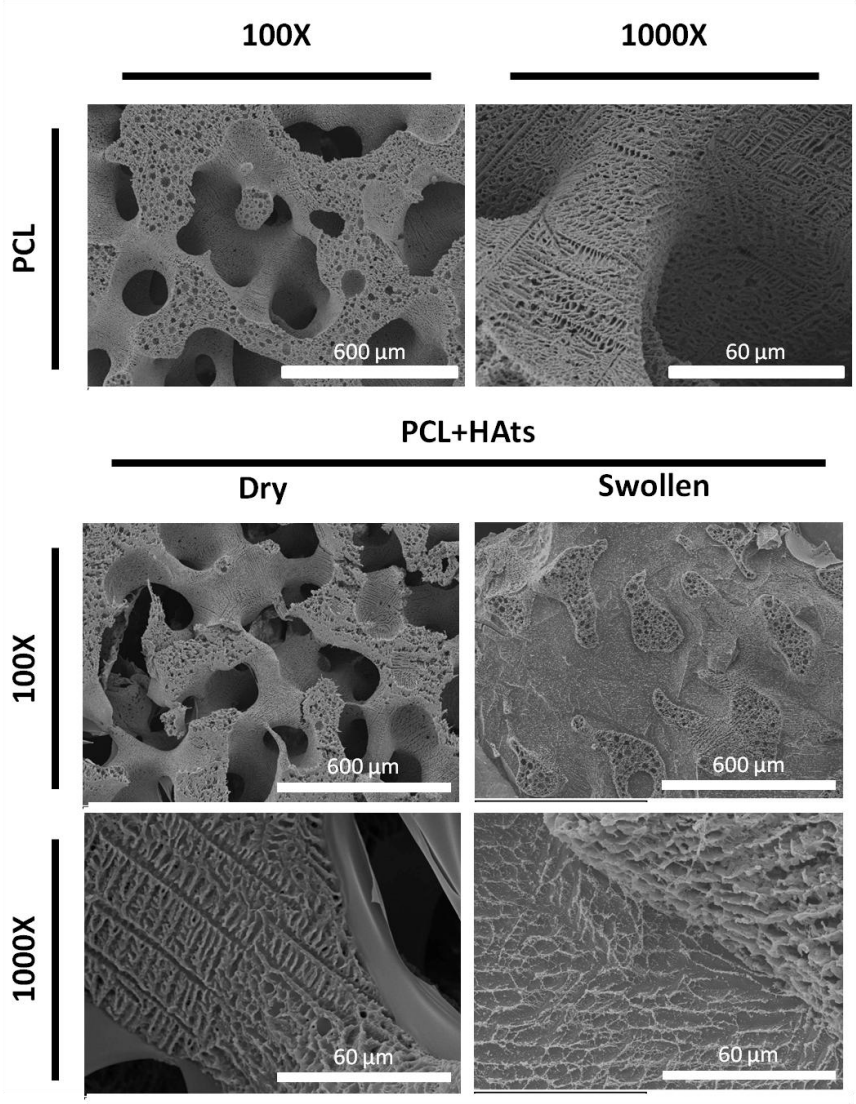

Figure 4-20. Scanning electron microscopy picture of PCL scaffold (A) and Scanning electron microscopy (dry samples) and Cryo-scanning electron microscopy (swollen samples) micrographs of PCL+HAts (B). (magnification/Scale bar = X100/600 µm and X1000/60 µm).

4.5.2. Initial adhesion of MSC to HA or FN-modified PCL scaffolds

In this work porcine MSCs were seeded at $3x10^5$ cells/scaffold and bovine chondrocytes at $1.2x20^6$ cells/alginate gel (sample ID showed in **table 4-8**). Cell seeding was determined as the number of cells present on cell-scaffold construct at day 1. Cell seeding efficiency was determined for mesenchymal stem cells with a MSC number vs. DNA standard curve determined for this purpose. Chondrocyte cell numbers were calculated on the basis of 7.7 pg DNA/cell[227]. MSCmFN and MSCcFN samples showed a cell seeding efficiency average of 35 ± 4%, not significantly different of the average efficiency for MSCmHA and MSCcHA (32 ± 9%). On the other hand alginate mould seeding efficiency was 59 ± 16% which combined with the results of scaffolds means that actual MSC: chondrocyte ratio was close to 1:7 for both scaffold types rather than the initially intended 1:4 ratio. To determine if cell seeding distribution was homogeneous through the scaffold and which cell receptors were involved in initial adhesion samples at day 1 were fixed and stained with haematoxylin staining or immunostaining as shown on **figure 4-21** and **figure 4-22** respectively. At day one cells seeded on MSCmFN and MSCcFN samples (**figure 4-21**) showed homogeneous cell dispersion through the scaffold pores, with cells showing an expanded morphology. On the other hand MSCmHA and MSCcHA at day one (**figure 4-21**) were completely filled with hyaluronic acid as observed on **figure 4-21**, with the cells showing a spherical shape as expected, and embedded homogeneously in the hydrogel phase. Immunostaining (**figure 4-22**) of MSC seeded in fibronectin coated samples showed an adhesion profile characterized by abundant β_1 integrin staining, less prominent α_5 and α_v staining and no staining for CD44. In contrast, MSC seeded in samples with hyaluronic acid expressed CD44 at day 1, as shown in **figure 4-22**. On the other hand integrin staining of α_5 was visible while β_1 and α_v staining was weak and only observed in some cells.

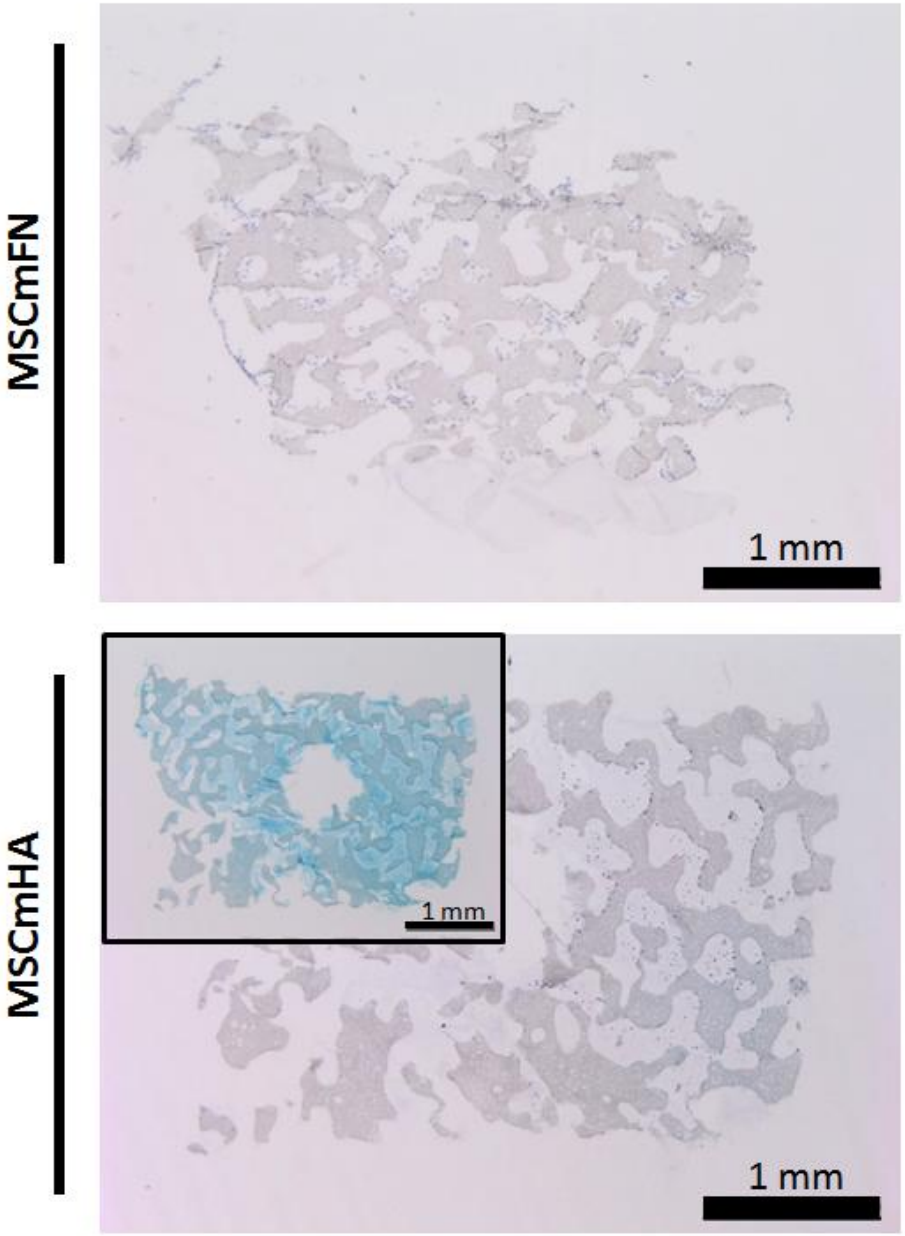

Figure 4-21. Hematoxylin staining for nucleus and Alcian Blue staining for glycosaminoglycans at day 1 in PCL+FN (FN) and PCL+HAts (HA) scaffolds. A: Cells appears in purple and glycosaminoglycans appear in blue. (magnification/Scale bar = X1.6/1mm).

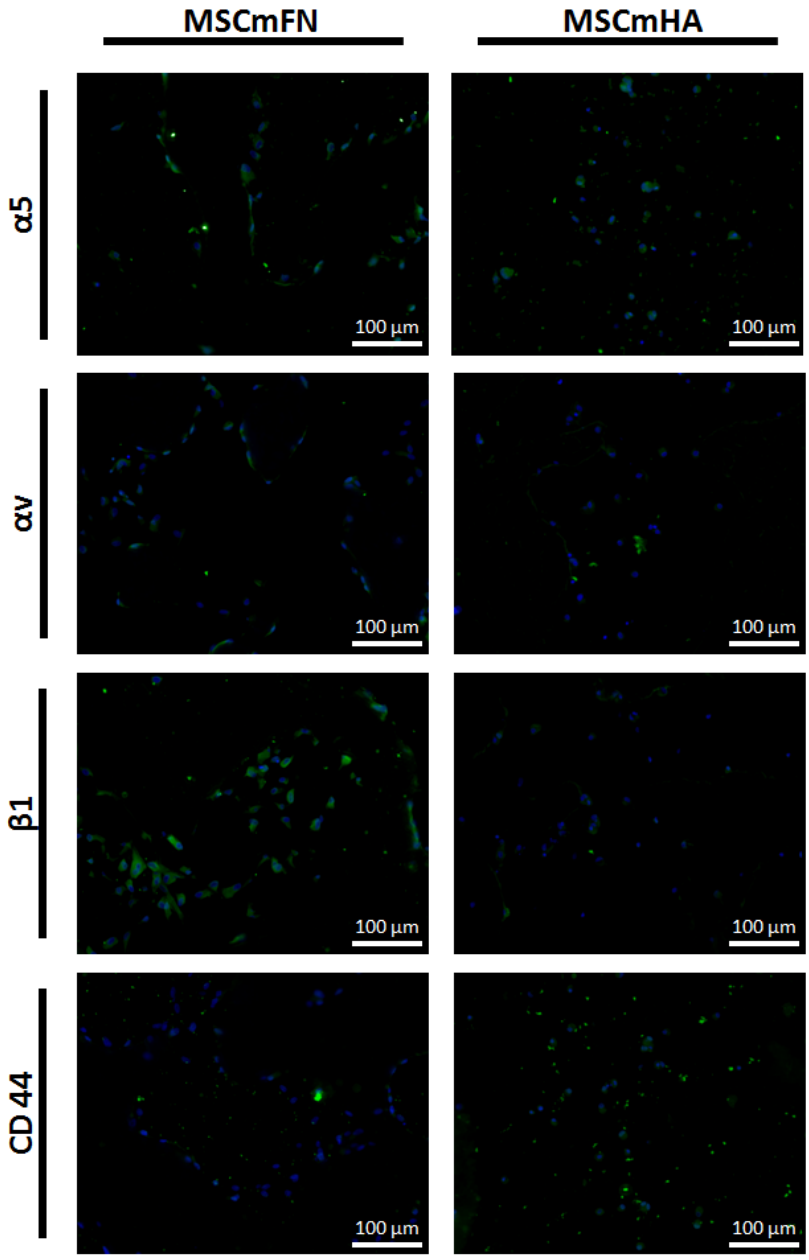

Figure 4-22. Microscopic views of anti-α5, αv, β1 and CD-44 immunohistochemical staining mesenchymal stem cells at day 1 in PCL+FN (FN) and PCL+HAts (HA) scaffolds. Cell nucleus appears blue and adhesion protein is green. (magnification/Scale bar = X20/100 µm).

4.5.3. DNA and proliferation

Cell population was studied at day 1, 17 and 35. DNA content (in **figure 4-23**) showed that MSCs proliferated with time in fibronectin coated samples while in hyaluronic acid filled samples cell number decreased with time. Coculture conditions improved cell proliferation significantly in MSCcFN compared to monoculture. On the other hand in hyaluronic acid filled samples coculture led to a stable cell number but there was no proliferation during the whole time of culture.

Chondrocytes proliferated in alginate hydrogel in all tested samples in coculture and monoculture conditions as shown in **figure 4-23**. In coculture, there was a decrement of DNA content with respect to monoculture control, showing that the behaviour of chondrocytes seeded into alginate gels was also affected by the presence of MSCs. This reduction of DNA content (**figure 4-23**) was statistically significant in CHOcFN samples where proliferation seemed to stop at day 35 while CHOcHA only showed a slightly lower DNA content than CHOmControl.

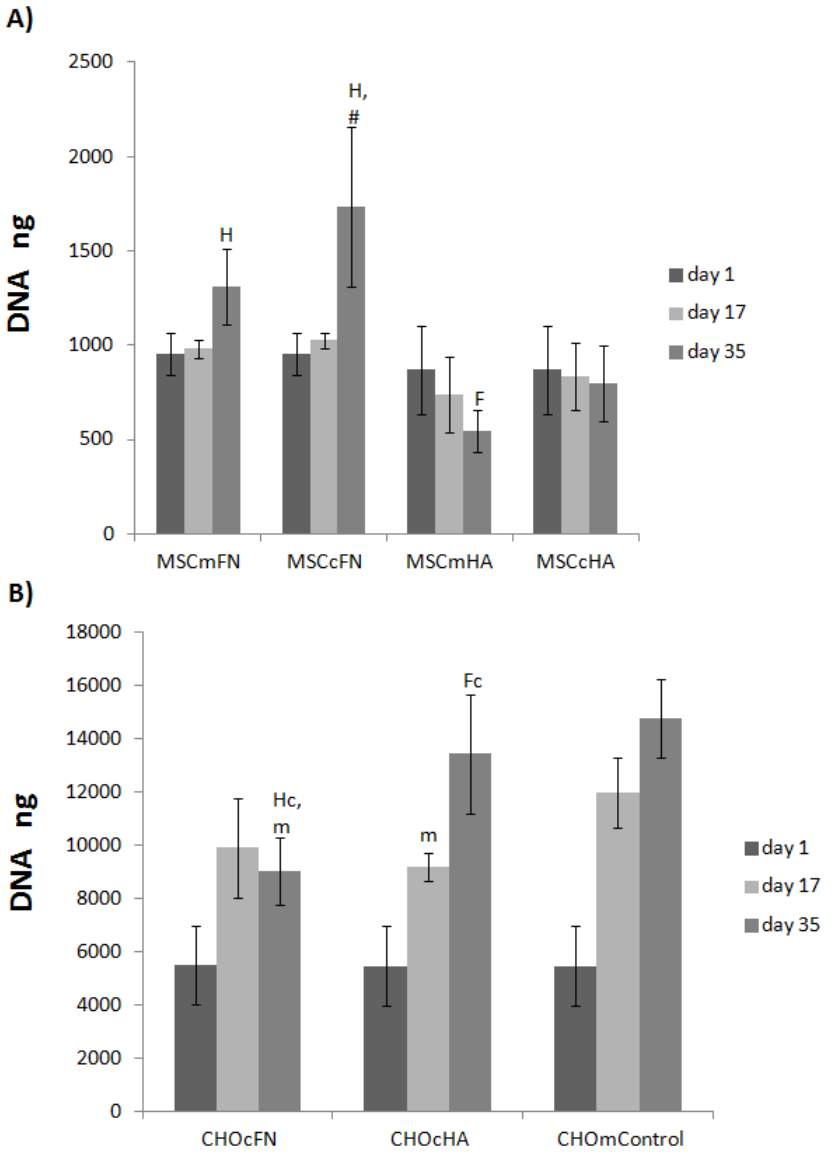

Figure 4-23. Total DNA of porcine mesenchymal stem cells after seeding at day 1, 17 and 35 in scaffolds (A) under monoculture (m) and coculture (c) and bovine chondrocytes (B) seeded in alginate in monoculture or coculture. Results are averaged from n=4 experiments. Significance ($p<0.05$) compared to similar group for normalized scaffolds is signalled as: (F) MSC_FN, (H) MSC_HA, (Fc) CHO_FN and (Hc) CHO_HA samples for each group at the same time and (#) cocultured sample from the same type at the same time.

4.5.4. Extracellular matrix synthesis

Extracellular matrix synthesis was evaluated as collagen and glycosaminoglycans content normalized to DNA content as shown in **figure 4-24** and **figure 4-25**. Regarding the central part of the construct where MSCs were seeded, normalized glycosaminoglycans and collagen content (**figure 4-24** and **figure 4-25**) increased with time in both scaffold types. Normalized collagen (**figure 4-24**) content was severely lowered by chondrocytes coculture with values several times lower than monoculture controls in both scaffold types without remarkable differences between them. On the other hand normalized glycosaminoglycans (**figure 4-25**) response to coculture was affected by the substrate. In FN coated samples, GAG content was higher in coculture conditions (MSCcFN>MSCmFN), while in HA filled samples, GAG content was higher in monoculture conditions (MSCmHA>MSCcHA). As a result GAG content was slightly higher in MSCcFN samples than in MSCcHA, while GAG content was significantly higher in MSCmHA than in MSCmFN.

Chondrocyte normalized ECM deposition, presented in **figure 4-24** and **figure 4-25** showed an increment with time for all tested samples. Extracellular matrix synthesis was affected by the coculture with MSC. Coculture improved glycosaminoglycans and collagen deposition in CHOcFN and CHOcHA compared to CHOmControl, but this difference was only significant for CHOcFN. On the other hand, CHOcFN had significantly higher normalized collagen and GAG content at day 35 than CHOcHA, showing that the material used to culture the MSCs influences their interaction with chondrocytes.

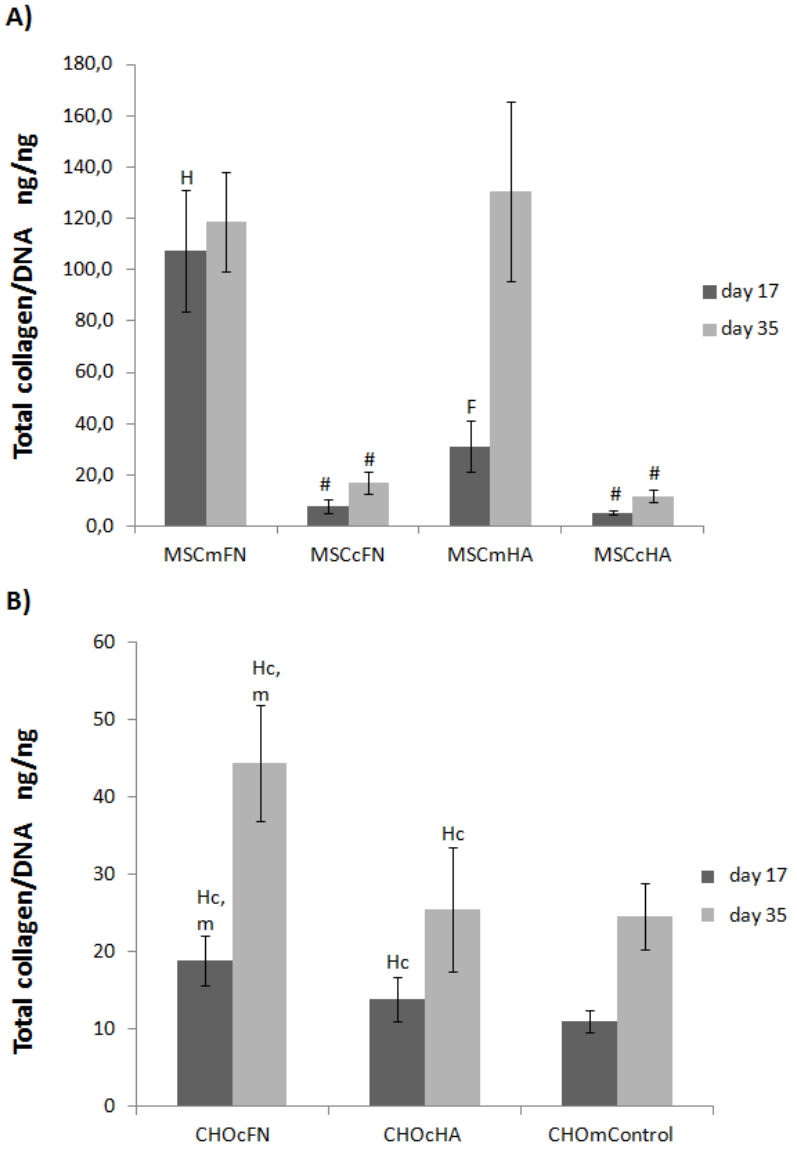

Figure 4-24: Collagen levels normalized to total DNA at day 17 and 35 in scaffolds (A) under monoculture (m) and coculture (c) and bovine chondrocytes seeded in alginate (B) in monoculture or coculture. Results are averaged from n=4 experiments. Significance ($p<0.05$) compared to similar group for normalized scaffolds is signalled as: (F) MSC_FN, (H) MSC_HA, (Fc) CHO_FN and (Hc) CHO_HA samples for each group at the same time and (#) cocultured sample from the same type at the same time.

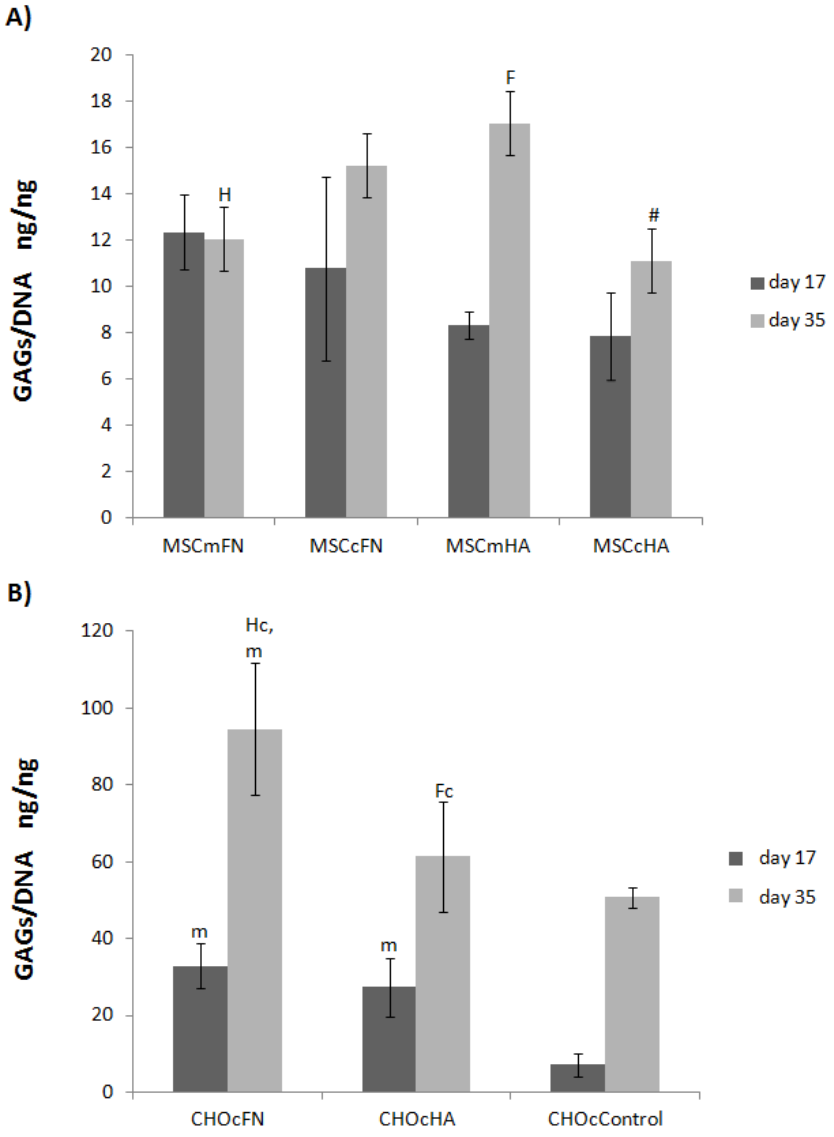

Figure 4-25: Glycosaminoglycans (GAGs) levels normalized to total DNA at day 17 and 35 in scaffolds (A) under monoculture (m) and coculture (c) and bovine chondrocytes seeded in alginate (B) in monoculture or coculture. Results are averaged from n=4 experiments. Significance ($p<0.05$) compared to similar group for normalized scaffolds is signalled as: (F) MSC_FN, (H) MSC_HA, (Fc) CHO_FN and (Hc) CHO_HA samples for each group at the same time and (#) cocultured sample from the same type at the same time.

4.5.5. Histological stains

Obtained constructs alginate/scaffold structure is shown in **figure 4-26** at day 35 with PCL+FN samples stained with Picrosirius red and PCL+HAts stained with Alcian blue to stain the HA inside the pores.

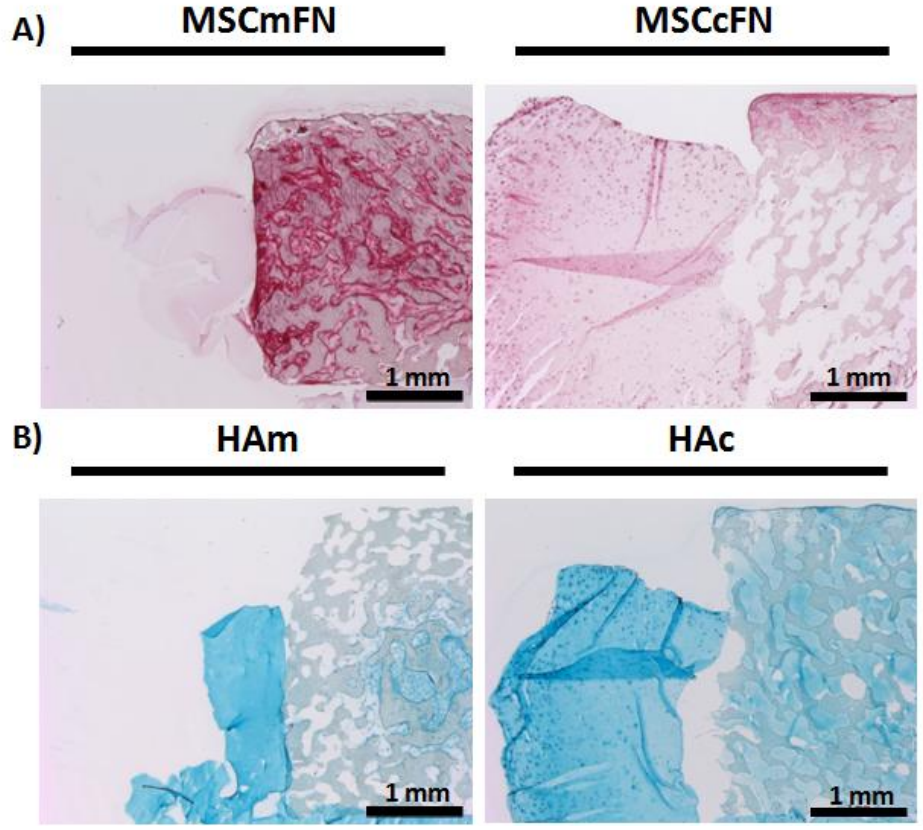

Figure 4-26. Picro-Sirius Red staining for collagen at day 35 in FNmo and FNco samples (A). Collagen appears in red and cells in purple. Alcian Blue staining for glycosaminoglycans at day 35 in HAmo and HAco samples (B). Glycosaminoglycans appears in blue and cells in purple. (magnification/scale bar = 1.6X/1mm).

Extracellular matrix distribution was evaluated by means of collagen and glycosaminoglycans staining (**figure 4-27** and **figure 4-28**) at day 17 and 35. Cell and ECM distribution varied depending of culture condition and the scaffold

composition. Monoculture of MSC seeded in MSCmFN and MSCmHA samples seems to induce fibroblastic cell shape, fibrous matrix distribution and high collagen deposition. Important differences between monoculture and coculture conditions were found in MSC cultured in fibronectin coated scaffolds. Collagen deposition is higher in monoculture as shown in **figure 4-27** with a marked staining pattern. MSC showed a fibroblastic shape and were distributed along the scaffold volume. In addition in monoculture the extracellular matrix showed a fibrous staining pattern. On the other hand MSC seeded in MSCcFN samples showed a cell distribution limited to scaffold top part with a less fibrous and softer ECM staining. Glycosaminoglycans (**figure 4-28**) showed a staining pattern similar to collagen but the staining was more intense in coculture conditions than in monoculture. Extracellular matrix distribution in hyaluronic acid filled samples (**figure 4-27** and **figure 4-28**) was different from MSCmFN and MSCcFN. The main difference was that cells adopted a spherical shape in hyaluronic acid filled samples. Coculture allowed retaining the spherical morphology of all mesenchymal stem cells cultured in MSCcHA scaffolds at day 35 (**figure 4-27**) while MSCmHA showed a collagen staining pattern similar to MSCmFN. In MSCcHA samples Picro Sirius red staining was found weakly in the thin cell layer on the surface of the scaffold and in the inside area where round cells were found. On the other hand Alcian blue staining (**figure 4-28**) showed that hyaluronic acid filled the pores homogeneously and remained intact during the 35 days of cell culture but hydrogel background did not allow studying the GAG distribution in MSCcHA.

Collagen and glycosaminoglycans distribution in chondrocyte seeded alginate moulds was studied (**figure 4-29**) and was localized as a weak staining ring surrounding cells but no significant differences were found between samples or culture conditions.

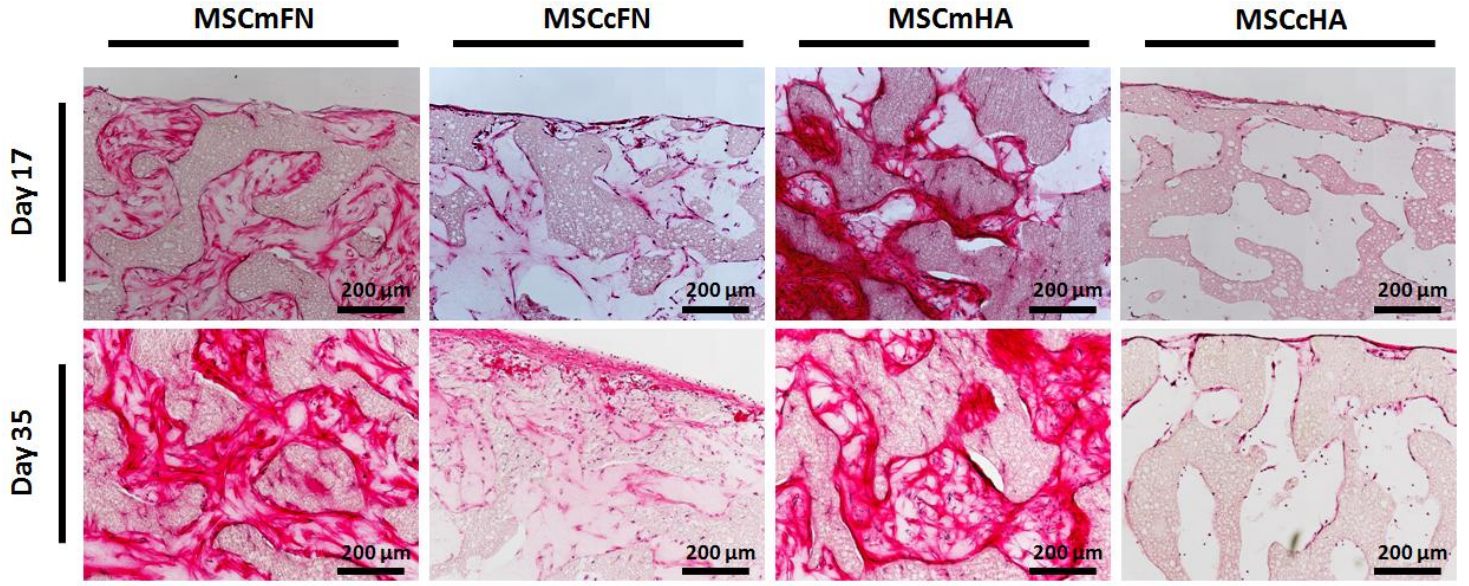

Figure 4-27. Picro-Sirius Red staining for collagen at day 17 and 35 under monoculture (m) and coculture (c) of MSC cultured in scaffolds. Collagen appears in red and cells in purple. (magnification/scale bar= 10X/200µm).

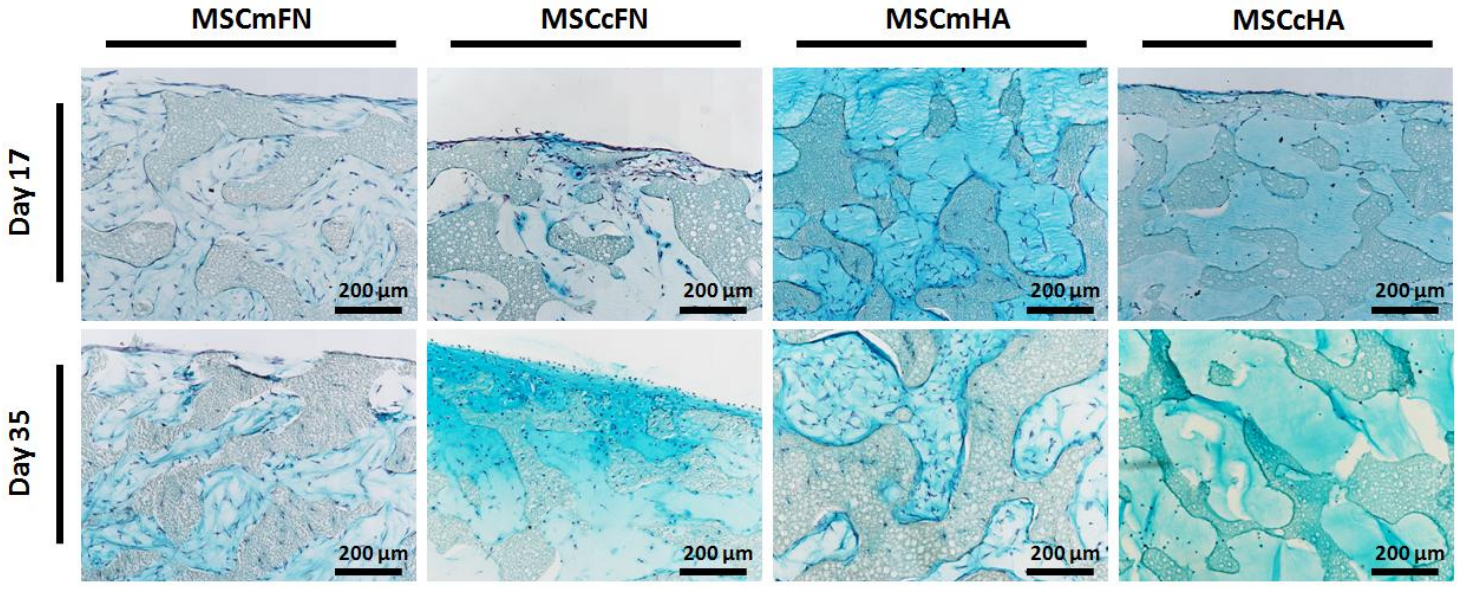

Figure 4-28. Alcian Blue staining for glycosaminoglycans at day 17 and 35 under monoculture (m) and coculture (c) of MSC cultured in scaffolds. Glycosaminoglycans appears in blue and cells in purple. (magnification/scale bar= 10X/200µm).

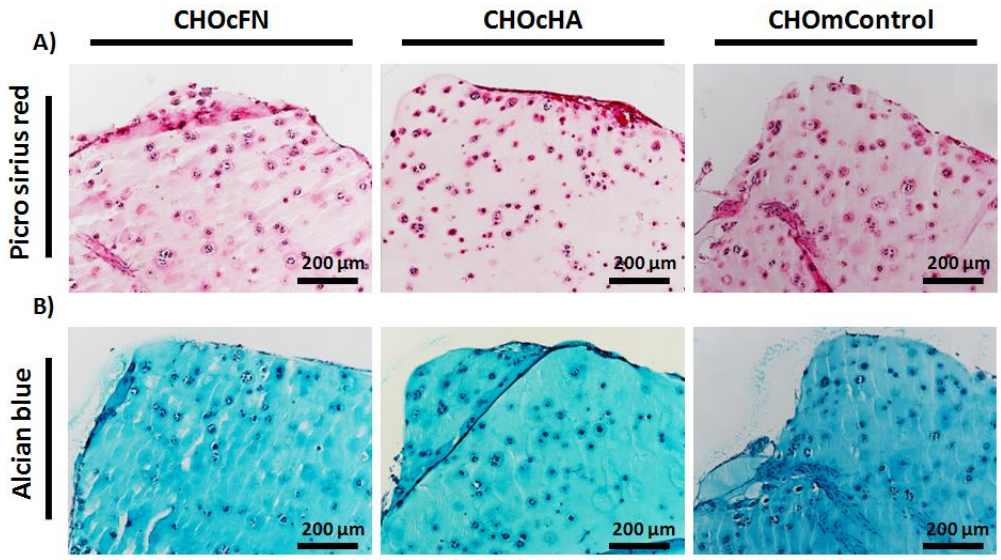

Figure 4-29. Picro-Sirius Red staining for collagen (A) and Alcian blue staining (B) at day 17 and 35 under monoculture (m) and coculture (c) of chondrocytes in alginate mould. Collagen appears in red, glycosaminoglycans appears in blue and cells in purple. (magnification/scale bar= 10X/200µm).

4.5.6. Expression of collagen type II

MSC differentiation to hyaline chondrocyte was studied measuring collagen type II compared to total collagen content. As can be observed in **figure 4-30** collagen type II content normalized to total collagen content showed significant differences between the different culture conditions: MSCcFN samples showed 16 times more normalized collagen type II deposition than MSCmFN. Normalized collagen type II deposition in MSCcHA samples (**figure 4-30**) showed the same response to culture conditions studied as MSCcFN but with values slightly lower.

Chondrocyte seeded samples showed an unexpected result because collagen type II levels (**figure 4-30**) were lower than 2%, extremely low compared with the 20% of MSCcFN or MSCcHA samples. On the other hand coculture showed a positive but not significant effect on collagen type II deposition.

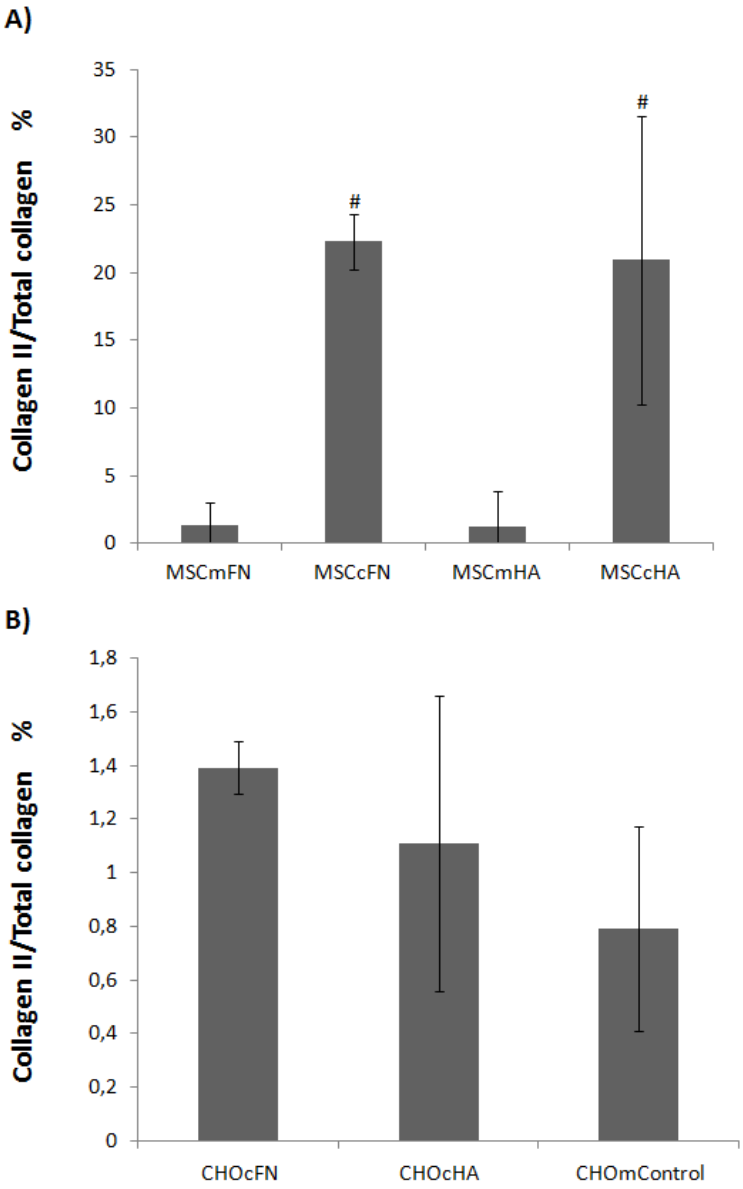

Figure 4-30. Collagen type II (collagen II) normalized to total collagen content at day 35 in scaffolds (A) and alginate mould (B). Results are averaged from n=4 experiments. Significance ($p<0.05$) compared to cocultured sample from the same type at the same time.

4.5.7. Expression of hypertrophic markers

Hypertrophic chondrocyte phenotype was evaluated for cultured MSC (**figure 4-31**) by means of ALP levels and collagen type X compared to total collagen content. Hypertrophic markers showed different patterns (**figure 4-31**). Normalized collagen type X (**figure 4-31**) showed a significantly higher percentage in coculture conditions than in monoculture but no sample presented values higher than 0.004% of collagen type X normalized to total collagen content. Nevertheless, Alkaline phosphatase release (**figure 4-31**) was several times higher in mesenchymal stem cells in monoculture compared to samples cultured under coculture conditions. On the other hand no significant differences between the different tested materials were found with respect to the response to coculture, but hyaluronic acid filled samples showed values higher than fibronectin coated samples for collagen type X and ALP.

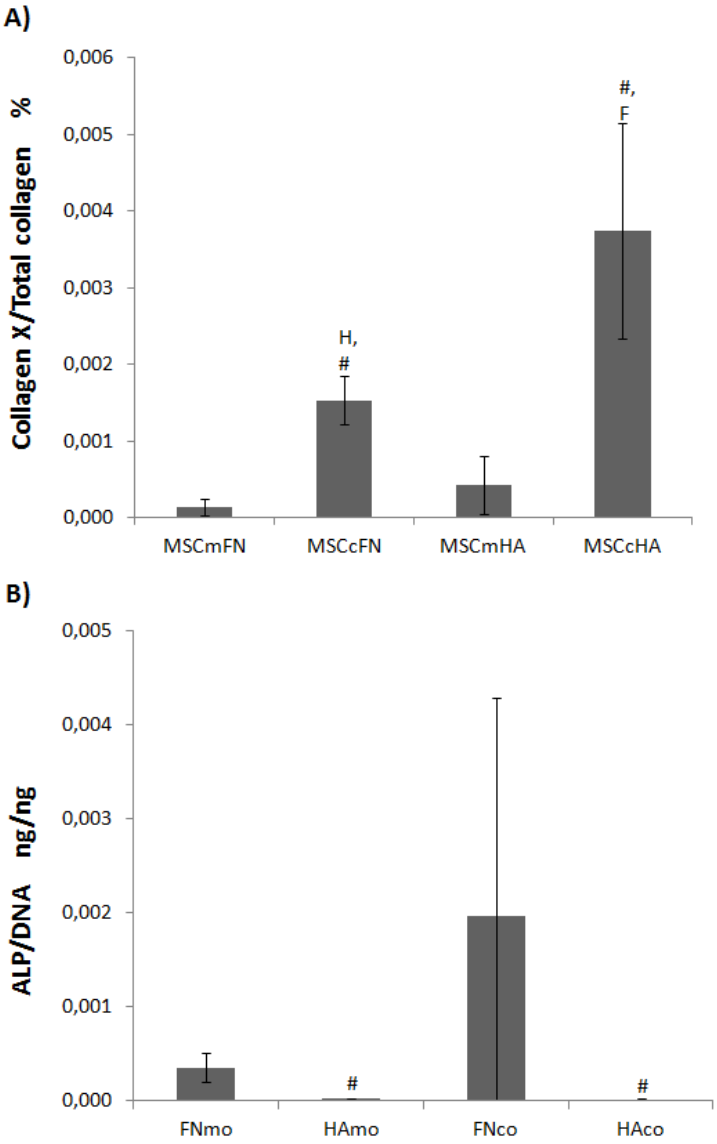

Figure 4-31. Collagen type X (collagen X) normalized to total collagen content (A) and alkaline phosphatase (ALP) released to culture media normalized to construct total DNA (B) at day 35 in scaffolds. Results are averaged from n=4 experiments. Significance ($p<0.05$) compared to similar group for normalized scaffolds is signalled as: (F) MSC_FN and (H) MSC_HA samples for each group at the same time and (#) cocultured sample from the same type at the same time.

4.5.8. Discussion

Different therapies used in clinics to resolve defects in articular cartilage shows that new formed tissue lacks the properties of hyaline cartilage and even if initially regenerated tissue histology presents some characteristics of native tissue, it soon degenerates towards fibrocartilage. Thus it seems that the environment found by the cells invading the defect (MSCs coming from subchondral bone) or transplanted (expanded chondrocytes or autologous MSCs) does not promote the *in vivo* acquisition of a hyaline chondrocyte phenotype.[13,62] This encourages the development of tissue engineered implants containing well characterized, previously *in vitro* differentiated chondrocytes that can be directly implanted in the site of the cartilage defect. In addition to the optimization of biophysical culture conditions (growth factors supply, hypoxia, mechanical stimulation) coculture of different cell types can generate a paracrine effect during *in vitro* culture that may direct cell fate towards the desired phenotype.[52] On the other hand, it is known that scaffolding material properties have a great deal of influence on the differentiation of stem cells and ECM deposition. In this work, we wanted to study the influence of the scaffolding material used to culture the mesenchymal stem cells on their response to a coculture with mature hyaline chondrocytes. Due to the separation of both cell types in our culture model, we would also be able to check whether the material where MSCs were seeded also would have an influence on chondrocyte behaviour despite of the fact that chondrocyte microenvironment would not change (alginate was used in every case). Obtained scaffolds (with or without hyaluronic acid) that showed a 80% of porosity and an elastic modulus in range with articular cartilage[22] were seeded with MSC for 35 days with chondrogenic culture media in coculture or monoculture. In the present work we use the alginate mould in which chondrocytes are seeded playing at the same time the role of the agarose moulds used in previous sections. However, cell seeding efficiency with alginate mould was around a half of that obtained in previous sections pointing that new mould did not

match perfectly with the scaffold size. Cell adhesion at 24 hours is shown in **figure 4-22** where it can be seen that MSC seeded in fibronectin coated scaffolds were attached to the surface through β1 integrin mainly and α5 and αv integrin. MSCs adhesion protein profile observed in MSCmFN and MSCcFN was expected because the α5β1 integrin mediates cell adhesion to fibronectin.[228] On the other hand MSC seeded in MSCmHA and MSCcHA showed CD44 attachment as expected. In **figure 4-22** α5 integrin staining is shown although cells were cultured in serum-free conditions pointing that cells seeded probably start secreting their own ECM proteins like fibronectin already in the first 24 hours.

Coculture has a positive effect on cell proliferation in MSCcFN and MSCcHA in contrast with the findings of other works were indirect coculture in transwell model or with two scaffolds in the same well did not show MSC proliferation improvement compared to monoculture control[140,146]. There was no proliferation in hyaluronic acid filled samples with a constant decrement in DNA content with time. One possible explanation to the observed differences is that α5β1 integrin adhesion to fibronectin, necessary for chondrocyte proliferation[228],was present in MSCmFN and MSCcFN but not in MSCmHA and MSCcHA samples. On the other hand coculture showed an important effect over ECM deposition, distribution and composition. Normalized collagen deposition in MSCmFN and MSCmHA was around 9 times lower compared to MSCcFN and MSCcHA. Obtained results are similar to results in static conditions obtained by Levorson *et al.*[146] In that work indirect coculture was performed with MSC and chondrocytes seeded separately in two scaffolds and cultured in the same well separated by a vertical piece of propylene mesh. Normalized glycosaminoglycans and collagen values deposited by MSCs in monoculture were higher than in coculture,[146] but normalized content differences between culture conditions were small and showed a great variability. On the other hand cartilage tissue typically shows a wet weight percentage of

proteoglycans (9%) and collagen (15%) [6] that can be defined as collagen/proteoglycans ratio of 1.67. In present study MSCmFN ratio of non-normalized collagen/ glycosaminoglycan was 9.8 whereas in MSCmHA it was 7.8. Ratio for both samples was far of theoretical 1.67 but the ratios of cocultured samples were around 1.1 for MSCcFN and MSCcHA much closer to the healthy tissue. These results suggest that coculture has a normalizing effect on ECM composition and that high collagen levels found in monoculture may be an anomalous secretion. Extracellular matrix was examined using Picrosirius red and Alcian blue staining to determine collagen and glycosaminoglycans distribution. The most important feature of monoculture staining was the intense collagen staining (consistent with the higher total collagen content found in monoculture) distributed along the scaffold with a visible fibrous staining. Such a pattern was already described previously in PCL scaffolds cultured in normoxia conditions (**section 4.3.** and **section 4.4.**). On the other hand MSC seeded in MSCcFN samples showed a less fibrous matrix deposition. These results are in good agreement with our previous hypothesis that monoculture induces a secretory profile that does not match that of hyaline cartilage. On the other hand cell distribution was affected by cell culture conditions. MSC seeded in MSCcHA were able to retain a spherical shape 35 days in contrast with MSCmHA suggesting that substrate alone was not enough to retain spherical shape. MSC cultured in MSCcFN were limited to the top part. This different cell distribution can be a consequence of deficient oxygen or/and nutrient distribution from outside to MSC seeded inside the scaffold. The mass transport could be affected because the chondrocytes that surrounded the scaffold consumed the main part of oxygen and nutrients and MSC migrate to the top part with a higher nutrient supply. Construct mechanical properties were studied at day 1, 17 and 35 but no significant differences (that could be related to huge differences of ECM components deposition or ECM distribution) were found. Results obtained are in contrast with the work of Bian *et al.*[145] with cells seeded on methacrylated

hyaluronic acid. Cells showed an ECM deposition increment in direct coculture compared to MSC control that was translated in a significant mechanical modulus increment.[145] If cell-scaffold construct mechanical elastic modulus can be roughly speaking a sum of the contributions of the scaffold modulus plus the extracellular matrix modulus (as in a parallel model for a two phase construct). Our results mean that ECM secreted by the cells has a small effect over the construct mechanical response as shown in previous sections. Vikingsson *et al.*[229] showed that the scaffold/hydrogel construct stiffness depends of hydrogel crosslinking degree because for low crosslink degree the scaffold's higher stiffness hides the contribution of the gel filling retaining water. On the other hand in cartilage tissue proteoglycans are entrapped in a collagen matrix mesh, which combination is responsible of cartilage unique properties.[6] This can explain why no differences in the mechanical properties were found at the end of culture between the studied culture conditions. In our samples collagen and proteoglycans probably are deposited randomly without a defined organization with a low crosslink degree between collagen and proteoglycans explaining the huge differences between culture conditions. Finally the eventual development of a hypertrophic phenotype was evaluated . MSCcFN and HAcFN showed the highest normalized collagen type II values that combined with collagen/GAGs shows that coculture improved ECM quality compared to monoculture, the later inducing a more fibroblastic phenotype. The effect of the coculture with mature chondrocytes seems thus to have a positive effect on MSCs since they showed a higher synthesis of collagen type II and reduced expression of ALP as is described in other works[138,141,147]. Nevertheless cocultured samples showed an overexpression of collagen type X compared with monocultures in contrast with other works [138,141]. It is worth note that anyway hypertrophic marker values obtained (**figure 4-31**) for collagen type X and ALP for all samples were extremely low what combined with absence of calcium deposits in

alizarin red staining points that hypertrophy was quite low regardless of the culture condition.

Chondrocyte redifferentiation usually was observed in direct coculture studies but literature suggests that non contact coculture had less effect on chondrocyte redifferentiation.[52] In the present work a paracrine effect of mesenchymal stem cells over chondrocytes was observed. Paracrine effect resulted in a decrement of cell proliferation and an increment of collagen and glycosaminoglycans synthesis. The effect of the presence of MSCs on chondrocytes evolution in coculture is clear independently of the type of support in which MSCs were seeded.

Finally obtained results showed a strong interaction between mature chondrocytes and MSCs in indirect coculture, so supporting previous findings in the same sense [138,141,147] but in contrast with other studies that points that only direct coculture works[140,145]. On the other hand differences with literature can be explained as coculture system is a highly modifiable study platform where different cell types, passage numbers, cell density and coculture system are used. All these parameters can strongly affect the results hampering direct comparison with the literature.[137]

4.5.9. Conclusions

Indirect coculture condition showed a high positive effect over MSC chondrogenesis. Coculture corrected the anomalous collagen/ glycosaminoglycan ratio and fibrillar extracellular matrix deposition observed on MSC cultured in monoculture. In addition coculture improved collagen type II synthesis and reduced ALP release. On the other hand coculture improved the effect of hyaluronic acid over cell morphology retaining the spherical morphology up to 35 days in culture.

Differences between tested materials were few: fibronectin coating improved MSC proliferation and hyaluronic acid improved slightly chondrogenic differentiation. Commented differences between substrates can be related with differential expression and interaction of cell surface receptors.

4.6. Chapter discussion

This chapter focuses on developing a cell-scaffold construct *in vitro* suitable for cartilage tissue engineering. The aim was to obtain a construct containing *in vitro* differentiated chondrocytes. We addressed the research in two directions: (a) developing scaffolds with different coatings and (b) differentiating *in vitro* MSCs seeded into the scaffolds by culturing under different chondrogenic conditions.

First developed prototype samples were based on PCL scaffolds coated with hyaluronic acid. PCL scaffold protect cells from excessive loading and hyaluronic acid provides a correct biological environment. Hyaluronic acid coating was crosslinked in two different ways (1 step and 2 steps). Samples had similar values of hyaluronic acid weight but in PCL+HA1s samples hydrogel partially fills the pore meanwhile on PCL+HA2s only coats the pore's walls. Developed samples improved hydrophilicity of PCL samples and showed an elastic modulus in range with cartilage[22]. Cell culture showed that coating allowed cell growth inside the pore using the hydrogel filler as substrate compared with PCL where cells grew stuck to the walls. On the other hand coating was not perfect, the PCL surfaces appears in some parts of the pore walls and cells attached to these zones showed a behaviour similar to cells in naked PCL scaffolds. Finally the main function of hyaluronic acid coating that was to improve chondrogenic phenotype through hyaluronic acid-CD44 interaction was successful: A high number of the cells seeded on PCL+HA samples showed positive CD44 staining. The obtained results were used to correct certain characteristics of the developed PCL+HA samples. PCL+HA1s showed the best cell response but had the worst cell seeding efficiency probably because the hyaluronic acid filled the pore. Modified scaffold PCL+HA1s-m showed a similar hyaluronic acid coating but did not fill the pore. On the other hand PCL+HA2s samples showed the highest cell seeding efficiency compared to PCL samples probably because it was more hydrophilic than PCL. To improve cell seeding on PCL samples PCL was

combined with Bioglass® providing the scaffold with higher hydrophilicity and increased initial cell adhesion[77]. Bioglass® is a bioactive glass widely used in bone tissue engineering but not in cartilage tissue engineering[9,77] New developed scaffolds were able to support cell proliferation and differentiation at similar levels to PCL control but showed worse results than PCL scaffolds in normoxia conditions. In addition PCL-5BG reduced their mechanical properties to the half in 35 days in acellular culture pointing that polymer degradation is probably too fast for cartilage tissue engineering. Finally cells were encapsulated inside a crosslinkable hyaluronic acid to obtain a support able to isolate them in a hydrogel environment. That new scaffold was able promote chondrogenesis. In spite that it showed a negative effect over cell proliferation it was able to retain round shape with the addition of extrinsic factors pointing that an external chondrogenic stimulus was still required.

The second part of the study was to analyze culture conditions in order to improve chondrogenesis. In a first study scaffold samples were tested with chondrocytes without chondrogenic media to determine if hyaluronic acid coating can rescue the phenotype in adverse conditions. Culture media used in the first chapter section contained FBS that is a probed dedifferentiating factor that represent an adverse culture condition.[188,191] The obtained results suggested that chondrocyte interaction with hyaluronic acid could improve chondrogenic phenotype expression. In the next studies a serum free culture medium was used containing chondrogenic factors such as transforming growth factor β3 or dexamethasone that promote chondrogenic ECM secretion.[125] On the other hand *in vivo* is a complex environment with different oxygen level tension, complex mechanical signals and cell interactions through paracrine signals or cell-cell contacts. In this work we used different culture conditions such as hypoxia, hydrostatic pressure or coculture to reproduce chondrogenic stimulus *in vitro*. Cartilage tissue *in vivo* is subjected to hypoxia that affect the cells through hypoxia inducible factors inducing

chondrogenic differentiation of mesenchymal stem cells.[209] Our results showed that hypoxia was a more decisive chondrogenic factor than the characteristics of the material substrate. PCL-5BG and PCL+HA1s-m failed in normoxia conditions to develop chondrogenic markers while results clearly improved under hypoxia. These results point that hypoxia is a key factor to obtain well functional constructs. Secondly hypoxia was improved with the application of hydrostatic pressure that is another chondrogenic stimulus[132]. In our work hydrostatic pressure improved *in vitro* construct allowing a better production of ECM components and better cell distribution. Hypoxia showed to be a key factor on MSC chondrogenesis and obtained results with the bioreactor showed that hydrostatic pressure was able to improve hypoxia effect. Finally coculture is a new platform to induce mesenchymal stem cell chondrogenesis and chondrocytes redifferentiation.[52] Indirect coculture was chosen as culture method to separate paracrine effect from cell-cell contact interaction trying to mimic cartilage cell interaction *in vivo*. It has been described in the literature that chondrocytes release to the culture media paracrine factors able to induce cell differentiation and inhibit hypertrophy.[137,138,141] In our work coculture improved chondrogenesis of MSCs and reduced the expression of ALP; in our system no significant production of hypertrophic collagen type X was found. In addition chondrocyte redifferentiation improvement was found in our coculture with MSCs. The main drawback in our coculture system was the deficient cell distribution along the scaffold at day 35. Our hypothesis is that the huge number of chondrocytes surrounding scaffold impair oxygen and nutrient diffusion as consequence of cell metabolism. We expect that reducing the alginate mould diameter and cell number or the use of a bioreactor to force nutrient diffusion can solve lack cell distribution.

Finally we use the collagen/proteoglycans ratio to establish a direct relationship between the obtained results and the effect of each extrinsic chondrogenic factor

studied. Healthy cartilage has a defined ratio of collagen and proteoglycans that has been reported to be 1.67[6]. In the first study about normoxia versus hypoxia culture conditions we observed that normoxia conditions showed aberrant ratios from 3 to 6.4 while hypoxia reduce the ratio to normal values around 1.5. When hydrostatic pressure was applied to improve the hypoxia results we obtained similar values between samples cultured hypoxia in free conditions or with mechanical loading. Values under hydrostatic pressure were more similar to the expected 1.67 ratio. Final study compared coculture with monoculture in normoxia conditions. Cells seeded in monoculture showed anomalous rates of 7.8 to 9.8 compared with cocultures that showed values of 1.1. As a conclusion, the obtained results point that suitable *in vitro* construct can be obtained with our hybrid scaffolds using a combination of different chondrogenic biophysical stimulus.

5. CONCLUSIONS

5. Conclusions

1) Freeze extraction and particle leaching mixed technique allow fabricating a macroporous scaffold with a bimodal porosity composed by micropores (few microns) and macropores (around 200 μm) suitable for cartilage and bone tissue engineering. The scaffolds obtained showed a porosity over 85%. Macropores allow cell colonization and tissue invasion meanwhile the micropores contribute to the diffusion of nutrients and residues. On the other hand scaffolds could be produced polylactide-polycaprolactone blends with the same technique and showed similar morphology than polycaprolactone scaffolds but with higher mechanical properties. Polymer blend scaffolds showed small spherical structures over scaffold surface due to polymer phase separation between polycaprolactone and polylactic acid.

2) Composite polymer scaffolds reinforced with mineral particles were obtained analogously. Morphology and porosity was similar to bare polymer scaffolds furthermore, mineral particles appear at the surfaces of the pore walls. The mechanical properties of the scaffold improves even for low mineral content. Besides hybrid scaffolds whose internal surfaces were coated with a layer biomimetic hydroxyapatite were obtained by immersion in simulated body fluid. Tested samples showed hydroxyapatite crystals with cauliflower like morphology.

3) Polymer blend scaffolds and composites showed different degradation response depending on the major polymer phase composition and the presence of hydroxyapatite. The degradation rate of polylactic acid phase

in the blends was faster than that polycaprolactone allowing modulating degradation kinetics of the scaffold blends. On the other hand hydroxyapatite introduction decreased polycaprolactone degradation rate in both, polycaprolactone and polylactic acid rich blends.

4) Developed composite scaffolds did not show cell cytotoxicity. On the other hand scaffolds with 5% of mineral reinforcement did not provoke any improvement in cell differentiation but enhanced the cell adhesion compared to pure polycaprolactone samples. *In vivo* study showed that studied scaffolds are able to promote bone regeneration in a rabbit critical size defect. Bone regenerated showed mechanical properties quite similar to health bone. The mechanical behaviour and biological response of developed biomaterials was similar to reference material used as control.

5) Coating of the pore walls with hyaluronic acid was performed with different protocols. This coatings did not affect scaffold mechanical properties but increased its hydrophilicity improving cell invasion. Hyaluronic acid morphology was different for each coating protocol employed. Filling pores and cross-linking in one step coating fills the pores with hyaluronic acid hindering cell seeding meanwhile one step modified to dry the coating simultaneously to cross-link and two step protocol in which a HA dry layer is first deposited and dried before crosslinking allows obtaining a functional coating leaving the macropores open for cell seeding. Polycaprolactone scaffolds coated with hyaluronic acid showed enhanced chondrogenic redifferentiation of adult human chondrocytes compared with non coated scaffolds. Cells in polycaprolactone scaffolds grown with

fibroblastic shape stuck to the surface and with reduced biosynthetic capacity showing high staining of collagen type I but reduced collagen type II and aggrecan. On the other hand binding of chondrocytes with HA chains in HA coated scaffold by CD44 receptor was proved. Chondrocytes in this environment showed higher ECM production and enhanced expression of chondrogenic markers compared to PCL scaffolds. PCL+HA scaffolds showed some nude PCL zones due to imperfect coating. In that zones cell attached and behave as in bare PCL scaffold. On the other hand hyaluronic acid substitution with tyramine was effective and crosslinked in presence of HRP and H_2O_2. Hydrogel repartition inside the scaffold was homogeneous filling all the pores but even in this case the mechanical properties of the scaffold were not affected.

6) Hypoxia positively affected chondrogenesis in any of the substrates considered. While under normoxic conditions expression of chondrogenic markers and production of ECM was deficient even with the addition of TGF-β3, hypoxia conditions maintained viability and regulated ECM synthesis enhancing collagen type II staining and reducing collagen type I. Collagen production levels were similar under normoxia or hypoxia but interestingly GAGs/cell ratio was improved under hypoxia conditions in hyaluronic acid coated and polycaprolactone scaffolds. On the other hand small composition changes in the scaffolding materials lead to different mesenchymal stem cells response to intermittent hydrostatic pressure. Polycaprolactone and PCL-5BG scaffolds showed an ECM production increment and a reduction of collagen type I staining meanwhile distribution and morphology of the deposited ECM was also greatly changed in presence

of hyaluronic acid coating. Finally MSCs cultured on synthetic rigid scaffolds proliferate and secrete ECM showing modulus values in the range of normal cartilage tissue and should thus be biomechanically apt for implantation.

7) In indirect coculture, interactions between chondrocytes and MSCs is mediated by soluble factors secreted by each of them. The presence of mature chondrocytes close but without direct contact with MSCs produce several significant changes in MSCs fate, thus as is observed on normalized collagen type II content and collagen/GAGs ratio. Samples in coculture showed a significant increment in normalized collagen type II and a collagen/GAGs ratio more close to healthy cartilage than monocultured samples. On the other hand effect of substrates over MSC only was observed in histological staining were cells shape and ECM distribution was different if cells were isolated in HA hydrogel or not. On the other hand the presence of MSCs affect redifferentiation of mature chondrocytes seeded in alginate gels. In particular normalized collagen, glycosaminoglycans and collagen type II content was improved in presence of MSC.

Glossary

ALP	Alkaline phosphatase
ARNT	Aryl hydrogen receptor nuclear translocator
BG	Bioglass®45S5
BSA	Bovine serum albumin
DMEM	Dulbecco's modified Eagle's medium
DPBS	Dulbecco's phosphate buffered saline
DPBSG	Dulbecco's phosphate buffered saline with 2g/l glucose
DSC	Differential scanning calorimetry
DVS	Divinyl sulfone
ECM	Extracellular matrix
EDX	Energy dispersive X-ray
FBS	Foetal bovine serum
FN	Fibronectin
FS	Free swelling
GAG	Glycosaminoglycan
HA	Hyaluronic acid
HAp	Hydroxyapatite
HIF-1α	Hypoxia inducible factor-1α

HP	Hydrostatic pressure
HRP	Horseradish peroxidase
HY	Hypoxia
MSC	Mesenchymal stem cell
NO	Normoxia
OC	Osteocalcin
PCL	Polycaprolactone
PEMA	Polyethylmethacrylate
PHD	Prolyl-4 hydroxylase
PLLA	Poly(L-lactic acid)
SEM	Scanning electron microscopy
TGA	Thermogravimetric analysis
VHL	E3 ubiquitin ligase Von Hippel-Lindau

Figure index

Table index

Literature

1. Marieb EN, Hoehn K. Human Anatomy & Physiology Seventh edition. Pearson Education, 2007. ISBN: 9780321372949

2. Kierszenbaum AL, Tres LL. Histology and Cell Biology: An Introduction to Pathology Third edition. Saunders, 2012. ISBN: 9780323078429

3. Raven P, Johnson G, Mason K, Losos J, Singer S. Biology, ninth edition. McGraw-Hill, 2011. ISBN: 9780073532226

4. Palmer LC, Newcomb CJ, Kaltz SR, Spoerke ED, Stupp SI. Biomimetic Systems for Hydroxyapatite Mineralization Inspired By Bone and Enamel. Chemical Reviews 2008; 108: 4754–4783

5. Rho JY, Kuhn-Spearing L, Zioupos P. Mechanical properties and the hierarchical structure of bone. Medical Engineering & Physics 1998, 20, 92-102

6. Ross MH and Pawlina W: Histology: A Text and Atlas 6th edition. Lippincott WIlliams & Wilkins, 2011. ISBN: 9780781772006

7. Yaszem MJ, Paynet RG, Hayes WC, Lange R , Mikos AG. Evolution of bone transplantation: molecular, cellular and tissue strategies to engineer human bone. Biomaterials 1996; 17: 175-165

8. Murugan R, Ramakrishna S. Development of nanocomposites for bone grafting. Composites Science and Technology 2005; 65: 2385–2406

9. Rezwan K, Chen QZ, Blaker JJ, Boccaccini AR. Biodegradable and bioactive porous polymer/inorganic composite scaffolds for bone tissue engineering. Biomaterials 2006; 27:3413-3431

10. Barrère F, Mahmood TA, de Groot K, van Blitteswijk CA. Advanced biomaterials for skeletal tissue regeneration: Instructive and smart functions. Materials Science and Engineering 2008; 59: 38-71

11. Brown PW, Martin RI. An Analysis of Hydroxyapatite Surface Layer Formation. The journal of physical chemistry B. 1999; 103: 1671-1675

12. Fawcett DW. Tratado de histología, 12ª edición. McGraw-Hill interamericana, 2000. ISBN:8448601078

13. Temenoff JS, Mikos AG. Review: tissue engineering for regenaration of articular cartilage. Biomaterials 2000; 21:431-440

14. Tsiridis E, Upadhyay N, Giannoudis P. Molecular aspects of fracture healing: Which are the important molecules? Injury 2007; 38: S11–S25

15. Marsell R, Einhom TA. The biology of fracture healing. Injury 2011; 42: 551-555

16. Porwit A, McCullough J, Erber WN. Blood and Bone Marrow Pathology Second edition. Elsevier, 2011. ISBN: 9780702031472

17. Herkowitz HN, Garfin SR, Eismont FJ, Bell GR, Balderston RA. Rothman-Simeone The Spine, sixth edition. Saunders, 2011. ISBN: 9781416067269

18. Dimitriou R, Tsiridis E, Giannoudis PV. Current concepts of molecular aspects of bone healing. Injury 2005; 36: 1392-1404

19. Phillips AM. Overview of the fracture healing cascade. Injury 2005; 36 S5-S7

20. Kelly DJ, Jacobs CR. The role of mechanical signals in regulating chondrogenesis and osteogenesis of mesenchymal stem cells. Birth Defects Research Part C: Embryo Today: Reviews 2010;90:75–85

21. Keating JF, McQueen MM. Substitutes for autologous bone graft in orthopaedic trauma. Journal of bone and joint surgery-british 2001; 83B:3-8

22. Sabir MI, Xu X, Li L. A review on biodegradable polymeric materials for bone tissue engineering applications. Journal of materials science 2009; 44: 5713-5724

23. Redman SN, Oldfield SF, Archer CW. Current strategies for articular cartilage repair. European Cells and Materials 2005; 9: 23-32

24. Beris AE, Lykissas MG,Papageorgiou CD, Georgoulis AD. Advances in articular cartilage repair. Injury 2005; 36: S14-S23

25. Hunziker EB. Articular cartilage repair: basic science and clinical progress. A review of the current status and prospects. Osteoarthritis and cartilage 2002; 10: 432-463

26. Hutmacher DW, Schantz JT, Lam CXF, Tan KC, Lim TC. State of the art and future directions of scaffold-based bone engineering from a biomaterials perspective. Journal of Tissue Engineering and Regenerative Medicine 2007; 1: 245-260

27. Lanza R, Langer R, Vacanti JP.Principles of tissue engineering, Third edition. Academic Press, 2011. ISBN: 9780080548845

28. Burg KJL, Porter S, Kellam JF. Biomaterial developments for bone tissue engineering. Biomaterials 2000; 21: 2347-2359

29. Kanczler JM, Oreffo ROC. Osteogenesis and angiogenesis: the potential for engineering bone. European Cells and Materials 2008; 15: 100-114

30. Santos MI, Reis RL. Vascularization in Bone Tissue Engineering: Physiology, Current Strategies, Major Hurdles and Future Challenges. Macromolecular Bioscience 2010; 10: 12-27

31. Xiao W-D, Zhong Z-M, Tang Y-Z,Xu Z-X, Xu Z, Chen J-T. Repair of critical size bone defects with porous poly(D,L-lactide)/nacre nanocomposite hollow scaffold. Saudi medical journal 2012; 33: 601-607

32. Roohani-Esfahani SI, Dunstan CR, Davies B, Pearce S, Williams R, Zreiqat H. Repairing a critical-sized bone defect with highly porous modified and unmodified baghdadite scaffolds. Acta Biomaterialia 2012; 8: 4162-4172

33. Salgado AJ, Coutinho OP, Reis RL. Bone Tissue Engineering: State of the Art and Future Trends. Macromolecular bioscience 2004; 4:743-765

34. Tate MLK, Niederer P, Knothe U. In Vivo Tracer Transport Through the Lacunocanalicular System of Rat Bone in an Environment Devoid of Mechanical Loading. Bone 1998; 22: 107-117

35. Puppi D, Chiellini F, Piras AM, Chiellini E. Polymeric materials for bone and cartilage repair. Prog Polym Sci 2010;35:403–40

36. Deplaine H, Gómez-Ribelles JL, Gallego-Ferrer G. Effect of the content of hydroxyapatite nanoparticles on the properties and bioactivity of poly(L-lactide) – Hybrid membranes. Composites science and technology 2010; 2010: 1805-1812

37. Kokubo T, Takadama H. How useful is SBF in predicting in vivo bone bioactivity? Biomaterials 2006;27:2907–2915

38. Deplaine H, Lebourg M, Ripalda P, Vidaurre A, Sanz-Ramos P, Mora G, Prósper F, Ochoa I, Doblaré M, Ribelles JLG, Izal-Azcárate I, Ferrer GG. Biomimetic hydroxyapatite coating on pore walls improves osteointegration of poly(L-lactic acid) scaffolds. Journal of Biomedical Materials Research Part B: Applied Biomaterials 2013; 101B:173–186

39. Lebourg M, Martinez-Díaz S, García-Giralt N, Torres-Claramunt R, Gómez-Ribelles JL, Vila-Canet G, Monllau JC. Cell-free cartilage engineering approach using hyaluronic acid–polycaprolactone scaffolds: A study in vivo. Journal of Biomaterials Applications 2014;28:1304–1315

40. Erggelet C, Neumann K, Endres M, Haberstroh K, Sittinger M, Kaps C. Regeneration of ovine articular cartilage defects by cell-free polymer-based implants. Biomaterials 2007; 28:5570-5580

41. Patrascu JM, Freymann U, Kaps C, Poenaru DV. Repair of a post-traumatic cartilage defect with a cell-free polymer-based cartilage implant: A follow-up at two years by MRI and histological review. Journal Bone & Joint Surgery 2010; 92: 1160-1163

42. Gotterbarm T, Richtera W, Jung M, Vilei SB, Mainil-Varlet P, Yamashita T, Breusch SJ. An in vivo study of a growth-factor enhanced, cell free, two-layered collagen–tricalcium phosphate in deep osteochondral defects. Biomaterials 2006; 27: 3387-3395

43. Efe T, Theisen C, Fuchs-Winkelmann S, Stein T, Getgood A, Rominger MB, Paletta JRJ, Schofer MD. Cell-free collagen type I matrix for repair of cartilage defects—clinical and magnetic resonance imaging results. Knee Surgery, Sports Traumatology, Arthroscopy 2012; 20: 1915-1922

44. Siclari A, Mascaro G, Gentili C, Cancedda R, Boux E. A Cell-free Scaffold-

based Cartilage Repair Provides Improved Function Hyaline-like Repair at One year. Clinical Orthopaedics and Related Research 2012; 470:910-919

45. Li WJ, Chiang H, Kuo TF, Lee HS, Jiang CC, Tuan RS. Evaluation of articular cartilage repair using biodegradable nanofibrous scaffolds in a swine model: a pilot study. Journal of Tissue Engineering and Regenerative Medicine 2009; 3: 1-10

46. Wakitani S, Imoto K, Yamamoto T, Saito M, Murata N, Yoneda M. Human autologous culture expanded bone marrow mesenchymal cell transplantation for repair of cartilage defects in osteoarthritic knees. Osteoarthritis and Cartilage 2002; 10: 199-206

47. Wakitani S, Nawata M, Tensho K, Okabe T, Machida H, Ohgushi H. Repair of articular cartilage defects in the patello-femoral joint with autologous bone marrow mesenchymal cell transplantation: three case reports involving nine defects in five knees. Journal of Tissue Engineering and Regenerative Medicine 2007; 1: 74-79

48. Martinez-Diaz S, Garcia-Giralt N, Lebourg M, Gómez-Tejedor JA, Vila G, Caceres E, Benito P, Pradas MM, Nogues X, Ribelles JLG, Monllau JC. In vivo evaluation of 3-dimensional polycaprolactone scaffolds for cartilage repair in rabbits. The American Journal of Sports Medicine 2010; 38: 509-519

49. Uematsu K, Hattori K, Ishimoto Y, Yamauchi J, Habata T, Takakura Y, Ohgushi H, Fukuchi T, Sato M. Cartilage regeneration using mesenchymal stem cells and a three-dimensional poly-lactic-glycolic acid (PLGA) scaffold. Biomaterials 2005;26:4273-4279

50. Hunzikerf EB. Articular cartilage repair: are the intrinsic biological constraints undermining this process insuperable? Osteoarthritis and cartilage. 1999; 7: 15-28

51. Maler JJ, Upton J, Langer R, Vacanti JP. Transplantation of cells in matrices for tissue regeneration. Advanced drug delivery reviews. 1998; 33: 165-182

52. Hubka KM, Dahlin RL, Meretoja VV, Kasper FK, Mikos AG. Enhancing Chondrogenic Phenotype for Cartilage Tissue Engineering: Monoculture

and Coculture of Articular Chondrocytes and Mesenchymal Stem Cells. Tissue Engineering Part B: Reviews

53. Vinatier C, Mrugala D, Jorgensen C, Guicheux J, Noël D. Cartilage engineering: a crucial combination of cells, biomaterials and biofactors. Trends in biotechnology 2009; 27: 307-14

54. Mobasheri A, Kalamegame G, Musumecif G, Batt ME. Chondrocyte and mesenchymal stem cell-based therapies for cartilage repair in osteoarthritis and related orthopaedic conditions. Maturitas 2014,78:188-198

55. Schnabel M, Marlovit S, Eckhoff G, Fichtel I, Gotzen I, Vecsei V, Schlegel J. Dedifferentiation-associated changes in morphology and gene expression in primary human articular chondrocytes in cell culture. Osteoarthritis Cartilage 2002; 10 :62–70

56. Brodkin KR, García AJ, Levenston ME. Chondrocyte phenotypes on different extracellular matrix monolayers. Biomaterials 2004; 25: 5929–5938

57. Darling EM, Athanasiou KA. Rapid phenotypic changes in passaged articular chondrocyte subpopulations. J Orthoped Res 2005;23: 425–432

58. Tuli R, Li WJ, Tuan RS. Current state of cartilage tissue engineering. Arthritis research & therapy 2003,5:235-238

59. Mano JF. Biomimetic Approaches for Biomaterials Development.; Wiley-VCH Verlag GmbH & Co. KGaA, 2012. ISBN:9783527329168

60. Gelse K et al. Molecular differentiation between osteophytic and articular cartilage clues for a transient and permanent chondrocyte phenotype. Osteoarthr and Cartil 2012; 20:162–171

61. Vinardell T, Sheehy EJ, Buckley CT, Kelly DJ. A comparison of the functionality and in vivo phenotypic stability of cartilaginous tissues engineered from different stem cell sources. Tissue Eng Part A 2012;18:1161-1170

62. Magne D, Vinatier C, Julien M, Weiss P, Guicheux J. Mesenchymal stem cell therapy to rebuild cartilage. Trends in molecular medicine. 2005, 11:

519-526

63. Nair LS, Laurencin CT. Biodegradable polymers as biomaterials. Progress in Polymer Science 2007; 32: 762-798

64. Bonzani IC, George JH, Stevens MM. Novel materials for bone and cartilage regeneration. Curr Opin Chem Biol 2006;10:568–575

65. Agrawal C.M., Ray R.B. Biodegradable polymeric scaffolds for musculoskeletal tissue engineering. Journal of biomedical materials research 2001; 55: 141-150

66. Wutticharoenmongkol P, Pavasant P, Supaphol P. Osteoblastic phenotype expression of MC3T3-E1 cultured on electrospun polycaprolactone fiber mats filled with hydroxyapatite nanoparticles. Biomacromolecules 2007;8:2602–2610

67. Shor L, Güçeri S, Wen X, Gandhi M, Sun W. Fabrication of three-dimensional polycaprolactone/hydroxyapatite tissue scaffolds and osteoblast-scaffold interactions in vitro. Biomaterials 2007;28:5291–5297

68. Chuenjitkuntaworn B, Inrung W, Damrongsri D, Mekaapiruk K, Supaphol P, Pavasant P. Polycaprolactone/hydroxyapatite composite scaffolds: preparation, characterization, and in vitro and in vivo biological responses of human primary bone cells. J Biomed Mater Res A 2010;94:241–51

69. Diba M, Kharaziha M, Fathi MH, Gholipourmalekabadi M, Samadikuchaksaraei A. Preparation and characterization of polycaprolactone/forsterite nanocomposite porous scaffolds designed for bone tissue regeneration. Compos Sci Technol 2012;72:716–23

70. Cannillo V, Chiellini F, Fabbri P, Sola A. Production of Bioglass® 45S5–polycaprolactone composite scaffolds via saltleaching. Compos struct 2010;92:1823–32

71. Lee HJ, Kim SE, Choi HW, Kim CW, Kim KJ, Lee SC. The effect of surface-modified nano-hydroxyapatite on biocompatibility of poly(ε-caprolactone)/hydroxyapatite nanocomposites. Eur Polym J 2007;43:1602–1608

72. Wei G, Ma PX. Structure and properties of nano-hydroxyapatite/polymer composite scaffolds for bone tissue engineering. Biomaterials 2004; 25: 4749-4757

73. Murphy WL, Kohn DH, Mooney DJ. Growth of continuous bonelike mineral within porous poly(lactide-co-glycolide) scaffolds in vitro. J Biomed Mater Res A 2000; 50:1549-3296

74. Ma PX, Zhang R, Xiao G, Franceschi R. Engineering new bone tissue in vitro on highly porous poly(a-hydroxyl acids)/hydroxyapatite composite scaffolds. J Biomed Mater Res 2000; 54:284-293

75. Woo KM, Seo J, Zhang R, Ma PX. Suppression of apoptosis by enhanced protein adsorption on polymer/hydroxyapatite composite scaffolds. Biomaterials 2007; 28:2622-2630

76. Peter M, Binulal NS, Nair SV, Selvamurugan N, Tamura H, Jayakumar R. Novel biodegradable chitosan–gelatin/nano-bioactive glass ceramic composite scaffolds for alveolar bone tissue engineering. Chem Eng J 2010;158:353–361

77. Wu J, Xue K, Li H, Sun J, Liu K. Improvement of PHBV scaffolds with Bioglass for cartilage tissue engineering. Plos One 2013;8

78. Boyan BD, Hummert TW, Dean DD, Schwartz Z. Role of material surfaces in regulating bone and cartilage cell response. Biomaterials 1996; 17: 137-146

79. Reilly GC, Engler AJ. Intrinsic extracellular matrix properties regulate stem cell differentiation. J. of Biomech 2010;43:55-62

80. Phillips JE, Petrie TA, Creighton FP, García AJ. Human mesenchymal stem cell differentiation on self-assembled monolayers presenting different surface chemistries. Acta Biomaterialia 2010;6:12-20

81. Katsanevakis E, Wen X, Shi D, et al. Biomineralization of polymer scaffolds. Key Eng Mater 2010; 441:269-295

82. Jiao Y-P, Cui F-Z. Surface modification of polyester biomaterials for tissue engineering. Biomedical materials 2007; 2: R24

83. Morent R, De Geyter N, Desmet T, Dubruel P, Leys Cristophe. Plasma Surface Modification of Biodegradable Polymers: A Review. Plasma processes and polymers 2011; 8: 171-190

84. Mondrinos MJ, Dembzynski R, Lu L, Byrapogu VKC, Wootton DM, Lelkes PI, Zhou J. Porogen-based solid freeform fabrication of polycaprolactone–calcium phosphate scaffolds for tissue engineering. Biomaterials 2006; 27:4399-4408

85. Lua Y, Zhu A, Wang W, Shi H. New bioactive hybrid material of nano-hydroxyapatite based on N-carboxyethylchitosan for bone tissue engineering. Appl Surf Sci 2010; 256:7228–7233

86. Zhao F, Grayson WL, Ma T, Bunnell B, Lu WW. Effects of hydroxyapatite in 3-D chitosan–gelatin polymer network on human mesenchymal stem cell construct development. Biomaterials 2006; 27:1859-1867

87. Li Z, Yubao L, Aiping Y, Xulein P, Xuejiang W, Xiang Z. Preparation and in vitro investigation of chitosan/nano-hydroxyapatite composite used as bone substitute materials. J Mater Sci Mater Med 2005; 16:213-219

88. Fabbri P, Cannillo V, Sola A, Dorigato A, Chiellini F. Highly porous polycaprolactone-45S5 Bioglass® scaffolds for bone tissue engineering. Composites Sci and Technol 2011; 70:1869-1878

89. Armentano I, Dottori M, Fortunati E, Mattioli S, Kennya JM. Biodegradable polymer matrix nanocomposites for tissue engineering: A review. Polymer degradation and stability 2010; 95: 2126-2146

90. Deb S, Mandegaran R, Di Silvio L. A porous scaffold for bone tissue engineering/45S5 Bioglass® derived porous scaffolds for co-culturing osteoblasts and endothelial cells. J Mater Sci Mater Med 2010; 21:893-905

91. Xynos ID, Edgar AJ, Buttery LD, Hench LL, Polak JM. Gene-expression profiling of human osteoblasts following treatment with the ionic products of Bioglass® 45S5 dissolution. Journal of Biomedical Materials Research 2001; 55:151–157

92. Weiss P, Fatimi A, Guicheux J, Vinatier C. Hydrogels for Cartilage Tissue

Engineering. Biomedical Applications of Hydrogels Handbook 2010; part III: 247-268

93. Balakrishnan B, Banerjee R. Biopolymer-Based Hydrogels for Cartilage Tissue Engineering. Chemical Reviews. 2011; 111: 4453-4474

94. Drudy JL, Mooney DJ. Hydrogels for tissue engineering: scaffold design variables and applications. Biomaterials. 2003; 24: 4337-4351

95. Steward AJ, Liu Y, Wagner DR. Engineering Cell attachments to Scaffolds in Cartilage tissue engineering. JOM 2011; 63:74-82

96. Adams JC, Watt FM. Regulation of development and differentiation by the extracellular matrix. Development 1993; 117: 1183-1198

97. Yoo HS, Lee EA, Yoon JJ, Park TG. Hyaluronic acid modified biodegradable scaffolds for cartilage tissue engineering. Biomaterials 2005; 26:1925-1933

98. Ishida O, Tanaka Y, Morimoto I, Takigawa M, Eto S. Chondrocytes Are Regulated by Cellular Adhesion Through CD44 and Hyaluronic Acid Pathway. Journal of Bone and Mineral Research 1997;12:1657–1663

99. Girotto D, Urbani S, Brun P, Renier D, Barbucci R, Abatangelo G. Tissue-specific gene expression in chondrocytes grown on threedimensional hyaluronic acid scaffolds. Biomaterials 2003;24: 3265–3275

100. Patti AM, Gabriele A, Vulcano A, Ramieri MT, Della Rocca C. Effect of hyaluronic acid on human chondrocyte cell lines from articular cartilage. Tissue Cell 2001;33:294–300

101. Grigolo B, De Franceschi L, Roseti L, Cattini L, Facchini A. Down regulation of degenerative cartilage molecules in chondrocytes grown on a hyaluronan-based scaffold. Biomaterials 2005;26: 5668–5676

102. Quinn TM, Grodzinsky AJ, Buschmann MD, Kim YJ, Hunziker EB. Mechanical compression alters proteoglycan deposition and matrix deformation around individual cells in cartilage explants. J Cell Sci 1998;111:573–583

103. Grodzinsky AJ, Levenston ME, Jin M, Frank EH. Cartilage tissue remodeling in response to mechanical forces. Annu Rev Biomed Eng 2000;2:691–713

104. Chung C, Burdick JA. Engineering cartilage tissue. Advanced Drug Delivery Reviews 2008;60:243–262

105. Chiang H, Jiang C-C. Repair of Articular Cartilage Defects: Review and Perspectives. Journal of the formosan medical association 2009; 108: 87-101

106. J.T. Connelly, A.J. García, M.E. Levenston. Inhibition of in vitro chondrogenesis in RGD-modified three-dimensional alginate gels. Biomaterials 2007; Vol 28:1071-1083

107. Steward AJ, Thorpe SD, Vinardell T, Buckley CT, Wagner DR, Kelly DJ. Cell–matrix interactions regulate mesenchymal stem cell response to hydrostatic pressure. Acta Biomaterialia 2012;8:2153-2159

108. Woodfield, T.B.F.; Miot, S.; Martin, I.; van Blitterswijk, C.A.; Riesle. The regulation of expanded human nasal chondrocyte re-differentiation capacity by substrate composition and gas plasma surface modification. J. Biomaterials 2006, 27, 1043-1053

109. Moutos FT, Guilak F. Composite scaffolds for cartilage tissue engineering. Biorheology 2008; 45:501-512

110. Berger J, Reist M, Mayer JM, Felt O, Peppas NA, Gurny R. Structure and interactions in covalently and ionically crosslinked chitosan hydrogels for biomedical applications. European Journal of Pharmaceutics and Biopharmaceutics 2004; 57:19-34

111. Darr A, Calabro, A. Synthesis and characterization of tyramine-based hyaluronan hydrogels. Journal of Materials Science: Materials in Medicine 2009; 20: 33-44

112. Tuan RS, Boland G, Tuli R. Adult mesenchymal stem cells and cell-based tissue engineering. Arthritis Res Ther 2003, 5:32-45

113. Huang AH, Farell MJ, Mauck RL. Mechanics and mechanobiology

of mesenchymal stem cell-based engineered cartilage. J. of Biomech 2010; 43:128-136

114. Crombrugghe BD, Lefebvre V, Nakashima K. Regulatory mechanism in the pathways of cartilage and bone formation. Current opinion in cell biology. 2001; 13: 721-728

115. Goldring MB, Tsuchimochi K, Ijiri K. The control of chondrogenesis. Journal of cellular biochemestry. 2006; 97: 33-34

116. DeLise AM, Fischer L, Tuan RS. Cellular interactions and signaling in cartilage development. Osteoarthritis and cartilage. 2000; 8: 309-334

117. Kobayashi T, Kronenberg H. Minireview: Transcriptional regulation in development of bone. Endocrinology. Endocrinology. 2005; 146: 1012-1017

118. Dreier R. Hypertrophic differentiation of chondrocytes in osteoarthritis: the developmental aspect of degenerative joint disorders. Arthritis research & therapy. 2010; 12: 216-227

119. Demarteau O, Schafer D, Hintermann B, Dick W, Heberer M, Martin I. Specific Growth Factors During the Expansion and redifferentiation of Adult Human Articular Chondrocytes Enhance Chondrogenesis and Cartilaginous Tissue Formation in Vitro. Journal of cellular bichemistry. 2001; 81: 368-377

120. Fermor B, Christensen SE, Youn I, Cernanec JM, Davies CM, Weinberg JB. Oxygen, Nitric Oxide And Articular Cartilage. European Cells and Materials 2007; 13:56-56

121. Huang LE, Franklin Bunn F. Hypoxia-inducible Factor and Its Biomedical Relevance. The journal of biological chemistry. 2003, 278:19575-19578

122. Araldi E, Schipani E. Hypoxia, HIFs and bone development. Bone. 2010; 47: 190-196

123. Duval E, Baugé C, Andriamanalijaona R, Bénateau H, Leclercq S, Dutoit S, Poulain L, Galéra P, Boumédiene K. Molecular mechanism of

hypoxia-induced chondrogenesis and its application in vivo cartilage tissue engineering. Biomaterials 2012;33:6042-6051

124. Makris EA, Hu JC, Athanasiou KA. Hypoxia-induced collagen crosslinking as a mechanism for enhancing mechanical properties of engineered articular cartilage. Osteoarthritis and Cartilage 2013; 21 :634-641

125. Welter JF, Solchaga LA, Baskaran H. Chondrogenesis from human mesenchymal stem cells: role of culture conditions. Stem Cells and Cancer Stem Cells 2012;5:269-280

126. Schulz RM, Bader A. Cartilage tissue engineering and bioreactor systems for the cultivation and stimulation of chondrocytes. European biophysics journal. 2007; 36: 539-568

127. Villanueva I, Weigel CA, Bryant SJ. Cell-matrix interactions and dynamic mechanical loading influence chondrocyte gene expression and bioactivity in PEG-RGD hydrogels. Acta Biomateralia 2009;5:2832-2846

128. Schagemann JC et al. The effect of scaffold composition on the early structural characteristics of chondrocytes and expression of adhesion molecules. Biomaterials 2010;31:2798–2805

129. Thorpe SC, Buckley CT, Vinardell T, O'Brien FJ, Campell VA, Kelly DJ. Dynamic compression can inhibit chondrogenesis of mesenchymal stem cells. Biochemical and biophysical research communications. 2008; 377: 458-462

130. Grad S, Eglin D, Alini M, Stoddart MJ. Physical stimulation of chondrogenic cells in vitro: A review. Clin Orthop. and Relat Res 2011;469: 2764-2772

131. Kessler MW, Grande DA. Tissue engineering and cartilage. Organogenesis 2008;4:28-32

132. Elder BD, Athanasiou KA. Hydrostatic pressure in articular cartilage tissue engineering: from chondrocytes to tissue regeneration. Tissue Eng Part B: Rev 2009;15:43-53

133. Wagner DR et al. Hydrostatic pressure enhances chondrogenic differentiation of human bone marrow stromal cells in osteochondrogenic medium. Ann of Biomed Eng 2008;36:813-820

134. Meyer EG, Buckley CT, Steward AJ, Kelly DJ. The effect of cyclic hydrostatic pressure on the functional development of cartilaginous tissues engineered using bone marrow derived mesenchymal stem cells. J. of the Mech Behav of Biomed Materials 2011;4:1257-1265

135. Wong M, Siegrist M, Goodwin K. Cyclic tensile strain and cyclic hydrostatic pressure differentially regulate expression of hypertrophic markers in primary chondrocytes. Bone 2003;33:685-693

136. Carroll SF, Buckley CT, Kelly DJ. Cyclic hydrostatic pressure promotes a stable cartilage phenotype and enhances the functional development of cartilaginous grafts engineered using multipotent stromal cells isolated from bone marrow and infrapatellar fat pad. J. of Biomech; In press.

137. Sayed KE, Zreiqat H, Ertel W, Schulze-Tanzil G. Stimulated Chondrogenesis via Chondrocytes Co-culturing. J Biochips & Tissue chips 2012; S2

138. Fischer J, Dickhut A, Rickert M, Richter W. Human Articular Chondrocytes Secrete Parathyroid Hormone–Related Protein and Inhibit Hypertrophy of Mesenchymal Stem Cells in Coculture During Chondrogenesis. Arthritis & rheumatism. 2010; 62: 2696-2706

139. Guo J, Chung U-I, Yang D, Karsenty G, Bringhurst FR, Kronenberg HM. PTH/PTHrP receptor delays chondrocyte hypertrophy via both Runx2-dependent and - ndependent pathways. Devolopmental biology. 2006; 292: 116-128

140. Acharya C, Adesida A, Zajac P, Mumme M, Riesle J, Martin I, Barbero A. Enhanced Chondrocyte Proliferation and Mesenchymal Stromal Cells Chondrogenesis in Coculture Pellets Mediate Improved Cartilage Formation. Journal of cellular physiology. 2012; 227: 88-97

141. Ahmed N, Dreier R, Gopferich A, Grifka J, Grassel S. Soluble

Signalling Factors Derived from Differentiated Cartilage Tissue Affect Chondrogenic Differentiation of Rat Adult Marrow Stromal Cells. Cellular phisiology and biochemistry. 2007; 20: 665–678

142. Liu X, Sun H, Yan D, Zhanga L, Lv X, Liu T, Zhanga W, Liu W, Cao Y, Zhou G In vivo ectopic chondrogenesis of BMSCs directed by mature chondrocytes. Biomaterials. 2010; 31: 9406-9414

143. Tsuchiya K, Chen G, Ushida T, Matsuno T, Tateishi T. The effect of coculture of chondrocytes with mesenchymal stem cells on their cartilaginous phenotype in vitro. Materials science and engineering: C. 2004; 24: 391-396

144. Mo X-T, Guo S-C, Xie H-G, Deng L, Zhi W, Xiang Z, Li X-G, Yang Z-M. Variations in the ratios of co-cultured mesenchymal stem cells and chondrocytes regulate the expression of cartilaginous and osseous phenotype in alginate constructs. Bone. 2009; 45: 42-51

145. Bian L, Zhai DY, Mauck RL, Burdick JA. Coculture of Human Mesenchymal Stem Cells and Articular Chondrocytes Reduces Hypertrophy and Enhances Functional Properties of Engineered Cartilage. Tissue engineering part A. 2011; 17: 1137-1145

146. Levorson EJ, Santoro M, Kasper FK, Mikos AG. Direct and indirect co-culture of chondrocytes and mesenchymal stem cells for the generation of polymer/extracellular matrix hybrid constructs, Acta Biomaterialia 2014;10:1824-1835

147. Hwang NS, Varghese S, Puleo C, Zhang Z, Elisseeff J. Morphogenetic Signals from Chondrocytes Promote Chondrogenic and Osteogenic Differentiation of Mesenchymal Stem Cells. Journal of cellular physiology. 2007; 212: 281-284

148. Collins MN, Birkinshaw C. Comparison of the Effectiveness of Four Different Crosslinking Agents with Hyaluronic Acid Hydrogel Films for Tissue-Culture Applications. Journal of applied polymer science, 2007; 104: 3183-3191

149. Ramamurthi A, Vesely I. Evaluation of the matrix-synthesis

potential of crosslinked hyaluronan gels for tissue engineering of aortic heart valves. Biomaterials 2005; 26: 999-1010

150. Choi JY, Lee BH, Song KB, Park RW, Kim IS, Sohn KY, Jo JS, Ryoo HM. Expression patterns of bone-related proteins during osteoblastic differentiation in MC3T3-E1 cells. Journal of cellular biochemistry 1996; 61:609-618

151. Ho MH, Kuo PY, Hsieh HJ, Hsien TY, Hou LT, Lai JY, Wang DM. Preparation of porous scaffolds by using freeze-extraction and freeze-gelation methods. Biomaterials 2004; 25: 129-138

152. Pyda M, Bopp RC, Wunderlich B. Heat capacity of poly(lactic acid). Journal of Chemical Thermodynamics. 2004;36:731-742

153. Yam WY, Ismail J, Kammer HW, Schmidt H, Kummerlowe C. Polymer blends of poly(ε-caprolactone) and poly(vinyl methyl ether) - Thermal properties and morphology. Polymer, 1999;40:5545-5552

154. Kafienah W, Sims TJ. Biochemical methods for the analysis of tissue-engineered cartilage. Methods in Molecular Biology 2004; 238: 217-229

155. Ignat'eva NY, Danilov NA, Averkiev SV, Obrezkova MV, Lunin VV, Sobol EN. Determination of hydroxyproline in tissues and the evaluation of the collagen content of the tissues. Journal of Analytical Chemistry 2007; 62: 51-57

156. Kruyt MC, Van Gaalen SM, Oner FC, Verbout AJ, De Bruijn JD, Dhert WJA. Bone tissue engineering and spinal fusion: the potential of hybrid constructs by combining osteoprogenitor cells and scaffolds. Biomaterials 2004; 25:1463-1473

157. Hench, LL. The story of Bioglass®. Journal of Materials Science: Materials in Medicine 2006; 17: 967-978

158. Ródenas-Rochina J, Ribelles JL, Lebourg M. Comparative study of PCL-HAp and PCL-bioglass composite scaffolds for bone tissue engineering. Journal of Materials Science: Materials in Medicine 2013;

24:1293-308

159. Meloan SN, Puchtler H. Chemical mechanisms of staining methods: von Kossa's technique. What von Kossa really wrote and a modified reaction for selective demonstration of inorganic phosphate. Journal of Histotechnology 1985; 8: 11–13

160. Kaysinger KK, Ramp WK. Extracellular pH modulates the activity of cultured human osteoblasts. Journal of Cellular Biochemistry 1998; 68: 83–89

161. Storrie H, Stupp SI. Cellular response to zinc-containing organoapatite: an in vitro study of proliferation, alkaline phosphatase activity and biomineralization. Biomaterials 2005; 26: 5492–5499

162. Boyde A, Corsi A, Quarto R, Cancedda R, Bianco P. Osteoconduction in large macroporous hydroxyapatite ceramic implants: Evidence for a complementary integration and disintegration mechanism. Bone. 1999;24:579-589

163. Barou O, Mekraldi S, Vico L, Boivin G, Alexandre C, Lafage-Proust M. Relationships between trabecular bone remodeling and bone vascularization: A quantitative study. Bone 2002; 30: 604-612

164. Cai L, Guinn AS, Wang S. Exposed hydroxyapatite particles on the surface of photo-crosslinked nanocomposites for promoting MC3T3 cell proliferation and differentiation. Acta Biomateralia 2011; 7: 2185–2199

165. Pitt CG, Zhong-wei G. Modification of the rates of chain cleavage of poly(ϵ-caprolactone) and related polyesters in the solid state. Journal of Controlled Release 1987; 4: 283-292

166. Matsuura T, Hosokawa R, Okamoto K, Kimoto T, Akagawa Y. Diverse mechanisms of osteoblast spreading on hydroxyapatite and titanium. Biomaterials 2000; 21: 1121-1127

167. Kilpadi KL, Chang PL, Bellis SL. Hydroxylapatite binds more serum proteins, purified integrins, and osteoblast precursor cells than titanium or steel. Journal of biomedical mater research 2001; 57:258–267

168. Lian JB, Stein GS. Concepts of osteoblast growth osteoblast growth and differentiation: modulation of bone cell development and tissue formation. Critical Reviews in Oral Biology & Medicine 1992; 3: 269–305

169. Al-Jallad HF, Nakano Y, Chen JLY, McMillan E, Lefebvre C, Kaartinen MT. Transglutaminase activity regulates osteoblast differentiation and matrix mineralization in MC3T3-E1 osteoblastcultures. Matrix Biology 2006; 25: 135–48

170. Wenstrup RJ, Fowlkes JL, Wittei DP, Florer JB. Discordant expression of osteoblast markers in MC3T3-E1 cells that synthesize a high turnover matrix. The journal of biological chemistry 1996; 271: 10271–10276

171. Varanasi VG, Saiz E, Loomer PM, Ancheta B, Uritani N, Ho SP, Tomsia AP, Marshall SJ, Marshall GW. Enhanced osteocalcin expression by osteoblast-like cells (MC3T3-E1) exposed to bioactive coating glass (SiO2–CaO–P2O5–MgO–K2O–Na2O system) ions. Acta Biomateralia 2009; 5: 3536–3547

172. Schneider GB, Perinpanayagam H, Clegg M, Zaharias R, Seabold D, Keller J, Stanford C. Implant surface roughness affects osteoblast gene expression. Journal of Dental Research 2003; 82: 372–376

173. Alliot-Licht B, Gregoire M, Orly I, Menanteau J. Cellular activity of osteoblasts in the presence of hydroxyapatite: an in vitro experiment. Biomaterials 1991; 12: 752–756

174. Prigodich RV, Vesely MR. Characterization of the complex between bovine osteocalcin and type I collagen. Archives of Biochemistry and Biophysics 1997; 345: 339–341

175. Franceschi RT, Iyer BS, Cui Y. Effects of ascorbic acid on collagen matrix formation and osteoblast differentiation in murine MC3T3-E1 cells. Journal of Bone and Mineral Research 1994; 9: 843–54

176. Lebourg M, Antón JS, Ribelles JLG. Porous membranes of PLLA–PCL blend for tissue engineering applications. European polymer journal 2008; 44: 2207-2218

177. Lebourg M, Antón JS, Ribelles JLG. Hybrid structure in PCL-HAp scaffold resulting from biomimetic apatite growth. Journal of materials science: materials in medicine 2010, 21: 33-44

178. Hutmacher DW. Scaffolds in tissue engineering bone and cartilage. Biomaterials 2000; 21: 2529-2543

179. Gaona LA, Ribelles JLG, Perilla JE, Lebourg M. Hydrolytic degradation of PLLA/PCL microporous membranes prepared by freeze extraction. Polymer Degradation and Stability 2012; 97: 1621-1632

180. Rodenas-Rochina J, Vidaurre A, Cortazár IC, Lebourg M. Effects of hydroxyapatite filler on long-term hydrolytic degradation of PLLA/PCL porous scaffolds. Submitted

181. Tsuji H, Ikada Y. Blends of aliphatic polyesters. II. Hydrolysis of Solution-Cast Blends from Poly(L-lactide) and Poly(ε -caprolactone) in Phosphate-Buffered Solution. Journal of Applied Polymer Science 1998; 67: 405-415

182. Fukushima K, Feijoo JL, Yang MC. Abiotic degradation of poly(DL-lactide), poly(ε-caprolactone) and their blends. Polymer Degradation and Stability 2012; 97: 2347-2355

183. Liao G, Jiang S, Xu X, Ke Y. Electrospun aligned PLLA/PCL/HA composite fibrous membranes and their in vitro degradation behaviors. Materials Letters 2012; 82: 159-162

184. Shikinami Y, Matsusue Y, Nakamura T The complete process of bioresorption and bone replacement using devices made of forged composites of raw hydroxyapatite particles/ poly L-lactide (F-u-HA/PLLA). Biomaterials 2005; 26: 5542–5551

185. Pearce AI, Richards RG, Milz S, Schneider E, Pearce SG. Animal models for implant biomaterial research in bone: A review. European Cells and Materials 2007; 13: 1-10

186. Bongio M, van den Beucken JJJP, Leeuwenburgh SCG, Jansen JA. Development of bone substitute materials: from 'biocompatible' to

‘instructive. Journal of materials chemistry 2010; 20: 8747-8759

187. Izquierdo R, Garcia-Giralt N, Rodríguez MT, Cáceres E, García SJ, Ribelles JLG, Pradas MM, Monllau JC, Suay J. Biodegradable PCL scaffolds with an interconnected spherical network for tissue engineering. Journal of Biomedical Materials Research Part A 2007; 85A: 25-35

188. Garcia-Giralt N, Izquierdo R, Nogués X, Perez-Olmedilla M, Benito P, Gómez-Ribelles JL, Checa MA, Suay J, Caceres E, Monllau JC. A porous PCL scaffold promotes the human chondrocytes redifferentiation and hyaline-specific extracellular matrix protein synthesis. Journal of Biomedical Materials Research Part A 2008; 85A: 1082-1089

189. Olmedilla MP, Lebourg M, Ivirico JLE, Nebot I, Giralt NG, Ferrer GG, Soria JM, Ribelles JLG.“In vitro” 3D culture of human chondrocytes using modified ε-caprolactone scaffolds with varying hydrophilicity and porosity. Journal Biomaterials Applications 2012; 27: 299-309

190. Gamboa-Martínez TC, Rodenas-Rochina J, Tortosa PR, Lebourg M, Ribelles JLG, Sanchez MS, Ferrer GG. Chondrocytes cultured in an adhesive macroporous scaffold subjected to stirred flow bioreactor behave like in static culture. Journal of Biomaterials and Tissue Engineering 2013; 3: 312-319

191. Lebourg M, Rochina JR, Sousa T, Mano J, Ribelles JLG. Different hyaluronic acid morphology modulates primary articular chondrocyte behavior in hyaluronic acid-coated polycaprolactone scaffolds. Journal of Biomedical Materials Research Part A 2013; 101A: 518–527

192. Woods A, Wang G, Beier F. Regulation of chondrocyte differentiation by the actin cytoskeleton and adhesive interactions. Journal of Cellular Physiology 2007; 213:1–8

193. Jakob M, Demarteau O, Schafer D, Stumm M, Heberer M, Martin I. Enzymatic digestion of adult human articular cartilage yields a small fraction of the total available cells. Connective Tissue Research 2003; 44: 173–180

194. Freyria AM, Cortial D, Ronzière MC, Guerret S, Herbage D.

Influence of medium composition, static and stirred conditions on the proliferation of and matrixprotein expression of bovine articular chondrocytes cultured in a 3D collagen scaffold. Biomaterials 2004; 25: 687–697

195. Wang Y, Liu L, Guo S. Characterization of biodegradable and cytocompatible nano-hydroxyapatite/polycaprolactone porous scaffolds in degradation in vitro. Polymer Degradation and Stability 2010; 95:207–213.

196. Pok SW, Wallace KN, Madihally SV. In vitro characterization of polycaprolactone matrices generated in aqueous media. Acta Biomaterialia 2010;6:1061–1068

197. Harrison KL, Jenkins MJ. The effect of crystallinity and water absorption on the dynamic mechanical relaxation behavior of polycaprolactone. Polymer International 2004;53:1298–1304

198. Samarza AJ, Athanasiou A. Design characteristics for the tissue engineering of cartilaginous tissues. Annals of Biomedical Engineering 2004;32:2–17

199. Shepherd DET, Seedhom BB. The instantaneous compressive modulus of human articular cartilage in joints of the lower limb. Rheumatology 1999;38:124–132

200. Nuernberger S, Cyran N, Albrecht C, Redl H, Vécsei V, Marlovits S. The influence of scaffold architecture on chondrocyte distribution and behavior in matrix-associated chondrocyte transplantation grafts. Biomaterials 2011;32:1032–1040

201. Hutmacher DW, Ng KW, Kaps C, Sittinger M, Klaring S. Elastic cartilage engineering using novel scaffold architectures in combination with a biomimetic cell carrier. Biomaterials 2003;24: 4445–4458

202. Sato T, Chen G, Ushida T, Ishii T, Ochiai N, Tateishi T, Tanaka J. Evaluation of PLLA–collagen hybrid sponge as a scaffold for cartilage tissue engineering. Materials Science and Engineering: C 2004;24:365–372

203. Discher DE, Janmey P, Wang Y. Tissue cells feel and respond to the

stiffness of their substrate. Science 2005;310:1139–1143

204. Choquet D, Felsenfeld DP, Sheetz MP. Extracellular matrix rigidity causes strengthening of integrin–cytoskeleton linkages. Cell 1997; 88:39–48

205. Grogan SP, Barbero A, Diaz-Romero J, Cleton-Jansen AM, Soeder S, Whiteside R, Hogendoorn PCW, Farhadi J, Aigner T, Martin I, Mainil-Varlet P. Identification of markers to characterize and sort human articular chondrocytes with enhanced in vitro chondrogenic capacity. Arthritis & Rheumatology 2007;56:586–595

206. Knudson CB. Hyaluronan and CD44: Strategic players for cell–matrix interactions during chondrogenesis and matrix assembly. Birth Defects Res C 2003;69:174–196

207. Stern R, Asari AR, Sugahara KN. Hyaluronan fragments: An information rich system. European Journal of Cellular Biology 2006;85:699–715

208. Lareu RR, Subramhanya KH, Peng Y, Benny P, Chen C, Wang Z, Rajagopalan R, Raghunath M. Collagen matrix deposition is dramatically enhanced in vitro when crowded with charged macromolecules: The biological relevance of the excluded volume effect. FEBS Lett 2007;581:2709–2714

209. Murphy CL, Thoms BL, Vaghjiani RJ, Lafont JE. HIF-mediated articular chondrocyte function: prospects for cartilage repair. Arthritis Research & Therapy 2009; 11:213-219

210. Gibson G, Lin D-L, Roque M. Apoptosis of Terminally Differentiated Chondrocytes in Culture. Experimental Cell Research 1997;233: 372 – 382

211. Lee HH, Chang CC, Shieh MJ, Wang JP, Chen YT, Young TH, Hung SC. Hypoxia Enhances Chondrogenesis and Prevents Terminal Differentiation through PI3K/Akt/FoxO Dependent Anti-Apoptotic Effect. Scientific Reports 2013;3 artículo 2683

212. Khan WS, Adesida AB,Hardingham TE .Hypoxic conditions

increase hypoxia-inducible transcription factor 2α and enhance chondrogenesis in stem cells from the infrapatellar fat pad of osteoarthritis patients. Arthritis Research & Therapy 2007, 9:R55

213. Sheehy EJ, Buckley CT, Kelly DJ. Oxygen tension regulates the osteogenic, chondrogenic and endochondral phenotype of BM derived mesenchymal stem cells. Biochemical and Biophysical Research Communications 2012; 417: 305–310

214. Zhu M, Feng Q, Bian L. Differential effect of hypoxia on human mesenchymal stem cell chondrogenesis and hypertrophy in hyaluronic acid hydrogels. Acta Biomaterialia 2014; 10: 1333–1340

215. Meretoja VV, Dahlin RL, Wright S, Kasper FK, Mikos AG. The effect of hypoxia on the chondrogenic differentiation of cocultured articular chondrocytes and mesenchymal stem cells in scaffolds. Biomaterials 2013;34: 4266-4273

216. Carter DR, Beaupré GS, Giori NJ, Helms JA. Mechanobiology of Skeletal Regeneration. Clinical Orthopaedics & Related Research 1998; 355: S41-S55

217. Zhu M, Feng Q, Bian L.Differential effect of hypoxia on human mesenchymal stem cell chondrogenesis and hypertrophy in hyaluronic acid hydrogels. Acta Biomaterialia 2014;10: 1333–1340

218. Markway BD, Tan G-K, Brooke G, Hudson JE, Cooper-White JJ, Doran MR. Enhanced Chondrogenic Differentiation of Human Bone Marrow-Derived Mesenchymal Stem Cells in Low Oxygen Environment Micropellet Cultures. Cell Transplantation 2010; 19: 29–42

219. Mansfield K, Rajpurohit R, Shapiro IM. Extracellular phosphate ions cause apoptosis of terminally differentiated epiphyseal chondrocytes.Journal of Cellular Physiology 1999;179:276-86

220. Rodenas-Rochina J, Kelly DJ, Ribelles JLG, Lebourg M. Compositional changes to synthetic biodegradable scaffolds modulate the influence of hydrostatic pressure on chondrogenesis of mesenchymal stem cells . Submitted

221. Gannon AR, Nagel T, Kelly DJ. The role of the superficial region in determining the dynamic properties of articular cartilage. Osteoarthritis and Cartilage 2012;20:1417-1425

222. Kim SY et al. Mechanical stimulation and the presence of neighbouring cells greatly affect migration of human mesenchymal stem cells. Biotechnol Lett 2013;35:1817-1822

223. Schipani E. Review: Hypoxia and HIF-1α in chondrogenesis. Seminars in Cell & Devolopmental Biology 2005;16:539–546

224. Bentovim L, Amarilio R, Zelzer E. HIF1α is a central regulator of collagen hydroxylation and secretion under hypoxia during bone development. Development 2012;139:4473-4483

225. Kurtis MS, Tu BP, Gaya OA, Mollenhauer J, Knudson W, Loeser RF, Knudson CB, Sah RL. Mechanisms of chondrocyte adhesion to cartilage: role of β1-integrins, CD44, and annexin. Journal of Orthopaedic Research 2001;19:1122-1130

226. Millward-Sadler SJ, Salter DM. Integrin-Dependent Signal Cascades in Chondrocyte Mechanotransduction. Annals of Biomedical Engineering 2004;32:435–446

227. Kim Y-J, Sah R, Doong J-Y, Grodzinsky A. Fluororometric assay of DNA in cartilage explants using hoechst 33258. Analytical Biochemistry 1988; 174:168–76

228. Enomoto-Iwamoto M, Iwamoto M, Nakashima K, Mukudai Y, Boettiger D, Pacifici M, Kurisu K, Suzuki F. Involvement of α5β1 Integrin in Matrix Interactions and Proliferation of Chondrocytes. Journal of bone and mineral research 1997; 12: 1124-1132

229. Vikingsson L, Ferrer GG, Gómez-Tejedor JA, Ribelles JLG. An in vitro experimental model to predict the mechanical behavior of macroporous scaffolds implanted in articular cartilage. Journal of the mechanical behavior of biomedical materials 2014; 32: 125-131